The University Of Sheffield.

Access to Electronic Thesis

Author:	Ian Packham
Thesis title:	Exploiting the Zebrafish Embyo as a Model to Determine the Role of Genes that Modulate Arteriogenesis
Qualification:	PhD
Date awarded:	14 September 2009

Exploiting the Zebrafish Embryo as a Model to Determine the Role of Genes that Modulate Arteriogenesis

Ian Michael Packham

A thesis submitted for the degree of PhD

Centre for Developmental and Biomedical Genetics

Department of Biomedical Sciences

University of Sheffield

February 2009

I. Acknowledgements

There are many people I wish to thank, first and foremost my supervisors. They have done nothing but offer support throughout, and have done far more than is necessary. From my first days Tim made me feel welcome and a valid part of the lab. Phil provided a nurturing atmosphere and a fantastic opportunity when he invited me to Singapore. I have thoroughly enjoyed my time in Sheffield.

There are a number of collaborators and colleagues without whom this research would not have been possible: Paul Heath, Marta Milo, Scott Reeve, Sue Newton, all the aquaria staff, the Ingham Lab, Vincent Cunliffe, Liz Seward and the members of CVRU.

A massive thank you also goes to all the members of facebook's "D38" group – they are really important people who mean a lot to me, and have had their bit parts in an important part of my life. You won't be forgotten, particularly if you keep inviting me back for those Thursday "lab meetings".

II. Abstract

Arteriogenesis, remodelling of pre-existing collateral vessels following occlusion has potential as therapy for diseases of arterial occlusion such as coronary heart disease. Although haemodynamic force is known to induce arteriogenesis, genetic modulation remains largely undetermined. Analysis of collateral remodelling in mammalian models occurs *post mortem* preventing serial *in vivo* observation. Zebrafish embryos have a number of advantages that permit serial *in vivo* observation of heart and vasculature.

I sought to determine if zebrafish embryos underwent arteriogenesis. *Gridlock* mutant embryos suffer complete and permanent occlusion of the aorta, but recover aortic blood flow from three to five days post fertilisation. To determine whether recovery was independent of *gridlock* mutation I performed laser-induced aortic occlusion of wildtype embryos preventing aortic blood flow distal to occlusion. Within 24 hours over 80% of embryos had recovered aortic blood flow, demonstrating zebrafish embryos undergo arteriogenesis. I next determined whether recovery occurred in a manner similar to mammalian arteriogenesis by demonstrating a similar modulation by nitric oxide.

To determine gene expression following reduced haemodynamic force occurring with arterial occlusion I performed microarray analysis of wildtype embryos lacking cardiac contraction and thus haemodynamic force (*tnnt2* morphants) at three timepoints in the first 60 hours of development. 290 genes were differentially expressed: 166 demonstrated increased expression and 124 decreased expression in *tnnt2* morphants compared to control (physiological haemodynamic force; ≥80% probability of ≥two-fold change in expression). I evaluated level and localisation of expression of two of these genes (*EFNB1* and *EDNRB*), and assessed the effect of inducing aberrant splicing by morpholino antisense oligonucleotide knockdown on general and vascular development, as well as the ability to recovery aortic blood flow by arteriogenesis.

III. Contents

IV. List of Figures

V. List of Abbreviations

Ab	absorption
ADP	adenosine diphosphate
ADRA2B	adrenoceptor 2B
Ang1	angiopoietin-1
Ang2	angiopoietin-2
aRNA	antisense RNA
At	aorta
ATP	adenosine triphosphate
BDM	2,3-butanedione monoxime
bFGF	basic fibroblastic growth factor
Bl	swim bladder
bp	base pair
Ca^{2+}	calcium ion
cAMP	cyclic adenosine monophosphate
cDNA	complementary DNA
CEBP1	CCAAT/enhancer binding protein 1
cGMP	cyclic guanosine monophosphate
CHD	coronary heart disease
CYP51	cytochrome P450, family 51
CYP26B1	cytochrome P450, family 26, subfamily b, polypeptide 1
dH_20	distilled water
DIC	differential interference contrast
DLAV	dorsal longitudinal anastomotic vessel
Dll4	delta-like 4
DMA	digital motion analysis
DNA	deoxyribonucleic acid
dNTP	deoxyribonucleotide triphosphate
EC	endothelial cell
ECM	extracellular matrix
EDNRB	endothelin receptor type B
EFNB1	ephrinB1
eGFP	enhanced green fluorescent protein
eNOS	endothelial nitric oxide synthase, formerly NOSIII
ENU	ethyl-nitrosourea
ET	endothelin-1
FADS	fatty acid desaturase 2
FSS	fluid shear stress

GFP	green fluorescent protein
GMCSF	granulocyte macrophage colony stimulating factor
GTP	guanine triphosphate
h	hour
HIF-1	hypoxia-inducible factor-1
hpf	hours post fertilisation
hpo	hours post occlusion
HUVEC	human umbilical vein endothelial cell
ICAM-1	intracellular adhesion molecule-1
IL-4	interlukin-4
iNOS	inducible nitric oxide synthase, formerly NOSII
INSIG1	insulin induced gene 1
ISH	*in situ* hybridisation
ISV	intersegmental/intersomitic vessel
MCP-1	monocyte chemotactic protein-1
MI	myocardial infarction
min	minute
mm	millimetre
MMP	matrix metalloprotease
MO	morpholino antisense oligonucleotide
MQ H_20	milliQ water
MRI	magnetic resonance imaging
N	notochord
NADPH	nicotinamide adenine dinucleotide phosphate
NCID	notch intracellular domain
nNOS	neuronal nitric oxide synthase, formerly NOSI
NO	nitric oxide
NOS	nitric oxide synthase
NPPA	natriuretic peptide precursor A
O_2	oxygen
PANTHER	protein analysis through evolutionary relationships
PBS	phosphate buffered saline
PCNA	proliferating cell nuclear antigen
PCR	polymerase chain reaction
Pi	inorganic phosphate
PI3-K	phosphatidylinositol 3-kinase
PLCγ-MAPK	phospholipase Cγ-mitogen activated protein kinase
PLS1	plastin
RBPJ	recombination signal binding protein for immunoglobulin kappa J region

RHO	rhodopsin
RNA	ribonucleic acid
ROI	region of interest
rpm	revolutions per minute
rtp	room temperature and pressure
RT-PCR	real-time polymerase chain reaction
s	second
SAGE	serial analysis of gene expression
SDF1	stromal-cell derived factor 1
sH_20	sterile water
SIV	subintestinal vessel
SNP	sodium nitroprusside
SR	sarcoplasmic reticulum
SSRE	shear stress response element
STAT1	signal transduction and activation of transcription 1
TNFα	tumour necrosis factor α
tnnt2	cardiac troponin T2
TSAd	T-cell-specific adapter molecule
V	cardinal vein
VEGF	vascular endothelial growth factor/VEGF-A
VEGFR	vascular endothelial growth factor receptor
VP	venous plexus
VSMC	vascular smooth muscle cells
WASp	Wiskott Aldrich syndrome protein

Chapter One
General Introduction

Chapter 1: General Introduction

1.1 Introductory Preamble

This introduction discusses, in general terms, research relevant to arteriogenesis. It also discusses the position of the zebrafish embryo as a model organism within cardiovascular research, in comparison to mammalian models. The introduction refers particularly to arterial vasculature, since it is arterial occlusion which results in arteriogenesis. For clarity, I refer to zebrafish of 1-5 days post fertilisation as embryos throughout, although they are often referred to as larvae from 2 days post fertilisation. Specific introductions relevant to experimental results (for example microarray technology) are found leading results chapters (Chapters 3-6).

1.2 Arteriogenesis and Neovascularisation

Arteriogenesis defines remodelling of pre-existing arterial communications into patent collateral vessels following arterial occlusion (Buschmann and Schaper, 1999), and is often described 'collateral vessel development' or 'remodelling'. It describes luminal enlargement of pre-existing vessels to redirect blood flow around an occlusion (figure 1.1) (Heilmann, Beyersdorf *et al.*, 2002).

Experiments demonstrate arteriogenesis to be driven by alterations in fluid shear stress (FSS), followed by infiltration of monocytes/macrophages (Van Royen, Piek *et al.*, 2001b). For example, sustained elevation of FSS following arterial ligation results in enhanced collateral blood flow (Eitenmuller, Volger *et al.*, 2006). Release of monocyte chemotactic protein-1 (MCP-1) leads to increased collateral density (Hoefer, van Royen *et al.*, 2001), while macrophage depletion by *pu.1* knockdown significantly reduces recovery of blood flow around the occlusion (Gray, Packham *et al.*, 2007).

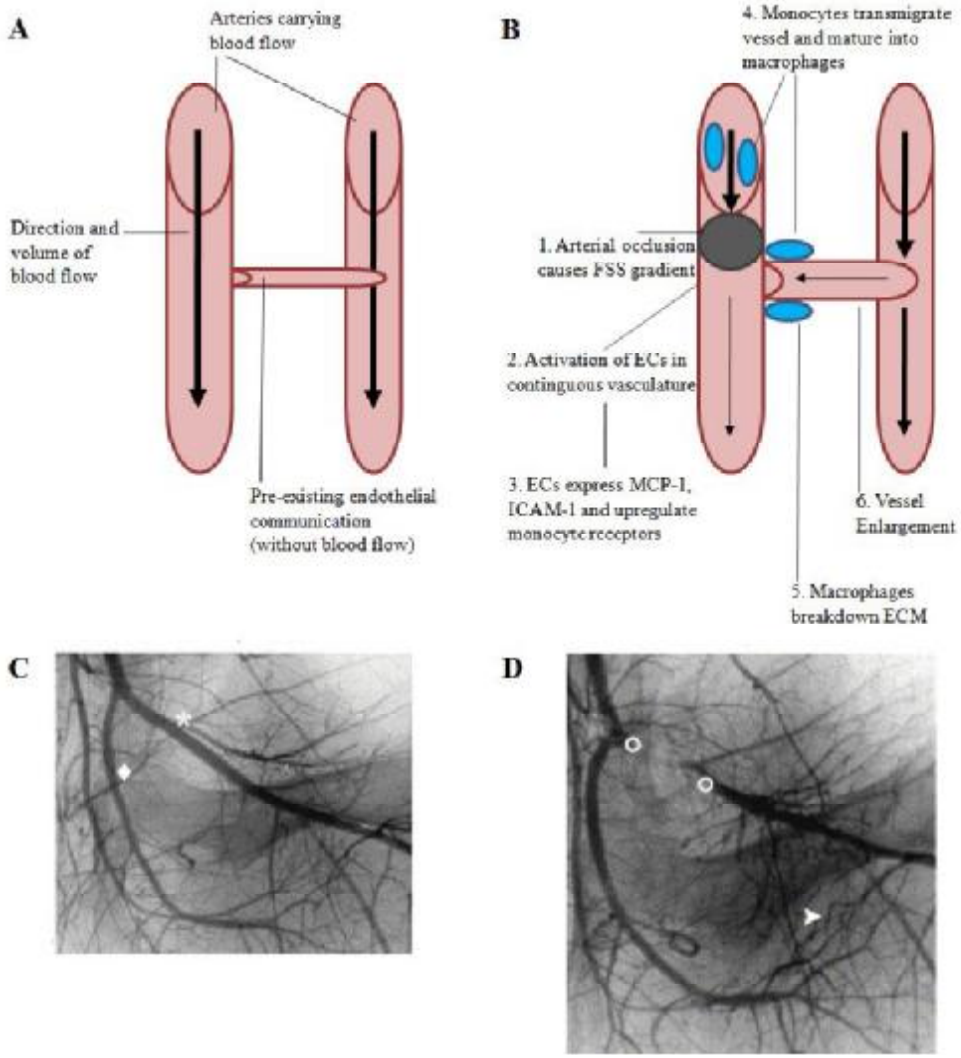

Figure 1.1 Collateral vessel development.

A and B depict the mechanism of arteriogenesis. Prior to occlusion (A), pre-existing endothelial communications transport little or no blood flow. Arterial occlusion initiates arteriogenesis (B), resulting in enlargement of the pre-existing endothelial communications and increased blood flow within them. C demonstrates *post mortem* X-ray angiography of unligated femoral artery in pig. * and ◊ mark femoralis superficialis and femoralis profunda respectively. D demonstrates the same arteries following double ligation (depicted by O). Arrowhead points to a collateral vessel which has remodelled to transport blood around occlusion site. C and D adapted from figure 6 Buschmann, Vokuil *et al.* (2003).

Arterial occlusion alters physiological levels of FSS in the vessel, causing elevations immediately anterior compared with posterior to occlusion (Schaper and Scholz, 2003). This results in attraction of monocytes/macrophages, whereupon it is believed they infiltrate the vessel and breakdown extracellular matrix (ECM), providing space for remodelling (Schaper and Buschmann, 1999). A more detailed discussion on mechanism follows in section 1.2.5, and figure 1.1 demonstrates key aspects.

1.2.1 Clinical Relevance of Arteriogenesis

Arteriogenesis is viewed as a potential therapeutic target for the millions suffering coronary artery occlusion (leading to Coronary Heart Disease; CHD) or peripheral artery occlusion (Peripheral Artery Disease) resulting from atherosclerosis (Heilmann, Beyersdorf *et al.*, 2002). Present therapeutic strategies are able to alleviate symptoms, but stimulate little or no disease regression (van Royen, Piek *et al.*, 2001a). Therapies are not tailored to individuals, potentially reducing efficacy. They aim to either prevent occlusion (blood-thinning drugs, statins) or revascularise/bypass vessels following occlusion (Heilmann, Beyersdorf *et al.*, 2002).

Blood-thinning drugs such as warfarin control occlusive disease by reducing likelihood of clot formation, while statins reduce low density lipoproteins responsible for atherosclerotic plaques (Weisfeldt and Zieman, 2007). Post-occlusion revascularisation (angioplasty, surgical bypass) are limited by restenosis and graft occlusion, prompting additional clinical intervention, and limited to patients meeting specific criteria (van Royen, Piek *et al.*, 2001a). Patients with severe or widespread vascular pathology may not be suitable (Buschmann and Schaper, 2000).

Therapies also do nothing to inhibit development of additional atherosclerotic plaques or their rupture (Van Royen, Piek *et al.*, 2001b), which would necessitate further treatment. A drug or growth factor induced stimulation of arteriogenesis could prevent or reduce the consequences of arterial occlusion. In addition, characterisation of arteriogenesis (for example gene expression profiling) could provide clinicians with a means of identifying individuals at risk prior to disease onset, and may also allow pharmacogenetics, tailoring treatments to ethnic or gene-specific groups (Weisfeldt and Zieman, 2007), giving a

greater likelihood of success. A similar strategy is envisaged for treatment of cancers, diseases in which pathological angiogenesis plays a leading role (personal communication, Professor R Bicknell).

1.2.2 Intra-species and Inter-species Variation

Collateral vessels do not occur in all individuals of a species, or in all species. For example, while canine hearts demonstrate a high number of collateral vessels, the porcine heart demonstrates such vessels only rarely (Maxwell, Hearse *et al.*, 1987). This has been hypothesised to be due to alterations in genetic predisposition to the position and quantity of collateral vessels that result (Buschmann and Schaper, 2000).

1.2.3 Mammalian Vascular Anatomical Development

Angioblasts - endothelial cell (EC) precursors, originating from embryonic and extra-embryonic mesoderm, migrate to sites of blood vessel formation to create 'strings' of non-lumenised ECs (Roman and Weinstein, 2000). Some evidence suggests the strings remodel into lumenised structures through fusion of intracellular vacuoles (Kamei, Saunders *et al.*, 2006) of ECs staked head to tail (Childs, Chen *et al.*, 2002), although other evidence suggests lumen are extracellular and lined by multiple ECs positioned side to side (Blum, Belting *et al.*, 2008). Vessels demonstrate an increasingly mature phenotype following vacuolisation when pericytes and vascular smooth muscle cells (VSMCs) migrate to the EC niche (Wang, Chen *et al.*, 1998).

Embryonic vascular patterning requires two processes: expression of a specific gene set coupled with onset of blood flow (Wang, Chen *et al.*, 1998). EC fate is partly determined at the angioblast stage by the gene *hey2* driving differentiation to arterial rather than venous fates (Peterson, Shaw *et al.*, 2004), thereby demonstrating that ECs undergo the fate decision before the onset of blood flow. Furthermore, arteries and veins possess distinct gene expression patterns observable before the onset of flow. For instance, arteries specifically express ephrinB2 and ephrinB4, and veins EphB4 (le Noble, Moyon *et al.*, 2004).

1.2.4 Vasculogenesis and Angiogenesis

Vasculogenesis, embryonic development of the vasculature through EC coalescence, occurs at two sites in mammals: internal and external to the embryo proper (Jones, le Noble *et al.*, 2006). Internally, vessels develop through differentiation and migration of angioblasts (Carmeliet, 2000); a VEGF-induced action (Carmeliet, Ferreira *et al.*, 1996). Externally, blood islands in the extra-embryonic membrane, comprising haematopoietic and ECs, expand over the yolk-sac forming the capillary plexus (Jones, le Noble *et al.*, 2006). The two vascular networks unite, allowing passage of blood with the commencement of cardiac contraction (Jones, le Noble *et al.*, 2006).

Further vascular development occurs by angiogenesis, the *de novo* sprouting of vessels from pre-existing vessels through proliferation and migration of ECs (Buschmann and Schaper, 1999). Vasodilatation (mediated by nitric oxide; NO) and increases in permeability (mediated by VEGF) result in infiltration of plasma proteins that provide the extravascular platform for EC migration (Carmeliet, 2000). Growth factors including VEGF activate ECs, resulting in release of matrix metalloproteases (MMPs) and leading to breakdown of the ECM, providing the physical space required for proliferation and migration (Rosen, 2002).

1.2.5 Mechanism of Arteriogenesis

Arterial occlusion results in a steep FSS gradient developing locally in vasculature contiguous with the occlusion site (Buschmann and Schaper, 1999). FSS anterior to the occlusion becomes elevated in comparison to FSS posterior to it (figure 1.1). Sustained elevated levels of FSS activate ECs in contiguous vasculature (Chen, Li *et al.*, 2001) (section 1.3.1), including collateral vessels. In man, approximately 30% of patients with partial or total occlusion of a coronary artery demonstrate the presence of collateral vessels on coronary angiography (Rentrop, Feit *et al.*, 1989). Collateral vessels were significantly more frequent in patients with total rather than partial occlusion (Rentrop, Feit *et al.*, 1989) suggesting a link between collateral vessel growth and disease progression. It remains unknown whether this holds for the general population not presenting with symptoms of coronary arterial disease.

Shear activated ECs express MCP-1 and adhesion molecules including intracellular adhesion molecule-1 (ICAM-1) (van Royen, Piek *et al.*, 2001a). EC monocyte receptors are also upregulated (van Royen, Piek *et al.*, 2001a). Circulating monocytes bind their receptor and transmigrate the vessel where they mature into macrophages (Bergmann, Hoefer *et al.*, 2006).

Monocytes are stabilised through upregulation of survival factors such as granulocyte macrophage colony stimulating factor (GMCSF), and are capable of releasing large quantities of growth factors (bFGF) (Buschmann and Schaper, 1999). Vessel localised macrophages secrete MMPs and factors including tumour necrosis factor α (TNFα) to breakdown the ECM (figure 1.2) (Heilmann, Beyersdorf *et al.*, 2002). The first wave of EC and VSMC mitosis now occurs (Heilmann, Beyersdorf *et al.*, 2002), permitting remodelling through physical enlargement of the vessel (figure 1.2).

1.2.6 Mammalian Blood Vessel Anatomy

In mammalian species arteries, arterioles, venules and veins have the same basic structure, comprising three distinct layers (figure 1.3). The *tunica intima* comprises a single layer of squamous ECs lining the vessel lumen and a surrounding basement membrane of connective tissue that includes pericytes (Armulik, Abramsson *et al.*, 2005), a cell of the same lineage as VSMCs (Benjamin, Hemo *et al.*, 1998). Pericytes are important in intracellular signalling, and in small vessels multiple ECs are found connected to a single pericyte by focal adhesion (Armulik, Abramsson *et al.*, 2005). Sited within the connective tissue is the internal elastic lamina, an elastic ring providing flexibility.

The medial layer, the *tunica media*, is the thickest. It comprises layers of circular elastic fibres, connective tissue, and VSMCs. The external elastic lamina separates the second and third layers. VSMCs are predominantly found in arteries. VSMCs provide arteries with the tone and elastic properties necessary to counteract the force of high pressure blood pumped directly from the heart, and also bestow vasoactive properties on the vessel.

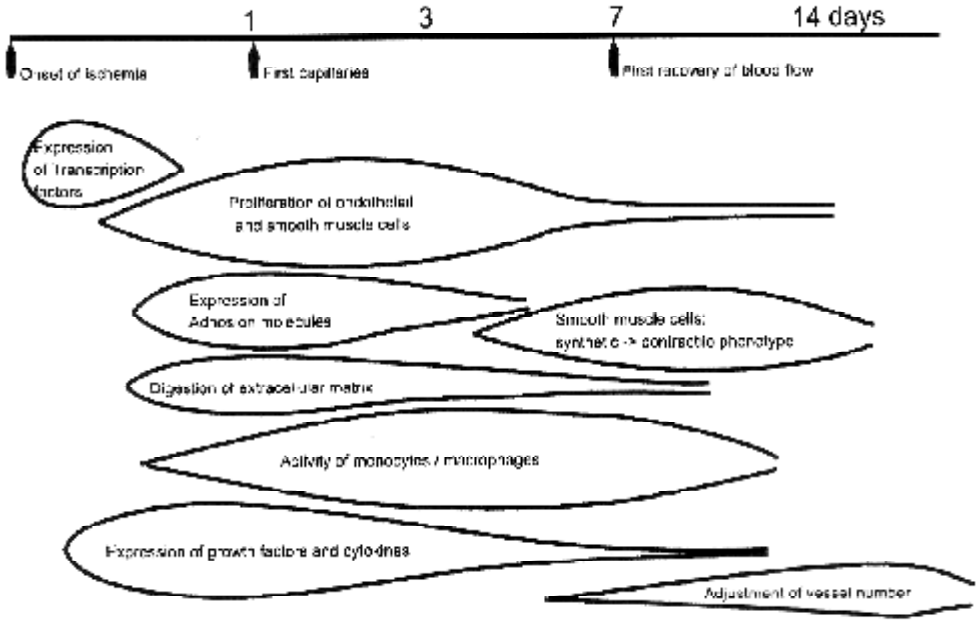

Figure 1.2 Time-course of collateral vessel remodelling during arteriogenesis.
The number of days recorded demonstrates the timing of collateral vessel development in a rabbit hindlimb femoral artery ligation model. Timing alters dependent upon the model organism studied. Femoral artery ligation also leads to ischaemia (Heilmann, Beyersdorf *et al.*, 2002), a response not observed in zebrafish embryos following arterial occlusion (Gray, Packham *et al.*, 2007). Expression of transcription factors follows onset of ischaemia. In turn, this results in proliferation of ECs and VSMCs, expression of adhesion molecules, growth factors and cytokines, and breakdown of ECM. Expression of adhesion molecules, growth factors and cytokines results in activation of monocytes/macrophages. A change in contractile phenotype of VSMCs follows, along with an adjustment of cell vessel number. Adapted from figure 1 Heilmann, Beyersdorf *et al.*, 2002.

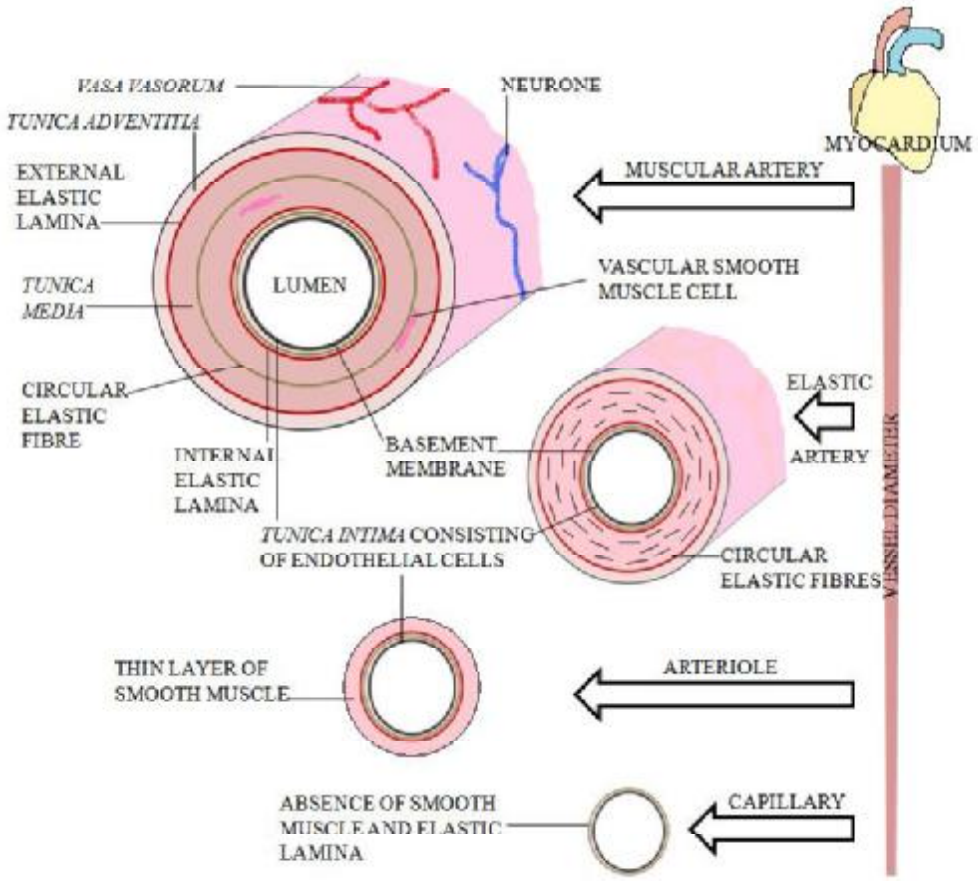

Figure 1.3 Standard anatomical detail of the mammalian arterial system.
As vessel diameter increases arterial anatomy changes. Capillaries comprise *tunica intima*, a single layer of squamous ECs lining the vessel lumen and a surrounding basement membrane of connective tissue, lacking elastic lamina and smooth muscle. Arterioles contain a small layer of smooth muscle and internal elastic lamina provides flexibility. The *tunica media* is thickest in muscular and elastic arteries. While elastic arteries contain large amounts of circular elastic fibres and connective tissue muscular arteries contain larger amounts of VSMCs. The external elastic lamina separates the second and third layers of the *tunica media*. VSMCs provide tone and elastic properties, and also bestow vasoactive properties on the vessel. In contrast, veins are unable to maintain tone due to thinner layers containing less elastic and muscular fibre. The *tunica adventitia* is predominantly connective tissue but also contains neurones necessary for VSMC innervation. In larger vessels a network of capillaries (*vasa vasorum*) supplies the vessel.

Veins are unable to maintain tone due to thinner layers containing less elastic and muscular fibre (Hong, Kume *et al.*, 2008). The outermost layer, the *tunica adventitia*, is predominantly connective tissue, but also contains neurones necessary for VSMC innervation. In larger vessels a network of capillaries (*vasa vasorum*) supplies the vessel with nutrients (Davies, Blakeley *et al.*, 2001).

1.2.7 Mammalian Arterial Physiology

The physiological role of arteries is transportation of nutrients, hormones and cells to tissues and organs. Innervation by the autonomic nervous system alters blood flow by innervating VSMCs found within the *tunica media* (Halka, Turner *et al.*, 2008). Vasoconstriction of VSMCs causes a decrease in luminal cross-sectional area and thereby blood flow. Vasodilatation has a contrary effect, increasing luminal cross-sectional area and blood flow.

Physical forces also play a key role in vessel physiology. FSS acts directly on ECs to modulate structure and function (Cunningham and Gotlieb, 2005) through alteration in gene expression (Garcia-Cardena, Comander *et al.*, 2001), release of vasoactive substances including NO (Lehoux, Castier *et al.*, 2006) and activation of cell populations such as monocytes (Buschmann, Voskuil *et al.*, 2003). In mice, the magnitude of FSS significantly increases at times the embryo is undergoing vascular remodelling (Jones, le Noble *et al.*, 2006). Reorganisation of intermediate filaments, microtubules, and F-actin stress fibres to forces such as FSS demonstrate a key role for cytoskeletal elements in force transmission in ECs (Terzi, Henrion *et al.*, 1997).

1.2.8 Collateral Vessel Architecture

Collateral vessels remodel from small EC lined vessels (Goncalves, Epstein *et al.*, 2001) into larger vessels composed of ECs surrounded by an internal elastic lamina, as well as one or two layers of VSMCs (Buschmann and Schaper, 1999). Increases in vessel diameter are not solely a result of vasodilatation, but also EC and VSMC proliferation (Lloyd, Yang *et al.*, 2001).

Collateral vessels often take on a tortuous, corkscrew-like appearance (Buschmann, Voskuil *et al.*, 2003). Figure 1.4 demonstrates the general histology of a collateral vessel. Although normal resting blood flow in collateral vessels is reached quickly, only 30-40% of maximal flow is ever reached (Eitenmuller, Volger *et al.*, 2006). This may be due to normalisation in FSS levels, since FSS falls with increases in diameter observed during arteriogenesis (Eitenmuller, Volger *et al.*, 2006). Blood flow is related to the fourth power of a vessel's radius (Poiseuille's formula), meaning minor changes in radius produce large alterations in flow (Davies, Blakeley *et al.*, 2001). Thus, maintaining the level of FSS may increase the percentage of maximal flow achieved, and similarly, further reductions in FSS may decrease the percentage of maximal flow observed. Reduced recovery of functionality in tissues may also have a role, limiting the utility of collateral vessels as a means of meeting tissue oxygen demand.

1.2.9 Comparison of Vasculogenesis, Angiogenesis and Arteriogenesis

While often occurring in concert, vasculogenesis, angiogenesis and arteriogenesis are distinct processes which may occur to different degrees dependent on the situation. Figure 1.5 demonstrates the similarities and differences between the three processes discussed below. While initiated by VEGF and bFGF, and with an undetermined role for TGFβ, vasculogenesis leads to an immature vasculature (Carmeliet, 2000). Stimulation of angiogenesis occurs when ischaemia results in the expression of hypoxia inducible factor-1 (HIF-1) (van Royen, Piek *et al.*, 2001a). HIF-1 expression in turn acts to increase transcription of genes including the nitric oxide synthase (NOS) enzymes and VEGF. Therefore, ischaemia initiates vasodilation (via NO release), increased vessel permeability, and enhanced EC proliferation (both via VEGF).

Arteriogenesis differs from angiogenesis in that there is no *de novo* vessel formation (Carmeliet, 2000), and that arteriogenesis takes place without the need for ichaemia (Heil, Eitenmuller *et al.*, 2006; Lee, Stabile *et al.*, 2004), which is a key driver of angiogenesis. The driving force for arteriogenesis appears to be alterations in FSS. All three processes share some level of modulation by VEGF, although the role of VEGF in arteriogenesis is not clearly defined, as discussed below.

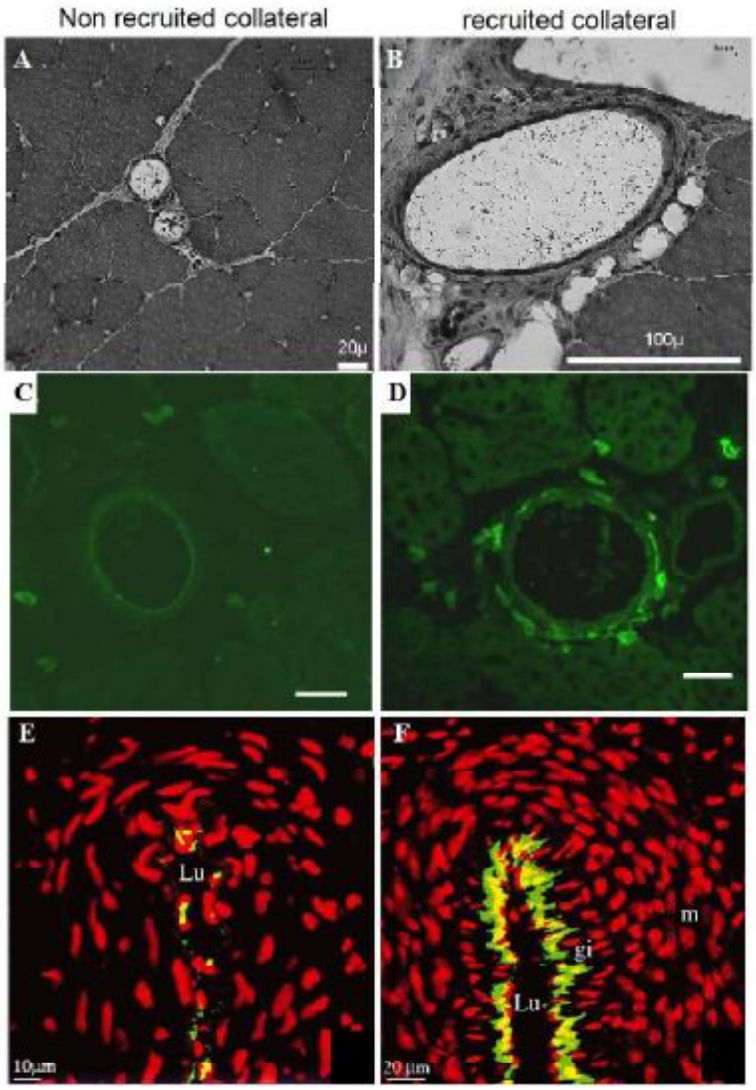

Figure 1.4 Basic histology of non recruited and remodelled collateral vessels.
Histology of non recruited (A, C, E) and recruited (B, D, F) collateral vessels following mouse femoral artery ligation (A-D) and dog cardiac collaterals (E, F). (A) The vessel demonstrates small quantities of blood flow (dark luminal staining) within a diameter of approximately 25µm. Scale bar = 20µm. (B) Mature collateral vessel 14 days post femoral artery ligation. The lumen of the remodelled collateral is clearly larger than the non recruited vessel in (A). Scale bar = 100 µm. A and B adapted from figure 9 Buschmann, Voskuil *et al.*, 2003. (C, D) Green fluorescent leukocytes in the collateral environment. In C a small number of leukocytes can be observed, while a larger number are observable 7 days post ligation demonstrating the role of leukocytes in arteriogenesis. Scale bar = 20µm. Images adapted from figure 4 Babiak, Schumm *et al.*, 2004. (E, F) eNOS expression (green) and nuclear staining (red). Yellow denotes overlap between colours. A larger lumen surrounded by cells expressing higher levels of eNOS is demonstrated in the recruited compared to non recruited vessel. Scale bar = 10 (E) and 20µm (F). lu = lumen, m = media, gi = growing intima, ad = adventitia. Images adapted from figure 1 Cai, Kocsis *et al.*, 2004.

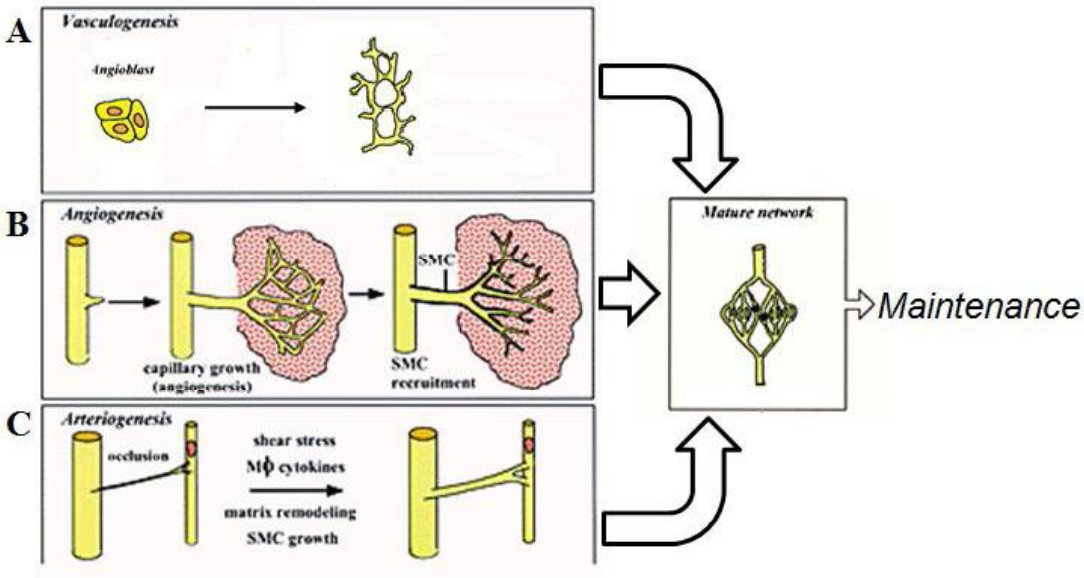

Figure 1.5 Comparison of vasculogenesis, angiogenesis, and arteriogenesis.
(A) Embryonic and adult vasculogenesis (differentiation of angioblasts) is driven by VEGF and bFGF leading to an immature vascular network. (B) Ischaemia is the stimulus for angiogenesis, leading to expression and activation of the transcription factor HIF-1 which in turn activates NO and VEGF. The result is vasodilatation (NO), increased vessel permeability and increased EC proliferation (VEGF). (C) Arteriogenesis can also be modulated by VEGF although the mechanism is not as clear as for vasculogenesis and angiogenesis. Arteriogenesis does not require ischaemia, with alterations in FSS levels stimulating the process. Figure adapted from figures 1 and 2 Carmeliet 2000.

1.3 Modulation of Arteriogenesis

Arteriogenesis undergoes modulation by a number of different factors. Factors may be systemic (alterations in FSS), local (for example NO and VEGF), circulating (infiltrating monocytes), or distant (bone marrow derived stem/progenitor cells). These factors are discussed in detail in the follow sections.

1.3.1 Fluid Shear Stress as a Modulator of Arteriogenesis

1.3.1.1 Fluid Shear Stress

FSS is force per unit area between two parallel layers, specifically, between vascular wall and blood (Nesbitt, Mangin *et al.*, 2006). FSS acts via mechanosensors on the EC surface to translocate signals to the nucleus. Signalling stimulates increases in DNA binding proteins which in turn bind shear stress response elements (SSREs). SSREs are lengths of base sequences within the promoter region of FSS-induced genes. Their binding leads to increased expression of genes such as monocyte adhesion molecules.

FSS is directly proportional to flow rate (volume/unit time) and inversely proportional to vessel diameter. Thus, as blood flow increases FSS also increases, while as vessel diameter increases FSS levels fall. Poiseuille's formula dictates that increases in luminal diameter, as occur during arteriogenesis, result in decreased flow (and thus haemodynamic force including FSS) since flow is related to the fourth power of the radius (Davies, Blakeley *et al.*, 2001). The relationship between FSS and flow rate also links FSS to heart rate, cardiac output, vascular resistance and blood pressure. For instance, increases in heart rate (contractions per minute) may result in increased cardiac output (total blood volume ejected by the heart in one minute) since cardiac output is the product of heart rate and stroke volume (blood volume ejected by each ventricle). It then follows that increased cardiac output may increase blood pressure and thus flow rate and FSS (Davies, Blakeley *et al.*, 2001).

1.3.1.2 Laminar and Non-laminar Blood Flow

The principle of laminar flow dictates that erythrocytes at the blood stream boundary have slightly lower velocity than those to the stream's centre, since they are prone to greater resistance from the vessel wall (Nesbitt, Mangin *et al.*, 2006). Blood also experiences non-uniform turbulent flow, characterised by 'eddies' distorting the pattern of laminar flow and significantly slowing a cell's passage (figure 1.6) (Nesbitt, Mangin *et al.*, 2006). Recent evidence suggests areas of turbulent flow such as bifurcations (figure 1.6) experience lower levels of FSS and are more disposed to developing atherogenic plaques (Yoshizumi, Abe *et al.*, 2003) demonstrating the importance of FSS to vessel homeostasis.

1.3.1.3 Studying the Role of Fluid Shear Stress in Modulating Arteriogenesis

Despite the importance of FSS to arteriogenesis little *in vivo* experimental work has looked directly at changes in gene expression induced by alterations in FSS. Surgery induces inflammation, altering gene expression through upregulation of non-specific inflammatory genes, which may also modulate collateral vessel development. To identify genes as vascular-specific careful *post mortem* excision would be necessary that may itself lead to altered gene expression. One group has performed such experimentation, to determine gene expression with FSS recovery after femoral artery ligation in mice (Lee, Stabile *et al.*, 2004). Entire adductor muscles were excised for RNA extraction, preventing identification of genes as vascular-specific, but limiting *post mortem* operation time. Inflammatory response-related genes formed the largest upregulated gene cluster. Genes relating to infiltration of inflammatory cells with no known association with arteriogenesis: neutrophils, lymphocytes, mast cells (Hoefer, Grundmann *et al.*, 2005) were also identified. Few of the other differentially expressed genes have been further implicated in arteriogenesis. This demonstrates the difficulties of determining gene expression with alterations in FSS *in vivo*. We therefore largely rely on extrapolation of results from microarray analysis of cell culture flow assays (discussed in section 4.1.9).

Figure 1.6 Blood rheology in an artery.
The figure demonstrates the possible variations in flow that occur in such a vessel during physiology and pathology. Arrows represent the direction of blood flow. The position of the arrow represents the type of flow likely in that specific region of the vessel. Uniform laminar flow becomes turbulent at bifurcation points. Stenosis can cause deceleration of flow at its entry point followed by acceleration across the stenotic narrowing before flow becomes more stable and uniform on exiting the stenotic region. Adapted from figure 1 Nesbitt, Mangin *et al.*, 2006.

1.3.1.4 Normalisation in Fluid Shear Stress Limits Collateral Vessel Conductance

Following experimental femoral artery ligation of control animals collateral flow has not been observed rising above 40% of maximal independent of species (Buschmann, Voskuil *et al.*, 2003; Lloyd, Yang *et al.*, 2001; Kondoh, Koyama *et al.*, 2004; Kumar, Branch *et al.*, 2008). Poiseuille's formula dictates that increases in luminal diameter, as occur during arteriogenesis, result in decreased flow (and thus haemodynamic force including FSS) since flow is related to the fourth power of the radius (Davies, Blakeley *et al.*, 2001). To determine whether FSS normalisation limited flow Eitenmüller, Volger, *et al.* (2006) adapted femoral artery ligation in rabbit to include an arterio-venous shunt. The shunt, positioned between the distal stump of the ligated artery and femoral vein, artificially enhanced the level of FSS in the collateral vasculature two-fold of control values. Large differences in pressure between ligation-end of collateral vessels and reentry into the femoral artery, caused blood flow in collateral vessels to increase. Maximal flow was achieved 28 days post shunt insertion at which point collateral vessels were capable of conducting double the maximum flow of control animals (Eitenmuller, Volger *et al.*, 2006), demonstrating *in vivo* the importance of FSS levels to collateral vessel development.

Similar experiments with femoral artery ligation in pigs demonstrate that sustained elevations in FSS not only significantly increase collateral vessel flow, but also lead to more prolonged EC and VSMC proliferation and differentiation (Pipp, Boehm *et al.*, 2004), again pointing to FSS elevations as of fundamental importance to arteriogenesis.

1.3.2 Endogenous Modulation of Arteriogenesis

A major body of work on the mechanisms of arteriogenesis focuses on two molecules: NO and VEGF which possess critical roles in arteriogenesis.

1.3.2.1 Nitric Oxide

NO is an important dilator of the vasculature. It also functions to inhibit VSMC proliferation, and protects ECs from platelet aggregation (Cai, Kocsis *et al.*, 2004a). NO forms through catalysis of L-arginine by the enzyme NOS in the presence of O_2 and

NADPH (Kibbe, Billiar *et al.*, 1999). There are three NOS isoforms. Endothelial NOS (eNOS, formerly NOSIII) is the predominant NO producer in vasculature (Cai, Kocsis *et al.*, 2004a). Inducible NOS (iNOS, NOSII) is expressed in VSMCs and cells of monocyte lineage, while neuronal NOS (nNOS, NOSI) is expressed mainly in neurones and skeletal muscle (Liu and Huang, 2008). eNOS activity is regulated by physical forces such as FSS (Jacobi, Sydow *et al.*, 2005), as well as signalling molecules such as VEGF (Hood, Meininger *et al.*, 1998).

NO freely diffuses into VSMCs where it activates soluble guanylate cyclase to catalyse GTP to cGMP (Villar, Francis *et al.*, 2006). cGMP activates serine/threonine-specific protein kinase G leading to phosphorylation of myosin light chain phosphatase (Ignarro, 1990). This leads to dephosphorylation of myosin light chains in VSMCs, resulting in vasodilatation.

1.3.2.2 NO is an Important Modulator in Remodelling of Collateral Vessels

Increases in collateral vessel blood flow resulting from three weeks exercise training in a rat model of femoral artery ligation are lost with inhibition of NO by the non-specific NOS inhibitor L-NAME (Lloyd, Yang *et al.*, 2001). eNOS deficient mice undergoing femoral artery ligation demonstrate decreased collateral blood flow during the first week post ligation, which returns to control levels by three weeks post occlusion (Mees, Wagner *et al.*, 2007). The authors hypothesise that absence of vasodilatation in eNOS deficient animals is responsible for the observation, stimulating continued remodelling of collateral vessels through sustained elevations in FSS long after FSS in wildtype control animals has normalised through dilatation (Mees, Wagner *et al.*, 2007). It has also been hypothesised that the inability of eNOS deficient mice to respond to VEGF is responsible for the observation (Yu, deMuinck *et al.*, 2005).

VEGF leads to dose-dependent release of NO from HUVECs through elevation of NOS in the cells (Hood, Meininger *et al.*, 1998). Conversely, NO production results in VEGF activity (Papapetropoulos, Garcia-Cardena *et al.*, 1997). Utilising femoral artery ligation, VEGF treatment has led to significant elevations in collateral vessel blood flow, while L-NAME administration diminished the effect (Yang, Yan *et al.*, 2001).

Thus, it appears that VEGF's role in arteriogenesis is dependent on production of NO, which is in part stimulated by VEGF.

1.3.2.3 Vascular Endothelial Growth Factor

1.3.2.3.1 VEGF Receptor Expression is Spatially Specific

The VEGF receptors are named VEGFR1 (Flt-1), VEGFR2 (Flk-1, KDR), and VEGFR3 (Flt-4) (Yancopoulos, Davis *et al.*, 2000); the first two of which bind VEGF-A, one of seven family members: VEGF-A to -F and Placental Growth Factor, PlGF (Siekmann, Covassin *et al.*, 2008; Pipp, Heil *et al.*, 2003; Otrock, Makarem *et al.*, 2007). VEGF-A acts predominantly by binding VEGFR2 (Siekmann, Covassin *et al.*, 2008), and is believed most important for vascular formation, initiating vasculogenesis and angiogenesis (Yancopoulos, Davis *et al.*, 2000). Alternative splicing results in six isoforms of which VEGF-A_{165} primarily mediates VEGF action (Tammela, Enholm *et al.*, 2005). For ease, VEGF-A_{165} is termed VEGF in further discussion. Functions of VEGF-B are undetermined, while VEGF-C and -D are primarily lymphaniogenic (Tammela, Enholm *et al.*, 2005). VEGF-E appears to be a potent angiogenic factor binding VEGFR2, and VEGF-F a VEGF antagonist (Otrock, Makarem *et al.*, 2007). PlGF has been described as 'disease-specific' with redundancy during vascular development and physiology, but inducing pathological angiogenesis (Fischer, Mazzone *et al.*, 2008). This information is summarised in the table below:

Isoform	**Main Role**	**Receptor Interactions**
VEGF-A	primary mediator of action	VEGFR1/R2
VEGF-B	undetermined	VEGFR1
VEGF-C	lymphangiogenic	VEGFR2/R3
VEGF-D	lymphangiogenic	VEGFR2/R3
VEGF-E	angiogenic	VEGFR2
VEGF-F	VEGF antagonist	VEGFR2
PlGF	pathological angiogenesis	VEGFR2

VEGF receptors are generally spatially specific, with expression on ECs alone, although VEGFR1 is also expressed on monocytes/macrophages (Hiratsuka, Minowa *et al.*, 1998). Deficiency of this gene leads to substantially reduced monocyte migration (Hiratsuka, Minowa *et al.*, 1998). VEGF receptors are receptor tyrosine kinases, and as such, ligand-receptor binding leads to receptor dimerisation. Dimerisation results in the autophosphorylation of specific tyrosine residues on the receptor, permitting signalling molecules to bind the phosphorylated tyrosines (Kowanetz and Ferrara, 2006).

1.3.2.3.2 VEGF Modulates Physiological and Pathological Vascular Activity

VEGF has participatory roles in the differentiation and migration of angioblasts (vasculogenesis), angiogenesis, vasodilatation, and vessel permeability. VEGFR2 is the predominant receptor for VEGF binding and intracellular signalling, with autophosphorylation of different tyrosine residues resulting in distinct downstream signalling. Autophosphorylation of VEGFR2 can lead to activation of phospholipase C-γ1 (PLC- γ1), phosphatidylinositol 3-kinase (PI3-K), mitogen activated protein kinase (MAPK) and T-cell-specific adapter molecule (TSAd) (figure 1.7) (Siekmann, Covassin *et al.*, 2008).

Deletion of a single VEGF allele results in lethal vascular abnormalities throughout murine embryos (Carmeliet, Ferreira *et al.*, 1996). Smaller quantities of ECs were observed in the aorta of these animals, further supporting the hypothesis that VEGF is a crucial factor in EC survival, and demonstrating its critical importance in maintenance and development of vasculature.

The predominant means of VEGF upregulation is binding of the HIF-1 α/β heterodimer to its binding site on the VEGF promoter (Forsythe, Jiang *et al.*, 1996), suggesting VEGF upregulation occurs under hypoxic conditions. However, arteriogenesis has been demonstrated to occur independently of hypoxia, which may suggest it is VEGF independent. Collateral vessel development was observed solely in the upper leg of rabbits with femoral artery ligation, an area unaffected by reduced blood flow as demonstrated by flow quantification at set pressure (Ito, Arras *et al.*, 1997).

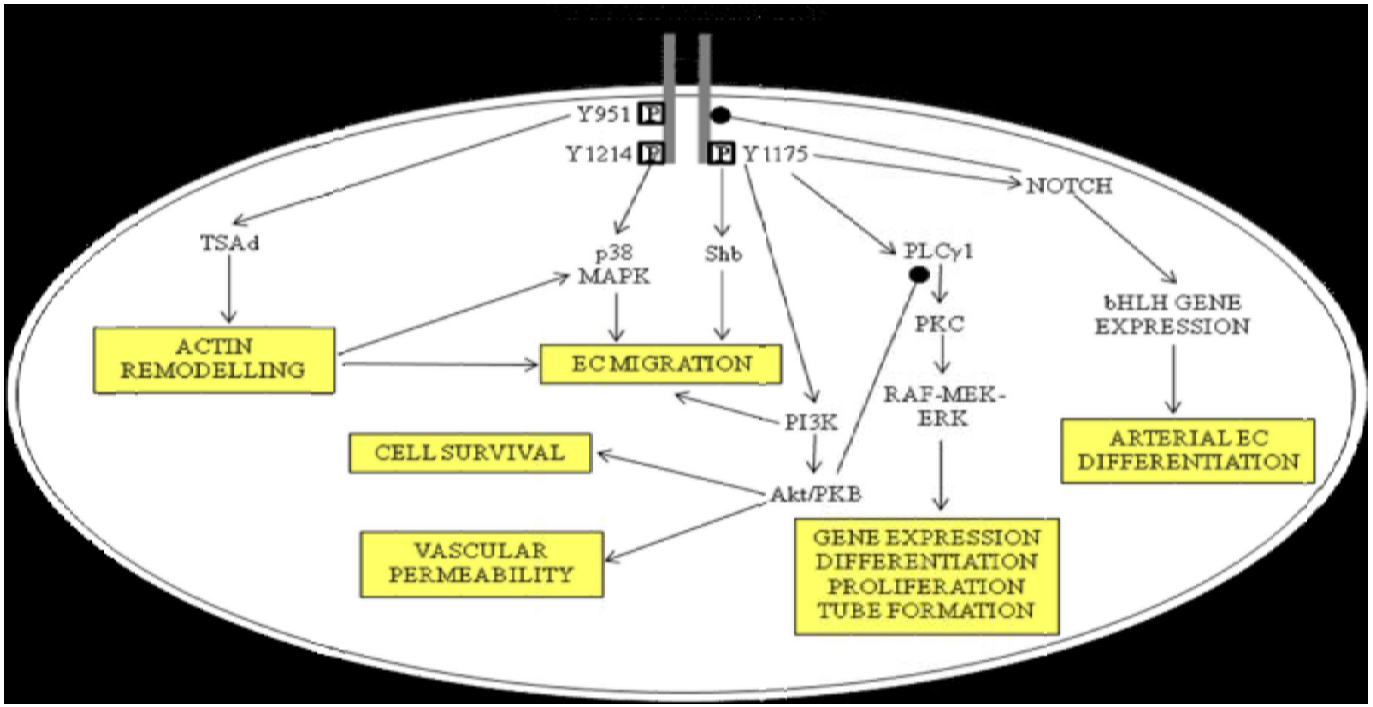

Figure 1.7 Signalling in endothelial cells through VEGF ligand binding to VEGFR2.

VEGFR2 dimerisation and serine/threonine phosphorylation events result in vascular remodelling through activity of numerous signalling pathways, each of which play a critical role in altering vessel physiology. Y951 binds to TSAd, modulating actin remodelling which ultimately affects EC migration, a component of arteriogenesis. Phosphorylation of Y1214 also modulates EC migration but via p38 MAPK. Y1175 leads to PLCγ1 signalling which via PKC and RAF-MEK-ERK results in gene expression, differentiation, proliferation and tube formation of ECs, factors all necessary for arteriogenesis to occur. Phosphorylation of Y1175 also results in activation of PI3K and Akt modulating EC migration and survival, as well as stimulating vascular permeability. Arrows represent activation, while filled circles represent inhibition of pathway components. Adapted from figures 1 and 4 Siekmann, Covassin *et al.*, 2008

No alteration in expression of hypoxia-induced lactate dehydrogenase A or HIF-1α mRNA was determined by Northern blot during collateral vessel development following femoral artery ligation in rabbit (Deindl, Buschmann *et al.*, 2001). Transfection of naked plasmid VEGF in rabbits with femoral artery ligation inducing ischaemia resulted in significant increases in collateral vessel number visualised by angiography (Takeshita, Weir *et al.*, 1996). Furthermore, fibroblasts excised, transfected with adenovirus including VEGF, and injected into the internal iliac artery following femoral artery excision in rabbit resulted in significantly increased numbers of collateral vessels and collateral conductance (Kondoh, Koyama *et al.*, 2004). These data thus demonstrate a role for VEGF in arteriogenesis. However, Deindl, Buschmann *et al.* (2001) determined no alteration in VEGF mRNA expression by Northern blot or VEGF protein by Western blot in growing collateral vessels isolated from non-ischaemic upper leg of rabbits following femoral artery ligation. The authors are clear to distinguish ischaemic from non-ischaemic regions of the hindlimb. Together, the data may suggest that VEGF is upregulated in ischaemic regions in response to hypoxia, but not upregulated in non-ischaemic regions, making VEGF modulation of arteriogenesis dependent on microenvironment.

1.3.3 Cellular Modulation of Arteriogenesis

1.3.3.1 Chemoattraction of Monocytes by MCP-1, GM-CSF, and TGF-β

Monocytes and macrophages are important to arteriogenesis. In rabbits, accumulation of monocytes to collateral vessels was reported from 12 hours post femoral artery ligation, reaching maximum after three days (Heilmann, Beyersdorf *et al.*, 2002). Accumulation correlated with upregulation of adhesion molecules such as ICAM-1 by ECs (Scholz, Ito *et al.*, 2000).

MCP-1 is released from shear activated ECs (Van Royen, Piek *et al.*, 2001b), and is the most potent stimulator of monocyte migration (Heilmann, Beyersdorf *et al.*, 2002). MCP-1 promotes monocyte recruitment to collateral vessels following ligation (van Royen, Hoefer *et al.*, 2003). Collateral conductance increased one week after ligation,

and returned to control levels by six months, suggesting a role for monocytes/macrophages during initiation of arteriogenesis. Collateral vessel density also increases after MCP-1 treatment (Heilmann, Beyersdorf *et al.*, 2002). In human, patients suffering acute myocardial infarction who develop angiographically observable coronary collateral vessels have shown significantly higher plasma MCP-1 levels then patients without collaterals (Park, Chang *et al.*, 2008), suggesting a link between MCP-1 expression and collateral development. This contrasts with previous data obtained from a chronic infarct model in rat which reported no difference in collateral vessel number following single injection of MCP-1 intra-myocardially six weeks post infarction (Schwarz, Meven *et al.*, 2004), and may again suggest a role for monocytes/ macrophages during initiation of arteriogenesis. Disruption of the MCP-1 receptor CCR-2 in mice inhibits nearly all collateral vessel development after ligation (Schaper and Scholz, 2003). Suppression of monocytes by 5-fluorouracil significantly delays arteriogenesis (Heil, Ziegelhoeffer *et al.*, 2002), while antibodies against ICAM-1 abolish MCP-1's effects (Van Royen, Piek *et al.*, 2001b).

GMCSF and TGF-β also increase arteriogenesis, probably via actions on monocytes (Van Royen, Piek *et al.*, 2001b). GMCSF inhibits monocyte/macrophage apoptosis, and TGF-β is believed to enhance monocyte transmigration into vessels and induce expression of growth factors by monocytes/macrophages (Van Royen, Piek *et al.*, 2001b). In addition, CXCR4a, expressed on macrophages, is the receptor for the chemokine SDF1. $CXCR4^{+}$ cells have been observed to induce revascularisation following MI in mice (Jin, Shido *et al.*, 2006; Morimoto, Takahashi *et al.*, 2007).

1.3.3.2 Modulation by Lymphocytes

Immunohistochemistry from experiments performed utilising mice has demonstrated positive lymphocyte staining in *adventitia* of remodelling collateral vessels with antibodies against CD3, CD4, and NK1.1 (van Weel, Toes *et al.*, 2007). Few positively stained cells were observed in non-operated contralateral legs. This data thus suggests a possible role for lymphocytes in modulation of arteriogenesis. In order to determine the subset of lymphocytes modulating arteriogenesis, the group performed antibody

depletion for $CD4^+$ T cells, Natural Killer cells, or control. Natural Killer cells comprise part of the innate immune system, mediating cytotoxicity and secreting inflammatory cytokines. CD4 and Natural Killer cell depletion resulted in significantly reduced collateral vessel formation (van Weel, Toes *et al.*, 2007). However, experiments in rabbits perfused with chemokines for monocytes (MCP-1) and lymphocytes (lymphotactin) following femoral artery ligation demonstrated that only MCP-1 induced a significant arteriogenic response (Hoefer, Grundmann *et al.*, 2005), making a role for lymphocytes in modulation of arteriogenesis unclear.

1.3.3.3 Modulation by Stem and Progenitor Cells

The potential role of stem or progenitor cells in arteriogenesis also remains unclear. Since arteriogenesis describes remodelling of pre-existing vasculature a role for such cells in the initial phases of arteriogenesis may be unlikely, although it is possible stem cells may incorporated into the enlarged smooth muscle layers. Bone marrow from GFP expressing mice has been transplanted into mice previously irradiated (Schaper and Scholz, 2003). Transplantation was followed by femoral artery ligation. No GFP expressing cells were observed within collateral vessels following histology, suggesting such bone marrow derived cells do not play a role in arteriogenesis, although these cells have been identified by specific markers in angiogenesis following artery ligation (Heilmann, Beyersdorf *et al.*, 2002). This hypothesis has been confirmed by similar murine transplantation and femoral artery ligation experiments which found no integration of multipotent adult progenitor cells within remodelling collateral vessels, but did observe improved collateral blood flow and cell integration within the skeletal muscle immediately surrounding remodelling collaterals (Huss, Heil *et al.*, 2004).

1.4 Studying Arteriogenesis in Current Models

1.4.1 Studying Arteriogenesis in Mammalian Models

1.4.1.1 Vascular Surgery

Vascular surgery is difficult and time-consuming. Complications can limit a study's endpoint and subject availability. Furthermore, inflammation resulting from surgery leads to the release of large numbers of non-specific cytokines including TNFα (Baik, Kwak *et al.*, 2008) that may themselves modulate vessel formation. Sham operations of contralateral limbs are an important and effective means of countering such non-specific inflammation and cytokine release.

1.4.1.2 Femoral Artery Ligation is an Acute Model of Arteriogenesis

Femoral artery ligation presents an acute model of mammalian arteriogenesis (Tang, Chang *et al.*, 2005). In contrast, arterial occlusion is a chronic disease spanning many decades. Thus, while results obtained from such experimentation will provide a broad framework of understanding, it may not be capable of unmasking the detailed pathophysiology involved during arteriogenesis.

To mimic arterial occlusion more closely several studies utilised ameroid constrictors ensheathing the femoral artery. Constrictors gradually absorb liquid and swell, causing progressive occlusion (Cai, Vosschulte *et al.*, 2000). Animals with constrictor implantation develop collateral vessels of significantly smaller diameter than animals undergoing femoral artery ligation (Tang, Chang *et al.*, 2005). The observation is perhaps a result of the rapid elevation in FSS in acute occlusion compared to progressive occlusion. While acute occlusion results in a sudden pressure gradient pre- to post occlusion which induces luminal enlargement to restore blood flow, gradual occlusion with constrictors may permit muscle to accommodate for decreases in blood flow through alteration of fibre type and energy metabolism (McGuigan, Bronks *et al.*, 2001), thereby reducing requirement for vessels of larger diameter. The longer timescale of gradual occlusion may permit collateral vessels to develop more fully, without significant levels of inflammation (Tang, Chang *et al.*, 2005).

1.4.1.3 Identification of Collateral Vessels in Mammals

The principle method for observing collateral vessels after arterial ligation is X-ray angiography (Babiak, Schumm *et al.*, 2004; Deindl, Buschmann *et al.*, 2001; Pipp, Boehm *et al.*, 2004). Collateral vessel remodelling cannot be observed serially or *in vivo*, and is dependent upon observation at a single endpoint *post mortem*. Furthermore, X-ray angiography allows visualisation of collateral vessels with a luminal diameter greater than 100μm, while collateral vessels are often of smaller luminal diameter (Mills, Fischer *et al.*, 2000). Magnetic resonance imaging (MRI) has been utilised to determine blood flow *in vivo*, and is non-invasive (Wagner, Helisch *et al.*, 2004). However, resolution is limited to approximately 100μm (Heil, Ziegelhoeffer *et al.*, 2004). Microcomputed tomography (microCT) permits three-dimensional observation of collateral vessels, and has a resolution of approximately 10μm, but like angiography occurs *post mortem* at a single timepoint (Duvall, Robert Taylor *et al.*, 2004).

1.4.2 Studying the Influence of FSS on Gene Expression Profiles by Cell Culture

Since different research groups perform cell culture assays and microarray analyses with different materials, cell populations, and methods, it becomes difficult to compare results and fully interpret collective significance. For instance, some groups performed experiments with mean FSS of around 12dyn/cm^2 (Himburg, Dowd *et al.*, 2007), while others have used double that value (McCormick, Eskin *et al.*, 2001). It is important to note that alterations in EC gene expression are observed *in vitro* with FSS of less than 1dyn/cm^2 (Hove, Koster *et al.*, 2003), and it is possible that ECs respond to varying FSS levels differently, making comparison of data obtained with different FSS levels difficult. In microarrays designed to examine the role of FSS on ECs *Jagged1* expression has been identified as upregulated with FSS of 25dyn/cm^2 (McCormick, Eskin *et al.*, 2001) and downregulated with FSS of 12dyn/cm^2 (Chen, Li *et al.*, 2001). Another important point to note is that these experiments were performed *in vitro* utilising culture assays. Cultured cells generally reside in an environment over a period of days, while ECs can reside in microenvironments for many months. This difference might translate to incomplete or deceptive mimicry of *in vivo* conditions (Staton, Lewis *et al.*, 2006). Additionally, *in vitro* systems are based primarily on single monolayers of

cells. *In vivo* cells undergo wide-ranging interactions, including with different cell populations. These issues are discussed in more detail in Chapter 4.

1.5 Utilisation of Zebrafish in Cardiovascular Research

Mammalian model organisms can suffer several innate disadvantages and limitations to their utilisation in studying cardiovascular development and pathology (section 1.4). Exploitation of novel model organisms that do not share these disadvantages, such as zebrafish, may permit alternative techniques that do not suffer the same limitations. The zebrafish (*Danio rerio*) is a freshwater tropical teleost belonging to the Cyprinidae (minnow) family. Adults reach a length of approximately 4cm (Froese & Pauly, 24/01/08). Zebrafish were first utilised as a developmental model by researchers including George Streisinger. Their potential importance as a novel model organism was demonstrated by two large scale mutagenesis screens (Boston and Tuebingen) during the 1990s. The AB wildtype line is the primary line utilised in generation of transgenic and mutant embryos from the Zebrafish International Resource Centre. The line was generated by crossing lines A and B purchased by Streisinger from pet shops. The line is maintained through screening for healthy haploid offspring from individual females and crossing them to males (Jason Cockington, University of Adelaide, Australia).

1.5.1 Advantages of Utilising Embryonic Zebrafish

1.5.1.1 Care and Breeding

In contrast to other commonly utilised non-mammalian model organisms (*Caenorhabditis elegans, Drosophila melanogaster,* yeasts) the zebrafish is a vertebrate, and therefore has closer evolutionary ties to mammalian species.

The small size of adult zebrafish enables large numbers to be reared in relatively small spaces, providing high density populations. Small size means zebrafish are also economically more viable. An adult zebrafish costs six pence per week to care for, compared to 105 pence per mouse (personal communication, Dr. S Francis).

While murine litter size ranges from 6-12, zebrafish have a prodigious fecundity with single pairs capable of producing hundreds of offspring, allowing more rapid turnover of experiments. In addition, embryos are age-matched to each other, and pairing can occur at regular intervals of 7-14 days.

1.5.1.2 Development

Development of zebrafish embryos is rapid compared to mammalian models, achieving development from one cell to a recognisable body plan within 24hpf (figure 1.8) at standard incubation temperatures of 28 degrees Celsius (Westerfield, 2000; Kimmel, Ballard *et al.*, 1995). Embryos undergo fertilisation and development externally of the adult. This permits observation of development *in vivo* without surgical intervention. In contrast, mammals develop internally and are maternally dependent for exchange of nutrients and waste products.

Embryos develop with an optical clarity unrivalled by other vertebrate models. Embryos are almost fully transparent between fertilisation and 3dpf (Isogai, Horiguchi *et al.*, 2001). With onset of pigmentation, the majority of the embryo is still easily observable with simple light microscopy. In addition, embryos can be chemically treated or genetically manipulated to inhibit pigmentation (Westerfield, 2000).

1.5.1.3 Genetic and Pharmacological Manipulation of Embryos

Another benefit is the ease of administering small non-peptide molecules. Many commonly used compounds, including the anaesthetic tricaine, readily diffuse into embryos (Chico, Ingham *et al.*, 2008). This obviates the need for gaseous or intravenous drug administration.

A number of techniques have been developed taking advantage of the ease of genetic manipulation in zebrafish embryos. Morpholino antisense oligonucleotides (MOs) are frequently used to knockdown genes of interest. MOs are short 25 base-pair nucleotides synthesised with a morpholine rather than ribose backbone (Summerton and Weller, 1997).

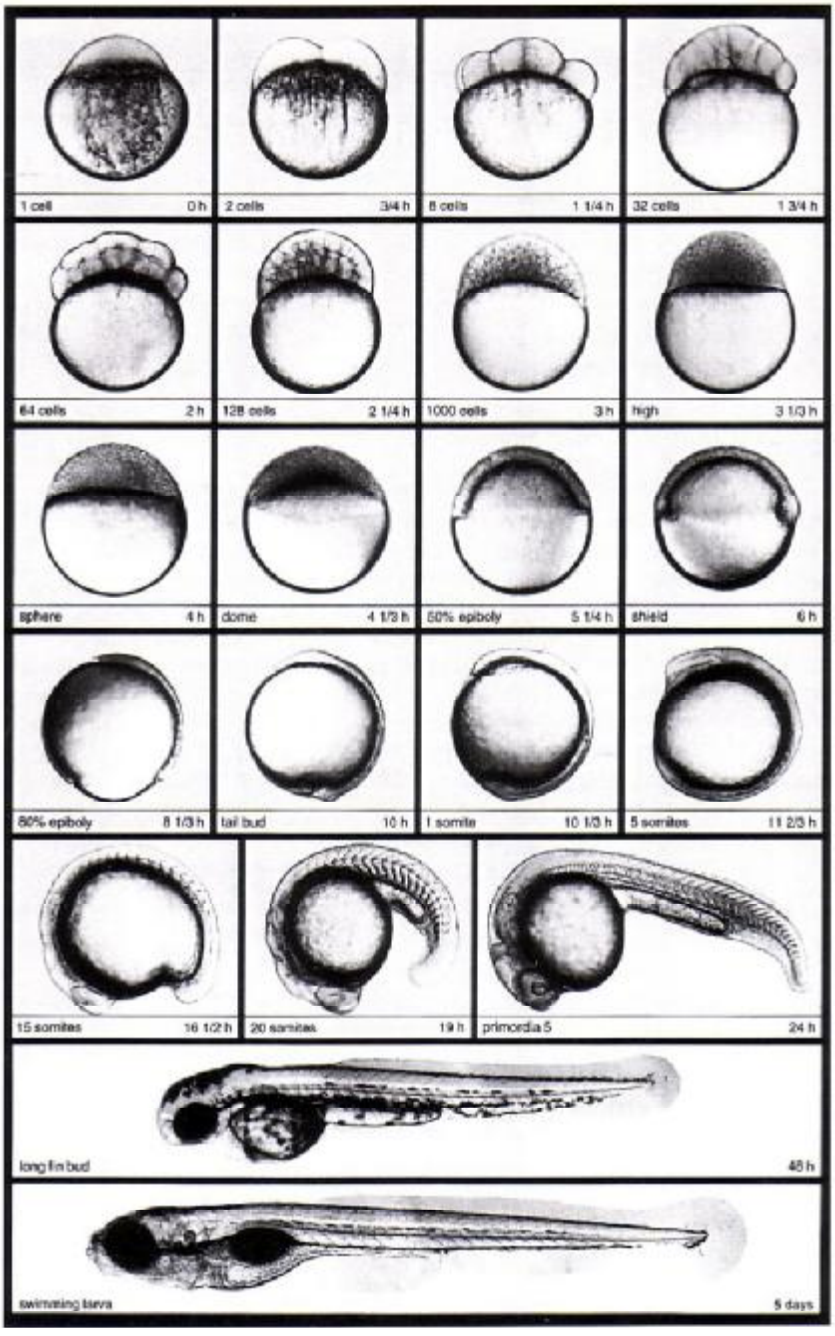

Figure 1.8 Differential Interference Contrast (DIC) images of live zebrafish embryos during the first five days of development.

The time in hours is given when embryos are incubated at 28.5°C. Embryos develop from a single cell to a recognisable body plan in 24 hours at standard conditions, allowing research a faster turnover time than may be possible with mammalian models. From Zebrafish A Practical Approach, Editors Christiane Nüsslein-Volhard and Ralf Dahm, Oxford, 2002.

The basic MO structure can be found in figure 1.9. MOs act via steric block to prevent translation of mRNA to peptide at the ribosome, and are complementary to a specific sequence in the mRNA. MOs are designed to act as either start-site blockers (generally binding to the transcript immediate 5' to the start codon) fully preventing translation, or splice-site blockers, resulting in modification of pre-mRNA splicing to knockdown a gene's functional sequence (Summerton, 2007).

Generation of stable germline transgenic lines (Motoike, Loughna *et al.*, 2000) permits non-invasive high-resolution *in vivo* time-lapse microscopy (Lawson and Weinstein, 2002). Promoters, such as transcription factors, drive fluorescent protein production (Peters, Rao *et al.*, 1995) that allows easy observation under ultraviolet light of cells in which promoter is present. For example, several lines have been generated which produce enhanced green fluorescent protein (eGFP) in vasculature. *Fli1* encodes a transcription factor expressed in cells of presumptive haemangioblast lineage, as well as cranial neural crest and a subset of myeloid cells (Lawson and Weinstein, 2002), permitting vascular visualisation although *fli1* is not vascular-specific (figure 1.10). A *flk1* (VEGFR2) transgenic line has also been generated, with eGFP expression specific to vasculature (Jin, Beis *et al.*, 2005). The flk1:eGFP line has been crossed with putative mutants demonstrating reduced blood flow in order to aid detailed examination of ECs *in vivo* (Jin, Herzog et al., 2007).

Generation of point mutations in spermatogonia of adult zebrafish by ethyl-nitrosourea (ENU) has been used to generate offspring heterozygotic, and through interbreeding homozygotic, for mutations (Haffter, Granato *et al.*, 1996; Driever, Solnica-Krezel *et al.*, 1996). Over 50 mutants have been described which affect the cardiovascular system (Chen, Haffter *et al.*, 1996). Their existence permits improved understanding of various aspects of cardiology and vascular biology including primary vessel formation (*gridlock*) (Weinstein, Stemple *et al.*, 1995), cardiac contraction (*silent heart*) (Sehnert, Huq *et al.*, 2002), heart rate (*slow mo*) (Baker, Warren *et al.*, 1997) and heart rhythm (*breakdance*) (Langheinrich, Vacun *et al.*, 2003).

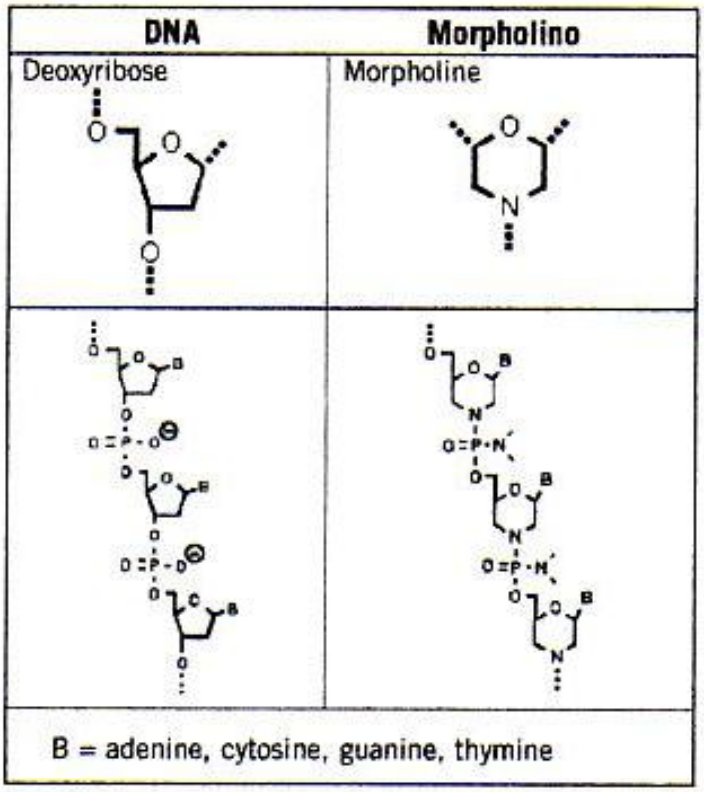

Figure 1.9 Comparison of DNA and morpholino antisense oligonucleotide (MO) structure.

The MO is constructed utilising a morpholine backbone, rather than the deoxyribose ring found in DNA. MOs are constructed utilising standard DNA bases (B) of adenine, cytosine, guanine, and thymine. Non-ionic phosphorodiamidate bonds bind each ring-based subunit. In nucleic acids, anionic phosphodiester bonds bind subunits. From Summerton, 2005.

Many of the genes responsible for zebrafish mutations are homologous or likely homologous to human genes causing diseases with similar characteristics or phenotypes (Warren and Fishman, 1998), which thereby allows study of human disease in a model with numerous other advantages.

1.5.2 Advantages of Utilising Embryonic Zebrafish in Cardiovascular Research

In addition to the advantages already discussed (section 1.5.1) in utilising zebrafish embryos as a model organism, there are many factors which make embryonic zebrafish advantageous to cardiovascular research. In 2001 Unger reviewed mammalian models and recent experimental approaches to studying collateral vessel development. In summary, Unger highlights model characteristics most advantageous to studying collateral vessel development. Unger points out that since arteriogenesis is a dynamic process, serial endpoints are most advantageous. Although serial endpoints are often not possible in mammalian models due to the techniques utilised to determine collateral vessel density, serial observation is possible in zebrafish embryos (Lawson and Weinstein, 2002). Unger also suggests animals small in size, easily maintained, and easily manipulated for experimentation (Unger, 2001). Zebrafish embryos can come close to matching these suggestions, while many mammals fail to do so.

1.5.2.1 The Embryonic Cardiovascular System

Unlike all mammalian species, there is no requirement for a functioning cardiovascular system during the first days of development in zebrafish, since oxygen demand is met through diffusion (Pelster and Burggren, 1996). This permits study of cardiac contraction, and the effect of environments free from haemodynamic force *in vivo*. It allows occlusion of major vessels within embryos providing insights into thrombosis (Thattaliyath, Cykowski *et al.*, 2005), and recovery of blood flow (Gray, Packham *et al.*, 2007).

The early function of the cardiovascular system is similar in zebrafish and mammalian embryos. For instance, increases in cardiac output, stroke volume and blood pressure, and a decrease in vascular resistance parallel development in mammals and zebrafish (Schwerte and Fritsche, 2003). Tissue oxygenation by simple diffusion during the first

days of development (Pelster and Burggren, 1996) permits study of the cardiovascular system without hypoxia, and in a way impossible in mammals.

At the heart-tube stage of development the heart of zebrafish is so highly conserved as to largely resemble that of human embryos (Fishman and Chien, 1997). In comparison, *C. elegans* has no heart; and the contractile dorsal vessel of *Drosophila* pumps a hemolymph directly to tissues at low pressure (Isogai, Horiguchi *et al.*, 2001); thus having little similarity to the mammalian cardiovascular system. Both early blood cell and early vascular development are conserved between vertebrates including zebrafish, which present with only minor modifications to a standard pattern of vascular development (Isogai, Horiguchi *et al.*, 2001), making zebrafish embryos an ideal model system through integrating simplicity with conservation.

Optical transparency of zebrafish embryos makes the heart and vasculature easily accessible for study, permitting observation with light microscopy (Bagatto and Burggren, 2006). It therefore also permits utilisation of techniques dependent upon light microscopy. Digital motion analysis (DMA; section 2.5.2) utilises movie files obtained with light microscopy to visualise blood circulatory paths (Schwerte and Pelster, 2000), and obviates the need for transgenic lines or costly equipment. However, since DMA is dependent upon motion between movie frames, interference can occur from physiological processes such as intestinal peristalsis even under anaesthesia. In addition, DMA only identifies blood vessels in which blood circulates.

1.5.3 Disadvantages of Utilising Embryonic Zebrafish

Though vertebrate, the zebrafish is a non-mammalian species, implying physiology and pathology to be more evolutionarily distant from human than mice, the most commonly utilised model organism. Although genes between zebrafish and human are often homologous, phenotypic characteristics of diseases caused by homologous genes in the two species can be very different (Weinstein, Stemple *et al.*, 1995; Gessler, Knobeloch *et al.*, 2002) making extrapolation from zebrafish to human difficult without recourse to mammalian models. Furthermore, following divergence from land vertebrates, the fish genome underwent partial duplication (Postlethwait, 2007). Zebrafish thus possess two

copies of many mammalian genes, making extrapolation of single gene manipulation in zebrafish to mammals difficult. It is therefore possible that zebrafish and their embryos may not reflect human processes such as arteriogenesis.

As a relatively novel model organism there remains a requirement for reagents, particularly antibodies suitable for immunohistochemical staining common in other model organisms.

1.5.4 Vasculature of Zebrafish Embryos

Despite divergent evolutionary paths, zebrafish and mammals share a basic pattern of myocardial and vascular development (Fishman and Chien, 1997). It is for this reason, and the advantages described above, that the zebrafish embryo is utilised in cardiovascular research. This section describes the development of the embryonic vascular system, laying down the foundation for understanding results obtained utilising zebrafish embryos to study arteriogenesis.

1.5.4.1 Formation of Vasculature Occurs through Vasculogenesis

The cardiovascular system begins functioning at approximately 24 hours post fertilisation (hpf), with the onset of cardiac contraction and lumenisation of major vessels (Chen, Haffter *et al.*, 1996). The circulation follows a single circulatory loop rather than the double loop observable in mammalian species. Circulation is brisk within head and trunk by 36hpf (Schwerte and Fritsche, 2003).

Embryonic vasculature, and hence circulation, begins as a simple loop (figure 1.10A) with blood exiting the heart through the *bulbus arteriosus* to the ventral aorta which divides into the aortic arches found on either side of the jaw. Blood then enters the paired lateral dorsal aortae before the vessels fuse to form the dorsal aorta (Weinstein, Stemple *et al.*, 1995). The dorsal aorta transports blood to trunk and tail, having its nomenclature altered to caudal artery distal to the urogenital opening (Isogai, Horiguchi *et al.*, 2001).

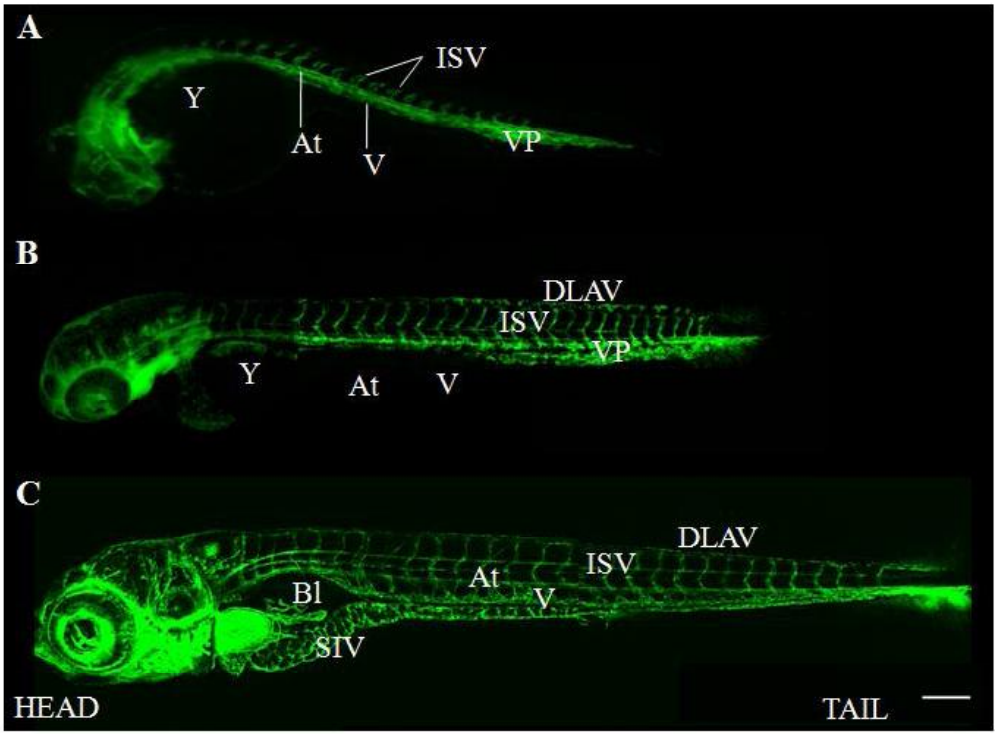

Figure 1.10 Development of the Embryonic Zebrafish Vasculature from 1-5dpf.

Lateral views of laser-scanning confocal microscopy images of fli1:eGFP transgenic embryos. The embryonic vasculature begins at 1dpf as a simple loop of aorta and cardinal vein transporting blood away from and back to the heart respectively (A). By 2dpf (B) the ISV are fully formed. At 5dpf, the embryo has developed a more mature vasculature that includes a complex subintestinal vasculature (C). At=aorta, V=cardinal vein, ISV=intersegmental vessels, SIV=subintestinal vessels, VP=venous plexus, DLAV=dorsal longitudinal anastomotic vessels, Bl=swim bladder. Each sub-figure composite of 4 images. See Chapter 2 for detailed methodology describing how I generated these images. Scale bar 200μm.

Blood is transported back towards the heart through the caudal vein, which at onset of circulation is formed of a plexus of vessels that remodel to a single vessel by approximately 3dpf (figure 1.10). Anterior to the plexus the vein is termed the cardinal vein. Close to the aortic bifurcation the cardinal vein divides, emptying into the duct of Cuvier or the common cardinal vein which cross the yolk sac replenishing the heart (Isogai, Horiguchi *et al.*, 2001).

1.5.4.2 Intersegmental Vessel Formation

At about the same time as cardiac contraction initiates, pairs of endothelial sprouts emerge from the dorsal aorta close to boundaries dividing the somites that make up the notochord. The sprouts extend between somites by extension and retraction of filopodia, mostly at the dorsal leading edge. By 28hpf, EC strands reach the roof of the neural tube and branch caudally and rostrally (Isogai, Lawson *et al.*, 2003). Anastomosing vessels fuse the EC strands to form two dorsal longitudinal anastomotic vessels (DLAVs). Each sprout forms an intersegmental vessel; paired at each somitic boundary.

Sprouts form from three ECs, with the first remaining within the aorta ventrally, sending a process out into the somatic boundary (Childs, Chen *et al.*, 2002). A second cell echoes this role but from the developing DLAVs (having originally migrated from the aorta). One or more cells then form a link between the first and second (Childs, Chen *et al.*, 2002). The cells do not appear to line up head to tail. All three appear to enclose the lumen on formation, suggesting a more complex development than originally envisaged (Blum, Belting *et al.*, 2008). By 2dpf the ISV are patent with an active circulation (Isogai, Horiguchi *et al.*, 2001).

1.5.4.3 Formation of Intestinal Vasculature

At 2dpf blood vessels that will supply the digestive system, the supraintestinal artery and subintestinal veins, begin developing. The supraintestinal artery is a continuation of the mesenteric artery, which branches from the dorsal aorta close to the kidneys. At this time, the subintestinal veins drain directly into the cardinal vein. By 3dpf the

subintestinal vein has begun to undergo angiogenesis broadening the intestinal vasculature (Isogai, Horiguchi *et al.*, 2001).

1.6 Concluding Remarks

The aim of this general introduction was to describe to date research performed with regard to arteriogenesis and factors which modulate its mechanism. Since the research was almost fully dependent upon mammalian models, I have described the development and physiology of mammalian vasculature. I have also described the development and physiology of zebrafish vasculature during embryonic phases (1-5dpf) to place the zebrafish embryo as a model within the context of cardiovascular research. Previous experimentation specifically related to my research is found in introductions to each results chapter (Chapters 3, 4, 5, and 6).

1.7 Project Aims and Objectives

From the evidence in this introduction I hypothesise that:

- zebrafish embryos can be exploited to generate a novel, non-mammalian model of collateral vessel development (arteriogenesis)
- collateral vessel development in zebrafish embryos will share some level of conservation with arteriogenesis observed in mammalian species
- zebrafish embryos can be exploited to determine the role of genes with differential expression in absent haemodynamic force.

The objectives of my research are therefore to:

- determine whether zebrafish embryos can undergo collateral vessel formation (arteriogenesis) after arterial occlusion

- determine the role of nitric oxide in collateral vessel development in order to determine whether conservation between zebrafish embryos and mammalian species occurs
- perform microarray analysis on genetically manipulated embryos without haemodynamic force to determine differential gene expression *in vivo*
- exploit the zebrafish embryo to determine the role of genes differentially expressed without haemodynamic force in modulating arteriogenesis in zebrafish embryos.

Chapter Two

Materials and Methods

Chapter 2: Materials and Methods

2.1 Chemical Acquisition

All chemicals were acquired from Sigma (Poole, UK) unless otherwise stated.

2.2 Recipes

2.2.1 E3 medium

10L of 10x stock was made with 28.7g 5mM NaCl, 1.27g 0.17mM KCl, 4.8g 0.33mM $CaCl_2$, 8.17g 0.33mM $MgSO_4$, and kept at rtp. A 1x working solution was made by diluting stock with dH_2O, and adding 3 drops of 0.01% Methylene Blue fungicide. The 1x solution was kept at 28.0°C (Nüsslein-Volhard & Dahm, 2002).

2.2.2 MS-222 (Tricaine)

Stock solution was made by combining 400mg MS-222 powder, 97.9ml dH_20, and 2.1ml 1M Tris (pH 9). pH was adjusted to 7 (Westerfield, 2000). A working dose of 50mg/l was utilised.

2.2.3 Low Melt-Point Agarose

1% low melt-point agarose was made up using E3 media, and heated until dissolved. 50mg/l MS-222 was added to ensure continued anaesthetisation of embryos. Prepared agarose was kept at 37°C to maintain liquidity.

2.2.4 Phosphate-Buffered Saline

1 Phosphate-Buffered Saline (PBS, Sigma) tablet was fully dissolved in 200ml milliQ H_2O and autoclaved to ensure sterility.

2.2.5 PBST

1x PBS + 0.1% Tween-20.

2.3 Zebrafish Husbandry

2.3.1 Home Office Regulation

All studies conformed to Home Office requirements for the use of animals in scientific research and were performed in accordance with project licence number 40/3031 issued to Dr TJA Chico.

2.3.2 Aquaria Light Cycle

The aquaria follow a 14:10 hour light:dark cycle.

2.3.3 Embryo Collection

Embryos were collected from adult tanks using a breeding trap that prevents adults from ingesting embryos by the presence of a physical mesh barrier. Embryos were sorted into groups of 40 fertilised offspring and placed in Petri dishes containing fresh E3 medium. Embryos were incubated at 28.0°C up to a maximum of 5.2dpf at which point they were destroyed using bleach.

2.3.4 Zebrafish Strains and Lines Utilised

2.3.4.1 Wildtype Strains

AB strain embryos were utilised throughout for experiments requiring wildtype embryos.

2.3.4.2 Transgenic Lines

The fli1:eGFP transgenic line expressing endothelial GFP was obtained from the Zebrafish International Resource Centre (University of Oregon, Eugene, Oregon, USA). Gata1:dsRED transgenic embryos expressing dsRED in erythrocytes were a gift of Dr. Leonard Zon (Howard Hughes Medical Institute, Maryland, USA). Fli1:eGFP and gata1:dsRED lines were crossed to produce fli1:eGFP/gata1:dsRED embryos. These fish

were crossed with *nacre* to produce the line in a pigment-free background. Homozygous *nacre* embryos lack melanophores due to a single base mutation in a gene homologous to the mammalian protein microphthalmia-associated transcription factor (Lister, Robertson *et al.*, 1999).

2.3.4.3 Mutant Strains

Homozygous *gridlock* mutants were a gift of Dr. Randall Peterson (MIT, Massachusetts, USA). Mutants were crossed with the fli1:eGFP transgenic line to produce *gridlocks* expressing GFP within endothelial cells (*gridlock*/fli1:eGFP).

2.4 Preparation of Embryos for Microscopy

2.4.1 Embryo Dechorionation

Embryos naturally hatch from their chorion at approximately 2.5dpf at 28.0°C. If required before this timepoint, embryos were manually dechorionated using Dumont #4 tweezers (WPI, Florida, USA).

2.4.2 Slide Preparation

Standard glass microscopy slides (25x75x10mm) were covered with 10 layers of insulating tape, and a chamber of approximately 25mm^2 excised from the centre using a scalpel.

2.4.3 Mounting Live Embryos

Embryos were first anaesthetised with 50mg/l MS-222 and then immobilised in 1% low-melt-point agarose with added MS-222 on a number 1.5 cover-slip. Embryos were positioned laterally with an inverted orientation to that finally desired for viewing, using a one-hair brush which permits orientation without injuring embryos. E3 with added MS-222 was used to fill the slide chamber. The cover-slip was positioned to fully cover the chamber, with the mounted embryo inside the chamber.

2.5 Light Microscopy

2.5.1 Inducing Mechanical Aortic Occlusion

2.5.1.1 Laser-induced Aortic Occlusion

4/5dpf wildtype AB or fli1:eGFP/gata1:dsRED embryos with/without chemical incubation as discussed were mounted as described (section 2.4.3). A pulsed UV air-cooled Micropoint nitrogen 337nm laser (VSL-337ND-S Spectra-Physics, California, USA) mounted on a Zeiss Axiophot 2 microscope was used to injure (Serluca and Fishman, 2001) and occlude the proximal/mid aorta by endothelial damage and subsequent clot formation. The procedure was repeated 3 hours post occlusion, at the same site, to maintain occlusion.

2.5.1.2 Observation of Laser-induced Aortic Occlusion Embryos

Following occlusion, embryos were serially observed by stereomicroscopy at 3 and 5h, then every 5h for 22-24 hours.

2.5.2 Digital Motion Analysis

Digital Motion Analysis (DMA) is a technique developed to visualise blood circulatory paths using video technology (Schwerte and Pelster, 2000) but I and others in Dr Chico's lab adapted this for use with digital recording apparatus. DMA provides a means of visually demonstrating paths taken by moving cells, such as erythrocytes through a vessel, without the need for transgenic animals or specialised equipment. However, since DMA is dependent upon motion, interference can occur from physiological processes such as intestinal peristalsis even with anaesthesia.

2.5.2.1 DMA Procedure

Each frame of a movie file is composed of pixels. Each pixel is denoted a greyscale value of 0 (black) to 255 (white), which alters from frame to frame. While the greyscale

value of non-altering pixels between two frames remains constant, the greyscale value of pixels in areas of the frame undergoing movement change.

Two consecutive frames were subtracted from one another utilising ImageJ software for the length of the movie file, so that each pixel making up a frame is subtracted from its counterpart pixel in the following frame. The result was a trace image of pixels that had altered in greyscale value between one frame and the next. Trace images were assigned colour through ImageJ lookup tables. ImageJ (Rasband) is a free to download Java based programme designed for analysis of image-based results.

2.5.3 Determination of Aortic Blood Velocity

To date, it has been difficult to determine haemodynamic parameters such as aortic blood velocity in zebrafish embryos. Their small size prevents the use of techniques, such as Doppler ultrasound, commonly performed in mammalian models. I developed a means of determining aortic blood velocity using light microscopy. In conjunction with bespoke software designed in collaboration with Scott Reeves (Cardiovascular Science, Medical School, Royal Hallamshire Hospital), the technique permitted rapid assessment of aortic velocity, allowing determination of erythrocyte acceleration during systole and deceleration during diastole (figure 2.1). During the course of the work, a similar technique was independently published by another group (Malone, Sciaky ***et al.***, 2007).

2.5.3.1 Recording Regions of Interest for Determination of Aortic Blood Velocity

1s of footage at 500 frames/s was recorded at three areas of the aorta, proximally at the highest point of the yolk-sac (ISV 6-8), at a midpoint (ISV 14-16), and distally (ISV 27-29) at 10x magnification using a high-speed camera (A504k, Basler, Germany) mounted on an Olympus IX81 inverted miscroscope (Hertfordshire, UK) and Video Savant software (Version 4.0, IO Industries, Ontario, Canada). Next, a Region of Interest (ROI) the length of the 3 ISV and of 1 pixel depth in the x dimension was created. Figure 2.2 demonstrates the position of the ROI within the aorta proximally. The data from the ROI was exported as a single .TIF file.

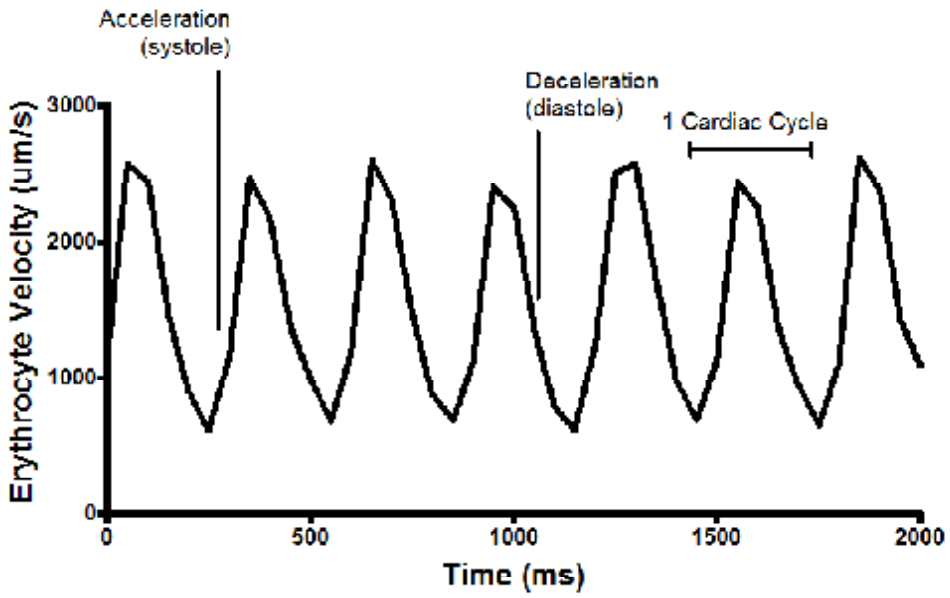

Figure 2.1 Determination of mean aortic velocity.
Measurements for aortic blood velocity were taken from the proximal aorta of a 5dpf wildtype embryo. A recording time of 2000ms provides information on a number of cardiac cycles, permitting data such as mean aortic velocity, acceleration, and deceleration to be calculated.

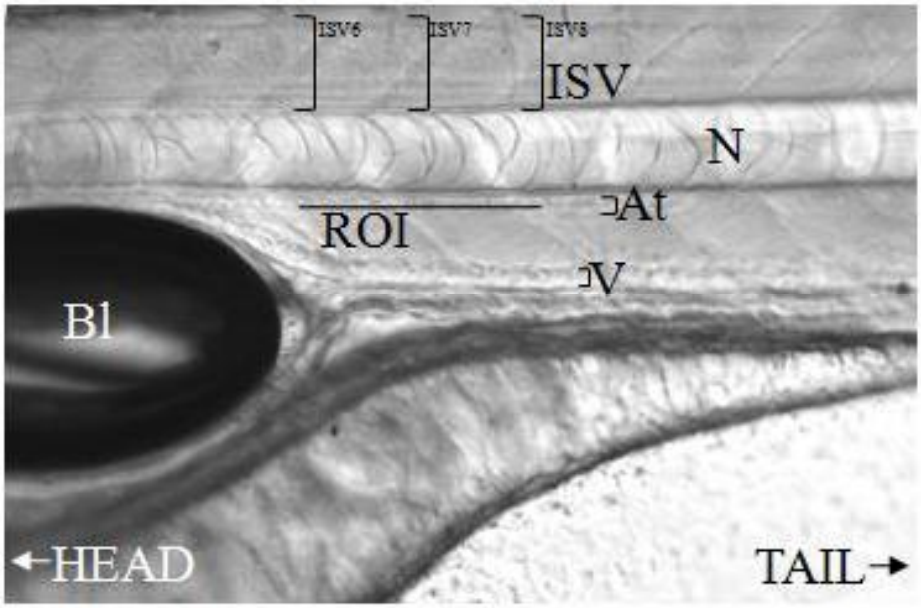

Figure 2.2 Position of the region of interest within the proximal aorta for measurement of aortic blood velocity.
An ROI of approximately 3 ISVs in length is positioned medially within the aorta. 1s of footage at 500 frames/s provides data on approximately 5 cardiac cycles. At=aorta, V=cardinal vein, ISV=intersegmental vessel, ROI=region of interest, Bl=swim bladder, N=notochord.

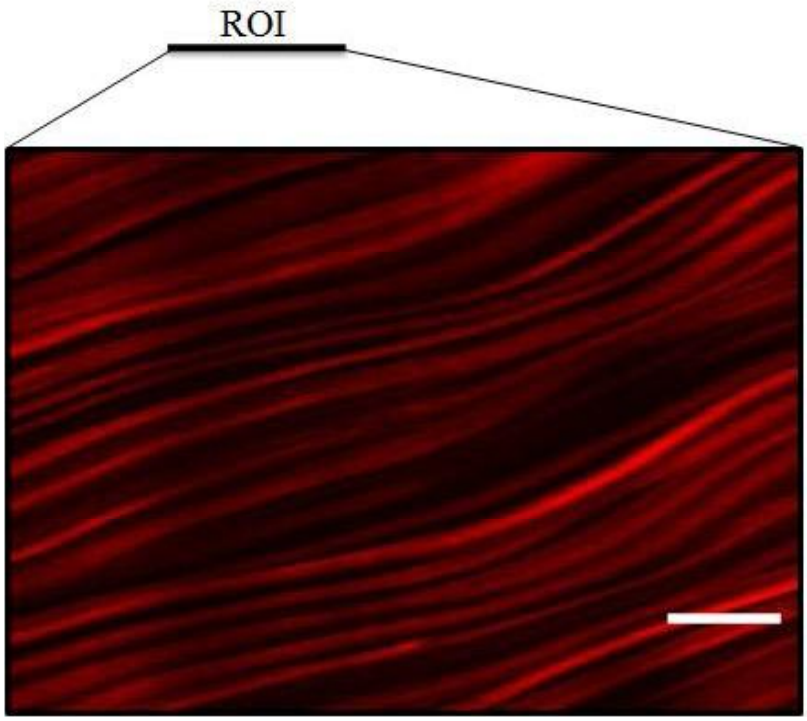

Figure 2.3 False-colour kymograph generated from video savant footage.
Repeated recording of the ROI permits generation of a kymograph demonstrating the movement of erythrocytes along the ROI (horizontal dimension) over time (vertical dimension). By determining an erythrocytes movement over time, velocity can be calculated. Each "streak" represents a single erythrocyte. Scale bar 200μm.

2.5.3.2 Bespoke Software Determines Aortic Blood Velocity Automatically

Bespoke software (Correlator v0.1-0.9 Scott Reeves, Cardiovascular Science, Medical School, Royal Hallamshire Hospital) was utilised to automate analysis. The software calculates movement of cells (in this case erythrocytes) using a routine of pattern matching (cross correlation). A ROI from a first time-step of a kymograph (figure 2.3) is compared with the ROI from a second time-step, and the best match identified.

The distance the ROI travels to identify the best match represents the distance travelled by the erythrocytes. The process is repeated for the same time-step with more ROI spread horizontally across the kymograph, and a mean value for ROI travel calculated for that time-step. The process is then repeated between subsequent time-steps and the mean erythrocyte velocity calculated by dividing by the size of the time-step.

2.5.3.3 Frame-frame Cell Tracking

In order to validate the automation software, individual erythrocytes from Video Savant recordings were tracked with ImageJ Manual Tracker plugin for approximately 100ms using the full 500 frames of movie file recorded. 15 erythrocytes were tracked per section of aorta.

2.6 Confocal Microscopy

Fli1:eGFP/gata1:dsRED double transgenic embryos in wildtype or *nacre* background were imaged using sequential scanning with a 10x or 20x objective on an Olympus FV-1000 laser-scanning confocal microscope using FV-10 ASW software (version 1.4). Analysis was performed using ImageJ software (Rasband). To produce Z stacks, slices of no more than 2μm were recorded for the full thickness of the ROI.

2.7 Preparation of Total RNA and cDNA

One of two protocols was utilised in extracting total RNA. All extractions associated with the microarray and its validation were performed using the Trizol method (section 2.7.2) followed by RNA clean-up (section 2.7.3). The Trizol method permits intervals

and storage at several steps without affecting purity, permitting multiple samples and timepoints to be extracted together limiting operator variability.

Other extractions were performed following the protocol of Nucleospin RNA II (section 2.7.4). Nucleospin RNA II is time-efficient, with extraction lasting no more than 1h. It does not require toxic compounds such as phenol/chloroform, and produces RNA of similar purity to the Trizol protocol.

2.7.1 Handling and Storage

To prevent degradation of RNA, extraction was performed on ice (4°C) and protective equipment worn throughout. On completion, RNA was immediately stored at -80°C.

2.7.2 Extraction of total RNA Utilising Trizol

Groups of embryos were transferred to 1.5ml tubes and all media removed. 200µl Tri reagent (Trizol) was added, and embryos roughly homogenised using a disposable pellet pestle (Sigma). Homogenate was passed through a 25G needle by syringe action (Becton Dickinson (BD), Oxford, UK) 5 times and a further 300µl Tri reagent added. 100µl phenol/chloroform was added to the sample and vortexed before centrifugation at 13,000rpm for 15min at 4°C. An interval can be taken at this point, storing the sample at 4°C. The colourless upper phase of the sample was transferred into an RNase free 1.5ml tube, and 250µl isopropanol added. The sample-isopropanol mixture was vortexed and incubated for 2 hours at -80°C. A longer interval can be taken at this point.

Having stood for 10min to fully defrost the sample, the sample was centrifuged at 13,000rpm for 20min to form a pellet. The liquid was removed, and 500µl 75% ethanol added before further vortexing to resuspend the pellet. The sample was then centrifuged at 8,000rpm for 15min. The ethanol was removed, and the pellet allowed to air dry for 5min. The pellet was resuspended in 100µl sH_2O, placed on a hot block at 55°C for 20min being pipetted up and down several times throughout.

2.7.3 Cleanup of total RNA

RNA cleanup followed the protocol of the Qiagen RNeasy Mini Handbook (fourth edition, April 2006). Briefly, RNA obtained in section 2.7.2 was applied to an RNeasy column and centrifuged for 15s at 8000rpm. Following transfer of the column to a new RNase free collection tube 500µl RPE buffer was pipetted onto the column, which was then centrifuged for 15s at 8000rpm. This step was repeated, discarding flow-through. Columns were transferred to new RNase free collection tubes and centrifuged for 60s at 15000rpm. Columns were transferred to RNase free 1.5ml tubes. 40µl of sH_2O was pipetted directly onto the filter membrane followed by centrifugation for 60s at 8000rpm. This step was repeated with elute from the previous stage.

2.7.4 Extraction of Total RNA Utilising Nucleospin RNA II

Extraction followed the Total RNA Isolation User Manual for Nucleospin RNA II (October 2007/Revision 8; Macherey-Nagel, Fisher Scientific, Loughborough, UK) protocol for Total RNA Purification from Cultured Cells and Tissue. Briefly, embryos were homogenised by mixing with 350µl RA1 + 3.5µl β-mercaptoethanol and passed through a 25G needle by syringe action (Becton Dickinson (BD), Oxford, UK) 5 times. Lysate was transferred to a filter column and centrifuged at 11000g for 60s. RNA binding conditions were adjusted by adding 350µl ethanol to lysate and mixed. Lysate was loaded onto a nucleospin RNA II column and centrifuged at 11000g for 30s. The column's silica membrane was desalted with 350µl membrane desalting buffer and centrifuged at 11000g for 60s. DNA was digested by addition of 95µl DNase reaction mixture (10µl reconstituted rDNase: 90µl reaction buffer for rDNase) and incubating at rtp for 15min. The membrane was washed and dried by a series of wash steps: 200µl RA2 at 11000g for 30s, 600µl RA3 at 11000g for 30s, 250µl RA3 at 11000g for 120s. RNA was eluted by adding 60µl RNase free H_20 and spun at 11000g for 60s.

2.7.5 Quantification of Total RNA

2.7.5.1 Quantification of Total RNA for Microarray-associated Extraction

Extracted and cleaned RNA was quantified using the NanoDrop ND100 spectrophotometer and quality assessed using an Agilent Bioanalyser 1000 Nanochip. The Bioanalyser quantifies RNA using microfluidics technology permitting automation and reduced operator variability. The Nanodrop requires only 0.5-1µl of sample, permitting quantification without substantially affecting the volume available for experimentation. Samples with purity (Ab^{260}/Ab^{280}) of 1.8-2.0 were used in microarray analysis.

2.7.5.2 General Quantification of Total RNA

Quantification of total RNA for other experiments was performed utilising a DU Series 500 spectrophotometer (Beckman, California, USA) with a 1:100 dilution of sample:sH_20, since the spectrophotometer was closely located making its utility more time-efficient. Samples with purity of 1.6-2.0 were used for further experiments.

2.7.6 Reverse Transcription of RNA for PCR

Reverse transcription of total RNA to cDNA was performed following the Reverse-iT 1st Strand Synthesis Kit or its replacement Verso cDNA Kit (ABgene, Surrey, UK) using a PTC-200 DNA Engine Cycler (Bio-Rad Laboratories, Hertfordshire, UK). Calculations were based on producing 0.5µg/ml cDNA.

2.8 Microarray Gene Analysis

Extracted and cleaned total RNA was passed to The Sheffield Microarray Core Facility (University of Sheffield). Sample handing, slide preparation, hybridisation and confocal image reading were performed by Dr. Paul Heath. The probabilistic model utilised for GeneChip analysis was developed and run by Dr. Marta Milo (Department of Biomedical Sciences, University of Sheffield) due to its high level of speciality and understanding.

2.8.1 Pair-mating of Adult Fish for Embryo Collection

Adult wildtype AB strain fish were individually pair-mated in tanks with a dividing wall to separate female and male the night before embryo collection. The following morning the dividing wall was removed, allowing time-specified embryo fertilisation to occur.

2.8.2 MO Injection

Embryos collected from a parent pair were sorted for fertilised embryos of one cell stage and divided into 2 equal groups to be simultaneously injected with [1nl] control or *tnnt2* MO (Sehnert, Huq *et al.*, 2002).

2.8.3 Time-points of Total RNA Extraction from MO Injected Embryos

Total RNA of control/*tnnt2* MO injected embryos was extracted at three timepoints: 36, 48, and 60hpf. 100-130 embryos were used per group, with three replicates per group.

2.8.4 Microarray Gene Analysis Methodology

Solutions and materials required for sample labelling, hybridisation and staining were purchased from Affymetrix (California, USA). Determination of gene expression took place using Affymetrix Zebrafish chips (1 chip per group, total 18) and standard Affymetrix protocol.

2.8.4.1 Affymetrix Microarray Gene Analysis Protocol

5µg of total RNA was used to produce cDNA through the addition of an oligo d(T) molecule with attached T7 polymerase binding site. T7 polymerase was then used to drive the production of antisense RNA with incorporated biotinylated nucleotides. Antisense RNA was fragmented by heating and included in the hybridisation solution injected into a GeneChip Zebrafish Genome array. Hybridisation (16h at 45˚C and 60 rpm) took place in a rotisserie oven. Post hybridisation washing and staining was carried out using the Fluidics station 400 (Affymetrix) following manufacturers' instructions; unincorporated material was removed by stringency washing. Biotinylated nucleotides were labelled using streptavidin-phycoerythrin.

Chips were scanned using the GeneChip Scanner 3000 (Affymetrix) and the resultant .DAT image converted to a .CEL file by GeneChip Operating Software. At appropriate points the integrity of the RNA molecules were monitored using the NanoDrop and Agilent Bioanalyser systems to ensure full quality control of materials.

2.8.5 Microarray Data Analysis

Data obtained by microarray gene analysis methodology was analysed by probabilistic model (Liu, Milo *et al.*, 2005; Sanguinetti, Milo *et al.*, 2005) using freeware available from http://www.bioinf.man.ac.uk/resources/puma. The model performed probe-level analysis of data, and provided each gene expression level an uncertainty measure to increase the robust nature of statistical analysis. Analysis is described in more detail in Chapter 4.

2.9 Identifying Base-Sequences of Genes of Interest in Zebrafish Embryos

2.9.1 Interspecies Gene and Protein Nomenclature

In order to provide consistency between groups a standard gene and protein nomenclature is utilised:

Species	**Gene Nomenclature**	**Protein Nomenclature**
Zebrafish	*gene*	Protein
Human	*GENE*	PROTEIN
Mouse	*Gene*	PROTEIN

For consistency, I refer to genes and proteins by their human nomenclature, unless clearly relating to other species.

2.9.2 Inter-Species Sequence Alignment

The sequences of genes of interest were aligned between human (*Homo sapiens*) mouse (*Mus musculus*), chick (*Gallus gallus*) and zebrafish using Ensembl Genome Browser release 47 and 52 (Oct 2007 and Feb 08, http://www.ensembl.org/-index.html) and ClustalW 1.83 and 2.0.10 (EMBL-EBI, accessed Nov 2007) to allow observation of regions of conservation between species. Such regions are likely to be regions of functionality within the gene sequence.

2.9.3 Reverse Transcription PCR Primer Design

The Ensembl database was utilised to identify proposed gene sequences in zebrafish. Primers of 20-25bp were designed using Primer3 version 0.4.0 software (http://frodo.wi.mit.edu/, accessed Nov 2007) against regions conserved between species. Primers were then purchased from Invitrogen (Paisley, UK).

2.9.4 Primer Sequences and Expected Band Size

EDNRB

Forward GCA GTG ATG AGT GCT CAA GG

Reverse AGA AGC TGA AAA GCC ACC AA

Expected Band Size 718bp

EFNB1

Forward TGA CCT GCA ACA AAC CAG AG

Reverse GCC AGA GTG CTG AGT GAC AG

Expected Band Size 579bp

GAPDH

Forward AGG CTT CTC ACA AAC GAG GA

Reverse GCC ATC AGG TCA CAT ACA CG

Expected Band Size 1019bp

2.9.5 Primer Dilution

Primers were diluted to 10µM using sH_2O.

2.9.6 PCR Controls

GAPDH was used as positive control. sH_2O was used as negative control.

2.9.7 Primer Combinations

F1:R1, F1:R2, F2:R1, F2:R2.

2.9.8 PCR Protocol

A 20µl reaction was prepared. 10µl 2x Biomix Red (Bioline, London, UK) vortexed, 1µl forward primer, 1µl reverse primer, and 1-2µl cDNA were mixed in a 200µl tube and made up to 20µl with sH_2O. The mixture was vortexed and spun down.

2.9.9 PCR programme

A PTC-200 DNA Engine Cycler (Bio-Rad Laboratories) was utilised.

Step 1: 94°C for 60s

Step 2: 94°C for 30s

Step 3: Annealing temperature for 30s

Step 4: 72°C for 60s

Step 5: Go to step 2 for 29 further cycles

Step 6: 72°C for 300s

Step 7: 10°C for ∞

2.9.10 Annealing Temperature

The annealing temperature (step 3 of the PCR programme) was taken as 2°C less than the combined forward and reverse primers' mean melting temperature (Tm) (1 M Na^+) taken from the provided datasheet.

2.9.11 Gel Electrophoresis

PCR product was run on a 1% multi-purpose agarose (Bioline) gel at 125V for approximately 20min using 10µl product with 7µl HyperLadder I or II (Bioline) which labels products of 10,000-200bp or 2,000-50bp in length respectively.

2.9.12 PCR Product Extraction from Agarose Gel

Following electrophoresis PCR product to be sequenced was excised from the agarose gel under UV light (Ultra-Violet Products, Cambridge, UK) by scalpel blade and extracted from the gel by performing the Qiagen Qiaquick Gel Extraction Kit protocol using a microcentrifuge.

2.9.13 Visualisation of PCR Product

Bands pertaining to PCR product were visualised and identified utilising UVItec apparatus (Cambridge, UK).

2.9.14 PCR Product Sequencing

PCR product at 50ng/µl was sequenced against my custom primers (section 2.9.3; ABI3730 capillary sequencer, Core Genomics Facility, University of Sheffield) to visualise possible alignment alterations between the Ensembl v47 sequence and sequence identified through custom primers. Products were purified to remove excess primer, dNTPs, and non-specific products at the facility. Data electropherograms were viewed using the free software Finch TV (version 1.4.0 2006, www.geospiza.com).

2.10 MO Injection

2.10.1 Purchase of MO

MOs were purchased from Gene Tools Inc, Oregon, USA. Custom MOs were designed using Gene Tools' free design service.

2.10.2 MO Storage

Prior to dilution, MO crystals were stored at rtp. Following dilution with sH_2O, MOs were stored at -20°C. Before injection, MOs were fully defrosted on ice and vortexed to ensure complete dissolution of the MO in the solution.

2.10.3 MO Sequences

STANDARD STOCK CONTROL

5'-CCTCTTACCTCAGTTACAATTTATA-3'

tnnt2

I utilised a previously published (Sehnert, Huq ***et al.***, 2002) start-site blocking MO.

5'-CATGTTTGCTCTGATCTGACACGCA-3'

ednrb

The MO was designed as a splice-site blocker, interacting at the intron:EXON boundary of exon 2.

5'-AGCCAGAAGCTGAAAAACAGGTACT-3'

efnb1

The MO was designed as a splice site blocker, also interacting at the intron:EXON boundary of exon 2.

5'-CACAAACCTGCAACACAAAGCATAC-3'

2.10.4 MO Injection Protocol

MOs were injected as standard (Westerfield, 2000), with the yolk-ball identified as injection site. 1.0mm glass filamentous capillary tubes (WPI, Florida, USA) were heated to a fine point using a Flaming/Brown Micropipette Puller (P-97, Sutter Instruments, California, USA) and filled with MO working solution via capillary action. The extreme tip was removed using Dumont #4 tweezers (WPI, Florida, USA). A 10mm/0.1mm division graticule (Pyser-Sgi, Kent, UK) was used to determine injection volume by calculating the volume injected into an oil-drop on the graticule.

One cell stage embryos were positioned along the edge of a standard microscopy slide on a 90mm Petri-dish lid for injection. Post-injection, embryos were placed in E3+10µl/ml Pen/Strep in groups of 40.

2.10.5 MO Dilution and Working Solution

The [50nM] MO crystals were diluted to [1nM] with sH_2O, and the solution divided into 5µl aliquots. Phenyl Red was added to aliquots at the dilution given for each experiment. Phenyl Red acts as a colorant making observation of injection easier, and also identifies pH. Over acidic MO dilutions can affect activity.

2.10.6 MO Injection Volume

To ensure injection volume would not affect response to MO injection, all MOs were injected at a volume of 1nl. For dose-response experiments concentration was altered through altering the dilution factor.

2.11 Whole Mount *in situ* Hybridisation Staining

Whole mount *in situ* hybridisation (ISH) is commonly utilised to determine gene expression patterns during early development by detecting specific nucleic acid sequences with RNA probes. In zebrafish embryos, ISH has a major advantage over antibody immunohistochemistry, since very few antibodies exist at present.

2.11.1 PTU Treatment of Embryos

Pigment cells can inhibit the observation of gene expression patterns. To prevent formation of pigment cells, embryos at 6hpf were treated with 0.0045% PTU (1-Phenyl-2-thiourea) solution.

2.11.2 Fixation of Embryos

Embryos of desired developmental stage were fixed with 4% paraformaldehyde in 1x PBS overnight at 4°C. The embryos were then dehydrated with 100% methanol and stored at -20°C for at least 12h.

2.11.3 Preparation of DNA Template with PCR Amplification

PCR for DNA template amplification were prepared and performed as described in sections 2.7 and 2.9.

2.11.4 Preparation of Vector-containing Bacteria

PCR product was inserted into plasmid vector and grown in *E. coli* TOP10 cells according to pCR 2.1-TOPO protocol (Version R, April 2004, Invitrogen). Figure 2.4 shows the vector map for pCR 2.1-TOPO. Cells were grown on Ampicillin selective agar plates (50µg/ml) to infer Ampicillin resistance.

2.11.5 Vector DNA Extraction

Vector DNA was extracted from the cells following the MinElute Gel Extraction Kit protocol (Qiaquick Spin Handbook, November 2006, Qiagen). DNA concentration was determined by quantitative analysis of 1µl on agarose gel with Hyperladder I (Bioline).

2.11.6 Antisense RNA Probe Synthesis

20µg vector DNA was linearised with HindIII restriction enzyme (NEB, London, UK) for 2h at 37°C. Purification was performed according to the HiSpeed Plasmid Purification Handbook (Qiagen, December 2001) using a Midi kit; and quantification by running a series on a 0.8% agarose gel with Hyperladder I (Bioline).

Antisense RNA probe was synthesised by 2h incubation at 37°C in transcription mix (1µl linearised DNA, 2µl transcription buffer, 2µl NTP-DIG-RNA, 1µl RNase inhibitor, 1µl T7 RNA polymerase, made up to 20µl with sH_2O; Roche). DNA was then digested with 2µl RNase free DNase (Roche) for 30min at 37°C.

Synthesis was stopped and RNA precipitated by adding 1µl EDTA 0.5M pH8, 2.5µl LiCl 4M and 75µl 100% ethanol to the mixture followed by incubation at -80°C for 30min. The mixture was centrifuged at 12,000rpm for 15min at 4°C, washed with 70% ethanol and resuspended in 20µl milliQ H_2O. The probe was tested to identify two bands on a 0.8% agarose gel and stored at -80°C as a 1:200 dilution of formamide.

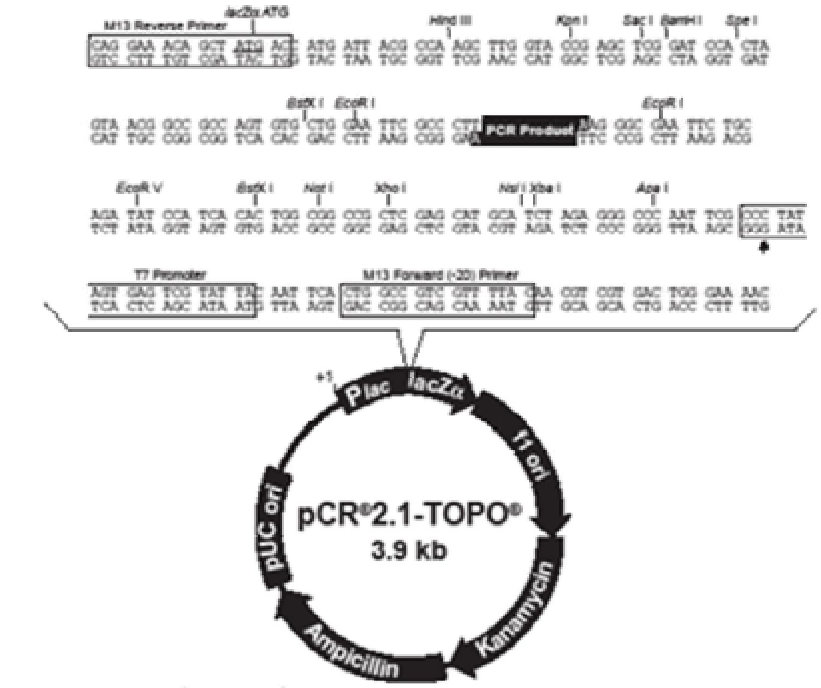

Comments for pCR®2.1-TOPO®
3931 nucleotides

LacZα fragment: bases 1-547
M13 reverse priming site: bases 205-221
Multiple cloning site: bases 234-357
T7 promoter/priming site: bases 364-383
M13 Forward (-20) priming site: bases 391-406
f1 origin: bases 548-985
Kanamycin resistance ORF: bases 1319-2113
Ampicillin resistance ORF: bases 2131-2991
pUC origin: bases 3136-3809

Figure 2.4 pCR 2.1-TOPO vector map.
Figure from pCR 2.1-TOPO protocol Version R, April 2004 (Invitrogen).

2.11.7 Whole Mount *in situ* Hybridisation Protocol

Whole mount ISH was performed as previously published (Thisse and Thisse, 2008) with minor modifications as described. All steps took place in 1.5ml tubes rather than 96-well plates.

Day 1. Embryos underwent a serial dilution of methanol in PBS: 75% (vol/vol), 50%, 25% each for 5min. Embryos were then washed 4 x 5min in PBST. Proteinase K treatment (10µg/ml) was performed for 15m at 24hpf, 30m at 48hpf, 60m at 72hpf and 90m at 96hpf to ensure total embryonic penetration to staining. Proteinase K digestion was stopped by incubating embryos for 20min in 4% PFA. Washes of 5 x 5min followed to remove residual PFA. Embryos were incubated in prehybridisation buffer (50ml of 50% formamide, 5xSSC, 0.1% Tween-20, citric acid pH6, 50µg/ml heparin, 500µg/ml tRNA) for 2h at 70°C horizontally on a heatblock. Embryos were then incubated in probe hybridisation buffer (prehybridisation buffer plus 1:200 dilution of probe in formamide) overnight at 70°C on a heatblock.

Day 2. Probe hybridisation buffer was removed before washing briefly in hybridisation wash (50% formamide, 5xSSC, 0.1% Tween-20, citric acid pH6) at 70°C. This was followed by a serial dilution of 75% wash:25% 2xSSC (vol/vol), 50% wash:50% 2xSSC, 25% wash:75% 2xSSC, 100% 2xSSC all at 70°C for 15min. 0.2xSSC at 70°C 2 x 30min. 75% 0.2xSSC:25 PBST, 50% 0.2xSSC: 50% PBST, 25% 0.2xSSC: 75% PBST, 100% PBST all at rtp for 10min. Embryos were incubated in blocking solution (PBST, 2% sheep serum, 2mg/ml BSA) for 2-4h and incubated in 1:4000 anti-DIG-AP shaking at 4°C overnight.

Day 3. Antibody solution was discarded and embryos washed briefly in PBST at rtp, followed by 6 further PBST washes at rtp for 15min each. Embryos were incubated three times, 5min each wash, with staining buffer (100mM tris HCl pH9.5, 50mM $MgCl_2$, 100mM NaCl, 0.1% Tween-20). Embryos were then incubated in staining solution (100mg/ml NBT, 50mg/ml BCIP in staining buffer) and monitored by dissecting microscope. Embryos were incubated in staining solution for 36hpf before the reaction was stopped with PBS pH 5.5 and 1mM EDTA.

2.11.7.1 Acquisition of tRNA

tRNA lyophilised powder from wheat germ type V (Sigma) was extracted three times with phenol/chloroform to remove protein.

2.11.8 Visualisation and Image Capture

For visualisation embryos were placed in a watch-glass and imaged utilising a colour camera attached to a Zeiss Axiovision microscope.

2.12 Statistical Analysis

2.12.1 Power Calculations

Statistical Power was calculated *post hoc* with OpenEpi 2.2.1 (Dean, Sullivan *et al.*, 2008).

2.12.2 Statistical Tests

Statistical analysis and graphical representations were created with GraphPad Prism 4.0 or 5.01 (GraphPad Software Inc., California, USA). N = one clutch of embryos. Data represents mean±SEM. Statistical comparison of two groups was by unpaired *t* test, and more than two groups by one-way ANOVA. Bonferroni post-tests were performed to identify groups demonstrating statistical significance.

2.12.3 Significance

* = $P<0.05$, significant difference from control

** = $P<0.01$, very significant difference from control

*** = $P<0.001$, highly significant difference from control.

Chapter Three

Exploiting the Zebrafish Embryo to Develop Models of Arteriogenesis

Chapter 3: Exploiting the Zebrafish Embryo to Develop Models of Arteriogenesis

In this chapter I determine whether zebrafish embryos can undergo collateral vessel formation (arteriogenesis) after arterial occlusion. I utilise two approaches: 1) *gridlock*, a mutant suffering a permanently occluded proximal aorta; and 2) mechanically-induced aortic occlusion of wildtype embryos. I demonstrate, by determination of the role of nitric oxide, that zebrafish arteriogenesis shares at least some level of conservation with arteriogenesis observed in mammalian species. As with Chapters 4, 5, and 6, I will start by describing the relevant background. Following the results (section 3.2) I will go on to discuss their relevance (section 3.3) within the context of the field.

3.1 Introduction

3.1.1 *Gridlock*

Gridlock mutant zebrafish were identified in the Boston mutagenesis screen and were identified by complete and permanent occlusion of the aorta at the bifurcation of the lateral dorsal aortae due to malformation during vasculogenesis (Peterson, Shaw *et al.*, 2004). *Gridlock* mutation is hypomorphic, leaving residual expression (Zhong, Childs *et al.*, 2001). Adult mutants are homozygous viable. Viability was credited to the possible development of collateral vessels transporting blood around the site of occlusion to more distal parts of the aorta (Gray, Packham *et al.*, 2007; Weinstein, Stemple *et al.*, 1995). However, this hypothesis has not been investigated directly, and possibilities such as abnormal vessel patterning may explain survival of *gridlock* mutant zebrafish.

Notch signalling leads to activation of a subfamily of basic helix-loop-helix (bHLH) transcription factors, hairy/Enchancer-of-split, including *Hey2*, to which the mutation responsible for the *gridlock* phenotype was subsequently positionally cloned (Zhong, Rosenberg et al., 2000). Activation of *Hey2* by Notch appears important for aortic angioblast cell fate determination (Zhong, Rosenberg *et al.*, 2000), leading to formation of arteries rather than veins.

Hey2 expression in vasculature of zebrafish embryos is restricted to arteries with expression along the length of the aorta (Zhong, Childs *et al.*, 2001). A dose-dependent pattern of aortic loss is demonstrated with *gridlock* MO knockdown; the bifurcation fusing the paired lateral dorsal aortae into the single dorsal aorta being the most vulnerable to reduced levels (Zhong, Childs *et al.*, 2001). *Hey2* expression has also been visualised in the developing heart field of zebrafish embryos, at regions representing cardiac precursor fields (Winkler, Elmasri *et al.*, 2003).

Gridlock mutation can be rescued irreversibly during the period of angioblast migration (12-24hpf) (Peterson, Shaw *et al.*, 2004). Rescue compounds upregulated VEGF expression to suppress the phenotype, pointing to the importance of VEGF in successful vascular development, as described in section 1.3.2.3.

3.1.2 *Hey2*

Zebrafish *gridlock* mutants have been described as a means of studying aortic coarctation (Weinstein, Stemple *et al.*, 1995), the narrowing of the aorta at the aortic arch, although there is no indication the mammalian *gridlock* orthologue *Hey2* is responsible for this disease. Mice deficient in *Hey2* do not appear to suffer abnormalities in arterial-venous fate decisions or aortic development. *Hey2* knockout mice do present with cardiomyopathy and defects in the ventricular septum, assumed to be a result of expression of *Hey2* within the heart (Gessler, Knobeloch *et al.*, 2002). In zebrafish, *Hey2* is known to be a negative regulator of cardiomyocyte proliferation (Jia, King *et al.*, 2007), supporting this hypothesis. *Hey2* limits heart growth by opposing *Gata5*, which promotes cardiomyocyte proliferation. *Gridlock* mutant zebrafish develop greater numbers of larger cardiomyocytes resulting from increased expression of early growth, and myocardial, genes. Conversely, upregulation of *Hey2* in wildtype embryos causes reduced heart size through decreased cardiomyocyte number and volume (Jia, King *et al.*, 2007).

One reason for differences in phenotypes observed between zebrafish and mammals may be that despite structural similarity (73.6% similarity, 67.6% identity) orthologues may have distinct roles in different species (Winkler, Elmasri *et al.*, 2003).

Differences may be associated with gene redundancy with other *hairy*-related genes, or differential evolution of *hey* function following genome duplication in zebrafish. Furthermore, *hey2* mutation in zebrafish (*gridlock*) is hypomorphic leaving residual expression (Weinstein, Stemple *et al.*, 1995), while mouse studies utilised complete knockout of *Hey2* by *lacZ* insertion (Gessler, Knobeloch *et al.*, 2002). It is possible that complete knockout in zebrafish would yield a phenotype different to that visualised with hypomorphic mutation, and which may reveal cardiac defects, since expression in the cardiac field has been visualised (Winkler, Elmasri *et al.*, 2003).

3.2 Results

3.2.1 *gridlock* Mutant Embryos Recover Blood Flow Distal to Occlusion Site

To determine rates of aortic blood flow recovery distal to occlusion binary counts recording presence or absence of aortic blood flow distal to occlusion were performed on *gridlock* mutant embryos from 2-5dpf.

At 2dpf no *gridlock* mutant embryo was observed with aortic blood flow. At 3dpf a minority of embryos (23.9±4.9%) had recovered aortic blood flow distal to site of occlusion. No blood cells were observed passing through the occlusion site. By 4dpf 57.3±0.3% of embryos had recovered aortic blood flow distal to occlusion. At 5dpf the majority (83.4±1.2%) of embryos recovered aortic blood flow (235 embryos; figure 3.1). Weinstein, Stemple *et al.* (1995) report embryos without distal blood flow at 7dpf. The group also report only mutants with remodelled (collateral) circulation survive beyond two weeks post fertilisation. At this timepoint diffusion is no longer sufficient for oxygenation (Pelster and Burggren, 1996). The data therefore suggests occlusion in *gridlock* mutants is complete and permanent, with survival of mutants occurring through transport of blood around the site of occlusion. The data does not exclude the possibility of mutant survival through abnormal vessel patterning during development transporting blood around the occlusion site.

Figure 3.1 Time-course of percentage recovery of aortic blood flow distal to the site of occlusion in *gridlock* mutant embryos.
The percentage of *gridlock* embryos with aortic blood flow distal to the site of occlusion rises from 0% at 2dpf to 83.4±1.2% by 5dpf. The occlusion remains intact throughout. It has been hypothesised (Weinstein, Stemple *et al.*, 1995) that survival of mutant fish beyond embryonic stages is dependent upon transport of blood around the occlusion site.

3.2.2 Vasculogenesis and Angiogenesis are Unaffected by *gridlock* Mutation

In order to determine whether abnormal vascular patterning was responsible for survival of *gridlock* mutant embryos I compared vasculogenesis (*de novo* vessel formation through *in situ* differentiation of angioblasts) and angiogenesis (growth and remodelling of primitive vascular networks) in wildtype and *gridlock* embryos. I performed laser-scanning confocal microscopy of *gridlock*/fli1:eGFP or wildtype fli1:eGFP embryos at 5dpf to produce representative images of embryonic vasculature (figure 3.2). 30 embryos per group were first observed under fluorescent stereomicroscopy. Four representative *gridlock* and two representative wildtype embryos were then imaged by confocal microscopy. By 5dpf vasculogenesis is complete and angiogenesis of ISVs, DLAVs, and SIVs has occurred, with embryos demonstrating a standard vascular pattern (Isogai, Horiguchi *et al.*, 2001). 5dpf is also the last timepoint at which I studied zebrafish embryos.

Of the approximately 30 *gridlock* embryos observed by fluorescent stereomicroscopy, all demonstrated normal patterning of aorta and cardinal vein on comparison with wildtype embryos, suggesting normal vasculogenesis, during which these vessels form (Isogai, Horiguchi *et al.*, 2001). *Gridlock* embryos demonstrated normal patterning and number of ISVs, and also normal development of communications between aorta, or cardinal vein, and SIVs. DLAVs developed normally in comparison to wildtype. The ISVs, SIVs and DLAVs form later than aorta and cardinal vein, during angiogenesis (Isogai, Horiguchi *et al.*, 2001). Their normal patterning in *gridlock* embryos suggests angiogenesis is unaffected by the mutation. Recovery of aortic blood flow through transport of blood around occlusion in *gridlock* embryos demonstrates the functional ability of aorta, ISVs and SIVs. Thus, despite complete absence of flow distal to occlusion in *gridlock* embryos, no vessels failed to form, and no vessel was found to have undergone aberrant angiogenesis by 5dpf.

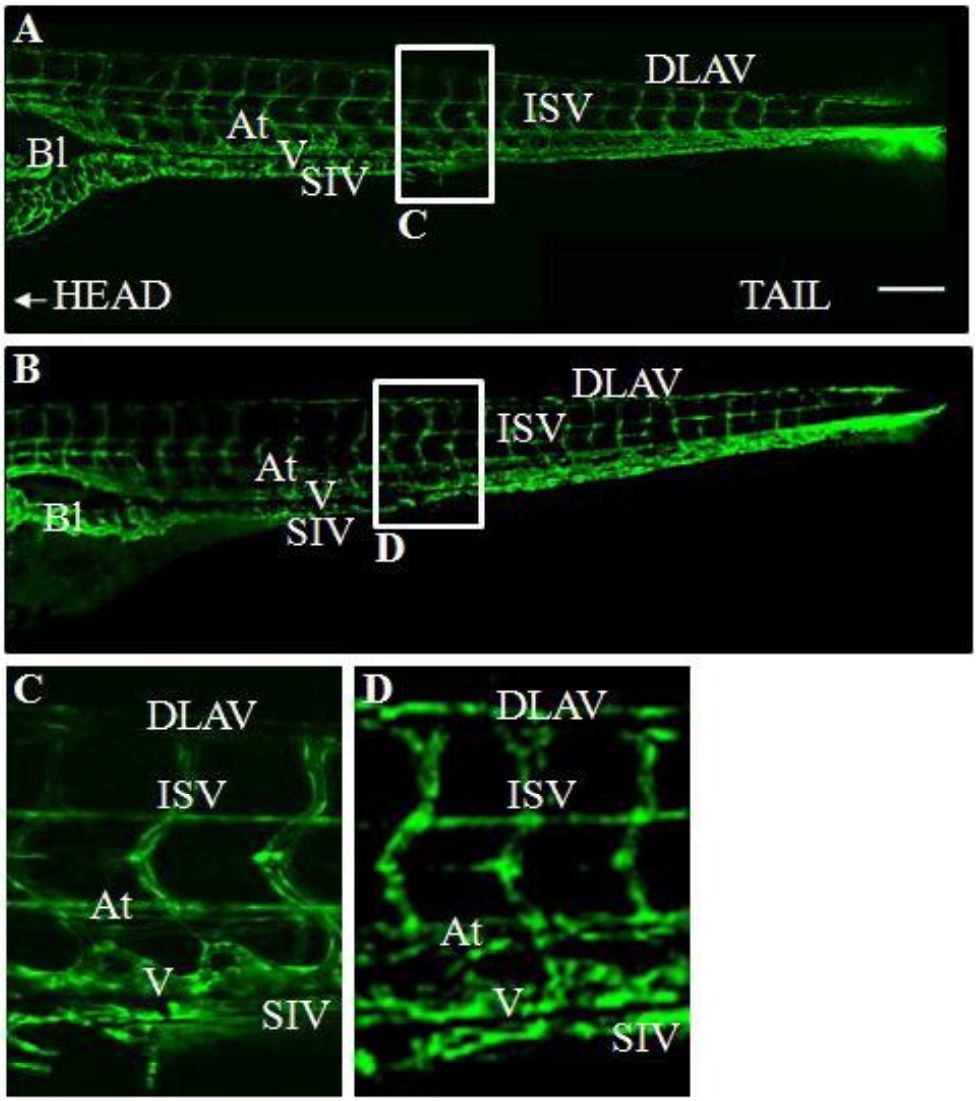

Figure 3.2 Laser-scanning confocal microscopy of *gridlock*/fli1:eGFP and fli1:eGFP embryos at 5dpf.

Representative lateral view of fli1:eGFP (A, and magnified section C) and *gridlock*/fli1:eGFP (B, and magnified section D) embryo at 5dpf. Aorta and cardinal vein, formed during vasculogenesis, of *gridlock* are normal compared to wildtype. ISVs, DLAVs, and SIVs, formed later by angiogenesis, are numerically and structurally normal also, on comparison with wildtype fli1:eGFP embryos. At=aorta, V=cardinal vein, ISV=intersegmental vessels, SIV=subintestinal vessels, DLAV=dorsal longitudinal anastomotic vessel. Each sub-figure composite of 4 images. Scale bar 200μm.

3.2.3 Pattern of *gridlock* Mutant 'Collateral' Blood Flow

In order to determine the origin of restored aortic blood flow in *gridlock* embryos the pattern of *gridlock* 'collateral' blood flow was observed by digital motion analysis (DMA) (Schwerte and Pelster, 2000). Consecutive frames from movie files are subtracted from one another resulting in a trace image. Trace images depict regions of movement (for example, blood flow) between frames, allowing observation of alterations in blood flow over time without harming embryos.

Figure 3.3 demonstrates representative DMA images of blood flow patterns in wildtype (A) and *gridlock* embryos (B) at 5dpf. In wildtype embryos, the majority of blood is transported along aorta and cardinal vein. Smaller volumes are transported by efferent and afferent ISVs to cardinal vein and from aorta respectively. The pattern of efferent and afferent ISVs is not fixed, except for the first four pairs (Isogai, Horiguchi *et al.*, 2001). Only very small volumes of blood enter SIVs, supplying the developing gut with blood, from communications with the aorta. Blood flows in multiple directions within SIVs, often reversing direction.

Gridlock aortic blood flow was restored in one of two ways (figure 3.3B and C). The majority of *gridlock* embryos (88%) acquired aortic blood flow via communications between aorta and subintestinal vasculature. Blood can also be restored to the aorta via reversal of flow in afferent ISVs (12%). Figure 3.3C is a diagrammatical representation of the pattern of blood flow in the *gridlock* mutant of B. As can be observed in figure 3.3B and C, the two forms of restored aortic blood flow are not exclusive, but can occur together at the same timepoints.

3.2.4 Laser-induced Aortic Occlusion Results in Recovery of Aortic Blood Flow Distal to the Occlusion Site

In order to demonstrate that recovery of aortic blood flow through remodelling of vessels in *gridlock* embryos was not a phenotypic characteristic of the mutation, but a spontaneous response to vascular occlusion observed in all embryos, I developed a means of occluding the proximal/mid aorta in wildtype embryos by focussed laser-induced injury.

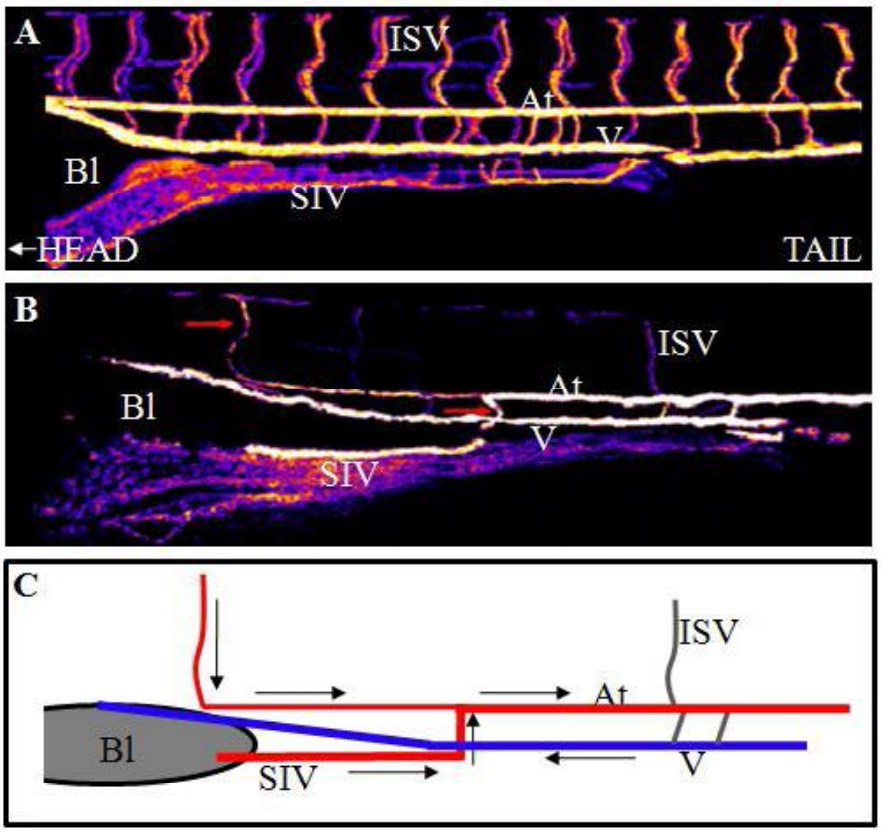

Figure 3.3 Pattern of 'collateral' blood flow in *gridlock* embryos resulting in aortic blood flow distal to occlusion.

Angiograms generated by DMA demonstrating representative lateral views of 5dpf wildtype (A) blood flow, and *gridlock* (B) 'collateral' blood flow. (C) diagrammatically represents the direct of blood flow in (B). At=aorta, V=cardinal vein, ISV=intersegmental vessels, SIV=subintestinal vessels, Bl=swim bladder. Red arrows in (B) denote collateral vessels. Directional arrows and coloured vessels in (C) denote direction of blood flow: red, away from the heart; blue, towards the heart; grey, undetermined. (A) and (B) composite of 4 images and generated by Caroline Gray.

Focussed laser-energy has previously been utilised to occlude the lateral dorsal aortae close to the bifurcation with the proximal aorta in zebrafish at approximately 12hpf, to observe the effect of absent FSS on kidney morphogenesis (Serluca and Fishman, 2001). A pulsed UV nitrogen 337nm laser was used to injure and completely occlude the proximal/mid aorta by endothelial damage and subsequent clot formation. Since I was to utilise clot formation to develop occlusion, I could not attempt laser-induced EC damage before 24hpf, at which time cardiac contraction begins (Chen, Haffter *et al.*, 1996). In order to phenocopy *gridlock* mutants as closely as possible, I directed EC damage to the proximal aorta, at a location just posterior to swim bladder (figure 3.4). I began by attempting aortic occlusion at 2 and 3dpf. Aortic occlusion at either timepoint would allow study of aortic blood flow recovery over a period of 72-96 hours. However, EC damage at these timepoints most frequently resulted in aortic rupture with severe trunk haemorrhage without occlusion, or fistula formation between aorta and cardinal vein. I therefore repeated the procedure in 5dpf embryos to determine if aortic occlusion was successful in more developed embryos. Laser-induced EC damage no longer resulted in vessel rupture or fistula formation. Occasionally, clot formation did not result in total vessel occlusion. On these occasions, EC damage was repeated immediately posterior to the initial attempt. In order to comply with Home Office regulation during envisaged longer post-occlusion observation, the procedure was repeated in 4dpf embryos. I found that by approximately 4h post occlusion clots began to degrade permitting passage of erythrocytes through the occlusion site, thereby preventing observation of aortic blood flow recovery over longer timepoints. In attempt to prevent clot degradation laser-induced EC damage was repeated at the occlusion site 3h post occlusion, generating an enlarged thrombus.

This secondary EC damage and clot build-up prevented clot degradation prior to 22h post occlusion in the vast majority of embryos. Only embryos which maintained occlusion until 22h post occlusion were included in the studies.

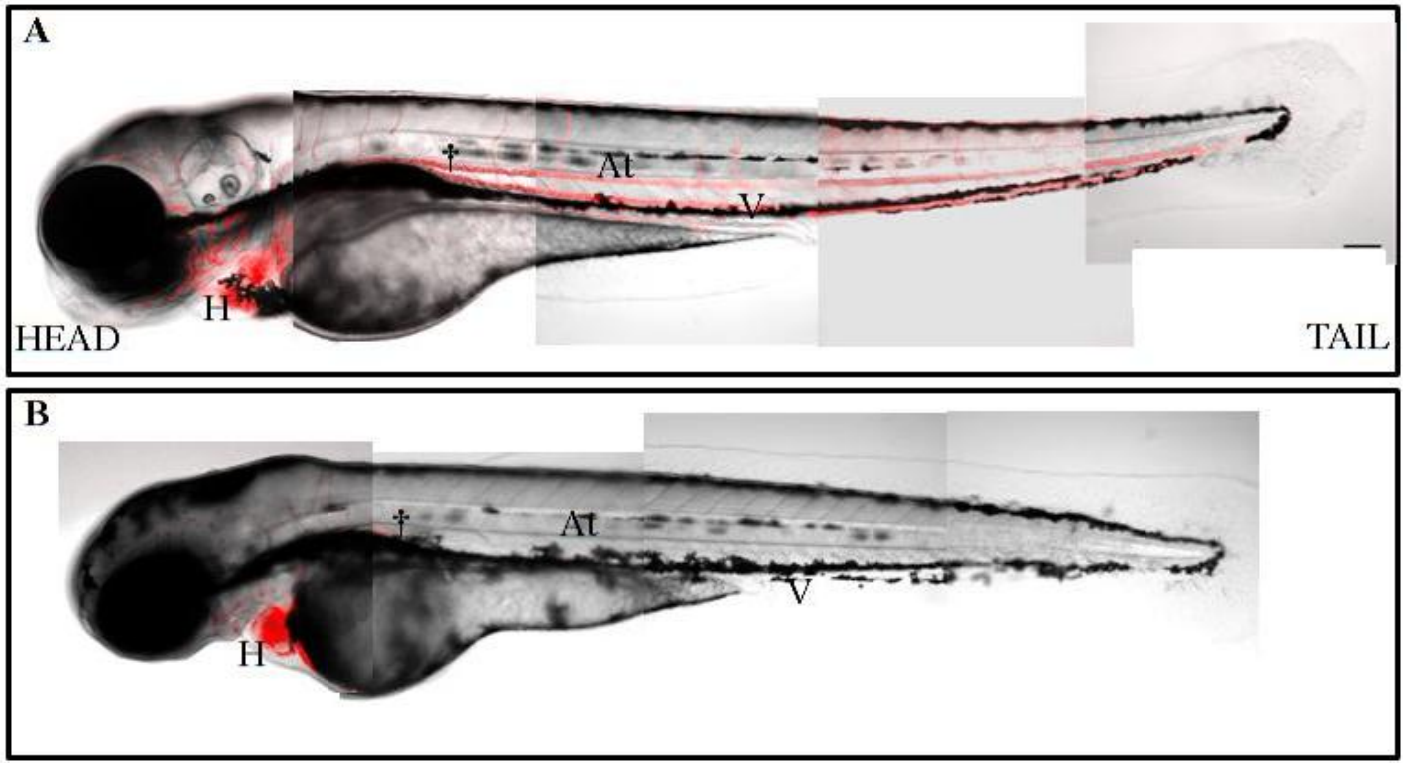

Figure 3.4 Laser-induced aortic occlusion of wildtype embryos at 5dpf.

Combined brightfield/DMA images demonstrating representative lateral views at 5dpf of wildtype embryo immediately before (A) and after (B) laser-induced aortic occlusion. Prior to occlusion blood flow (red) is normal, with the majority of flow in aorta and cardinal vein. Immediately post occlusion (B), no blood flow was observed distal to occlusion (†). However, the heart continued to contract regularly, and some flow can be observed within the head. At=aorta, V=cardinal vein, H=heart. Figures composite of 5/6 images. Scale bar 200µm.

Immediately after laser-induced aortic occlusion (5 replicates, total of 65 embryos) in 8.7% of embryos a small number of erythrocytes were observed to enter the aorta via communications with the subintestinal vasculature (figure 3.5). This is presumably a passive process permitting the movement of erythrocytes along a vessel of sufficient luminal diameter induced by the sudden change in pressure difference between occluded distal aorta and patent SIVs. The movement of erythrocytes in this manner ceased within five minutes, possibly as a result of further alterations in intravascular pressure. However, by 3h post occlusion 50.0% of embryos had recovered aortic blood flow from the same type of communications between aorta and SIVs. Angiograms generated using DMA demonstrate a close similarity in development of communications between *gridlock* and wildtype occluded embryos (compare figures 3.3 and 3.6). By 22h post occlusion 90.7% of embryos had restored aortic blood flow (figure 3.5). Occlusions began to fail following this timepoint, due to degradation of the clot, preventing later observation.

3.2.5 Restoration of Aortic Blood Flow Distal to Occlusion Occurs via Pre-existing Communications

DMA allows observation of alterations in blood flow over time. However, DMA is dependent upon shifts in pixel greyscale values between frames resulting from movement. It is therefore not possible to observe patent vessels with absent blood flow, and difficult to observe vessels with very low volumes of blood flow. Laser-scanning confocal microscopy of transgenic embryos permits observation of cardiovascular development over time, and is not dependent upon movement. fli1:eGFP/gata1:dsRED double transgenic embryos expressing endothelial GFP and erythrocyte dsRED allow the interaction between vasculature and blood to be observed. A defining feature of arteriogenesis is remodelling of *pre-existing* vessels (Buschmann and Schaper, 1999; Carmeliet, 2000). The presence of pre-existing vessels prior to occlusion, and their recruitment post occlusion, demonstrates that vasculogenesis or angiogenesis are not inducing recovery of aortic blood flow.

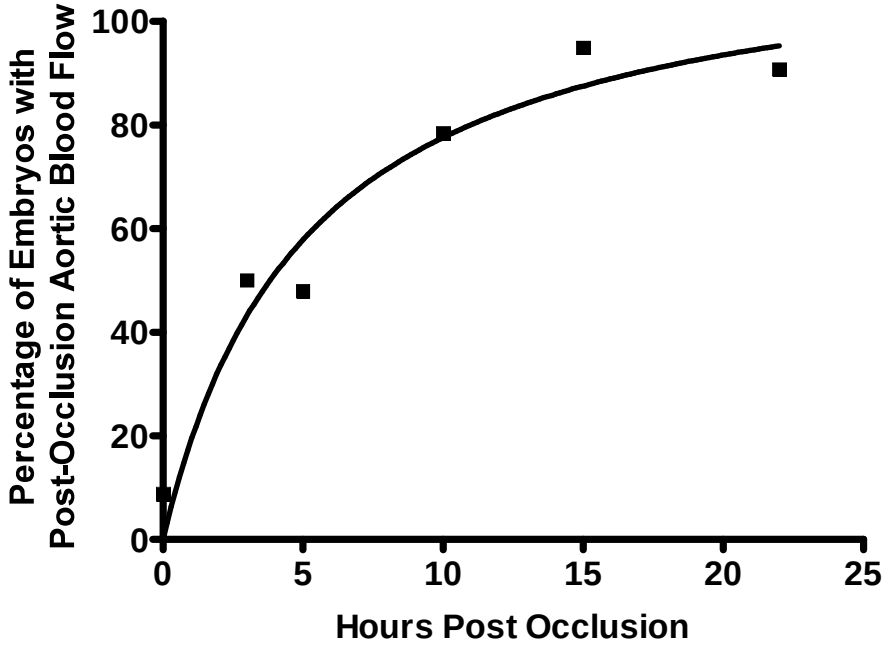

Figure 3.5 Time-course of wildtype embryos recovering aortic blood flow distal to the site of laser-induced occlusion.

The percentage of wildtype embryos (n=65) with aortic blood flow distal to the site of laser-induced occlusion rises from 0% immediately following occlusion to 90.7% in a 22h period. The occlusion remained intact throughout.

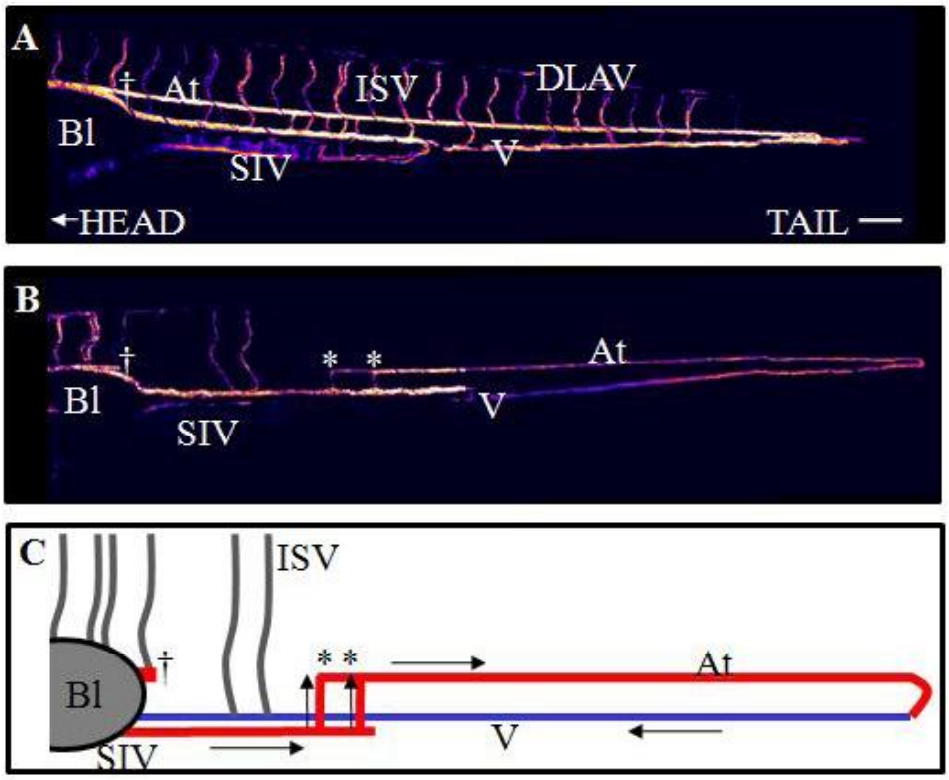

Figure 3.6 Pattern of 'collateral' blood flow in wildtype embryos following laser-induced aortic occlusion.

Angiograms generated by DMA demonstrate representative lateral views of a 5dpf wildtype embryo prior (A) and 22h post occlusion (B). (C) diagrammatically represents the direct of blood flow in (B). At=aorta, V=cardinal vein, ISV=intersegmental vessels, SIV=subintestinal vessels, Bl=swim bladder. † denotes occlusion site and * communications recovering blood to the aorta distal to the occlusion site. Directional arrows and coloured vessels in (C) denote direction of blood flow: red, away from the heart; blue, towards the heart; grey, undetermined. (A) and (B) composite of 4 images. Scale bar 200μm.

Laser-scanning confocal microscopy of 4dpf fli1:eGFP/gata1:dsRED wildtype embryos prior to and following laser-induced aortic occlusion was performed. The aim of this experiment was to determine in wildtype embryos the presence of vessels prior to occlusion which undergo recruitment as 'collateral' vessels following occlusion. The experiment would thus enable identification of pre-existing 'collateral' vessels. It would also exclude the possibility of occlusion inducing vasculogenesis or angiogenesis as a means of developing collateral blood flow.

Figure 3.7 demonstrates the same 4dpf embryo immediately prior to and 5h post occlusion. Immediately prior to occlusion the embryo has standard wildtype blood flow. As described by Isogai, Horiguchi *et al.* (2001) the majority of blood is pumped from heart to aorta, returning through the cardinal vein. Smaller volumes are transported through efferent and afferent ISVs. Smaller volumes are also transported through SIVs, only very small volumes of which enter SIVs via communications with the aorta. Within SIVs, blood flows in multiple directions often changing direction.

Immediately post occlusion, blood flow halts posterior to occlusion. Blood flow continues within the head, and the heart continues to contract normally. A small minority of embryos (8.7%; discussed in the previous section) are observed to have small numbers of erythrocytes entering the aorta, which ceases within five minutes. On observation at 3h post occlusion 50.0% of embryos have recovered aortic blood flow via communications connecting SIVs and aorta. Exactly the same communications are observed prior to occlusion; transporting little or no blood flow. This suggests vasculogenesis and angiogenesis are not involved in the development of 'collateral' vessels. It suggests that 'collateral' blood flow develops through pre-existing vessels, a feature key to the definition of arteriogenesis (Buschmann and Schaper, 1999). Observation of a communication pre- and post occlusion in the same animal is not possible in mammalian species (as discussed in section 1.4), and thus this experiment also highlights an advantage of exploiting zebrafish embryos for such research.

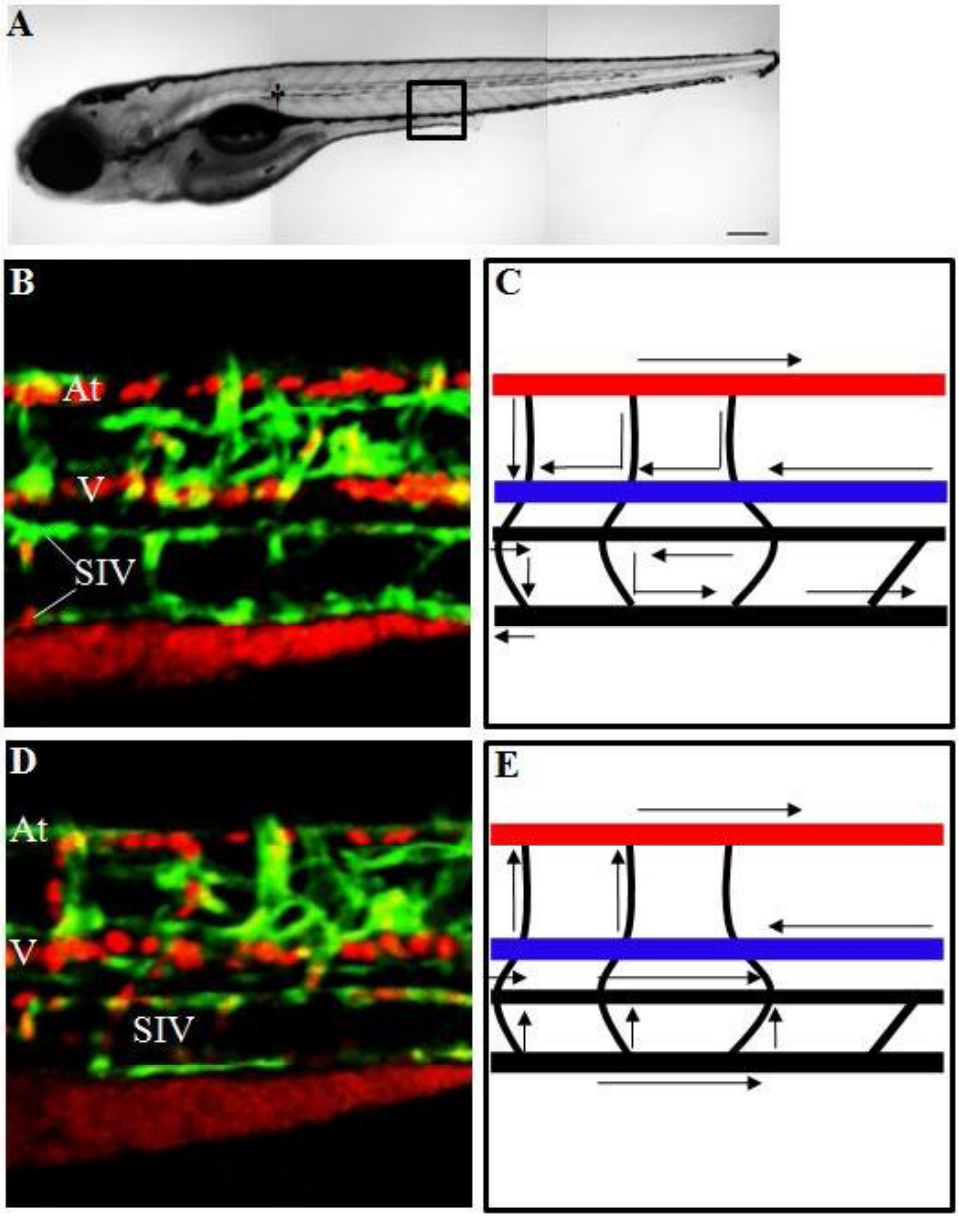

Figure 3.7 Recovery of aortic blood flow distal to the site of occlusion is the result of flow redistribution in pre-existing vessels *(legend continued overleaf)*.

Figure 3.7 Recovery of aortic blood flow distal to the site of occlusion is the result of flow redistribution in pre-existing vessels ***(continued).***

Representative lateral laser-scanning confocal microscopy image of a fli1:eGFP/gata1:dsRED wildtype embryo at 4dpf immediately prior to laser-induced aortic occlusion (B), and 5h after occlusion (D). Box in (A) depicts area imaged in (B) and (D). (C) and (E) are diagrammatical representations of blood flow in (B) and (D) respectively. The diagrammatical representations demonstrate the high degree of blood flow alteration following aortic occlusion. While direction of flow in aorta and cardinal vein remains constant before and after occlusion, direction of flow in ISVs and SIVs varies. For example, before occlusion, blood flows ventrally within ISVs, while after occlusion, blood flow in ISVs is dorsal. Arrows depict direction of blood flow, vessels without arrows demonstrate absent flow. At=aorta, V=cardinal vein, ISV=intersegmental vessels, SIV=subintestinal vessels. † in (A) denotes occlusion site. (A) composite of 3 images, scale bar 200μm.

3.2.6 The Effect of NOS Inhibition on Recovery of Aortic Blood Flow in *gridlock* Mutants

NO has been shown to modulate collateral vessel formation in a wide range of species and models (Cai, Kocsis *et al.*, 2004a; Lloyd, Yang *et al.*, 2001; Yu, deMuinck *et al.*, 2005). To determine if zebrafish embryo 'collateral' vessel remodelling shares this modulation I determined the effect of pharmacological inhibition of all NOS isoforms by the non-specific inhibitor L-NAME (Fritsche, Schwerte *et al.*, 2000).

An advantage of zebrafish embryos is the ability of applying small molecule inhibitors at different timepoints during cardiovascular development through media incubation and subsequent diffusion into embryos (Chico, Ingham *et al.*, 2008) to test their effects without requiring direct intervention. I was therefore able to assess the effect of NOS inhibition on restoration of aortic blood flow in *gridlock* embryos. I was also able to assess the possible role of NO-mediated vasodilatation in collateral vessel development through NOS inhibition.

Gridlock embryos (n=6-30 embryos/replicate, 8 replicates/group) were incubated in [1mM] L-NAME from 1-5dpf, the L-NAME solution being replaced at 24h intervals. Treatment with L-NAME from 1-5dpf induced a very significant decrease ($P<0.01$) in the percentage of embryos recovering aortic blood flow compared to untreated control siblings (control 75.14±4.23%, L-NAME 42.99±8.85%; power 100%) (figure 3.8). This suggests that as in other species and models (Cai, Kocsis *et al.*, 2004a; Lloyd, Yang *et al.*, 2001; Yu, deMuinck *et al.*, 2005), NO modulates collateral vessel formation in zebrafish embryos.

NO mediates vasodilatation, and so to exclude inhibited vasodilatation as the cause of decreased percentages of *gridlock* embryos recovering aortic blood flow I performed additional experiments to determine the time dependence on NO production. 3h L-NAME washout with fresh medium at 5dpf demonstrated no significant change from the decrease in aortic blood flow recovery described, suggesting inhibition of NO-mediated vasodilatation is not responsible for decreased aortic blood flow recovery in *gridlock* embryos.

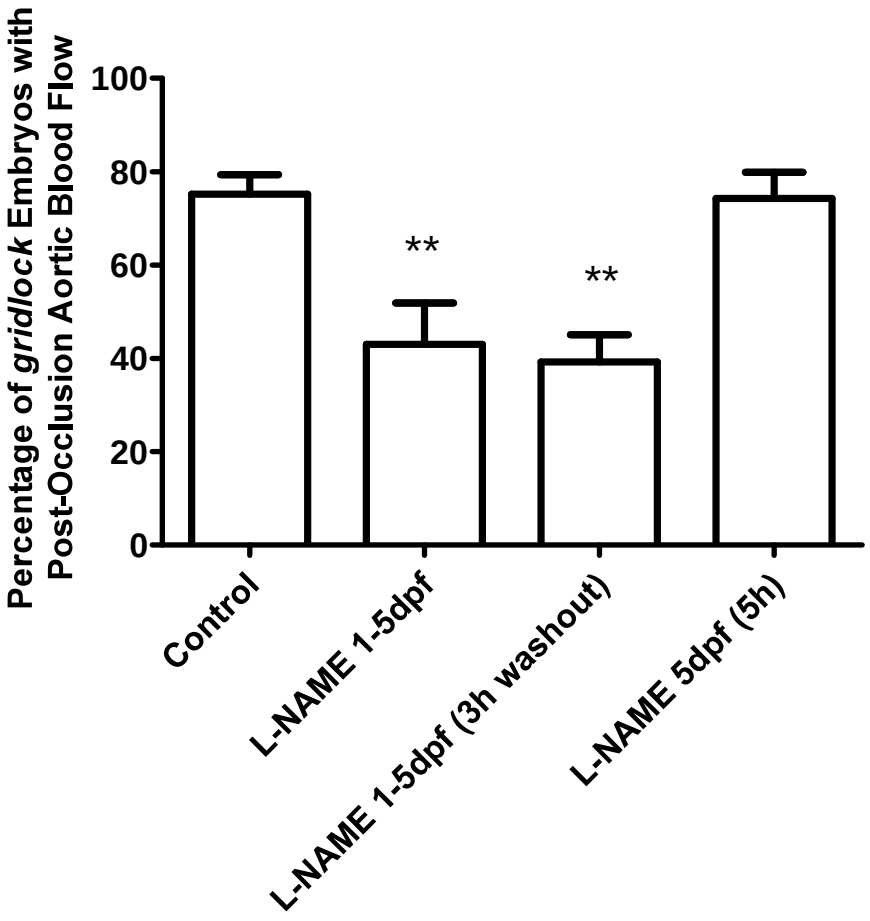

Figure 3.8 Effect of NOS Inhibition on Recovery of Aortic Flow by 'Collateral' Vessel Remodelling in *gridlock* Mutant Embryos.

Treatment with [1mM] L-NAME from 1-5dpf led to a very significant reduction in recovery of aortic flow ($P<0.01$) compared to control sibling embryos. 3h Washout at 5dpf did not significantly affect this result, excluding a role for NOS inhibition in vasoactivity as the cause of reduction in recovery of aortic flow. In addition, treatment for 5h at 5dpf did not result in reduced recovery of aortic flow compared to control siblings, providing further evidence for the exclusion of inhibited NO-mediated vasodilatation as the cause.

Further supporting this notion, *gridlock* embryos treated with L-NAME (for 5h) only at 5dpf demonstrated no significant difference in recovery of aortic blood flow on comparison to untreated control embryos (figure 3.8). Thus, inhibition of NO-mediated vasodilatation for 5h at 5dpf did not result in a reduced recovery of aortic blood flow as might be expected if NO-mediated vasodilatation was responsible for recovery of blood flow in *gridlock* embryos.

3.2.7 The Effect of NOS Inhibition on Recovery of Aortic Blood Flow following Laser-induced Aortic Occlusion

As discussed in section 3.2.6 NO has been shown to modulate arteriogenesis in a range of species and models. To determine if zebrafish embryo 'collateral' vessel remodelling following laser-induced aortic occlusion shares this modulation I determined the effect of pharmacological inhibition of NOS by L-NAME. Wildtype embryos were treated with [1mM] L-NAME 16h prior to laser-induced occlusion, and for the subsequent length of experimentation. The recovery of aortic blood flow was observed at 22h post occlusion, the timepoint at which the greatest percentage of embryos had recovered aortic blood flow via 'collateral' vessels following laser-induced occlusion.

At 22h post occlusion the percentage of embryos having recovered aortic blood flow had decreased highly significantly ($P<0.001$) in L-NAME treated embryos compared to controls (control 85±8% L-NAME 30±8%; n=15 embryos control, 28 L-NAME, power 96.8% or 92.8% with continuity correction) (figure 3.9). This suggests that, like other species and models (Cai, Kocsis *et al.*, 2004a; Lloyd, Yang *et al.*, 2001; Yu, deMuinck *et al.*, 2005), NO mediates 'collateral' vessel development in wildtype zebrafish embryos suffering induced aortic occlusion.

3.2.8 NOS Inhibition Affects Heart Rate but not Aortic Blood Velocity

In addition to its role in vasodilatation, NO also modulates cardiac contraction and so heart rate. This has been demonstrated through inhibition of NOS by L-NAME in mice, which resulted in a significant decrease in heart rate (Jacobi, Sydow *et al.*, 2005).

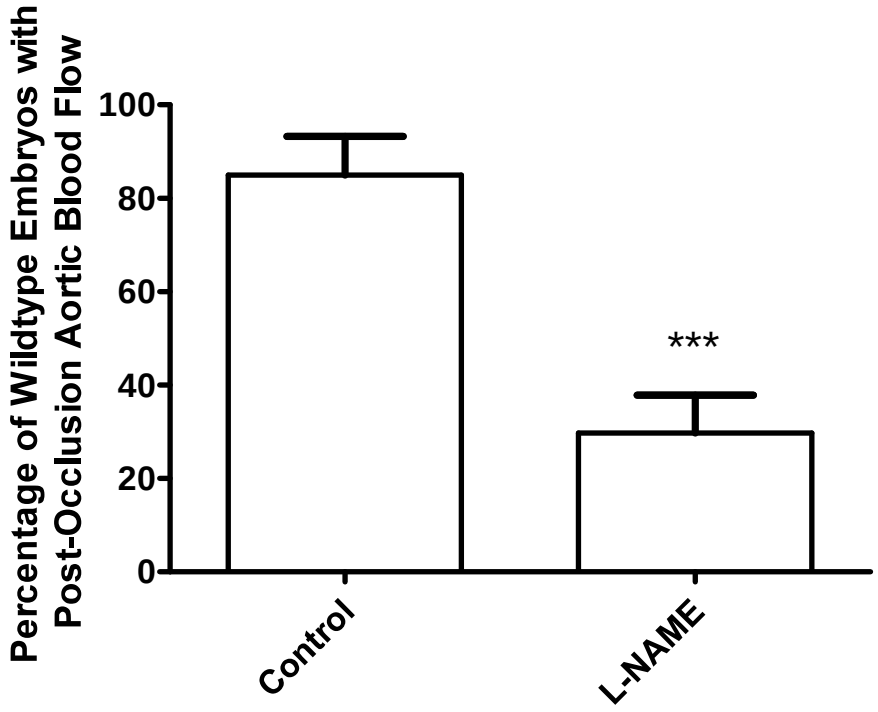

Figure 3.9 Percentage of wildtype embryos with blood flow distal to the occlusion site 22h post laser-induced occlusion following NOS inhibition.
NO synthase inhibition by [1mM] L-NAME treatment resulted in a highly significant decrease ($P<0.001$) in the ability of embryos to remodel vessels to perfuse the aorta with blood flow compared to control 22h post occlusion.

It is therefore possible that NOS inhibition in zebrafish embryos decreases the percentage recovery of aortic blood flow following occlusion through altered modulation of cardiac contraction. For example, decreased heart rate may lead to decreased blood flow, intravascular pressure, and FSS in remodelling communications, resulting in decreased remodelling. Decreased stroke volume may also result in decreased blood velocity, since blood volume may be reduced. In zebrafish, eNOS expression has been demonstrated from 3dpf in cardiomyocytes, dorsal aorta, and cardinal vein (Fritsche, Schwerte *et al.*, 2000). Vasoactivity of L-NAME and SNP at concentrations I have utilised has also been found (Fritsche, Schwerte *et al.*, 2000).

To determine whether recovery of aortic blood flow following occlusion was influenced by NO modulation of cardiac contraction, heart rate and aortic blood velocity in wildtype L-NAME or SNP treated embryos were studied at 5dpf. As with previous NOS inhibition studies embryos were treated with [1mM] L-NAME for 16h prior to observation. Figure 3.10 demonstrates the effect of NOS inhibition on heart rate at 5dpf.

Heart rate was significantly decreased ($P<0.05$, n=10 per group) following L-NAME treatment compared to control sibling embryos (control: 132.2±6.5 beats/minute; L-NAME 113.2±3.1; power 100%), concurring with mammalian data (Jacobi, Sydow *et al.*, 2005). This result suggests the possibility that decreased blood flow caused by the fall in heart rate may cause a decrease in the percentage of embryos recovering aortic blood flow. However, treatment of sibling embryos with the NO donor SNP demonstrated no significant difference in heart rate on comparison to control embryos (figure 3.11; $P>0.15$, n=8 per group, control: 168.3±4.0 beats/minute; SNP: 159.8±3.9; power 99.1%), suggesting super-physiological levels of NO do not affect heart rate.

I then wished to determine the effect of decreased heart rate on aortic blood velocity. It has been difficult to determine haemodynamic parameters such as aortic blood velocity in zebrafish embryos. Their small size prevents use of techniques such as Doppler ultrasound, commonly performed in mammals. I developed a means of determining aortic blood velocity by calculating erythrocyte movement through time.

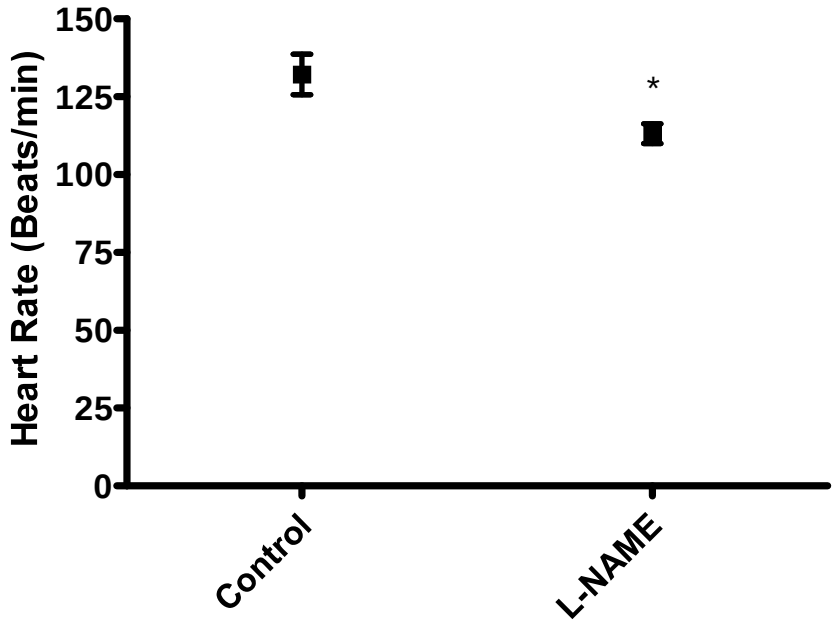

Figure 3.10 Effect of NOS inhibition on the heart rate of wildtype embryos at 5dpf.

NOS inhibition by [1mM] L-NAME treatment resulted in a significant decrease in heart rate ($P<0.05$) in wildtype embryos compared to control sibling embryos at 5dpf.

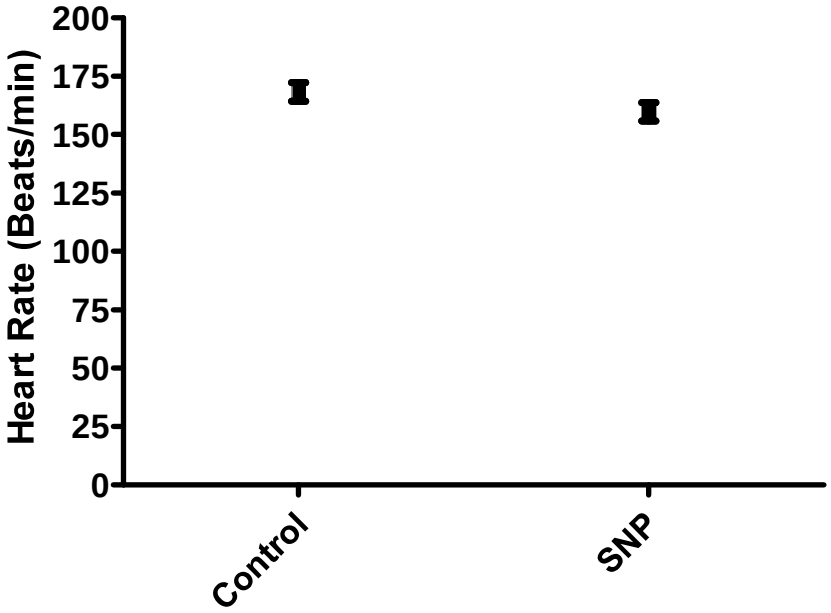

Figure 3.11 Effect of NOS elevation on the heart rates of wildtype embryos at 5dpf.

Enhancement of NOS activity by [1mM] SNP treatment did not significantly alter heart rate in wildtype embryos at 5dpf compared to control ($P>0.05$).

Velocity was determined at three areas of the aorta, proximally at the highest point of the yolk-sac (ISV 6-8), at a midpoint (ISV 14-16), and distally (ISV 27-29). Velocity was determined utilising wildtype embryos at 5dpf. Aortic blood velocity has demonstrated significant reduction at the proximal portion of the aorta in a concentration dependent manner to anaesthetic (MS-222) treatment earlier during embryonic development at 2dpf (Malone, Sciaky *et al.*, 2007). This demonstrates that the technique has the sensitivity required to measure subtle alterations in haemodynamic parameters in zebrafish embryos. It also demonstrates that embryos at the earliest stages of development have the physiological processes necessary for alterations in haemodynamics.

I found no significant difference at any of three points along the aorta in aortic blood velocity (figure 3.12) following the same L-NAME treatment performed above ($P>0.05$; proximal aorta: control 1139±79μm/s, L-NAME 1041±115, power 10.3%; mid aorta: control 779±87μm/s, L-NAME 801±110; distal aorta: control 432±57μm/s, L-NAME 434±55; n=14-15 per group). This result suggests aortic blood velocity is not affected by decreased heart rate. It is possible that inhibition of vasodilatation by NOS inhibition limits the effect of decreased heart rate on aortic blood velocity, maintaining velocity via decreased luminal diameters in vessels. SNP treatment identical to heart rate studies also demonstrated no significant difference in aortic blood velocity (figure 3.13; $P>0.05$; proximal aorta: control 1058±130μm/s, SNP 973±926, power 30.3%; mid aorta: control 635±72μm/s, SNP 728±116; distal aorta: control 325±72μm/s, SNP 337±53; n=10/group).

The novel Correlator software utilised in determining embryonic aortic blood velocity was compared to the technique of frame-frame cell tracking to determine correlation and disagreement between the techniques. Figure 3.14 demonstrates correlation between techniques which results in a slope of 0.84, suggesting a highly correlative association. A Bland-Altman disagreement plot (figure 3.15) of the same data demonstrates that percentage differences between techniques are as high as 50%, with a bias of 7.63.

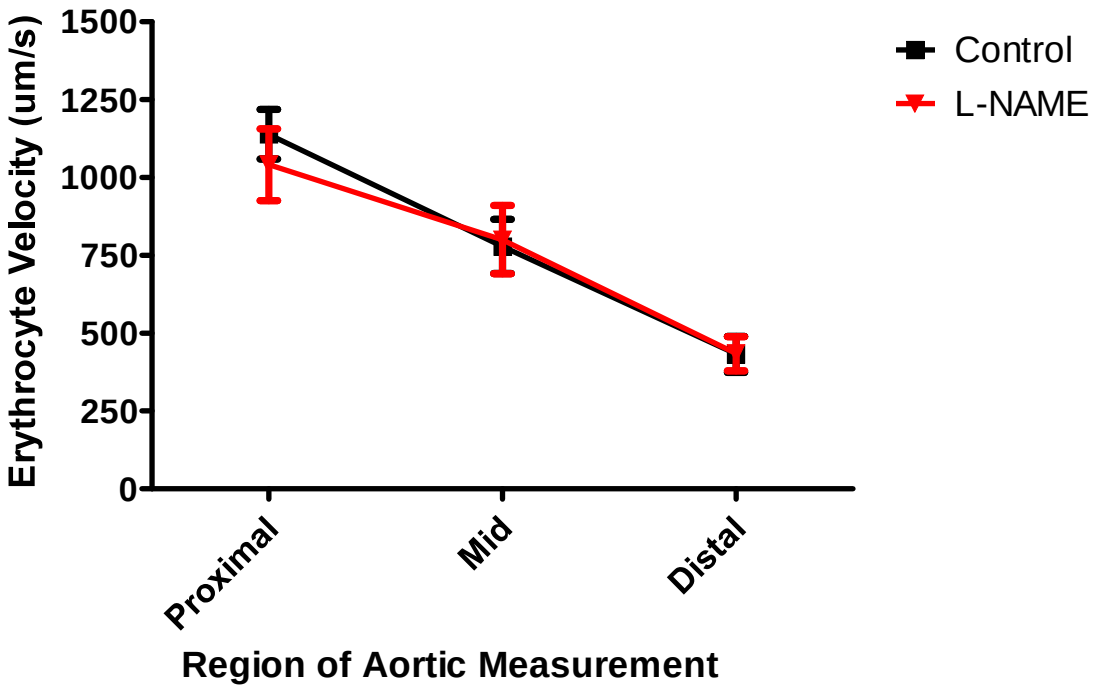

Figure 3.12 Effect of NOS inhibition on aortic blood velocity of wildtype embryos at 5dpf.

NOS inhibition by [1mM] L-NAME treatment did not significantly effect aortic blood velocity ($P>0.05$) in any region of the aorta measured (proximal, mid, distal) in wildtype embryos at 5dpf compared to control siblings.

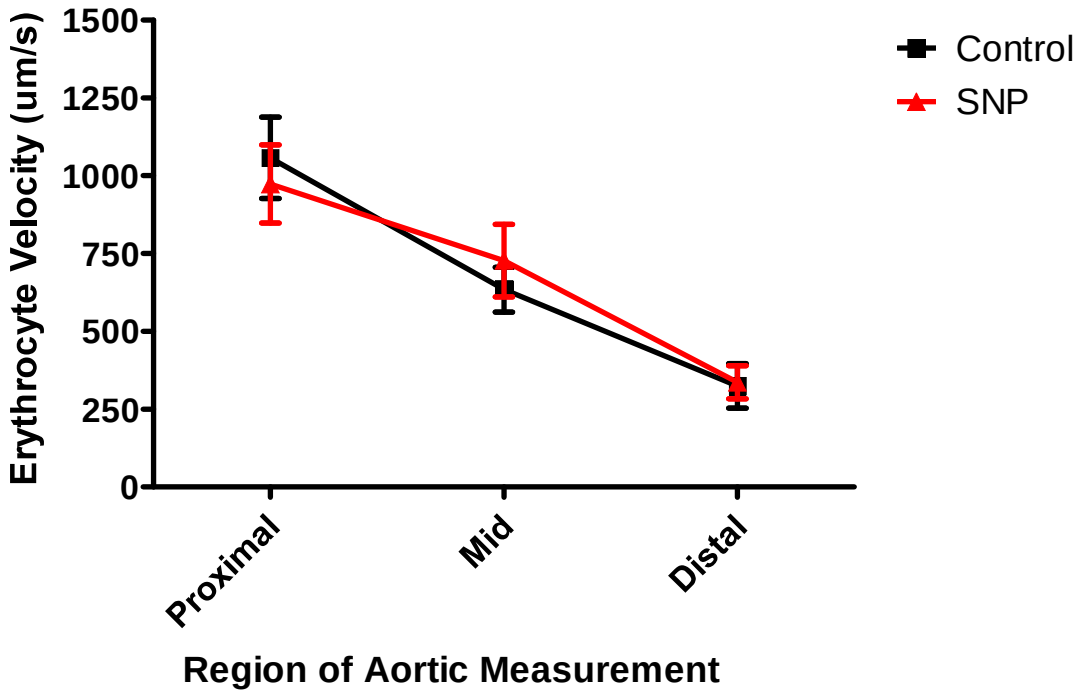

Figure 3.13 Effect of NO donor SNP on aortic blood velocity of wildtype embryos at 5dpf.

Enhancement of NOS activity by [1mM] SNP treatment did not significantly effect aortic blood velocity ($P>0.05$) in any region of the aorta measured (proximal, mid, distal) in wildtype embryos at 5dpf compared to control.

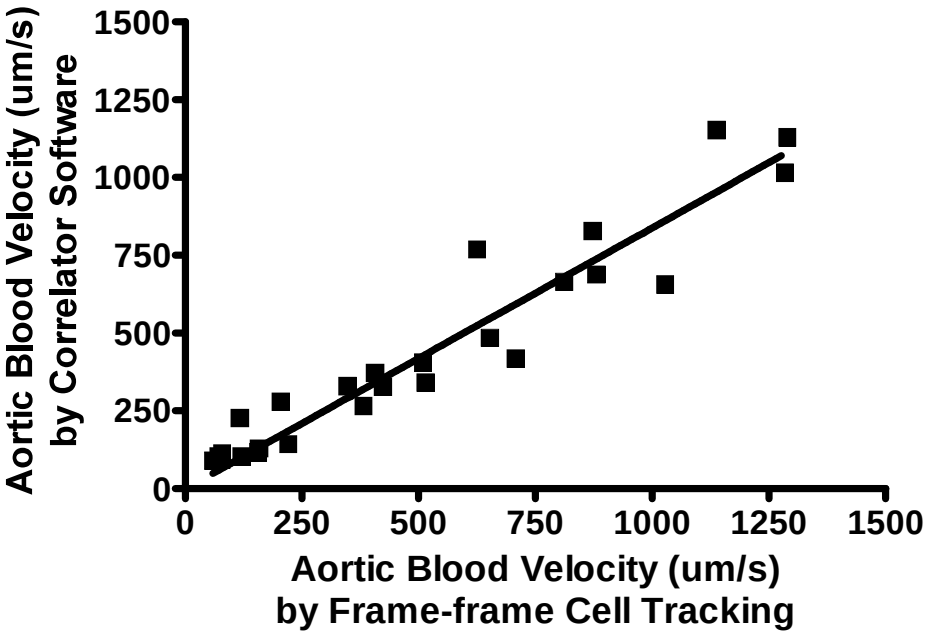

Figure 3.14 Validation of correlator software through comparison with manual frame-frame cell tracking.

Using data obtained from all 3 aortic areas of the aorta (proximal, mid, and distal) for wildtype fish at 5dpf (26 recordings) the Correlator software and frame-frame cell tracking were compared. The plot of identity, comparing methods with a slope of 0.84±0.03 by linear regression, demonstrates a good correlation between techniques.

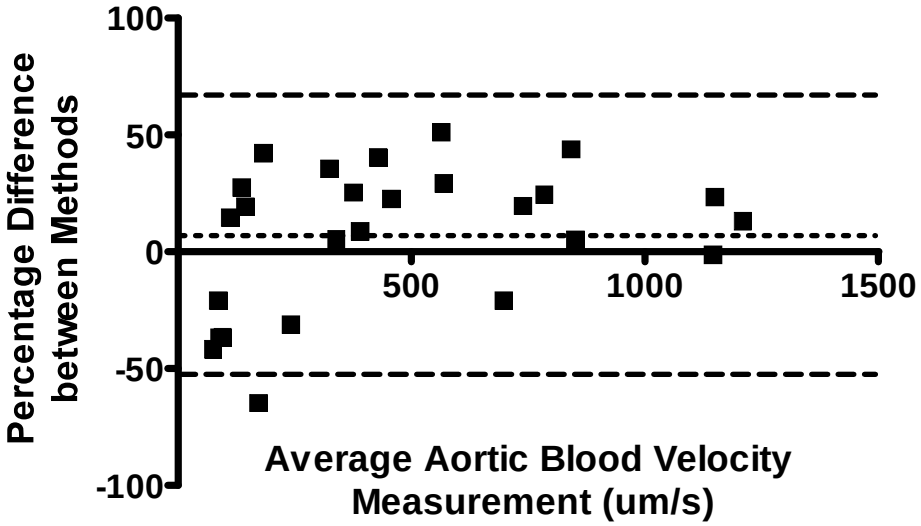

Figure 3.15 Bland-Altman disagreement plot identifying disagreement between correlator software and frame-frame cell tracking.

Bland-Altman disagreement plot using the same data as figure 2.4. A bias of 7.63 exists between the two methods. Crossed line=mean difference, dashed lines=95% confidence intervals.

3.3 Discussion

3.3.1 *gridlock* Mutant Embryos Recover Aortic Blood Flow Distal to Occlusion Site

Gridlock mutant zebrafish were identified by complete and permanent occlusion of the aorta at the bifurcation of the lateral dorsal aortae due to malformation during vasculogenesis (Peterson, Shaw *et al.*, 2004). As they develop a minority of embryos undergo swelling of the yolk-sac; however all other vasculature is described as physiologically normal, including cranial vasculature. At the onset of circulation at approximately 36hpf, occlusion prevents all blood flow distal to it (Weinstein, Stemple *et al.*, 1995). Despite this, adult mutants are homozygous viable. Viability has been credited to possible development of collateral vessels transporting blood around the site of occlusion to more distal parts of the aorta (Gray, Packham *et al.*, 2007; Weinstein, Stemple *et al.*, 1995). However, this hypothesis had not been investigated directly. Other possibilities, such as abnormal vessel patterning, may have explained survival of *gridlock* mutant zebrafish. To determine rates of recovery of aortic blood flow distal to occlusion in *gridlock* mutant embryos binary counts were performed from 2-5dpf (235 embryos).

Despite complete aortic occlusion in *gridlock* mutant embryos, recovery of aortic blood flow was observed between 3 and 5dpf, the last observed timepoint (figure 3.1). While no mutant embryo was observed with aortic blood flow at 2dpf; percentages of aortic blood flow increased thereafter. Almost one quarter of embryos at 3dpf demonstrated recovery of aortic blood flow. At 4dpf over half, and at 5dpf over 80%, of embryos had recovered aortic blood flow. The gradual increase in numbers of embryos demonstrating aortic blood flow from 3-5dpf could result from genetic variability between siblings of different parent pairs, or differences in haemodynamic parameters which are known to vary widely during the first days of embryonic development. For instance, greater cranial blood velocity in some embryos may result in greater FSS levels, a key stimulus for vascular remodelling.

Percentages of aortic blood flow recovery do not continue to increase until all embryos recovery flow. *Gridlock* embryos are observed without aortic blood flow at 7dpf and 2.5

weeks (Weinstein, Stemple *et al.*, 1995), suggesting not all *gridlock* recover aortic blood flow. Recovery of flow also appears critical for survival since only mutants with recovered flow survive to this later timepoint (Weinstein, Stemple *et al.*, 1995) when diffusion is no longer sufficient for tissue oxygenation (Pelster and Burggren, 1996). The data therefore suggests occlusion in *gridlock* mutants is complete and permanent, with survival of mutants occurring through vascular remodelling transporting blood around occlusion. However, the data does not exclude the possibility of mutant survival resulting from abnormal vessel patterning during development transporting blood around occlusion.

Exploiting *gridlock* mutant embryos provides an easy resource for determining blood flow recovery following occlusion. Occlusion is present from aortic formation (Peterson, Shaw *et al.*, 2004) and embryonic optical clarity enables visualisation of blood vessels with light microscopy. *Gridlock* embryos would also therefore provide a means of rapid high-throughput screening of drugs (particularly small non-peptide molecules that diffuse into tissues) and genes (Chapters 5 and 6) for possible modulation of arteriogenesis. In contrast, there is presently no mammalian mutation resulting in complete and permanent occlusion of a major artery, and such mutation might prove embryonic lethal. Surgical intervention is thus required to induce occlusion. Determination of blood flow recovery is most common utilising indirect techniques such as Doppler ultrasound (Heil, Ziegelhoeffer *et al.*, 2004), preventing direct observation. Zebrafish embryos therefore demonstrate advantages over mammalian models in determining recovery of blood flow after occlusion.

3.3.2 Recovery of Aortic Blood Flow is Independent of Vasculogenesis and Angiogenesis

To determine whether *gridlock* mutant survival resulted from abnormal vessel patterning during development transporting blood around occlusion I utilised embryos with the fli1:eGFP transgene to compare vasculogenesis and angiogenesis in wildtype and *gridlock* by laser-scanning confocal microscopy. By 5dpf *de novo* formation (vasculogenesis) of aorta and cardinal vein is complete (Isogai, Horiguchi *et al.*, 2001).

Growth and remodelling of ECs (angiogenesis) for ISV, DLAV and SIV formation has also occurred, following a standard pattern (Isogai, Horiguchi *et al.*, 2001). Any defect in patterning in *gridlock* compared to wildtype is thus easily observable.

Gridlock embryos demonstrated normal patterning of aorta and cardinal vein when compared to wildtype embryos (figure 3.2), suggesting vasculogenesis is unaffected by hypomorphic *hey2* mutation. Patterning of ISVs, DLAVs and SIVs was comparable between *gridlock* and wildtype embryos. ISV number demonstrated no difference. Normal development of communications between aorta, or cardinal vein, and SIVs was also observed in *gridlock* compared to wildtype embryos. The ISVs and SIVs form during angiogenesis, later than the aorta and cardinal vein (Isogai, Horiguchi *et al.*, 2001). These data demonstrate defective patterning during angiogenesis is not responsible for recovery of aortic blood flow in *gridlock* mutants. Further supporting this data, *Hey2* deficient mice demonstrate no apparent abnormality in vasculogenesis or angiogenesis (Gessler, Knobeloch *et al.*, 2002). Comparable vasculogenesis and angiogenesis in *gridlock* and wildtype embryos therefore demonstrates recovery of aortic blood flow in *gridlock* does not result from abnormal vessel patterning during development, and is independent of vasculogenesis and angiogenesis. It must be noted however that no histological techniques were performed to compare molecular characterisation of wildtype and *gridlock* embryos, and it therefore cannot be determined with certainty that *gridlock* vasculature is equivalent to wildtype vasculature. Such histology would provide valuable additional data.

3.3.3 Pattern and Recovery of Aortic Blood Flow Distal to Occlusion Site is not a Phenotype of *gridlock* Mutation

Angiograms generated by digital motion analysis (DMA) (Schwerte and Pelster, 2000) permitted determination of the origin of restored aortic blood flow in *gridlock* mutant embryos by determining the pattern of *gridlock* 'collateral' blood flow. In wildtype embryos (figure 3.3A) at 5dpf the majority of blood flow is transported along aorta and cardinal vein. Smaller volumes are carried by efferent ISVs transporting blood to cardinal vein, and afferent ISVs transporting blood from aorta. Only very small volumes

enter SIVs, from communications with the aorta. Blood flows in multiple directions within SIVs, reversing direction frequently.

Gridlock mutant embryos recovered aortic blood flow in one of two ways (figure 3.3B and C). Almost 90% of *gridlock* embryos restored aortic blood flow via communications between aorta and SIVs, while the remainder restored blood to the aorta via reversal of flow in afferent ISVs. As can be seen from figure 3.3B and C, both means of recovering aortic blood flow distal to occlusion can occur within the same embryo at the same time. There is no apparent difference in recovery of aortic blood flow between the two means, which may suggest these vessels most susceptible to remodelling or endogenous factors such as vasoactivity.

To demonstrate recovery of aortic blood flow in *gridlock* mutant embryos was not a phenotypic characteristic of the mutation, but a response to vascular occlusion observable in all embryos, I developed a means of occluding the proximal/mid aorta in wildtype embryos (figure 3.4) by focussed laser-energy. Previous studies demonstrated the feasibility of utilising focussed laser-energy to occlude the lateral dorsal aortae in early development (12hpf) (Serluca and Fishman, 2001; Serluca, Drummond *et al.*, 2002), however, after preliminary experimentation a later timepoint (4dpf) for aortic occlusion was found necessary. Earlier timepoints resulted in aortic rupture or fistula. Aortic ligation was not possible due to the practical difficulty of performing surgery in embryos of approximately 5mm total length at 4dpf.

Embryos with laser-induced aortic occlusion were found to recover aortic blood flow distal to occlusion. Less than 10% of embryos were observed with small numbers of erythrocytes entering the aorta immediately after occlusion, which ceased within five minutes. A passive process resulting from sudden alterations in pressure between distal aorta and patent SIVs is proposed to account for this movement. *Gridlock* mutant embryos do not demonstrate similar movements of erythrocytes. Since *gridlock* occlusion is present from earliest aortic development (Peterson, Shaw *et al.*, 2004) sudden pressure alterations might not be expected. Passive erythrocyte movement has not been observed in mammals with arterial ligation. Human arterial occlusion is generally gradual, allowing tissue time to adapt to altering pressure (Tang, Chang *et al.*,

2005), while sudden pressure alterations induced by acute occlusion requires recruitment and morphogenesis of larger magnitudes of tissue (Buschmann, Voskuil *et al.*, 2003) than in zebrafish embryos, as discussed below.

The majority of wildtype occluded embryos were observed with recovery of aortic blood flow by 22h post occlusion (figure 3.5). Angiograms generated by DMA demonstrate close similarity in development of communications between *gridlock* and wildtype occluded embryos, as is observable in figures 3.3 and 3.6. Both *gridlock* and wildtype occluded embryos recover aortic blood flow distal to occlusion by flow of blood from SIVs to aorta via short length communications. Other embryos recovered aortic blood flow through reversal of flow in afferent ISVs, as was also observed in *gridlock* embryos.

It can thus be concluded that recovery of aortic blood flow in *gridlock* mutant embryos is not a phenotypic response to hypomorphic *hey2* mutation, but a response to vascular occlusion that can occur in all zebrafish embryos. The pattern of aortic blood flow recovery in *gridlock* and wildtype occluded embryos is similar, suggesting occlusion of proximal aorta leads to similar redistributions of intravascular pressure and blood flow that then leads to similar patterns of 'collateral' blood flow. *Gridlock* mutant embryos are therefore a robust model in which to observe recovery of aortic blood flow.

Development of collateral blood flow in mammalian species after ligation surgery can occur over longer timepoints than is necessary for observation of aortic blood flow recovery in either wildtype occluded or *gridlock* zebrafish embryos. Following femoral artery ligation in mice 50% recovery of arterial blood flow is observed between three days and three weeks dependent on strain (Heil, Ziegelhoeffer *et al.*, 2004), meaning with preparation, surgery and *post mortem* analysis a single experiment might take up to two months. Timepoints can increase further as model size increases because of the time required to generate the amount of new tissue necessary for morphogenesis of vessels in larger animals (Buschmann, Voskuil *et al.*, 2003). Models of blood flow recovery in zebrafish embryos therefore provide a means of performing experiments more rapidly.

3.3.4 Recovery of Aortic Blood Flow Distal to Occlusion Site Occurs through Pre-existing Arterial Communications

It is widely accepted that arteriogenesis involves remodelling of *pre-existing* arterial communications into patent collateral vessels following arterial occlusion (Buschmann and Schaper, 1999). To provide further evidence that the mechanism of aortic blood flow recovery distal to occlusion was not vasculogenesis or angiogenesis, but rather arteriogenesis, double transgenic fli1:eGFP/gata1:dsRED wildtype embryos underwent laser-induced aortic occlusion (figure 3.7). Utilising double transgenic embryos with laser-scanning confocal microscopy provided a means of observing interactions between vasculature and blood temporally. Presence of pre-existing vessels prior to occlusion, and their recruitment following occlusion, would demonstrate independence from vasculogenesis and angiogenesis since both processes induce new vessel growth extending the vascular network (Isogai, Horiguchi *et al.*, 2001). *In vivo* observation of endothelial communications pre- and post occlusion in the same animal is difficult in mammalian species (section 1.4). Although *in vivo* X-ray angiography is achievable, communications smaller than 100µm in diameter are not identified (Mills, Fischer *et al.*, 2000). Doppler ultrasound and MRI provide indirect evidence through demonstration of blood flow in the vessels (Wagner, Helisch *et al.*, 2004). My experiment provides direct evidence of remodelling through recruitment of pre-existing vessels in arteriogenesis. It highlights one advantage of exploiting zebrafish embryos for such research. The pattern and recovery of aortic blood flow in zebrafish embryos following occlusion has already been discussed in section 3.3.3 and will therefore not be repeated here. Laser-induced aortic occlusion in transgenic embryos demonstrated existence of communications between aorta and SIVs prior to onset of occlusion. Observation of the same embryos 5h after occlusion demonstrated recovery of aortic blood flow through those same communications, suggesting 'collateral' blood flow develops through recruitment of pre-existing vessels, a key defining feature of arteriogenesis (Buschmann and Schaper, 1999).

3.3.5 Different Time-course for Recovery of Aortic Blood Flow Distal to Occlusion in *gridlock* Mutants Compared to Laser-induced Occlusion of Wildtype Embryos

Between 2dpf, when no *gridlock* mutant embryo is observed with aortic blood flow, and 5dpf over 80% of *gridlock* embryos recover aortic blood flow distal to occlusion through recruitment of pre-existing vessels. A similar percentage (90.7%) of wildtype embryos having undergone laser-induced aortic occlusion recover aortic blood flow distal to occlusion after 22h through recruitment of pre-existing vessels. I hypothesise that the more rapid recovery of aortic blood flow distal to occlusion in wildtype occluded embryos results from higher levels of haemodynamic forces prior to occlusion compared to *gridlock*. Occlusions developed by focussed laser-injury must abruptly withstand levels of force developed under powerful fully-circulating blood flow rather than cranial-only circulation of *gridlock* mutants. *Gridlock* occlusion, permanent and present from earliest aortic development, must only withstand force developed by cranial circulation, which could be much lower than haemodynamic force of full circulation. In mammalian models, falls in FSS back to physiological pre-ligation levels after onset of collateral blood flow is seen as the cause of low-level conductance in collateral vessels (Eitenmuller, Volger *et al.*, 2006). Artificially elevating levels of FSS results in significantly higher levels of conductance within collateral vessels in rabbit following femoral artery ligation (Eitenmuller, Volger *et al.*, 2006), supporting the notion of higher haemodynamic force inducing recovery of aortic blood flow more rapidly than lower levels.

Although collateral vessel development occurs at different rates dependent upon various factors including species, strain, and site of occlusion (Babiak, Schumm *et al.*, 2004; Deindl, Buschmann *et al.*, 2001; Pipp, Boehm *et al.*, 2004; Heil, Ziegelhoeffer *et al.*, 2004) it appears to follow a standard plan (figure 1.2) in mammals (Heilmann, Beyersdorf *et al.*, 2002). Occlusion results in differential gene expression, leading to release of growth factors, cytokines, and adhesion molecules (Scholz, Ito *et al.*, 2000). Monocyte/macrophage activity has also been observed at this stage (Bergmann, Hoefer *et al.*, 2006). Cell proliferation has yet to take place (Heilmann, Beyersdorf *et al.*, 2002). It is likely that I am observing only the early stages of blood vessel remodelling, which may correspond to the phase immediately post-occlusion in mammals. Gene expression

profiling of embryos without haemodynamic force has demonstrated differential gene expression within 12h between these and physiologically normal embryos (Chapter 4). Genes differentially expressed included growth factors (VEGF), cytokines (SDF-1), and adhesion molecules (integrin α2b). The importance of myeloid cells to zebrafish aortic blood flow recovery has also been demonstrated with *pu.1* knockdown resulting in significantly decreased percentages of *gridlock* with aortic flow recovery (Gray, Packham *et al.*, 2007). In mammals, proliferation and migration of ECs and VSMCs then follows (Heilmann, Beyersdorf *et al.*, 2002), before first recovery of blood flow (figure 1.2). I did not determine cell proliferation (for example, by BrdU labelling). It is presumed zebrafish aortic blood flow recovery can occur prior to cell proliferation, since recovery was observed as early as 3h post occlusion in wildtype occluded embryos, providing little time for proliferation and migration.

3.3.6 The Effect of NOS Inhibition on Recovery of Aortic Blood Flow Distal to Occlusion

Nitric oxide has been demonstrated to modulate collateral vessel formation in a wide range of species and models (Cai, Kocsis *et al.*, 2004a; Lloyd, Yang *et al.*, 2001; Yu, deMuinck *et al.*, 2005). Genetic knockout (Mees, Wagner *et al.*, 2007) and pharmacological inhibition (Lloyd, Yang *et al.*, 2001) of NOS result in delayed collateral vessel remodelling following femoral artery ligation in mammals. eNOS expression has been demonstrated in zebrafish from 3dpf in cardiomyocytes, aorta and cardinal vein (Fritsche, Schwerte *et al.*, 2000). To determine if zebrafish embryo 'collateral' vessel remodelling shares NO modulation I determined the effect of pharmacological inhibition of all NOS isoforms by the non-specific inhibitor L-NAME. L-NAME has been previously reported to cause vasoconstriction in zebrafish embryos from 3dpf (Fritsche, Schwerte *et al.*, 2000), demonstrating the early development of haemodynamic control, as well as the activity of L-NAME in zebrafish embryos. An advantage of zebrafish embryos over other models is the ability to apply small molecule inhibitors through media incubation and subsequent diffusion into embryos (Chico, Ingham *et al.*, 2008). I was therefore able to assess the effect of NOS inhibition on recovery of aortic blood flow in *gridlock* mutant embryos, and wildtype embryos

undergoing laser-induced aortic occlusion. I was also able to assess the possible role of NO-mediated vasodilatation in 'collateral' vessel formation through NOS inhibition.

Gridlock embryos were observed with only 57% of control levels of aortic blood flow recovery following L-NAME treatment from 1-5dpf ($P<0.01$; figure 3.8), suggesting that as in other species and models of vascular occlusion NO modulates 'collateral' vessel formation in zebrafish embryos following aortic occlusion. In further support of this notion, I assessed whether 'collateral' vessel remodelling of wildtype occluded embryos also shared NO modulation. At 22h, the last observation timepoint following laser-induced aortic occlusion, L-NAME treated embryos were observed with only 35% of control levels of aortic blood flow recovery ($P<0.001$; figure 3.9). This data provides further evidence to suggest that like other previously studied species NO modulates 'collateral' vessel development in zebrafish embryos following aortic occlusion.

3.3.7 NO Modulation of Embryonic Zebrafish Arteriogenesis does not Result from Modulation of Vasoactivity or Aortic Blood Velocity

NO mediates vasodilatation and cardiac contractility. To determine whether the significant decreases in percentages of embryos recovering aortic blood flow following occlusion were mediated via these processes I first treated *gridlock* embryos with L-NAME from 1-5dpf and followed it by washout for several hours. If inhibited vasodilatation was responsible for decreased percentages of blood flow recovery, L-NAME washout would rapidly return percentages to control levels, since NO-mediated vasoactivity is responsive within minutes (Fritsche, Schwerte *et al.*, 2000). Washout did not alter the percentage of aortic blood flow recovery following L-NAME treatment, suggesting inhibited NO-mediated vasodilatation does not cause decreased flow recovery. To confirm these results, I treated *gridlock* embryos for 5h at 5dpf. Again, if inhibited NO-mediated vasodilatation was responsible for decreased aortic blood flow recovery rates *gridlock* treated with L-NAME for 5h would decrease flow recovery. However, no decrease in flow recovery was observed. Therefore, it appears NO modulation of arteriogenesis in zebrafish embryos does not result from NO-mediated vasoactivity, concurring with mammalian data. Despite the volume of mammalian research linking NO to arteriogenesis little evidence suggests NO-mediated

vasodilatation is the primary modulatory role for NO in collateral vessel development, although some evidence demonstrates inhibited NO-mediated vasodilatation causing reduced blood flow in recruited collateral vessels of eNOS deficient mice (Yu, deMuinck *et al.*, 2005). Transgenic mice overexpressing human eNOS are found with increased collateral blood flow immediately after femoral artery ligation; however this did not lead to any effect on arteriogenesis (Mees, Wagner *et al.*, 2007).

NOS inhibition has been shown to cause significant reductions in heart rate in mice (Jacobi, Sydow *et al.*, 2005), demonstrating NO modulation of cardiac contractility. It is therefore possible that L-NAME inhibition of NOS in zebrafish embryos decreases percentage recovery of aortic blood flow following occlusion through modulation of cardiac contraction. Decreased heart rate may result in decreased blood flow, intravascular pressure, and FSS in remodelling communications resulting in decreased remodelling of those communications. Decreased stroke volume may also result in decreased blood velocity, because blood volume may be decreased.

To determine if recovery of aortic blood flow following occlusion was influenced by NO modulation of cardiac contractility, heart rate and aortic blood velocity in wildtype L-NAME or SNP treated embryos were studied at 5dpf. L-NAME treatment resulted in heart rates of 86% of control rates ($P<0.05$; figure 3.10), thus concurring with mammalian data which demonstrated heart rate falls by half with L-NAME treatment (Jacobi, Sydow *et al.*, 2005). This may suggest that decreased volumes of blood flow caused by falls in heart rate result in decreased percentages of embryos with aortic blood flow recovery. Treatment of sibling embryos with SNP led to no significant change in heart rate compared to untreated control sibling embryos (figure 3.11). SNP has previously been reported to have no significant affect on heart rate or stroke volume in zebrafish until 12dpf, utilising identical concentrations as I utilised (Pelster, Grillitsch *et al.*, 2005). Human intracoronary injection of SNP resulted in increased heart rate compared to control (Parham, Bouhasin *et al.*, 2004), as was also observed following intravenous administration in conscious dogs where heart rate was 88±20% of control (Pagani, Vatner *et al.*, 1978). It thus appears that NO donation causes alterations in heart

rate in developed adult mammalian hearts, but does not affect heart rate of developing zebrafish embryos.

To determine the effect of decreased heart rate on aortic blood velocity I developed a means of determining aortic blood velocity by calculating movement of erythrocytes with respect to time. Previously, it has been difficult to determine haemodynamic parameters in zebrafish embryos due to their small size preventing the use of techniques commonly performed in mammals. Aortic blood velocity has demonstrated significant reduction in the proximal aorta in a concentration dependent manner to MS-222 at 2dpf (Malone, Sciaky *et al.*, 2007), demonstrating the technique has the sensitivity required to measure subtle alterations in haemodynamic parameters in zebrafish embryos. It also demonstrates that embryos at the earliest stages of development have the physiological processes necessary for controlling haemodynamics. Although correlation between the novel Correlator software and frame-frame cell tracking was demonstrated as positive with a slope of 0.84 (figure 3.14), a Bland-Altman disagreement plot (figure 3.15) demonstrated percentage differences of up to 50%. This suggests there is significant difference between the two techniques, perhaps in the measurement of outliers, and demonstrates the importance of determining such disagreement.

L-NAME treatment did not result in significant alterations in aortic blood velocity compared to control siblings (figure 3.12) suggesting aortic blood velocity is not affected by decreased heart rate. It is possible that inhibition of vasodilatation by NOS inhibition limits the effect of decreased heart rate on aortic blood velocity, maintaining velocity via decreased vessel luminal diameters. It should be noted the power of this experiment was limited to 10.3% proximally, making it more difficult to identify changes in velocity. Erythrocyte numbers entering ISVs of 5 and 6dpf zebrafish embryos decrease significantly on L-NAME treatment, as a result of decreased vessel diameter (Fritsche, Schwerte *et al.*, 2000). However, aortic blood velocity was not determined. L-NAME treatment did not affect non-ischaemic (physiologically normal) blood flow in rat muscles (Lloyd, Yang *et al.*, 2001), while it has significantly reduced limb perfusion in mice (Jacobi, Sydow *et al.*, 2005), perhaps suggesting measurement of different indices accounts for alternative results. Fritsche, Schwerte *et al.* also

demonstrated an increased erythrocyte passage with SNP treatment, resulting from increased vessel diameter. I found no significant difference in aortic blood velocity compared to control siblings with SNP treatment (figure 3.13; power 30.3% proximally). Transgenic eNOS overexpressing mice demonstrate increases in tissue perfusion only immediately after arterial ligation compared to wildtype animals (Mees, Wagner *et al.*, 2007), described as resulting from maximal vasodilatation of vessels. Non-ischaemic hindlimb blood flow was unaffected by SNP injected in wildtype mice (Kumar, Branch *et al.*, 2008). Thus, it appears SNP treatment does not induce changes in blood velocity.

3.4 Limitations and Future Work

3.4.1 Zebrafish Embryonic Arteriogenesis is observed at its Earliest Stages

Although studying the remodelling of blood vessels into collateral vessels following occlusion in the very early zebrafish (1-5dpf) has resulted in the discovery that zebrafish undergo arteriogenesis, and has demonstrated the possibility that arteriogenesis in zebrafish embryos shares conservation with mammalian arteriogenesis, it is likely that only early stages of blood vessel remodelling are observed. Independent of model, mammalian arteriogenesis follows a standard plan (section 3.3.5; figure 1.2). At the earliest phases occlusion induces changes in gene expression and monocyte/macrophage activity (Heilmann, Beyersdorf *et al.*, 2002), both processes observed in zebrafish embryos following aortic occlusion (Chapter 4 and Gray, Packham *et al.*, 2007). Only after this first phase is cell proliferation and maturation observed. Zebrafish embryos have numerous advantages that make their exploitation in studying arteriogenesis an addition to the field. Of particular utilisation is embryonic optical transparency permitting easy observation of collateral vessel development, and gene knockdown by morpholino antisense oligonucleotides. Optical transparency decreases as embryos increase in size and develop greater amounts of pigmentation. Morpholinos remain active for only the first days of development. Thus, although research at later timepoints in zebrafish should be performed in order to further consolidate zebrafish and

mammalian arteriogenesis, zebrafish are best exploited at embryonic stages for this research.

3.4.2 Binary Assay for Determining Aortic Blood Flow Distal to Occlusion Site may limit the Nature of Data Obtained

To determine aortic blood flow recovery distal to occlusion a simple binary assay of presence or absence of aortic flow was utilised. The assay's speed permits high-throughput experimentation, and can be performed using simple light microscopy without needing to mount embryos. However, the assay prevents the determination of haemodynamic measurement such as aortic blood velocity.

Techniques now exist to permit determination of haemodynamic performance. Experimentation to determine possible blood velocity changes in collateral vessels and aorta during remodelling would provide information on vascular performance during arteriogenesis in an *in vivo* model. However, the means of determining aortic velocity I have utilised requires a large sample size to result in any significant experimental power.

Particle Image Velocimetry (PIV) could be utilised to similar effect, and would be able to determine velocity within an entire field, over multiple timepoints, resulting in two- and three-dimensional velocity maps of a vessel.

3.4.3 Zebrafish Embryonic Collateral Vessels Lack Molecular Characterisation

The research outlined within this chapter was performed to determine whether exploitation of zebrafish embryos could yield new models of arteriogenesis: remodelling of pre-existing communications following arterial occlusion. Having determined that pre-existing vessels do remodel following arterial occlusion, an important next step is to characterise the nature of collateral vessels further. To fully exploit these novel models of arteriogenesis, physiological and molecular characterisation of collateral vessels should be determined. In this way it would be possible to further determine whether arteriogenesis in zebrafish embryos is conserved with mammalian arteriogenesis, or whether the mechanisms are different yet share some degree of conservation (for example, response to NOS inhibition, as demonstrated).

Methods for physiological characterisation such as BrdU staining to determine cell proliferation, and molecular characterisation such as *in situ* hybridisation and Western blot analysis, are performed with *ex vivo* tissue or tissue samples, but may still yield novel data. Utilisation of *ex vivo* tissue contradicts a key advantage of exploiting zebrafish embryos for such research: that of an *in vivo* model system. In addition, the number of antibodies available for Western blot analysis in zebrafish remains small.

3.5 Conclusion

My data demonstrates that zebrafish embryos are able to undergo a process akin to arteriogenesis to perfuse the aorta with blood flow through pre-existing communications following aortic occlusion. I have demonstrated that the process is not a phenotypic response to *gridlock* mutation, but a response to vascular occlusion that can occur in wildtype embryos following laser-induced aortic occlusion.

I have shown that like mammalian arteriogenesis, recovery of aortic blood flow distal to occlusion site in *gridlock* mutants and wildtype embryos having undergone laser-induced aortic occlusion is modulated by NOS inhibition. I have also demonstrated that modulation by NOS inhibition is not a result of modulating vasoactivity or aortic blood velocity.

In short, I have exploited the zebrafish embryo to develop two models, one high-throughput (*gridlock* mutant embryos) and one low-throughput (laser-induced aortic occlusion of wildtype embryos) useful for the study of collateral vessel remodelling. With its many advantages, I believe using zebrafish embryos to study collateral vessel remodelling adds a complementary tool to mammalian models for further elucidating arteriogenesis.

Chapter Four

Role of Haemodynamic Force in Altering Gene Expression

Chapter 4: Role of Haemodynamic Force in Altering Gene Expression

Having exploited zebrafish embryos to develop two models of arteriogenesis (Chapter 3) I wanted to further exploit the advantages of zebrafish embryos to investigate the role of haemodynamic force in modulating gene expression. Many pro-arteriogenic genes are differentially expressed with altered levels of haemodynamic force (Schaper and Ito, 1996). Development of collateral vessels is induced when ECs previously experiencing little or no haemodynamic force are exposed to the force. Gene expression following onset of cardiac contraction, with ECs suddenly exposed to haemodynamic force, may be analogous to collateral vessels suddenly exposed to haemodynamic force. Therefore, in this chapter I describe combining the advantages of zebrafish embryos with current microarray technology to identify candidate genes with the potential to modulate arteriogenesis, through comparing gene expression under physiological levels of haemodynamic force and its absence.

4.1 Introduction

4.1.1 Cardiac Contraction

Myocytes are the contractile cells of the myocardium and are comprised of myofibrils, which are in turn constructed of myofilaments, constructed of sarcomeres (figure 4.1A). Sarcomeres consist of filaments of actin and myosin, which slide past one another during excitation-contraction coupling, leading to sarcomere shortening, myocyte shortening, and thus at the whole organ scale, muscle contraction.

Actin forms a filament consisting of two α-helical strands of globular actin molecules. With tropomyosin and troponin molecules the actin filament forms a regulatory complex controlling binding of the myosin head to the filament. Between the two strands of the actin filament lies a rod shaped tropomyosin molecule, upon which binds troponin-T, -C, and -I.

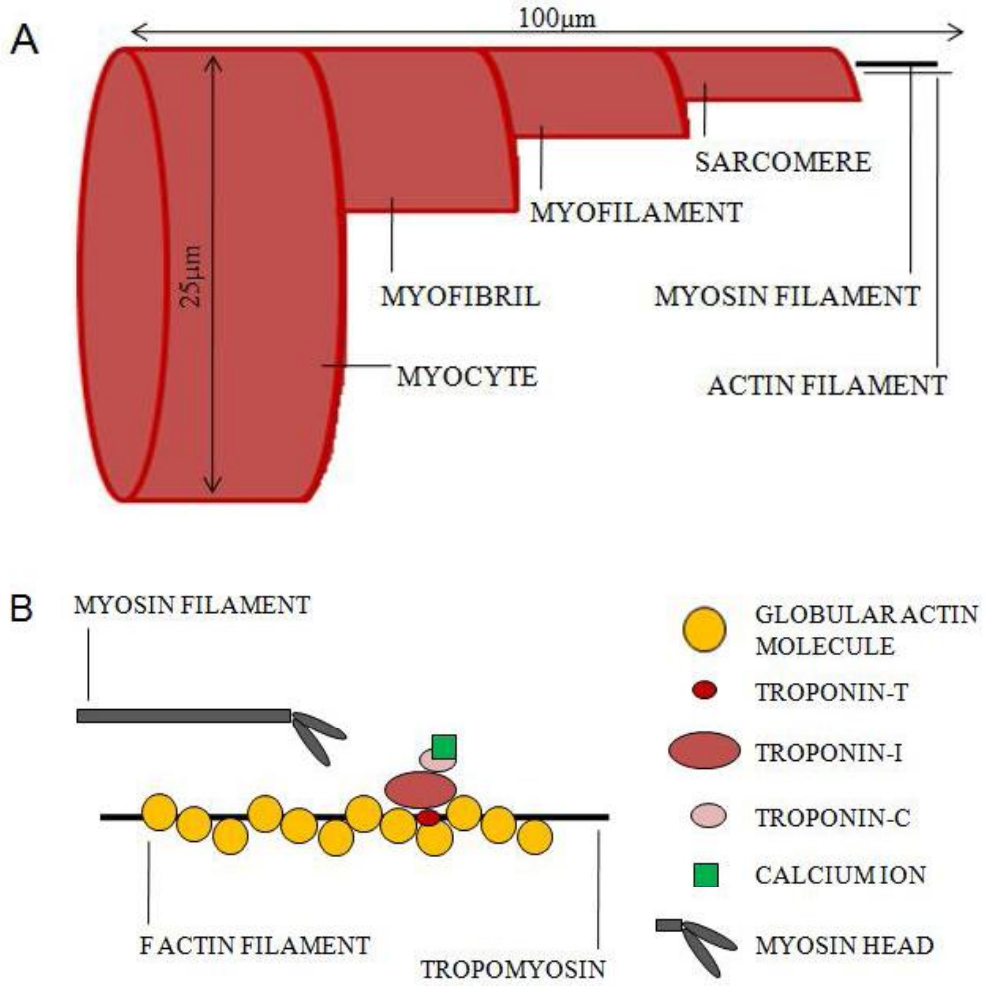

Figure 4.1 Anatomical and molecular composition of myocytes.
A, Simplified diagram of myocyte anatomy demonstrating the different structures which comprise the myocyte. B, Actin-myosin association during cross-bridge formation. Troponin-T binds the rod-shaped tropomyosin molecule, while troponin-I inhibits the myosin head binding site of the F actin filament. Calcium ions bind to troponin-C to initiate the conformational change of the troponin complex which frees the myosin head binding site.

Troponin-T binds the tropomyosin molecule, while troponin-C serves as a binding site for free intracellular Ca^{2+}, and troponin-I blocks the myosin ATP-dependent binding site on the actin filament (figure 4.1B) (Klabunde, 2005; Bers, 2002). At low $[Ca^{2+}]_i$ myosin head binding sites on the actin filament are inhibited by tropomyosin's positioning.

4.1.2 Excitation-Contraction Coupling

Upon myocyte depolarisation L-type calcium channels on the plasma (sarcolemma) membrane alter to an open conformation allowing influx of Ca^{2+} into myocytes. The influx leads to calcium-induced calcium release of Ca^{2+} within the sarcoplasmic reticulum (SR) through the activation of ryanodine receptors on the SR membrane (Davies, Blakeley *et al.*, 2001). Free cytosolic Ca^{2+} binds troponin-C causing a conformational change that alters the position of tropomyosin against the actin filament, thereby exposing the myosin head binding site. ATP hydrolysis to ADP + Pi provides the energy necessary for a conformational change resulting in a 'ratchet' action of the myosin head, pulling the actin filament towards the centre of the sarcomere (Bers, 2002), decreasing sarcomere length and resulting in muscle contraction when scaled up to the myocardial level. Ca^{2+} entry into myocyte cytoplasm slows, allowing uptake into SR by Ca^{2+}-ATPases, sarcolemmal Na^{+}/Ca^{2+} exchanger, and mitochondrial Ca^{2+} uniporter. This results in less free Ca^{2+} to bind troponin-C, and a reverse conformational change occurs so that tropomyosin competitively inhibits the myosin head binding site (Bers, 2002; Klabunde, 2005; Levy, 2005).

4.1.3 Zebrafish *silent heart* Mutation

The zebrafish mutant *silent heart* has been shown to result from reduced *tnnt2* expression caused by mutated protein sequence. Phenotypically, *silent heart* embryos present a non-contractile heart. During development, pericardial oedema forms, and the endocardial lining separates from the surrounding myocardium (Sehnert, Huq *et al.*, 2002). Death ensues by 7dpf (Sehnert, Huq *et al.*, 2002).

4.1.4 Microarray Technology

Microarrays allow quantitative assessment of target samples: be they cDNA, mRNA, protein, or tissue (Jayapal and Melendez, 2006). This section focuses on cDNA and oligonucleotide microarrays, utilising mRNA, since I wished to determine differential gene expression with altered haemodynamic force. These microarrays permit assessment of expression levels of thousands of genes in a single experiment, providing a means for assessing alterations in gene expression at the genome level (Affymetrix). Other techniques for determining gene expression such as Northern blots, *in situ* hybridisation, and reverse transcription PCR are unsuitable for multiple gene expression analysis (Jayapal and Melendez, 2006) since the number of genes analysed in one experiment is limited (Lockhart, Dong *et al.*, 1996; McCormick, Eskin *et al.*, 2001). Oligonucleotide microarrays (such as Affymetrix GeneChips) are versatile, sensitive and specific while providing standardisation and reproducibility (Jayapal and Melendez, 2006). These factors result from *in situ* oligonucleotide synthesis of probe sets defined by their ability to hybridise target genes (Jayapal and Melendez, 2006). Oligonucleotide design allows regions homologous to other genes to be avoided, thereby avoiding non-specific hybridisation (Gerhold, Rushmore *et al.*, 1999). Oligonucleotide probes also remove requirement for maintaining cDNA clones necessary for cDNA microarrays (Gerhold, Rushmore *et al.*, 1999). Oligonucleotide microarrays consist of numerous DNA sequence probes sets (11-20 probe pairs) synthesised to substrate at known locations (Liu, Milo *et al.*, 2005). Each probe pair consists of perfect match and mismatch probes, in which a single base is made complimentary to a base on the perfect match probe (Liu, Milo *et al.*, 2005). The slight alteration in probe sequence allows measurement of non-specific hybridisation, which occurs when target mRNA sequences are not perfectly complimentary to probe (Liu, Milo *et al.*, 2005). Probe sets are used in qualification and quantification of target binding, detected through fluorescent labelling of target RNA (Affymetrix). Specific detail regarding methodology for performing oligonucleotide (Affymetrix) microarrays can be found in section 2.8.4. Samples are hybridised separately on different chips utilising a single fluorescent label (Lockhart, Dong *et al.*, 1996). cDNA microarrays (Schena, Shalon *et al.*, 1996), in contrast, label nucleotides before simultaneous hybridisation onto the same array (Lockhart, Dong *et al.*, 1996).

Limitations to microarray technology include possible differences between mRNA and protein levels, cost, and requirement for skilled personnel (Jayapal and Melendez, 2006).

4.1.5 Influence of Laminar Flow on Gene Expression

Haemodynamic force, comprising FSS, cyclic stretch and other less studied forces such as longitudinal stretch, influence gene expression (Schaper and Scholz, 2003), and many pro-arteriogenic genes are differentially expressed with altered levels of haemodynamic force (Schaper and Ito, 1996). Microarray analysis of HUVECs following 24h FSS exposure mimicking physiological laminar flow rheology of arteries demonstrated a significant downregulation of *endothelin-1* (*ET*) and *MCP-1*, and upregulation in *Tie-2* and *Jagged1* (McCormick, Eskin *et al.*, 2001), genes known to have roles in vessel formation and remodelling. A sustained decrease in ET mRNA and peptide levels was also observed in bovine aortic ECs following FSS exposure compared to no flow cultures, which was maintained for several hours after the removal of FSS from the system (Malek, Greene *et al.*, 1993), suggesting *ET*, *MCP-1* and other genes differentially expressed are partially regulated by haemodynamic force. Similar analysis in human aortic ECs led to differential expression of 125 genes compared to no flow cultures. Genes upregulated included *Notch4*, *VEGFR2*, *Tie-2*, and *vimentin*, while those downregulated included *Jagged1* (Chen, Li *et al.*, 2001). Once more, these genes are noted for their involvement in controlling cardiac performance (e.g. *VEGFR2* (Jacobi, Tam *et al.*, 2004), or cell shape (e.g. *vimentin*), which necessarily undergo alteration during remodelling (Cai, Kocsis *et al.*, 2004b). These studies provide evidence of EC gene expression under approximate physiological conditions (i.e. ECs under FSS), and therefore provide us with knowledge desirable in determining changes in gene expression under pathological conditions. Atherosclerotic plaques, for instance, develop at areas of turbulent rather than laminar flow conditions (Yoshizumi, Abe *et al.*, 2003).

4.1.6 Influence of Turbulent Flow on Gene Expression

Microarray analysis of HUVECs treated with turbulent rather than laminar flow for 24h resulted in gene expression closest to that of no flow cultures (Garcia-Cardena, Comander *et al.*, 2001). HUVECs exposed to laminar flow demonstrated differential expression of 100 genes compared to HUVECs under turbulent flow of similar force (Garcia-Cardena, Comander *et al.*, 2001). The results demonstrate the capacity of ECs to detect differences in flow patterns (Ohura, Yamamoto *et al.*, 2003). Several cytoskeletal elements including vimentin demonstrated significant upregulation with laminar flow compared to no flow cultures, supporting the hypothesis that active remodelling of cytoskeletal elements takes place when ECs are exposed to FSS (Garcia-Cardena, Comander *et al.*, 2001). Similar experiments were performed to observe the affect of turbulent flow on pig aortic ECs compared to laminar flow. The aortic ECs demonstrated significant upregulation of vascular specific genes such as the ET precursor *preproendothelin* with turbulent flow (Himburg, Dowd *et al.*, 2007), concurring with previous studies that demonstrate a downregulation in ET in conditions of laminar flow (Malek, Greene *et al.*, 1993), and suggesting a flow-related regulation of ET. *MCP-1* follows a similar pattern of expression. Laminar flow demonstrated downregulation (Malek, Greene *et al.*, 1993), while turbulent flow led to upregulation (Himburg, Dowd *et al.*, 2007). Also significantly upregulated under turbulent flow was *PCNA, proliferating cell nuclear antigen*, a gene expressed during cell proliferation, suggesting turbulent flow induces proliferation.

4.1.7 Influence of Haemodynamic Force on EC-VSMC Interactions

The vasculature is not formed of ECs in isolation. ECs are physically close to, and interact with, other cell types, particularly VSMCs and pericytes. It is thus important to observe the influence of haemodynamic force on EC-VSMC interaction.

A co-culture of human aortic ECs and human aortic VSMCs was submitted to 4h or 24h FSS. The two cell populations were then separated, and underwent microarray analysis independently (Heydarkhan-Hagvall, Chien *et al.*, 2006). ECs demonstrated differential expression of nearly 700 genes following 4h FSS, this number falling to approximately 300 after 24h FSS (Heydarkhan-Hagvall, Chien *et al.*, 2006); providing further evidence

of the temporal nature of gene expression under the influence of FSS. Following 24h FSS in VSMCs, 200 genes were differentially expressed. Of most interest, 20 genes were upregulated and 36 downregulated in both ECs and VSMCs at the 24h timepoint (Heydarkhan-Hagvall, Chien *et al.*, 2006) demonstrating the importance of considering EC-VSMC interaction. For instance co-culture resulted in increased expression of *MCP-1* compared to EC monoculture when determined by RT-PCR (Chiu, Chen *et al.*, 2004). On addition of FSS to co-cultured cells, altered gene expression was lost, perhaps suggesting an atheroprotective role for FSS in downregulating expression of pathological genes induced by EC-VSMC interactions.

4.1.8 Influence of Cyclic Stretch on Gene Expression

Stretch of VSMCs cultured on deformable substrate has demonstrated regulation of proliferation, migration and apoptosis of cells, as well as ECM breakdown (Haga, Li *et al.*, 2007) by mechanical force. It has been suggested that the influence of cyclic stretch on gene expression is of greater importance than FSS, since it has a force two orders of magnitude higher (Heil and Schaper, 2004). VSMCs mechanically deformed with low levels of stretch resulted in three of 5000 possible genes upregulated and 13 downregulated two-fold (Feng, Yang *et al.*, 1999). *MMP1* demonstrated significant downregulation, perhaps in order to inhibit breakdown of ECM required to withstand stretch. HUVECs under cyclic stretch upregulate expression of MCP-1 mRNA and protein (Demicheva, Hecker *et al.*, 2008). In contrast, increased FSS had no effect on *MCP-1* expression, although ECs adapted to low FSS demonstrate significant *MCP-1* downregulation with increasing FSS levels (Demicheva, Hecker *et al.*, 2008). A further study demonstrated differential expression of 11 of 4000 genes arrayed in HUVECs under conditions of cyclic stretch (Frye, Yee *et al.*, 2005), suggesting cyclic stretch is not an important gene expression regulator in ECs or that stretch induces a highly specific gene set. Some genes (*heat shock proteins 10*, *47*, and *90β*) upregulated were linked to oxidative stress. One, *TGFβ* stimulating proliferation, has been associated with arteriogenesis (Van Royen, Piek *et al.*, 2001b).

4.1.9 Studying Modulation of Gene Expression by Haemodynamic Force *in vivo*

Despite attempts to more closely mimic *in vivo* physiology, such as the co-culture of ECs and VSMCs (Heydarkhan-Hagvall, Chien *et al.*, 2006), studies to determine the modulation of gene expression by haemodynamic force and alterations in haemodynamic force have been performed *in vitro* utilising cell culture flow assays. It is difficult to extrapolate *in vitro* studies to the *in vivo* situation, since more complex interactions occur including interactions with non-vascular cell-types (Clayton, Chalothorn *et al.*, 2008). Likewise, arteriogenesis requires the cooperation of vascular and non-vascular cell-types (Heilmann, Beyersdorf *et al.*, 2002) as well as endogenous modulation (Lloyd, Yang *et al.*, 2001), and therefore the study of haemodynamic force and its relationship to arteriogenesis is best studied in an *in vivo* setting. Furthermore, while effects of FSS or cyclic stretch have been studied independently, *in vivo* many haemodynamic forces interact simultaneously.

It is difficult to modulate haemodynamic performance in mammalian models for *in vivo* microarray analysis. Surgery induces inflammation and necrosis. Manipulation of blood flow can induce ischaemia, which itself alters gene expression (Flamant, Toffoli *et al.*, 2009), and to which arteriogenesis has been demonstrated to be independent (Heil, Eitenmuller *et al.*, 2006). One study set out to determine gene expression profiles in an active area of collateral vessel growth following femoral artery ligation in mice compared to sham operated animals (Lee, Stabile *et al.*, 2004). 783 genes demonstrated at least two-fold change in expression in ligated animals compared to sham controls at one or more of five timepoints ranging from six hours to 14 days. Genes with known roles in arteriogenesis such as *MCP-1* and *TGFβ* were upregulated in ligated animals, however the largest functional group of genes identified with significant differential gene expression were those involved in inflammation. The zebrafish embryo does not suffer hypoxia under standard incubation conditions (Schwerte, Uberbacher *et al.*, 2003) prior to 14dpf even in the absence of blood flow (Pelster and Burggren, 1996). Necrosis and inflammation are rarely observed in gene knockdown through MO injection (Summerton and Weller, 1997), the technique I employed. Furthermore, the advantages of the model can be exploited to more rapidly elucidate the role of candidate genes in modulation of arteriogenesis than can occur with mammalian models.

4.2 Results

4.2.1 Embryonic Development is Unaffected by *tnnt2* Knockdown

Wildtype embryos were injected with *tnnt2* or standard control MO at the 1-4 cell stage and observed microscopically for cardiac contraction at 30hpf, allowing time for any contraction to initiate. In wildtype embryos, contraction begins at approximately 26hpf (Chen, Haffter *et al.*, 1996). Contraction was not observed in the vast majority of *tnnt2* morphants (approximately 95% of morphants over the course of experimentation). *tnnt2* morphants with contraction were removed prior to RNA extraction. All control morphants were observed with contraction and blood flow. *tnnt2* morphants developed normally, dechorionating without mechanical aid from 48hpf like control morphants. They responded to touch stimuli, demonstrating non-cardiac muscle to be unaffected by *tnnt2* knockdown. However, by 60hpf *tnnt2* morphants developed pericardial oedema, as reported by Sehnert, Huq *et al*. (2002).

4.2.2 Vasculogenesis and Angiogenesis are Unaffected by *tnnt2* Knockdown

In order to demonstrate whether vasculogenesis and angiogenesis occurred comparably to standard control MO injected sibling embryos under conditions of absent blood flow (*tnnt2* morphant embryos), I performed laser-scanning confocal microscopy of fli1:eGFP embryos injected with *tnnt2*/control MO at 60hpf, the latest timepoint at which the microarray analysis was performed.

Vasculature of approximately 20 morphants per group was observed under fluorescence stereomicroscopy and representative morphants (2 per group) randomly chosen for confocal microscopy. Figure 4.2 demonstrates representative lateral views of morphant embryonic vasculature. All *tnnt2* morphants demonstrated normal patterning and formation of aorta and cardinal vein compared to control morphants. As reported in previous chapters, aorta and cardinal vein develop *de novo* during vasculogenesis by *in situ* differentiation of angioblasts during the first 24hpf (Isogai, Horiguchi *et al.*, 2001). Their normal patterning and formation in *tnnt2* morphants suggests vasculogenesis is not affected by *tnnt2* knockdown in zebrafish embryos.

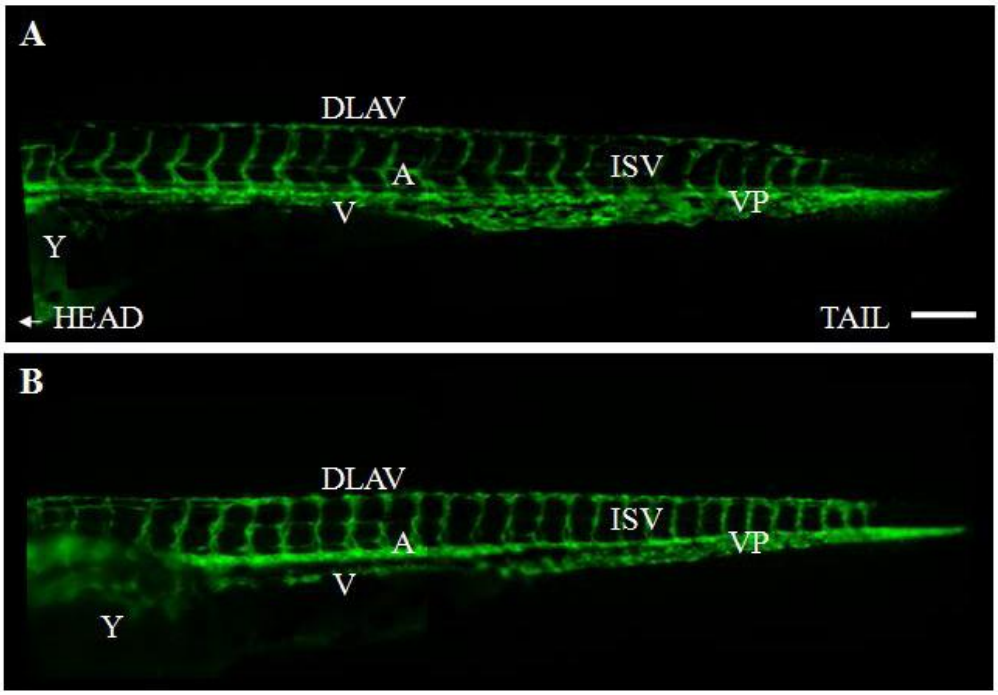

Figure 4.2 Laser-scanning confocal microscopy of fli1:eGFP transgenic embryos at 60hpf injected with *tnnt2*/control MO.

Lateral view of a representative fli1:eGFP transgenic embryo at 60hpf injected with control (A) or *tnnt2* (B) MO. Absent blood flow does not affect vasculogenesis or angiogenesis. Yolk-sac swelling can be just determined in *tnnt2* morphants. At=aorta, V=cardinal vein, VP=venous plexus, ISV=intersegmental vessels, DLAV=dorsal longitudinal anastomotic vessels, Y=yolk-sac. A and B composed of 4 images. Scale bar 200μm.

These vessels in *tnnt2* morphants appeared collapsed, presumably due to absence of blood flow. *tnnt2* morphants demonstrated normal patterning and number of ISVs. DLAVs and SIVs also developed normally when compared to control morphants. ISVs, DLAVs, and SIVs develop after aorta and cardinal vein by growth and remodelling of these vessels in angiogenesis (Isogai, Horiguchi *et al.*, 2001). Normal development of vessels formed during angiogenesis suggest the process is unaffected by *tnnt2* knockdown.

4.2.3 Absent Blood Flow Results in Differential Gene Expression Profiles During Early Development

The microarray was designed to demonstrate alterations in gene expression that may occur with changes in haemodynamic forces since this is a stimulus of arteriogenesis. In order to determine the effect of absent blood flow, and therefore absent haemodynamic force, on gene expression during early embryonic development *in vivo* a total of 18 Affymetrix GeneChip Zebrafish Genome arrays were utilised. The chips corresponded to 18 groups of 100-130 age-matched *tnnt2*/control MO injected wildtype embryos. Total RNA was extracted with Trizol (Sigma, Poole, UK) at three timepoints: 36, 48, and 60hpf. These timepoints were chosen since they represent the first 2.5 days during which blood circulates vasculature in wildtype embryos (Isogai, Horiguchi *et al.*, 2001). Although a timepoint prior to onset of circulation may have been beneficial to demonstrate gene expression of *tnnt2* mutants was comparable to wildtype embryos, the aim of the microarray was to observe the effect on gene expression of *changes* in haemodynamic forces, since this results in induction of arteriogenesis. Prior to RNA extraction at 36hpf, all embryos underwent manual dechorionation with Dumont #4 tweezers (WPI, Florida, USA), since natural dechorionation had yet to occur. Embryos injured during dechorionation were excluded. At 48 and 60hpf morphants that had not yet naturally dechorionated underwent manual dechorionation. At each timepoint RNA was extracted from three replicate groups of *tnnt2* or control morphants. Each *tnnt2* replicate group was matched to control derived from the same parent pair, with equal numbers of morphants in groups. RNA cleanup was performed with Qiagen RNeasy Mini Kit, and resulting RNA quantified and quality assessed by NanoDrop. Samples

with purity (Ab^{260}/Ab^{280}) of 1.8-2.0 were used in microarray analysis. To prevent degradation, RNA extraction was performed on ice (4°C) and protective equipment worn. On completion, RNA was immediately stored at -80°C. RNA was quality assessed again immediately prior to generation of cDNA, the first step of gene expression analysis (section 2.8.4.1), and at appropriate points during analysis.

Data was analysed by probabilistic model performing probe-level analysis (Liu, Milo *et al.*, 2005; Sanguinetti, Milo *et al.*, 2005). A cut-off of a two-fold change in gene expression with 80% probability was used to identify a list of candidate genes with differential expression between control/*tnnt2* morphants. Candidate genes were clustered using GeneSpring GX (version 7.3.1, Agilent Technologies), and Gene Cluster 3.0 (de Hoon, Imoto *et al.*, 2002) and Treeview 1.6 software (Eisen, 2002). Protein Analysis Through Evolutionary Relationships (PANTHER) gene ontology (Thomas, Campbell *et al.*, 2003) classified genes into groups based on biological process, and was used to determine fractional difference of *tnnt2* compared to control. The number of differentially expressed genes in each biological process against the total number of genes (differentially + undifferentially expressed) categorised to each process: (number of genes observed in biological process – number of genes expected in biological process)/number of genes expected in biological process.

Experiments conformed to the Minimum Information About a Microarray Experiment (MIAME) proposal (Brazma, Hingamp *et al.*, 2001), which seeks to define the minimum information required to ensure data is easily interpretable. The data has been deposited in the Gene Expression Omnibus http://www.ncbi.nlm.nih.gov/geo/ Accession GSM207470 and will be freely available following publication of the data. Pubmed literature searches (www.pubmed.gov) were performed to identify genes of interest.

Replicate gene array chips for both control and *tnnt2* demonstrated a low degree of variability (figure 4.3). Variability was improved by normalisation (figure 4.4). Both control and *tnnt2* demonstrated a trend of increasing total gene expression from 36-48hpf, followed by a decrease from 48-60hpf (figure 4.5).

290 genes were differentially expressed by the parameters. 166 genes had a significant decrease in gene expression ratio in *tnnt2* compared to control (1.1% of total genes on chip). 124 genes had a significant increase in gene expression ratio in *tnnt2* (0.8% of total genes on chip) compared to control (figure 4.6). Seven, encoding genes of metabolism such as the cytochrome P450 system (*CYP26B1*) had expression ratios which increased and decreased in *tnnt2* compared to control. This may result from presence of different gene isoforms on the GeneChip. Figures 4.7 and 4.8 demonstrate diagrammatically changes in gene expression over the three timepoints in *tnnt2* morphants compared to control.

The majority of genes (71.4%) with decreased expression ratios in *tnnt2* compared to control were observed at 48hpf and included genes linked to developmental patterning (*ephrinB1*/*EFNB1*) (Frisen, Holmberg *et al.*, 1999) and those of myeloid lineage (*SPI1*/*PU.1*). As well as its involvement in cell fate during patterning, ephrinB1 also modulates vessel development during angiogenesis (Adams, Wilkinson *et al.*, 1999), a process part driven by haemodynamic force (Carmeliet, 2000). *EphrinB1'*s decreased expression in absent blood flow concurs with data from the related ligand ephrinB2, which demonstrates decreased mRNA and protein levels with falls in blood flow induced by ligation of the chick vitelline artery (le Noble, Moyon *et al.*, 2004). SPI1 is a myeloid-specific transcription factor which plays an important role in monocyte development (Lieschke, Oates *et al.*, 2002). Monocytes are directed to sites of injury by a series of processes induced by altered haemodynamic force (Heilmann, Beyersdorf *et al.*, 2002), and thus a decreased *SPI1* expression might be expected in conditions of absent force. 37 genes (18.9%) demonstrated decreased expression ratios at the earliest timepoint of 36hpf. These genes included adrenoceptors such as *adrenoceptor 2B* (*ADRA2B*), *2C* and *2Da*, as well as *endothelin receptor B* (*EDNRB*).

Their decreased expression might suggest absent haemodynamic force limits expression, since there would be less requirement for vascular control compared to control siblings. ENDRB is expressed on ECs and VSMCs (Murakoshi, Miyauchi *et al.*, 2002; Bagnall, Kelland *et al.*, 2006), the latter responding to cyclic stretch induced by blood flow.

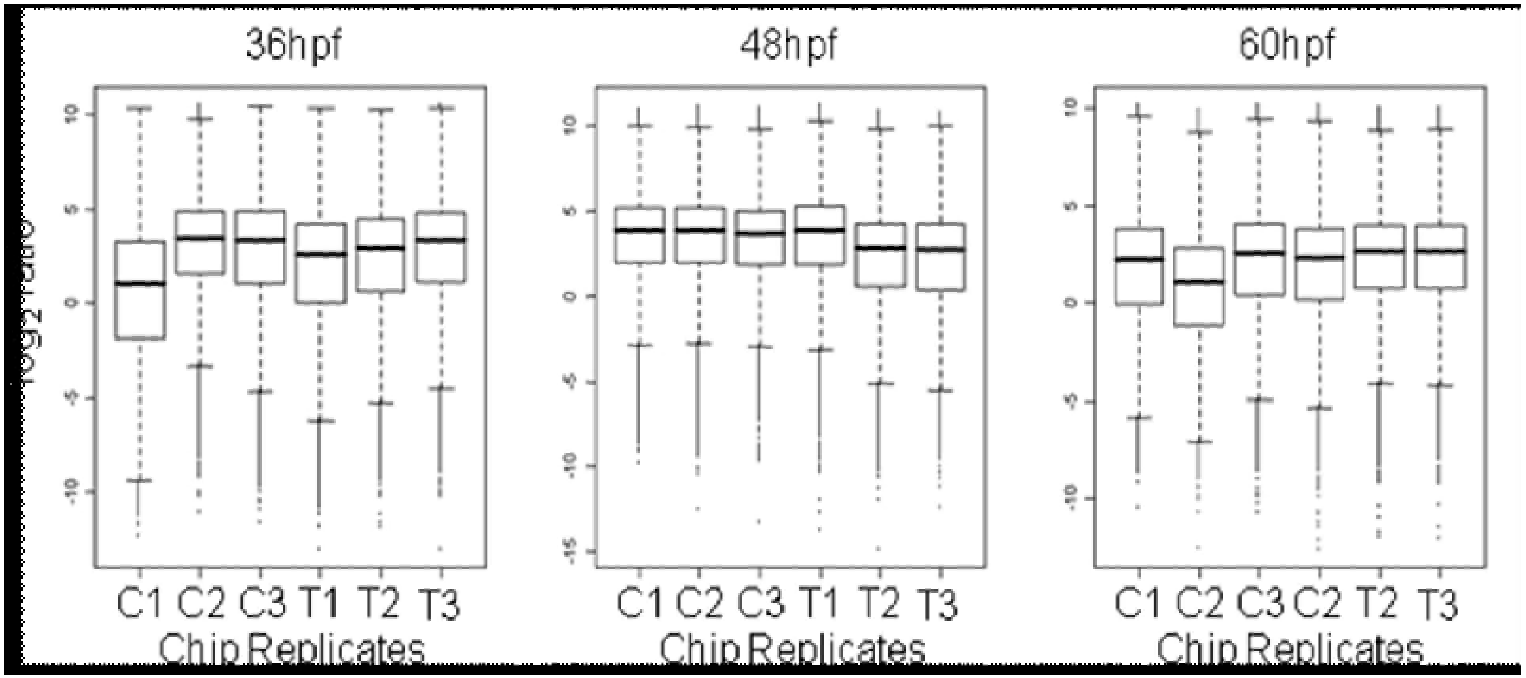

Figure 4.3 Replicate gene array chips for control and *tnnt2* morphants demonstrate a low degree of variability.
In both control and *tnnt2* gene array chips, variability was demonstrated to be low between replicate chips at all three timepoints. C=control, T=*tnnt2*.

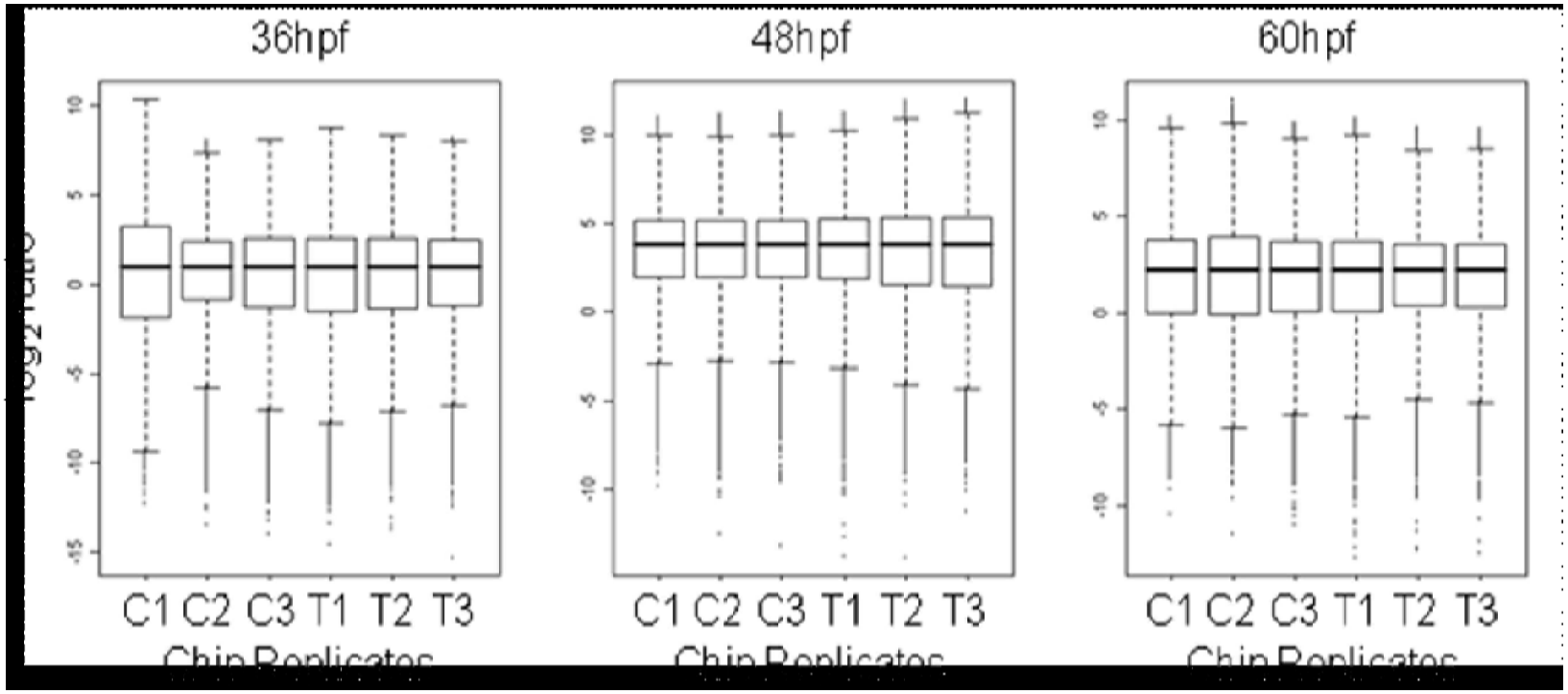

Figure 4.4 Variability between replicate gene array chips was improved by normalisation.
The variability observed between replicate gene array chips was improved by normalisation. C=control, T=*tnnt2*.

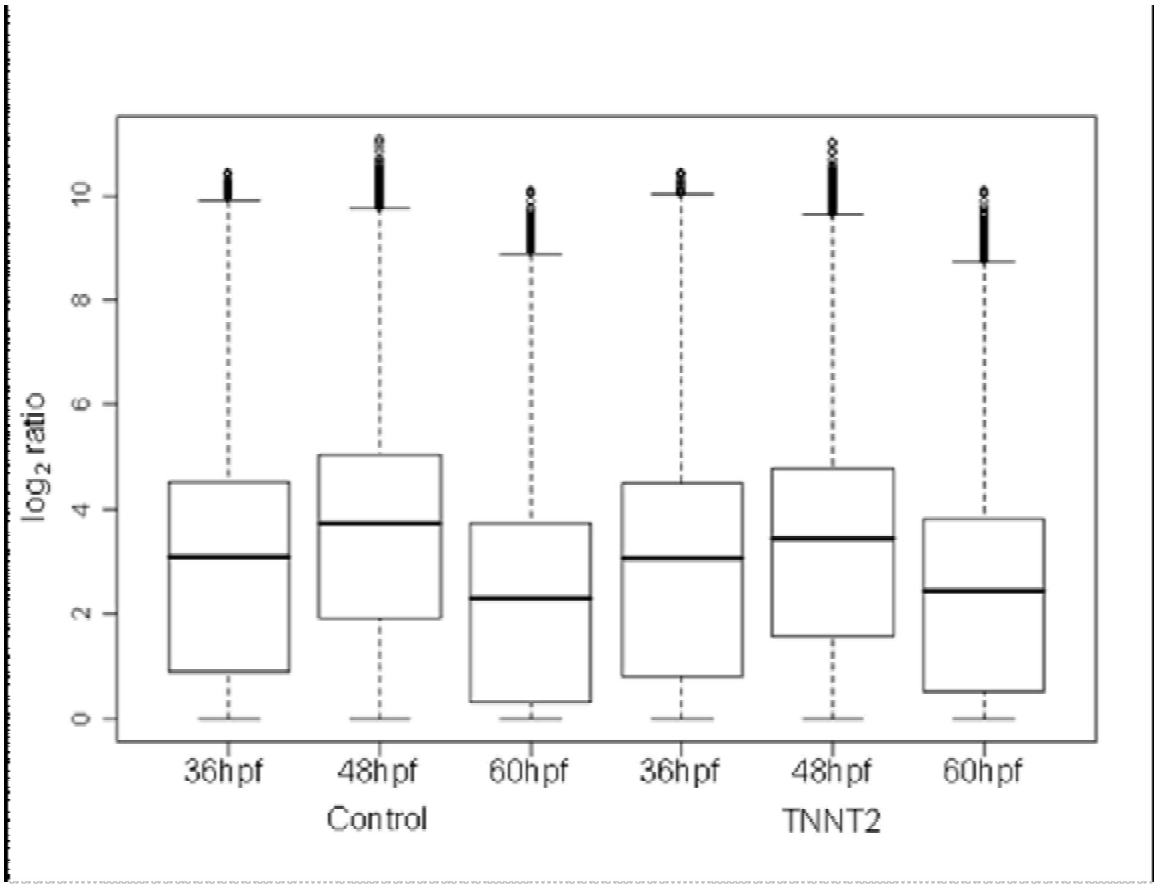

Figure 4.5 Total gene expression levels of control and *tnnt2* over time.
In both control and *tnnt2* groups, a trend of increasing total gene expression is demonstrated from 36-48hpf, followed by a decrease from 48-60hpf.

Concurring with my data, onset of cyclic stretch induced significant upregulation of EDNRB mRNA (Cattaruzza, Dimigen *et al.*, 2000). The smallest number of genes (19 of 166) with decreased expression ratios was observed at 60hpf, including *rhodopsin* (*RHO*), a molecule important in light perception. A very small number of genes demonstrated decreased expression ratios at more than one timepoint, including *adrenoceptor 2Da* differentially expressed at 36 and 48hpf. The sustained depression in expression of these genes may highlight the importance of their relationship with haemodynamic force. No genes demonstrated decreased expression ratios at all three timepoints.

Of genes with increased expression ratios in *tnnt2* compared to control, the majority were observed at 60hpf (91 of 124). This group included *VEGF*, whose receptors are specific to ECs and monocytes/macrophages (Hiratsuka, Minowa *et al.*, 1998), cell types involved in vessel remodelling following alterations in haemodynamic force. Indeed, VEGF induces vessel growth following alterations in haemodynamic force (Babiak, Schumm *et al.*, 2004). *VEGF* upregulation predominantly occurs through binding of HIF-1 to the VEGF promoter (Forsythe, Jiang *et al.*, 1996) under hypoxic conditions. However, *HIF-1*, and other hypoxia-induced genes such as *lactate dehydrogenase A* (Deindl, Buschmann *et al.*, 2001) did not demonstrate differential expression in *tnnt2* despite their presence on the GeneChip, suggesting increased *VEGF* expression in this microarray is not in response to hypoxia.

22 genes (17.4%) demonstrated increased expression ratios at 36hpf, including *plastin 1* (*PLS1*). At 48hpf the same number of genes demonstrated increased expression ratios. These included *CXCR4a*, the receptor for stromal-cell derived factor-1 (SDF-1), expressed on macrophages (Jin, Shido *et al.*, 2006). It has been demonstrated that $CXCR4^{+}$ cells induce neovascularisation following MI in mice (Morimoto, Takahashi *et al.*, 2007), again linking monocytes/macrophages with haemodynamic force and subsequent vessel remodelling. Very small numbers of genes demonstrated increased expression ratios at two or all three timepoints.

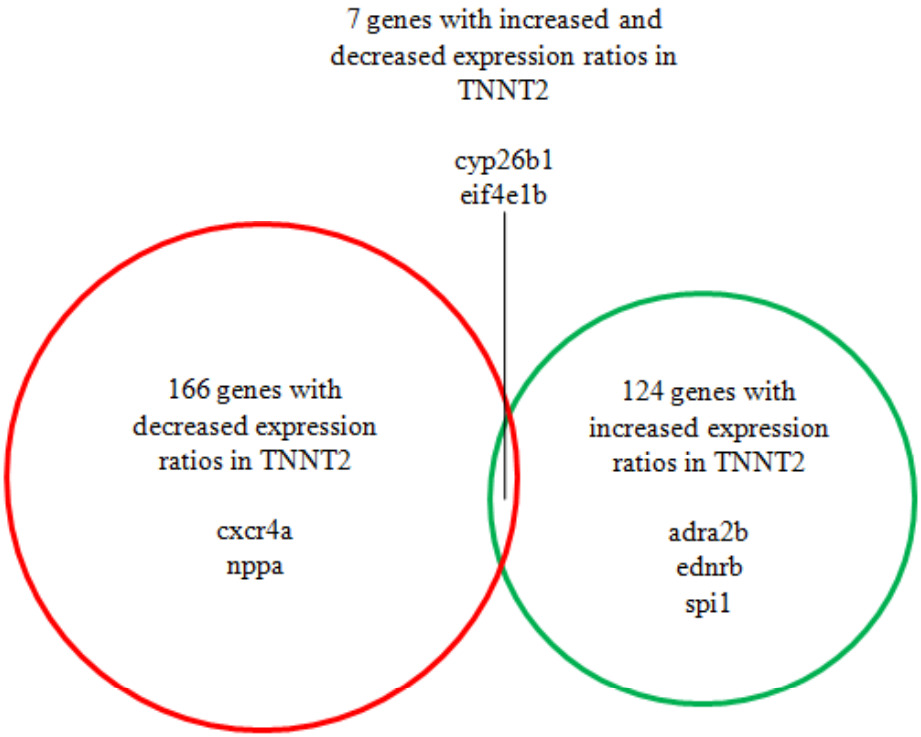

Figure 4.6 Venn diagram of differential gene expression in *tnnt2* compared to control groups.

Genes were classed as differentially expressed if there was ≥two-fold difference in expression between *tnnt2* and control with ≥80% probability. Genes listed in the figure represent examples differentially expressed in that group. In total 290 genes were differentially expressed. 166 (red circle) demonstrated a decrease in expression ratio in *tnnt2* compared to control including *CXCR4a* and *natriuretic peptide precursor A* (*NPPA*). 124 demonstrated an increase (green circle) including *adrenoceptor 2B* (*ADRA2B*), *endothelin receptor B* (*EDNRB*) and *SPI1*. 7 genes demonstrated both increased and decreased expression ratios. These encoded genes of general metabolism such as the cytochrome P450 system (*CYP26B1*) and *eukaryote translation initiation factor* (*EIF4E1B*).

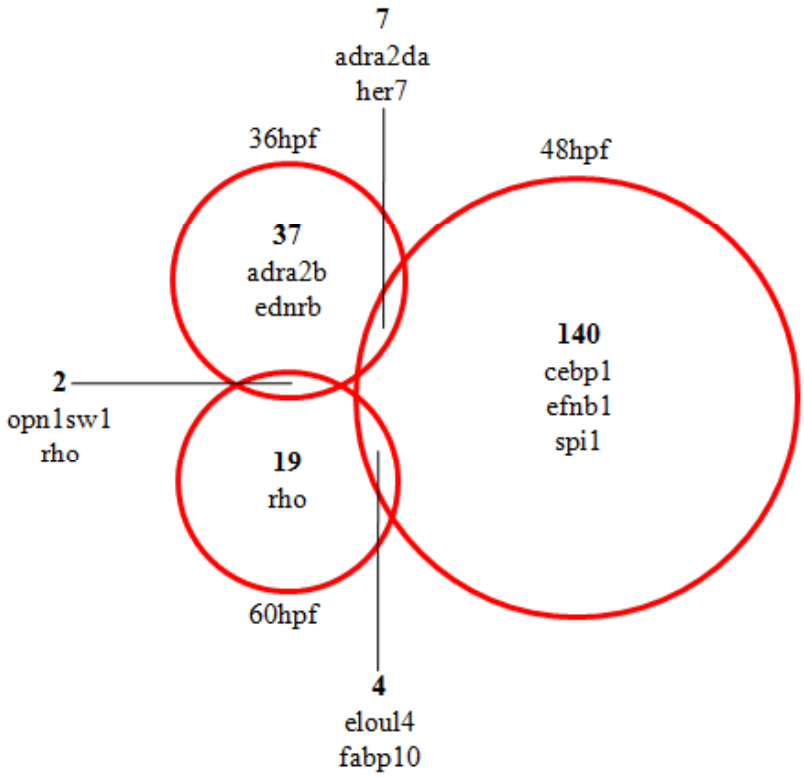

Figure 4.7 Venn diagram demonstrating temporal nature of genes with decreased expression ratio in *tnnt2* compared to control.

The numbers in the figure represent numbers of genes differentially expressed. The majority of genes with decreased expression ratios in *tnnt2* compared to control occurred at 48hpf. These included *CCAAT/enhancer binding protein* (*CEBP1*), *ephrinb1* (*EFNB1*) and *SPI1*. Smaller numbers of genes had decreased expression rations at 36h, including adrenoceptors (*ADRA2B*) and *endothelin receptor B* (*EDNRB*). 19 genes demonstrated decreased expression ratios at 60hpf, including *rhodopsin* (*RHO*). Small numbers of genes were identified with differential expression at more that one timepoint. Of these, the most interesting shared differential expression at 36 and 48hpf, including adrenoceptors (*ADRA2Da*) and *hairy and enhancer of split 7* (*HER7*). No genes demonstrated decreased differential expression at all three timepoints.

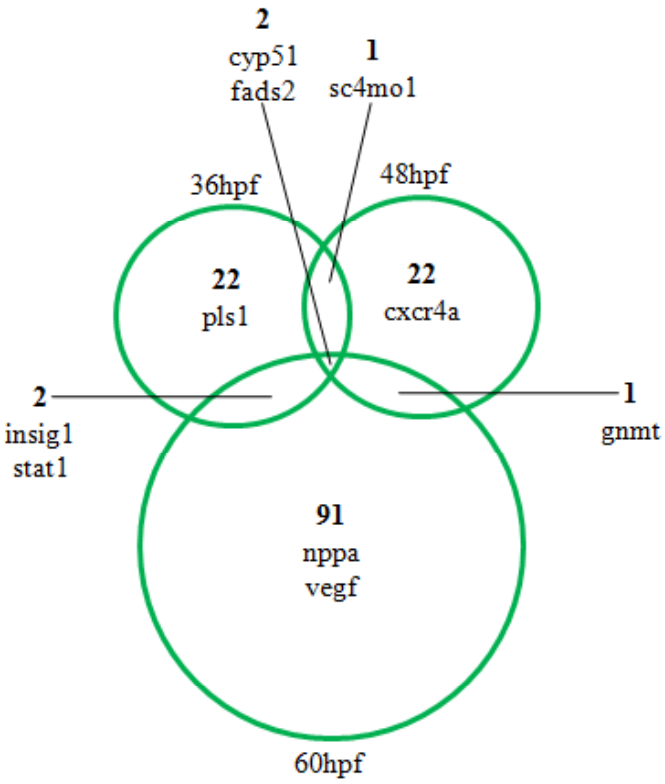

Figure 4.8 Venn diagram demonstrating temporal nature of genes with increased expression ratio in *tnnt2* compared to control.

The numbers in the figure represent numbers of genes differentially expressed. The majority of genes with increased expression ratios in *tnnt2* compared to control occurred at 60hpf, and included *natriuretic peptide precursor A* (*NPPA*) and *VEGF*. At 36hpf 22 genes demonstrated increased expression ratios, including *plastin 1* (*PLS1*). 22 genes also had increased expression ratios at 48hpf. These included *CXCR4a*. Very small numbers of genes demonstrated differential expression at more than one timepoint. Many, such as *insulin induced gene 1* (*INSIG1*) and *signal transduction and activation of transcription 1* (*STAT1*) differentially expressed at both 36 and 60hpf represent genes of metabolism. 2 genes were also identified with increased expression ratios at all three timepoints: a cytochrome P450 family member (*CYP51*), and *fatty acid desaturase 2* (*FADS2*).

Genes in these groups were associated with growth and metabolism, such as *CYP51*, part of the cytochrome P450 system.

4.2.4 Analysis of Differentially Expressed Genes

4.2.4.1 Classification of Differentially Expressed Genes by Gene Ontology

Protein Analysis Through Evolutionary Relationships (PANTHER) gene ontology (Thomas, Campbell *et al.*, 2003) enables classification of genes into groups based on their molecular function, involvement in biological processes, or the cellular components they are associated with by utilising published evidence and prediction based upon evolutionary relationships. I first determined which biological process (for instance *signal transduction* or *visual perception*) each gene belonged. This allowed me to identify which biological processes were most affected by differential gene expression of *tnnt2* compared to control at each timepoint. Figure 4.9 demonstrates graphically the number of named differentially expressed genes assigned to each biological process at each timepoint.

At 36hpf a small number of genes are seen to be differentially expressed (37 with decreased expression, 22 with increased expression in *tnnt2*). These genes represent the majority of biological processes, although no gene represents either *apoptosis* or *antigen presentation*, suggesting *tnnt2* knockdown has not affected general development since cellular apoptosis has not been induced. At 48hpf all biological processes are represented. The largest numbers of genes are observed with decreased expression and represent *signal transduction*, *protein transcription/translation*, and *morphogenesis*. At 60hpf the biological processes with highest numbers of differentially expressed genes have increased expression in *tnnt2* compared to control, and represent the processes with decreased gene expression at 48hpf. At 48 and 60hpf the number of differentially expressed genes representing *apoptosis* and *antigen presentation* remain very low (*apoptosis*: total of 2 differentially expressed genes at both timepoints; *antigen presentation*: 4).

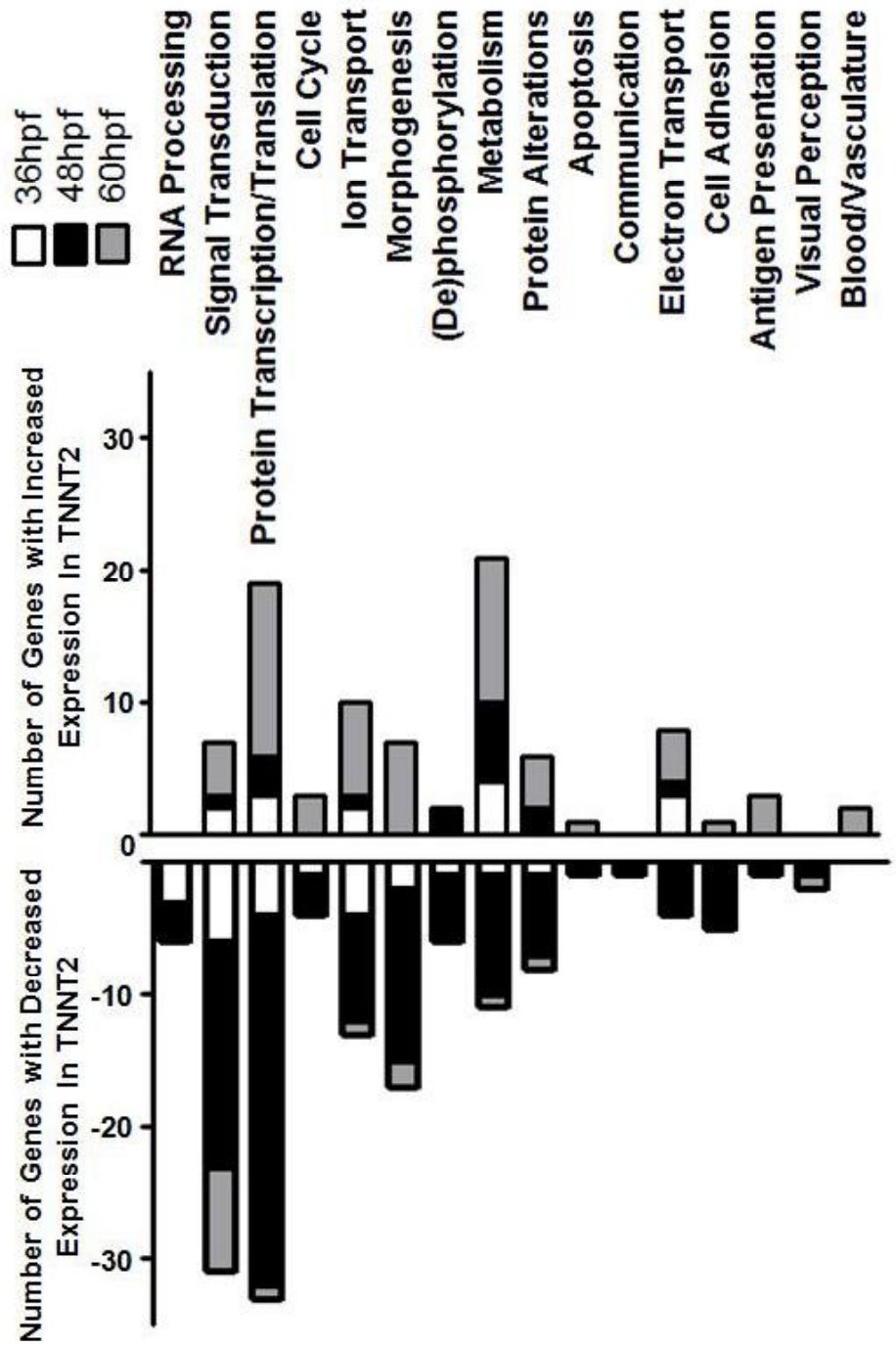

Figure 4.9 Gene ontology provides data describing the biological processes of differentially expressed genes.

A graphical representation of the number of genes with increased and decreased expression following *tnnt2* knockdown compared to control MO knockdown at 36, 48, and 60hpf.

Over the three timepoints the largest groups of genes represent *signal transduction*, *protein transcription/translation* and *morphogenesis*, resulting in part from these processes high representation at 48hpf.

Gene ontology can also be utilised to determine whether numbers of differentially expressed genes from a specific biological process is an under- or over-representation of the number expected, the fractional difference. Fractional difference increases with the number of genes from a specific process differentially expressed compared to the total number of genes in that process (for example, the total number of genes in a process listed on the GeneChip). Fractional difference was determined at each timepoint (figure 4.10 and figure 4.17 in the appendix at end of this chapter) by comparing the number of differentially expressed genes in each biological process against the total number of genes (differentially + undifferentially expressed) categorised to each process: (number of genes observed in biological process – number of genes expected in biological process)/number of genes expected in biological process. Positive fractional differences therefore demonstrate over-representation of genes in a biological process, while negative fractional differences demonstrate under-representation. Over the three timepoints eight biological processes demonstrated significant under- or over-representation ($P \leq 0.05$; Binomial statistical test). These included significant over-representation of *cholesterol metabolism* and *steroid metabolism* at 36 and 48hpf. Over-representation might suggest a failure for *tnnt2* embryos to metabolise cholesterol and steroids required during physiology, and could contribute to the cardiac failure observed at 60hpf. There was a significant under-representation of *cell proliferation and differentiation* at 48hpf and *cell cycle* at 60hpf. This under-representation might suggest a reduced embryonic growth of *tnnt2* morphants at later timepoints, although no visible manifestation has been observed of decreased proliferation in this study (particularly regarding the vasculature, section 4.2.2) or by Sehnert, Huq *et al.* (2002). Of most interest may be significant over-representation of genes classified to *G-protein mediated signalling* at 48hpf, a process which includes vasoregulatory genes such as *EDNRB*. Evidence suggests zebrafish embryos respond to decreased haemodynamic force by vasoconstriction even at this early developmental stage (Pelster, Grillitsch *et al.*, 2005).

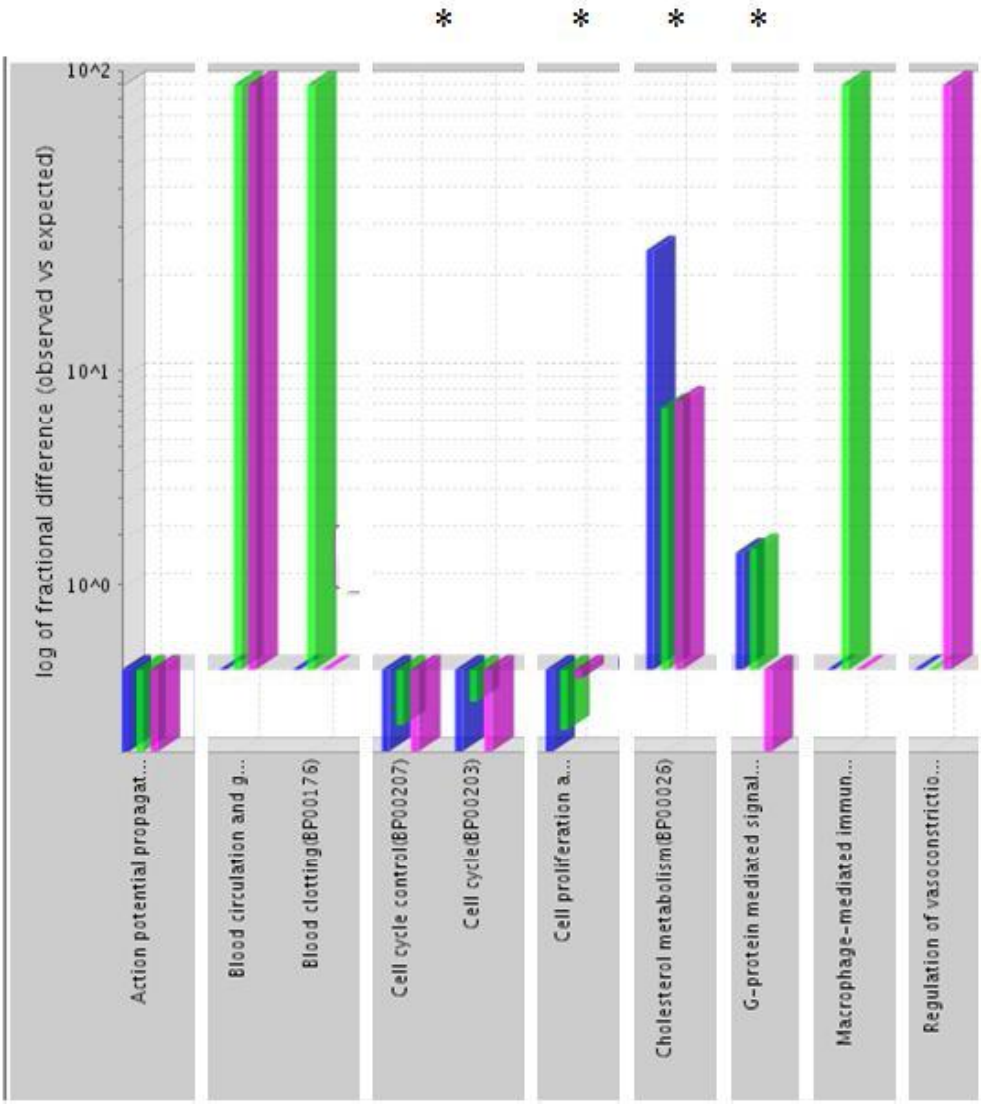

Figure 4.10 Fractional difference demonstrates under- and over-representation of differentially expressed genes.

Selected regions of a graph of log fractional difference, demonstrating biological processes with significant under- or over-representation of differentially expressed genes, including statistical significance. Blue columns represent differentially expressed genes at 36hpf, green at 48hpf, and red at 60hpf. * = $P<0.05$, Binomial statistical test.

Significant over-representation might thus suggest an attempt to control falls in haemodynamic force in *tnnt2* morphants through vasoconstriction.

A series of interesting biological processes demonstrated increased but non-significant over-representation. *Blood circulation*, *blood clotting*, *macrophage-mediated immunity*, and *regulation of vasoconstriction* all demonstrated non-significant over-representation. Over-representation of genes classified to *blood circulation* (*cytoglobin*, *NPPA*) and *blood clotting* (*coagulation factor IX*, *thrombospondin 3*) is conceivably directly related to absent cardiac contraction and blood pooling which results in *tnnt2* morphants, and is thus caused by *tnnt2* knockdown and not by absence of haemodynamic force. Over-representation of *macrophage-mediated immunity* might result from induction of altered haemodynamic force in *tnnt2* morphants mirroring conditions inducing vessel remodelling (Heilmann, Beyersdorf *et al.*, 2002). As discussed in the previous paragraph (in discussing *G-protein mediated signalling*), over-representation of genes classified to *regulation of vasoconstriction* might occur in *tnnt2* morphants in an attempt to raise low haemodynamic force by vasoconstriction.

4.2.4.2 Clustering of Differentially Expressed Genes

Clustering of differentially expressed genes provides data on similarities in expression over time. Genes demonstrating differentially increased or decreased expression in *tnnt2* morphant GeneChips compared to control were hierarchically clustered into gene trees in order to demonstrate similarity of gene expression pattern over time. Gene trees are illustrated in figure 4.11 (genes with decreased expression in *tnnt2* morphant GeneChips compared to control) and 4.13 (genes with increased expression in *tnnt2* compared to control). Figure 4.12 illustrates isolated branches of the gene tree for genes with decreased expression in *tnnt2* compared to control. The branch in figure 4.12A contains four genes involved in modulation of vasculature, three adrenergic receptors (*2B*, *2C*, and *2Da*), and *EDNRB*. As discussed in section 4.2.3, these genes are involved in vasoregulation. Their decreased expression with absent haemodynamic force might suggest less control of vasoactivity it required with reduced blood flow. The cluster in figure 4.12A also contains *angiopoietin-like 2b* (*ANGPTL2B*).

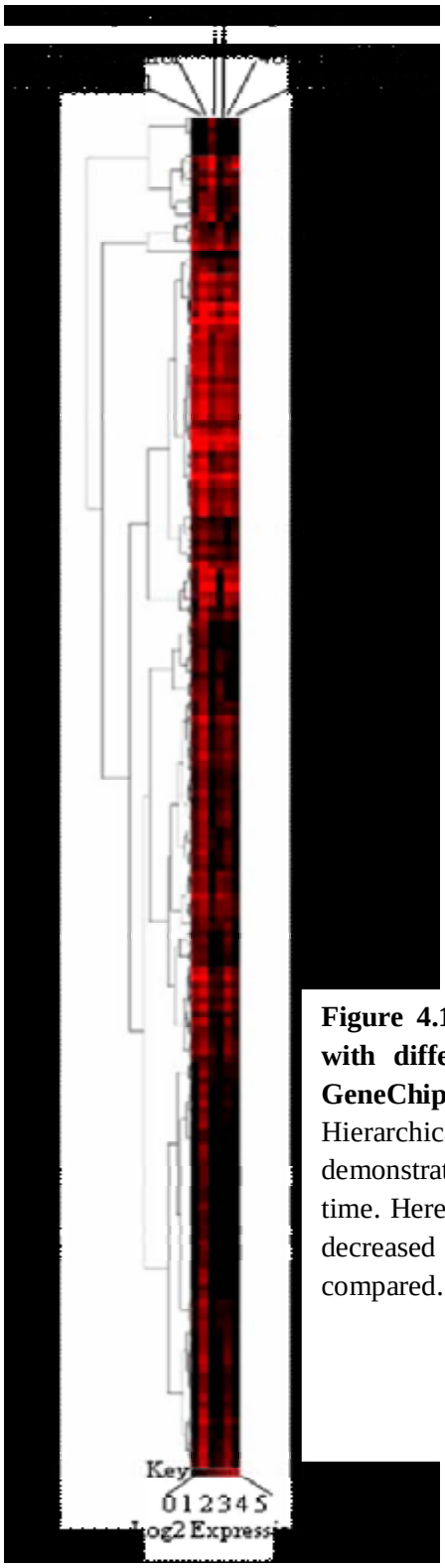

Figure 4.11 Tree of hierarchically clustered genes with differentially decreased expression in *tnnt2* GeneChips.

Hierarchical clustering into gene trees permits demonstration of similarity of gene expression over time. Here, clustering enables similarity of genes with decreased expression in *tnnt2* versus control to be compared.

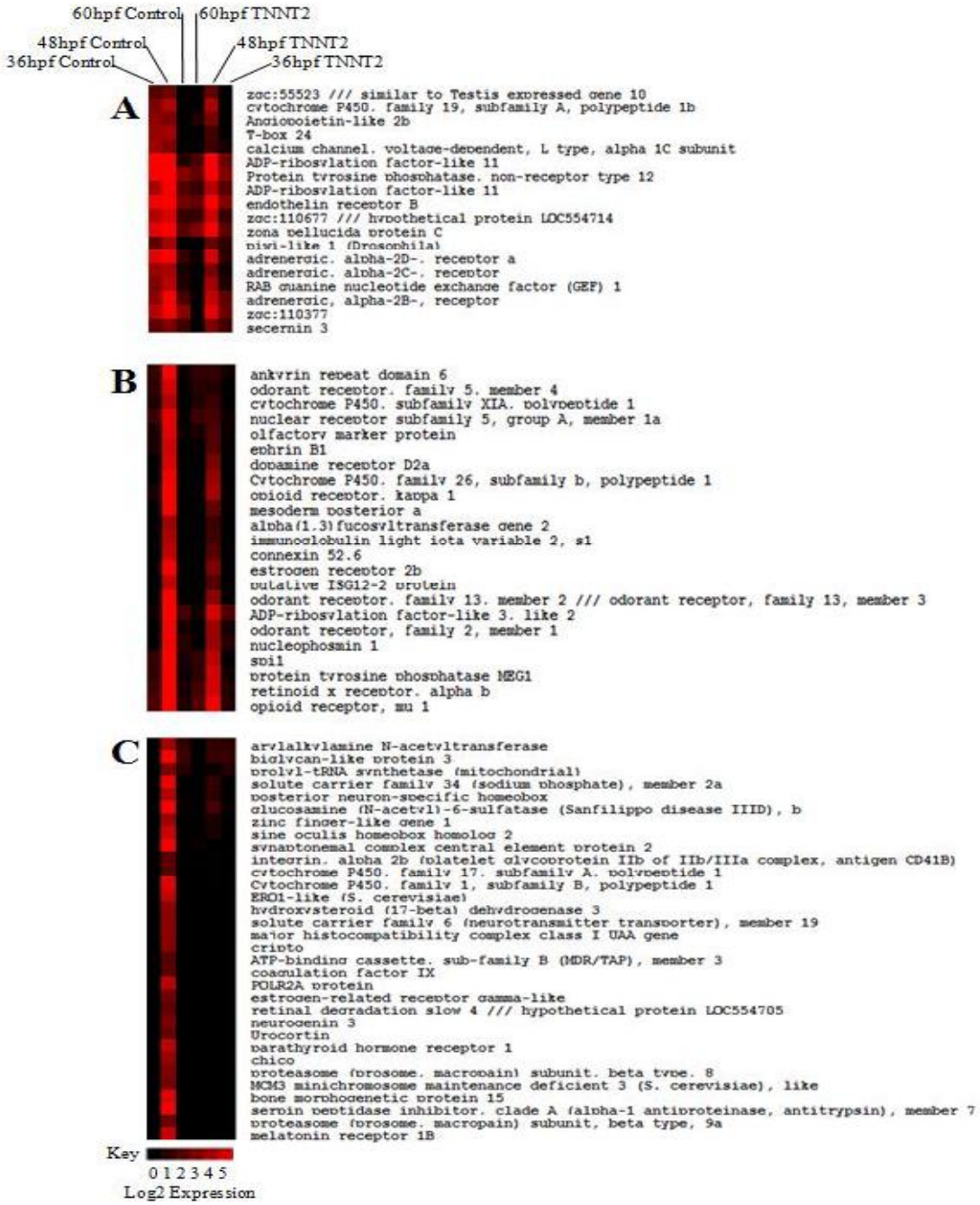

Figure 4.12 Hierarchical clustering provides information on similarity of gene expression over time. Figures A-C represent branches of the tree of genes with significantly decreased expression in *tnnt2* GeneChips compared to control in figure 4.11. For instance, A, demonstrates similar clustering and thus gene expression of several vasoactive genes including adrenoceptors and EDNRB.

ANGPTL2B is expressed in skeletal muscle and heart, as well as other tissues such as intestine (Hato, Tabata *et al.*, 2008), and has been shown to induce sprouts in porcine pulmonary arterial ECs, suggesting a role in angiogenesis (Kim, Moon *et al.*, 1999), a process modulated by haemodynamic force as related elsewhere. Gene knockdown in zebrafish embryos resulted in death at 72hpf due to pericardial effusion (Kubota, Oike *et al.*, 2005). When knocked down in combination with *angiopoietin-like 1*, ISVs and DLAVs failed to form, suggesting they act in concert to inhibit angiogenesis (Kubota, Oike *et al.*, 2005). The genes contained within the branch in Figure 4.12B demonstrate decreased expression patterns in *tnnt2* morphant GeneChips compared to control chips primarily at 48hpf. Genes within this branch include *EFNB1* and *SPI1*. The role of these genes and their relationships to haemodynamic force have been discussed in section 4.3.2, and thus will not be repeated here.

Figure 4.12C presents a branch with very different patterns of gene expression between groups. The genes in this branch demonstrate little expression at 36 or 60hpf in either *tnnt2* or control GeneChips. At 48hpf, gene expression in *tnnt2* remains very low in comparison to control gene expression. Genes include *integrin* α_{2b} (*platelet GPIIb*). Integrins are cell surface receptors capable of cell-ECM attachment and signalling, with evidence linking integrin function to induction of angiogenesis through expression on platelets and bone-marrow derived cells (Feng, McCabe *et al.*, 2008). For instance, pharmacological inhibition of $\alpha_{2b}\beta_3$ led to 35% reduction in angiogenesis in mice (Rhee, Black *et al.*, 2004), while murine $\alpha_V\beta_3$ knockout enhanced angiogenesis (Reynolds, Wyder *et al.*, 2002), suggesting a complex role for integrins in vessel remodelling.

Figure 4.14A illustrates a branch of the gene tree for genes with differentially increased expression in *tnnt2* GeneChips compared to control (figure 4.13). Figure 4.14A contains genes with increased expression compared to control at the earliest timepoint of 36hpf. The branch includes a member of TNF receptor superfamily. TNFα is known to be secreted from macrophages during vessel remodelling in order to breakdown ECM, allowing migration and proliferation of ECs (Heilmann, Beyersdorf *et al.*, 2002), as well as undergoing increased expression in inflammation (Baik, Kwak *et al.*, 2008).

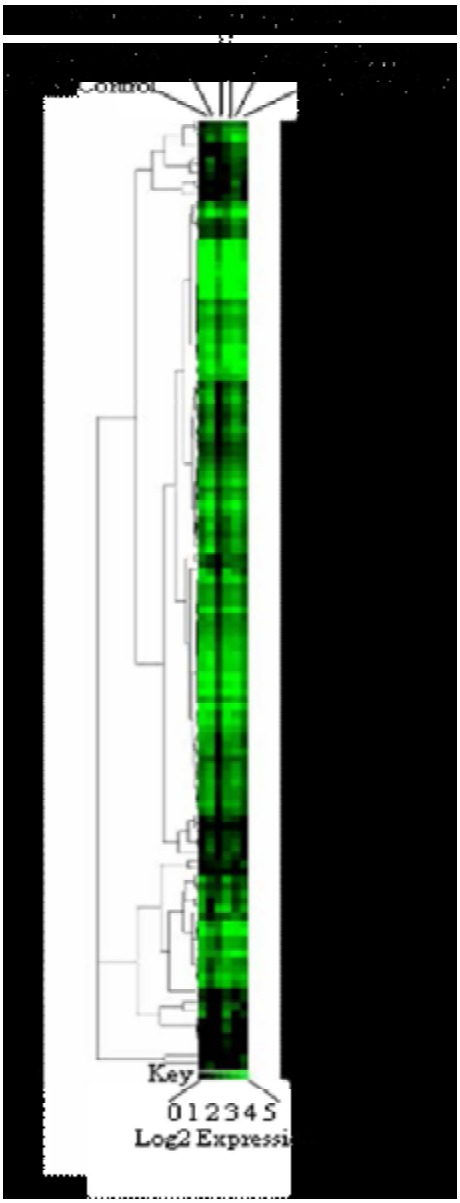

Figure 4.13 Tree of hierarchically clustered genes with differentially increased expression in *tnnt2* GeneChips.
This clustering enables the similarity of expression in genes with increased expression in *tnnt2* compared to control GeneChips to be compared.

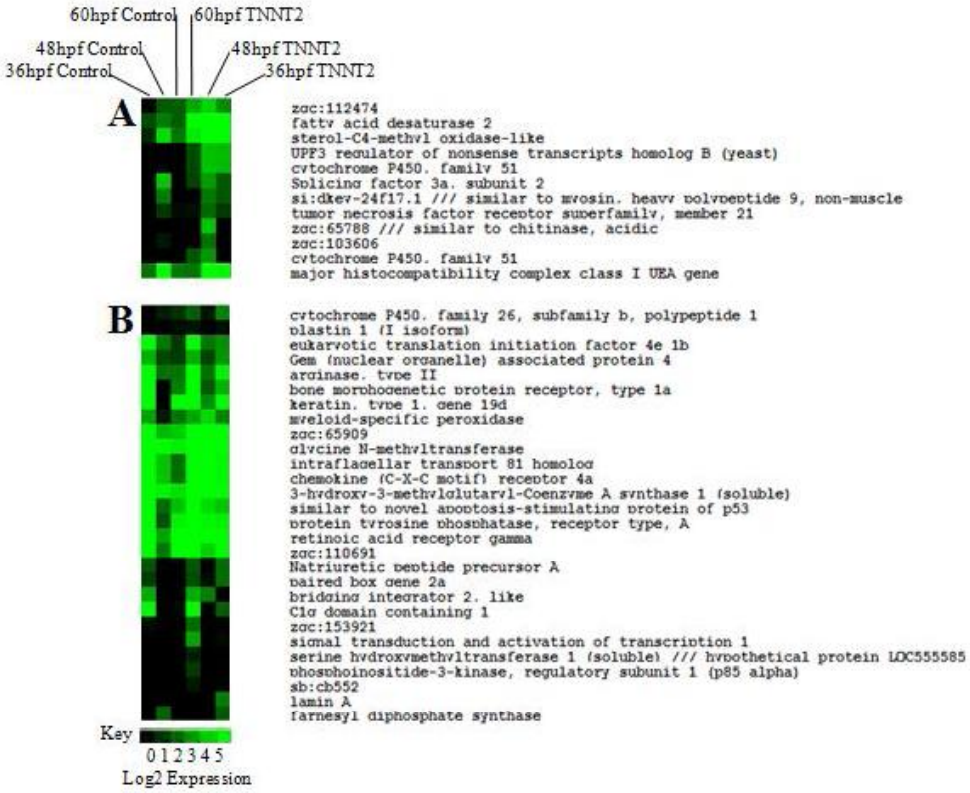

Figure 4.14 Clustering provides information on the similarity of gene expression over time in genes with increased expression in *tnnt2*.

Branches isolated from the gene tree generated by hierarchical clustering of genes with significantly increased expression in *tnnt2* GeneChips compared to control (figure 4.13) provide information on the similarity of gene expression over time. (A) contains genes with increased expression compared to control at the earliest timepoint of 36hpf. The branch includes a member of TNF receptor superfamily. TNFα is known to be secreted from macrophages during vessel remodelling in order to breakdown ECM, allowing migration and proliferation of ECs. B demonstrated increased expression at 48hpf in *tnnt2* GeneChips. This branch includes *CXCR4a*, the receptor for the chemokine SDF (stromal-cell derived factor) 1, expressed on macrophages.

Increased expression of a member of the TNF receptor superfamily in *tnnt2* may suggest a desire for increased sensitivity to TNFs, perhaps to induce greater vascular remodelling, since conditions of reduced haemodynamic force mirror conditions which induce remodelling. The genes continue to demonstrate increased expression in comparison to control at 48 and 60hpf.

Genes within the branch of Figure 4.14B demonstrated increased expression at 48hpf in *tnnt2* GeneChips. This branch includes *CXCR4a*, the receptor for the chemokine SDF (stromal-cell derived factor) 1, expressed on macrophages. $CXCR4^{+}$ cells have been observed to induce revascularisation following MI in mice (Jin, Shido *et al.*, 2006; Morimoto, Takahashi *et al.*, 2007), and angiogenesis necessary for tumour growth (Feng, McCabe *et al.*, 2008). CXCR4a has therefore been demonstrated to modulate remodelling in processes which are commonly devoid of physiological levels of haemodynamic force.

A body of evidence demonstrates the importance of haemodynamic forces such as FSS and cyclic stretch to vascular development, remodelling, and gene expression. Much of this work comes from *in vitro* studies, with disadvantages I discussed in section 4.1.9. Exploiting advantages of zebrafish embryos I have been able to determine gene expression in the absence of haemodynamic force *in vivo*.

4.3 Discussion

4.3.1 Embryonic Development is Unaffected by *tnnt2* Knockdown

To determine the effect of *tnnt2* knockdown on embryonic development sibling wildtype embryos at the 1-4 cell stage (figure 1.6) were injected with either *tnnt2* or standard control MO. Their development was observed by stereomicroscopy to 60hpf, the latest timepoint for microarray analysis. Control morphants demonstrated normal development under standard incubation conditions at 28°C (Westerfield, 2000), including normal vascular development (section 4.3.2 below). Cardiac contraction of control morphants occurs at approximately 26hpf, again concurring with published data (Chen, Haffter *et al.*, 1996). No other developmental defect is visible by 60hpf. *tnnt2*

morphants were observed developing comparably to control morphants. Cardiac contraction was inhibited in almost all morphants (approximately 95%), demonstrating the success of *tnnt2* knockdown. Despite *tnnt2* knockdown, *tnnt2* morphants were able to dechorionate from 48hpf without mechanical intervention. Morphants responded to touch stimuli, demonstrating non-cardiac muscle was unaffected by *tnnt2* knockdown. By 60hpf, *tnnt2* morphants developed pericardial oedema, as observed by Sehnert, Huq *et al.* (2002). Pericardial oedema at this later timepoint may suggest heart failure, and it is possible that gene expression changes observed at this timepoint are a result of cardiac abnormalities rather than absent haemodynamic forces alone.

4.3.2 Vasculogenesis and Angiogenesis are Unaffected by Absent Blood Flow

The complete absence of blood flow through the vasculature that occurs due to inhibition of cardiac contraction in *tnnt2* morphant embryos prevents development of physiological levels of FSS that occur in control morphants. Development of the vascular system has been shown to require genetic predetermination, as well as onset of blood flow (Wang, Chen *et al.*, 1998). Arterial and venous ECs are molecularly distinct. For example, arterial cells express *EFNB2* and venous cells its receptor *EPHB4* (Wang, Chen *et al.*, 1998) before the onset of circulation. No-flow chick embryos demonstrated normal development of the vascular plexus (le Noble, Moyon *et al.*, 2004). *In situ* hybridisation demonstrated expression of EFNB2 to be spatially distinct, with some areas of plexus expressing EFNB2 and others staining negatively, suggesting arterial-venous differentiation without flow. In zebrafish embryos, inhibition of *Notch* resulted in expression of venous markers in arteries (Lawson, Scheer *et al.*, 2001) suggesting *Notch* specifies an arterial fate, while its absence induces a venous fate. However, local vascular conditions are also important. Arterial EC grafts from quail were able to colonise chick vein, with expression of specific arterial/venous markers changing with relocation (le Noble, Fleury *et al.*, 2005). Studies utilising fli1:eGFP transgenic zebrafish embryos have demonstrated vessels made up of aortic-derived ECs are able to form venous vessels (Isogai, Lawson *et al.*, 2003). These data suggest that despite early genetic differentiation, plasticity remains. Plasticity might be one way in which vascular remodelling is possible.

To determine whether vasculogenesis and angiogenesis occurred comparably to standard control MO injected sibling embryos under conditions of absent blood flow (*tnnt2* morphant embryos), I performed laser-scanning confocal microscopy of fli1:eGFP transgenic embryos injected with either *tnnt2*/control MO at 60hpf, the latest timepoint at which microarray analysis was performed. Approximately 20 *tnnt2*/control morphants were observed by fluorescent stereomicroscopy, and two representative morphants randomly chosen for confocal microscopy at 60hpf (figure 4.2). In control morphants vasculature developed as described by Isogai, Horiguchi *et al.* (2001), with aorta traversing laterally to the tail, before joining the cardinal vein which will return blood to the heart at onset of circulation. The caudal-most end of the cardinal vein forms the venous plexus at this time. By 1.5dpf ISVs had began to form, sprouting from dorsal aorta migrating dorsally (Childs, Chen *et al.*, 2002; Isogai, Lawson *et al.*, 2003) to form DLAVs by 2dpf. The ISVs became patent at 2dpf, and SIVs began to develop at this timepoint (Isogai, Horiguchi *et al.*, 2001).

On comparison with control morphant embryos, *tnnt2* morphants appeared to have developed a normal vascular patterning. *tnnt2* morphants demonstrated normal development of aorta and cardinal vein, suggesting vasculogenesis is not affected by *tnnt2* knockdown since vasculogenesis is the process responsible for formation of these vessels (Isogai, Horiguchi *et al.*, 2001). However, aorta and cardinal vein appear collapsed, presumably resulting from absence of blood flow. *tnnt2* morphants also demonstrated normal patterning and number of ISVs, DLAVs, and SIVs when compared to control morphants. These vessels develop through growth and remodelling of aorta and cardinal vein during angiogenesis (Isogai, Horiguchi *et al.*, 2001). Normal development of these vessels suggests angiogenesis is unaffected by *tnnt2* knockdown. This data concurs with previous observation of vascular development in these morphants (Isogai, Lawson *et al.*, 2003), as well as findings from vessel occlusion during early zebrafish development in studies of kidney morphogenesis which determined no alteration in development to 72hpf without blood flow (Serluca, Drummond *et al.*, 2002).

4.3.3 Zebrafish Embryos Permit Determination of Differential Gene Expression Unfeasible Utilising Alternative Model Systems

Microarray technology utilising *in vitro* cell culture assays of different vascular cell populations from differing sources have consistently demonstrated changes to the expression of genes involved in vascular performance and vascular control under conditions of altered haemodynamic force (McCormick, Eskin *et al.*, 2001; Chen, Li *et al.*, 2001). For instance, microarray analysis of human aortic ECs under conditions of laminar flow demonstrated upregulation of *VEGFR2* (Chen, Li *et al.*, 2001), which mediates vasculogenesis and angiogenesis (Yancopoulos, Davis *et al.*, 2000). Upregulation of *VEGFR2* expression was also determined in collateral vessels of canine hearts in immunohistochemical studies (Cai, Kocsis *et al.*, 2004b), demonstrating the ability for microarray analysis of *in vitro* assays to successfully replicate *in vivo* evidence. However, given the complexities of the vasculature, with interaction of vascular and non-vascular cell populations (Clayton, Chalothorn *et al.*, 2008), haemodynamic force, and endogenous modulation, vasculature is difficult to mimic accurately *in vitro* (Weinstein, 2002), making extrapolation into the *in vivo* setting challenging. Although effects of FSS or cyclic stretch have been studied independently *in vitro*, *in vivo* many haemodynamic forces interact simultaneously. Utilisation of mammalian models for *in vivo* microarray analysis is difficult since manipulation of blood flow can induce hypoxia and ischaemia. Furthermore, surgery has the potential of inducing inflammation and necrosis, a result observed following microarray analysis of collateral vessel remodelling after femoral artery ligation in mice (Lee, Stabile *et al.*, 2004).

Zebrafish embryos permit determination of differential gene expression following complete absence of physiological levels of haemodynamic force *in vivo* for microarray analysis, as I have demonstrated. At the timepoints my microarray was performed, zebrafish embryos do not suffer from hypoxia under standard incubation conditions (Schwerte, Uberbacher *et al.*, 2003), allowing determination of gene expression *in vivo* without ischaemia for the first time. Gene knockdown through MO injection at appropriately determined concentrations limits inflammation and necrosis which obstructs *in vivo* mammalian models (Summerton and Weller, 1997). Exploiting

zebrafish embryos therefore overcomes difficulties intrinsic to cell culture. The simplicity of MO injection also limits risks of indirect responses in gene expression resulting from inflammation and necrosis, possible with difficult surgery necessary in mammalian models to perform similar experiments.

4.3.4 Absent Blood Flow Results in Differential Gene Expression Profiles During Early Development of Zebrafish Embryos

18 Affymetrix Zebrafish GeneChips were used in determining the effect of absent haemodynamic force *in vivo* on gene expression during early embryonic development. Experimentation resulting in generation of RNA for microarray analysis was designed to reduce variability and ensure quality as much as possible. Morphant groups were paired, with equal numbers of 100-130 age-matched *tnnt2*/control MO injected sibling wildtype embryos from the same parent pair. Morphants were manually dechorionated as necessary. Morphants injured during manual dechorionation were removed, and morphant numbers equalised again. Three replicates per timepoint (36, 48, and 60hpf) were generated. In order to prevent degradation of RNA, extractions were performed on ice (4°C) and protective equipment worn throughout. On completion, RNA was immediately stored at -80°C. At each timepoint total RNA was extracted using Trizol (Sigma, Poole, UK) since the protocol permits storage at several steps without affecting purity. This allows multiple samples and timepoints to be extracted simultaneously, reducing operator variability. RNA cleanup was performed with Qiagen RNeasy Mini Kit to purify RNA samples. Only samples with purity (Ab^{260}/Ab^{280}) of 1.8-2.0, as determined by NanoDrop, were used in microarray analysis. RNA quality was determined again immediately prior to generation of cDNA necessary for analysis, and at appropriate points during analysis. Experimentation was performed in this way to reduce variability and maintain quality.

Replicate GeneChips for both control and *tnnt2* demonstrated a low degree of variability (figure 4.3), despite MO injection and total RNA extraction occurring independently for each replicate group. The low variability is suggestive of an accurate determination of differential gene expression in response to the altered physiology of *tnnt2* morphant embryos compared to control morphant embryos, rather than indirect effects such as

inflammation caused by either MO injection or *tnnt2* knockdown. Excluding cardiac-specific activity of *tnnt2*, *tnnt2* morphant embryos have been described as physiologically, if not phenotypically, normal at the timepoints the microarray was performed (Sehnert, Huq *et al.*, 2002). The low variability observed was reduced further by normalisation (figure 4.4).

Genes were classed as differentially expressed if there was ≥two-fold difference in expression between groups with ≥80% probability. Since changes in haemodynamic force, including during arteriogenesis, results in infiltration of monocytes, breakdown of ECM, and release of endogenous mediators, we may expect to observe gene expression changes in at least some genes related to these processes. As described in more detail in the following paragraphs such gene expression changes are observed, with, for example *SPI1*, *CXCR4a*, and *VEGF*.

290 genes (1.95% of total genes represented on the GeneChip) were identified as differentially expressed at one or more timepoint (figure 4.6). Seven, encoding genes of metabolism such as members of the cytochrome P450 system (*CYP26B1*) had expression ratios which increased and decreased in *tnnt2* compared to control. 166 genes demonstrated a significant decrease in gene expression ratio in *tnnt2* compared to control (figure 4.7). 19% of genes (37 genes) demonstrated decreased expression in *tnnt2* at 36hpf, including a number associated with vasoregulation: *adrenoceptor 2B, 2C, 2Da*, and *EDNRB*. These genes may demonstrate decreased expression since absent haemodynamic force might make control of vasoactivity unnecessary. *EDNRB* is expressed on ECs and VSMCs (Murakoshi, Miyauchi *et al.*, 2002), and therefore its regulation may result from decreased expression by ECs (modulated by FSS) or VSMCs (modulated by cyclic stretch). Onset of cyclic stretch induced significant upregulation of EDNRB mRNA in VSMCs (Cattaruzza, Dimigen *et al.*, 2000). Microarray analysis of HUVECs following exposure to FSS for 24h demonstrated significant downregulation of *endothelin* (McCormick, Eskin *et al.*, 2001). On comparison to no flow cultures, bovine aortic ECs exposed to FSS also demonstrated sustained decreases in endothelin mRNA and peptide (Malek, Greene *et al.*, 1993). These data demonstrate regulation of

EDNRB and *endothelin* expression by haemodynamic force and concur with my finding of decreased expression of *EDNRB* in absence of haemodynamic force.

Almost 72% of genes with decreased expression in *tnnt2* demonstrated differential expression at 48hpf. These included genes associated with developmental patterning (*EFNB1*) and the myeloid lineage (*SPI1*). Like other members of the ephrin family such as EFNB2, specifically expressed on arterial EC (section 4.2.3), EFNB1 is also involved in cell fate decisions. For example, EFNB1 has been localised to regions of cartilage differentiation during mouse development (Davy, Aubin *et al.*, 2004). Additionally, EFNB1 is implicated in angiogenesis *in vitro* (Huynh-Do, Vindis *et al.*, 2002) and *in vivo* (Kojima, Chang *et al.*, 2007) (Chapter 6), and therefore might undergo modulation by alterations in haemodynamic force. Decreased expression in *tnnt2* compared to control did not result in any visible defect in angiogenesis, with *tnnt2* morphant vasculature developing comparably to control siblings. *EFNB1* has not previously been reported with differential expression with alterations in haemodynamic force. The related ligand ephrinB2 demonstrates decreased mRNA and protein levels with falls in blood flow induced by ligation of the chick vitelline artery (le Noble, Moyon *et al.*, 2004). The receptor EphB2, which has affinity for EFNB1, demonstrated significant downregulation in human aortic ECs with FSS (Heydarkhan-Hagvall, Chien *et al.*, 2006). These data therefore suggest possible regulation of Ephrin-Ephs by haemodynamic force. SPI1 is a myeloid-specific transcription factor which plays an important role in monocyte development (Lieschke, Oates *et al.*, 2002). Monocytes are directed to sites of injury by a series of processes induced by altered haemodynamic force (Heilmann, Beyersdorf *et al.*, 2002), and thus a decreased *SPI1* expression might be expected in *tnnt2* which demonstrate similar conditions compared to control. 19 genes demonstrated significantly decreased expression in *tnnt2* at 60hpf, including *rhoposin* (*RHO*). A very small number of genes demonstrated decreased expression at more than one timepoint. *Adrenoceptor 2Da* was differentially expressed at 36 and 48hpf. Sustained decreased expression may highlight the importance of their association with haemodynamic force. No genes demonstrated decreased expression ratios at all three timepoints.

124 genes demonstrated significantly increased gene expression in *tnnt2* compared to control (figure 4.8). 22 genes (17.4%) demonstrated increased expression ratios at 36hpf, including *plastin 1* (*PLS1*). At 48hpf the same number of genes demonstrated increased expression, including *CXCR4a*. CXCR4a is the receptor for stromal-cell derived factor-1 (SDF-1), expressed on macrophages (Jin, Shido *et al.*, 2006). $CXCR4^{+}$ cells induce neovascularisation following MI in mice (Morimoto, Takahashi *et al.*, 2007), demonstrating the link between monocytes/macrophages and haemodynamic force with subsequent vessel remodelling. MCP-1 is a key chemokine for attraction of monocytes to sites of vessel remodelling. *MCP-1* demonstrates significantly decreased expression in aortic ECs exposured to laminar FSS (Malek, Greene *et al.*, 1993), while turbulent flow led to significantly increased expression (Himburg, Dowd *et al.*, 2007). This data suggests monocyte attraction and maturation is most important at sites of low haemodynamic force, as with *tnnt2* morphants.

The majority of genes with increased expression occurred at 60hpf (73%). *VEGF* was one such gene. VEGF receptors are specific to ECs and monocytes/macrophages (Hiratsuka, Minowa *et al.*, 1998), cell types involved in vessel remodelling following alterations in haemodynamic force. VEGF is known to induce vessel growth following alterations in haemodynamic force (Babiak, Schumm *et al.*, 2004). Human aortic ECs exposured to FSS demonstrated significantly increased expression of *vegfr2* on comparison to no flow cultures (Chen, Li *et al.*, 2001), suggesting a requirement for increased VEGF signalling. VEGFR2 is the predominant receptor for VEGF-A_{165} (which I have termed simply VEGF throughout) (Siekmann, Covassin *et al.*, 2008), the isoform believed most important for VEGF's modulation of vasculogenesis and angiogenesis (Yancopoulos, Davis *et al.*, 2000; Tammela, Enholm *et al.*, 2005). VEGF upregulation predominantly occurs through binding of HIF-1 to the VEGF promoter (Forsythe, Jiang *et al.*, 1996) under hypoxic conditions. However, *HIF-1*, and *lactate dehydrogenase A*, another hypoxia-induced gene (Deindl, Buschmann *et al.*, 2001) did not demonstrate differential expression in *tnnt2* despite their presence on the GeneChip, suggesting increased VEGF expression is not in response to hypoxia in this study. Very small numbers of genes demonstrated increased expression ratios at two or all three

timepoints. Genes in these groups were associated with growth and metabolism, such as *CYP51*, part of the cytochrome P450 system.

Although data resulting from microarray analysis can be determined from analysing possible roles of individual differentially expressed genes, as I have performed above, additional information can be obtained by grouping genes by similarity. Gene ontology classifies genes sharing biological process, molecular function, or pathway; while clustering divides genes into branches sharing similar levels of expression.

4.3.5 Gene Ontology Provides Analysis on the Biological Processes of Differentially Expressed Genes

I first utilised Protein Analysis Through Evolutionary Relationships (PANTHER) gene ontology (Thomas, Campbell *et al.*, 2003) to determine which biological processes were most affected by differential gene expression in *tnnt2* compared to control at each timepoint (figure 4.9). At 36hpf small numbers of genes are differentially expressed (59, of which 37 demonstrated decreased expression in *tnnt2*). These genes are classified to the majority of biological processes however no gene is classified to *apoptosis* or *antigen presentation*. This suggests *tnnt2* knockdown has no affect on general development since cellular apoptosis has not been induced. It also demonstrates an advantage of utilising zebrafish embryos for microarray analysis, and suggests macrophage-associated genes are differentially expressed due to absence of haemodynamic force and not inflammation. The largest group of differentially expressed genes in microarray analysis of thigh muscle following femoral artery ligation in mice was inflammatory response-related genes (Lee, Stabile *et al.*, 2004). The genes within this group included monocyte/macrophage-related genes such as *MCP-1*, but also genes of neutrophil infiltration (*ENA-78*) and inflammatory resolution (*lipocortin 1*), suggesting these genes may have been induced by surgical intervention rather than vessel occlusion. Genes, including the *interleukin 1 receptor precursor*, associated with inflammation have also been induced *in vitro*, following exposure to FSS (McCormick, Eskin *et al.*, 2001). At 48hpf all biological processes are represented. The largest numbers of genes are observed with decreased expression and represent *signal transduction*, *protein transcription/translation*, and *morphogenesis*. These processes

frequently include large numbers of genes in microarray analysis studying haemodynamic force (McCormick, Eskin *et al.*, 2001; Chen, Li *et al.*, 2001), presumably due to their high numbers in the genome and wide-ranging roles. At 60hpf the biological processes with highest numbers of differentially expressed genes have increased expression in *tnnt2* compared to control. They represent processes with decreased gene expression at 48hpf. At the two latest timepoints the number of differentially expressed genes representing *apoptosis* and *antigen presentation* remained very low. This again suggests that genes associated with inflammation (such as *MCP-1* and *CXCR4a*) differentially expressed in *tnnt2* undergo differential expression as a result of absent haemodynamic force and not indirect inflammation induced by MO injection.

I then utilised gene ontology to determine whether differentially expressed genes classified to specific biological processes under- or over-represented their process. This is termed fractional difference and was determined for each timepoint (figure 4.10 and figure 4.17 in the appendix at the end of the chapter). Fractional difference increases with the number of genes in a process differentially expressed compared to total numbers of genes on the GeneChip classified to that process. Eight biological processes demonstrated significant under- or over-representation ($P<0.05$, Binomial statistical tests) over the three timepoints. *Cholesterol metabolism* and *steroid metabolism* demonstrated significant over-representation at 36 and 48hpf. Genes classified to metabolic groups demonstrate differential expression with stimulation or alteration in a number of microarray studies *in vivo* (Lee, Stabile *et al.*, 2004), *in vitro* (Chen, Li *et al.*, 2001), and following EC-VSMC co-culture (Heydarkhan-Hagvall, Chien *et al.*, 2006). This suggests metabolism of cells exposed to haemodynamic force alters with specific local conditions. It is known ECs are capable of detecting and responding to different flow patterns (Ohura, Yamamoto *et al.*, 2003), which may come some way to explaining why atherosclerosis develops in regions of low haemodynamic force (Yoshizumi, Abe *et al.*, 2003). *Cell proliferation and differentiation* demonstrated significant under-representation at 48hpf, and *cell cycle* at 60hpf. This might suggest reduced embryonic growth of *tnnt2* morphants at 48 and 60hpf, however observation in this and previous

studies (Sehnert, Huq *et al.*, 2002) did not visualise differences compared to control siblings at these timepoints.

G-protein mediated signalling demonstrated significant over-representation at 48hpf. This group includes vasoregulatory genes such as *EDNRB*. Zebrafish embryos induce vasoconstriction in response to decreased haemodynamic force at this timepoint (Pelster, Grillitsch *et al.*, 2005). Several microarray studies on haemodynamic force have reported differential expression of vasoregulatory genes like *EDNRB*, demonstrating their association with haemodynamic force. HUVECs exposed to 24h laminar flow downregulated *endothelin* (McCormick, Eskin *et al.*, 2001), while sustained decreases in endothelin mRNA and peptide levels was observed in bovine aortic ECs following laminar flow exposure compared to no flow cultures (Malek, Greene *et al.*, 1993). Aortic ECs demonstrated significant upregulation of vascular specific genes such as the endothelin precursor *preproendothelin* with turbulent flow (Himburg, Dowd *et al.*, 2007), concurring with previous studies that demonstrate a downregulation in ET exposed to laminar flow, and suggesting a flow-related regulation of such genes. Significant over-representation might thus suggest an attempt to control falls in haemodynamic force in *tnnt2* morphants through vasoconstriction.

Although not significantly over-represented several biological processes associated with vascular remodelling demonstrated non-significant over-representation: *blood circulation*, *blood clotting*, *macrophage-mediated immunity*, and *regulation of vasoconstriction*. Over-representation of genes classified to *blood circulation* and *blood clotting* is conceivably directly related to absent cardiac contraction and blood pooling resulting from *tnnt2* knockdown, and thus results from *tnnt2* inhibition of cardiac contraction and not absent haemodynamic force. Over-representation of *macrophage-mediated immunity* (genes such as *MCP-1*) might result from induction of altered haemodynamic force in *tnnt2* morphants mirroring conditions inducing vessel remodelling (Heilmann, Beyersdorf *et al.*, 2002). Laminar flow led to downregulation of *MCP-1* in HUVECs (McCormick, Eskin *et al.*, 2001), while exposure to turbulent flow resulted in upregulation in aortic ECs (Himburg, Dowd *et al.*, 2007). HUVECs under cyclic stretch upregulate expression of MCP-1 mRNA and protein (Demicheva, Hecker

et al., 2008). These data thus demonstrate the possible association between induced expression of genes of macrophage-mediated immunity and haemodynamic force. Over-representation of genes classified to *regulation of vasoconstriction* has been discussed, with the example of *EDNRB*, in the previous paragraph.

4.3.6 Clustering of Differentially Expressed Genes Provides Analysis on Similarities in Gene Expression over Time

Genes differentially up- or downregulated in *tnnt2* morphant GeneChips compared to control were hierarchically clustered into gene trees in order to demonstrate similarity of gene expression over time. Figure 4.11 illustrates the gene tree for genes differentially downregulated in *tnnt2* morphant GeneChips compared to control and figure 4.13 the tree for genes differentially upregulated in *tnnt2* compared to control. Figure 4.12 illustrates isolated branches of the gene tree for genes differentially downregulated in *tnnt2* compared to control. The branch in figure 4.12A contains genes (*adrenergic receptors 2B, 2C, 2Da, EDNRB*) involved in vasoregulation and vascular development (Cruz, Parnot *et al.*, 2001). As discussed in section 4.3.5, this finding concurs with the role of the genes in modulating vessel tone, since vasoactivity will be dependent in part on the volume of flow within a vessel. The branch also contains *angiopoetin-like 2b* (*ANGPTL2B*). *ANGPTL2B* is expressed in a number of tissues including skeletal muscle and heart (Hato, Tabata *et al.*, 2008). ANGPTL2B induces sprout formation on porcine pulmonary arterial ECs, suggesting a role in vascular remodelling (Kim, Moon *et al.*, 1999), a process modulated by haemodynamic force. Knockdown in zebrafish embryos caused death by 72hpf resulting from pericardial effusion (Kubota, Oike *et al.*, 2005), but when knocked down in combination with *angiopoietin-like 1*, ISVs and DLAVs failed to form. This may suggest the two genes act in concert to inhibit angiogenesis (Kubota, Oike *et al.*, 2005). These data demonstrates a role for *ANGPTL2B* in vascular remodelling, and may suggest its clustering to other genes linked to vascular control and development.

The genes contained within the branch in Figure 4.12B demonstrate expression patterns significantly downregulated in *tnnt2* morphant GeneChips compared to control primarily at 48hpf. Genes within this branch include *EFNB1* and *SPI1*. Both genes are

involved in developmental processes. While EFNB1 plays a role in modulating embryonic development (Compagni, Logan *et al.*, 2003), including vascular development (Adams, 2002), SPI1 is critical for myelopoiesis (Lieschke, Oates *et al.*, 2002), as discussed in section 4.3.4. Figure 4.12C presents a branch with severe patterns of gene expression. The genes in this branch, such as *integrin* α_{2b} (*platelet GPIIb*), demonstrate very little expression at 36 or 60hpf in either *tnnt2* or control GeneChips. At 48hpf, gene expression in *tnnt2* remains very low in comparison to control gene expression. Evidence links integrin function to induction of angiogenesis, through expression on platelets and bone-marrow derived cells (Feng, McCabe *et al.*, 2008). Pharmacological inhibition of $\alpha_{2b}\beta_3$ led to 35% reduction in angiogenesis in mice (Rhee, Black *et al.*, 2004), while murine $\alpha_V\beta_3$ knockout enhanced angiogenesis (Reynolds, Wyder *et al.*, 2002). Data regarding roles of integrins in vascular remodelling remain contradictory, and might be explained by complex roles in which integrins can be both pro- and anti-angiogenic dependent on precise conditions.

Figure 4.14A illustrates a branch of the gene tree for genes differentially upregulated in *tnnt2* GeneChips compared to control (figure 4.13). Figure 4.14A contains a branch of genes upregulated in *tnnt2* at 36hpf. The genes continue to be upregulated in comparison to control at 48 and 60hpf. One gene is a member of TNF receptor superfamily (member 21). TNFα is secreted from macrophages during vessel remodelling to breakdown ECM, thus allowing migration and proliferation of ECs (Heilmann, Beyersdorf *et al.*, 2002). *TNFα* also undergoes increased expression during inflammation (Baik, Kwak *et al.*, 2008). Increased expression of the TNF receptor superfamily in *tnnt2* may suggest a desire for increased sensitivity to TNFs, perhaps to induce greater vascular remodelling, since conditions of reduced haemodynamic force mirror conditions which induce remodelling. The genes contained within the branch of Figure 4.14B were upregulated at 48hpf in *tnnt2* GeneChips such as *CXCR4a*, the receptor for the cytokine SDF1. CXCR4a has been shown to modulate arteriogenesis in mammalian models through stem cell recruitment to the ischaemic area (Jin, Shido *et al.*, 2006). Furthermore, $CXCR4^+$ cells induce revascularisation following MI in mice (Morimoto, Takahashi *et al.*, 2007). Concurring with this, other members of Dr Chico's lab have demonstrated

that inhibition of *CXCR4a* through MO knockdown or pharmacological antagonism inhibits arteriogenesis (Ms Caroline Gray; manuscript in preparation).

Meta-analysis of this microarray together with other microarrays seeking to determine gene expression profiles in arteriogenesis or vascular remodelling may also provide further insight. It may enable a determination of genes expressed in different models and different species including mammalian and non-mammalian species. Thus, meta-analysis may help determine the evolutionary pathway of arteriogenesis, and differences in gene expression essential for the process to occur.

4.4 Limitations and Future Work

4.4.1 Differential Gene Expression Analysis Utilised Total Embryonic RNA

Microarray analysis of differential gene expression of control compared to *tnnt2* morphant embryos were performed utilising total RNA of zebrafish embryos. The advantage of this method is technical ease, as well as the ability to begin RNA extraction immediately, capturing gene expression profiles as close to conditions of *in vivo* physiology as is possible. This is particularly relevant when the goal is determination of haemodynamic force on gene expression profiles.

Techniques for isolating vascular tissue are technically complex and time-consuming in such a small organism, making capture of gene expression during conditions of *in vivo* physiology difficult. In addition, isolation ignores interactions between other cell-types, physical forces, and endogenous mediators which may also modulate gene expression. FAC sorting technology could also have been utilised, to isolate cells of vascular and non-vascular types before undergoing microarray analysis (Covassin, Amigo *et al.*, 2006). Once more however, this would involve removing cells from conditions of *in vivo* physiology, as well as from the complex of interactions that may be necessary for modulation of gene expression.

4.4.2 Microarray Validation

Microarray validation by real-time PCR was to be performed utilising RNA extracted and used in microarray analysis in order to limit variability. However, it was difficult to combine extraction of high quality ($Ab^{260/280}$ of 1.8-2.0) and high yield RNA necessary for each microarray timepoint, resulting in repeated rounds of MO injection and RNA extraction which extended experimentation considerably beyond the timeframe originally envisaged. Additionally, high quality RNA generated was used entirely in generation of cDNA for microarray, making it necessary to repeat MO injection and RNA extraction again for validation. Thus, time was reduced for validation and further experimentation. Had more time been available, I would have been able to perform real-time PCR for genes of interest (Chapters 5 and 6) at all three timepoints. It would have been interesting to perform Northern blots of genes of interest to determine changes in RNA levels, and Western blots to observe levels of protein. It would also have been interesting to compare gene expression levels in *tnnt2* with those observed following induced inhibition of cardiac contraction by pharmacological inhibitors such as BDM (2,3-butanedione monoxime). BDM blocks myofibrillar ATPase (Bartman, Walsh *et al.*, 2004), so that at high enough concentrations cardiac contraction is inhibited or reduced to the extent that blood flow is prevented. This experimentation would allow determination of at which point in early development of zebrafish embryos inhibited contraction had the most affect on gene expression.

4.5 Conclusion

In Chapter 3, I exploited zebrafish embryos to develop two models of arteriogenesis, a process in part modulated by haemodynamic force. In this chapter, I wanted to further exploit advantages inherent to zebrafish embryos in comparison to mammalian species to increase understanding of the role haemodynamic force plays in modulating arteriogenesis. Many arteriogenesis-associated genes are differentially expressed with alterations in haemodynamic force. In this chapter I described combining the advantages of zebrafish embryos with current microarray technology to identify candidate genes with potential to modulate arteriogenesis, through comparing gene expression under physiological levels of haemodynamic force and in its absence. To my knowledge, this

is the first time determination of gene expression without haemodynamic force has been performed *in vivo* with a model of haemodynamic force (rather than FSS or cyclic stretch) without induction of ischaemia. The microarray has demonstrated a potentially important role for vasoactive genes such as adrenoceptors and EDNRB in stimulation of arteriogenesis.

Chapter Five

Modulation of Arteriogenesis by Endothelin Receptor B

Chapter 5: Modulation of Arteriogenesis by Endothelin Receptor B

In Chapter 4 microarray technology was utilised to identify a gene set differentially expressed under conditions of absent blood flow, and thereby absent haemodynamic force, compared to controls under physiological levels of blood flow. 290 genes differentially expressed were scrutinised by performing literature searches to create a list of candidate genes with known functions within vasculature. One panel of genes which demonstrated significant expression and over-representation in multiple forms of analysis were a group of vasoactive genes including several adrenoceptors and *Endothelin receptor B* (*EDNRB*). The role of *EDNRB* in arteriogenesis has not been studied. *EDNRB* is known to have roles within tumour angiogenesis, which shares some genetic and molecular components with arteriogenesis. This chapter thus discusses utilisation of the zebrafish embryo models of arteriogenesis discussed in Chapter 3 to extrapolate on the microarray analysis obtained in Chapter 4 to determine the role of *EDNRB* in modulating arteriogenesis. The introduction discusses previous research which led me to hypothesise roles for *EDNRB* in modulating arteriogenesis.

5.1 Introduction

5.1.1 The Endothelin System

5.1.1.1 Endothelin-1 and Endothelin Receptors

Endothelin-1 (ET) is a vasoconstrictor peptide released predominantly by ECs, but also expressed on cells including VSMCs, monocytes, and macrophages (Miyauchi and Masaki, 1999). ET exerts its functions by binding the seven transmembrane G-protein coupled endothelin receptor A or B. Endothelin receptor A is located predominantly on VSMCs and endothelin receptor B (EDNRB) primarily on ECs, as well as VSMCs (Murakoshi, Miyauchi *et al.*, 2002; Bagnall, Kelland *et al.*, 2006). While VSMC

receptor expression leads to vasoconstriction on ligand binding, EC EDNRB activation leads to release of vasodilators such as NO (Murakoshi, Miyauchi *et al.*, 2002). In VSMCs, ligand binding leads to activation of phospholipase C, which in turn activates Protein Kinase C leading to increased $[Ca^{2+}]_i$ stimulating muscle contraction and thus vasoconstriction (Takigawa, Sakurai *et al.*, 1995). EDNRB also clear circulating ET (Pollock and Schneider, 2006). Mammalian species have EDNRB subsets, termed EDNRB1 and EDNRB2, while zebrafish have a single *ednrb* gene analogous to *EDNRB1* (Kelsh, Harris *et al.*, 2008). There is no equivalent to *EDNRB2* in zebrafish (Kelsh, Harris *et al.*, 2008).

5.1.1.2 Endothelin Receptor B and Vascular Control

Through its vasoconstrictive properties ET is involved in regulation of blood pressure. EDNRB may influence blood pressure through regulation of vascular tone, alterations in renal haemodynamics, clearance of circulating ET, or a combination of these mechanisms (Bagnall, Kelland *et al.*, 2006). Blood flow measurement in *EDNRB* loss of function mutant mice demonstrated significantly elevated systolic blood pressure compared to wildtype animals, attributed to development of salt-sensitive hypertension (Murakoshi, Miyauchi *et al.*, 2002). In another study, EC-specific inactivation of *EDNRB* led to increased concentrations of plasma ET and reduced endothelial-dependent vasodilatation, but did not alter blood pressure (Bagnall, Kelland *et al.*, 2006). It has also been demonstrated that EDNRB is not required for ET-activated vasoconstriction in human branchial arteries (Berthiaume, Yanagisawa *et al.*, 2000).

Experiments utilising VSMCs in culture demonstrated significant EDNRB mRNA upregulation following onset of cyclic stretch, mimicking increases in blood pressure, maintained for 12h after abolishment of stretch (Cattaruzza, Dimigen *et al.*, 2000). Elevated EDNRB mRNA levels resulted in significantly increased VSMC apoptosis, and it was hypothesised by Cattaruzza, Dimigen *et al.* (2000) that increased apoptosis was a means of permitting arterial remodelling to occur. *EDNRB* deficient mice experience reduced levels of vascular remodelling following ligation of the right common carotid artery (Murakoshi, Miyauchi *et al.*, 2002). Animals present with enlarged areas of neointimal formation and stenosis compared to wildtype animals.

Concurring, EDNRB antagonism in wildtype mice leads to similar levels of neointima and stenosis developing (Murakoshi, Miyauchi *et al*., 2002).

ET promotes proliferation and migration of ECs, a key constituent of angiogenesis, *in vitro* as well as *in vivo* (Cruz, Parnot *et al*., 2001). EC migration is also important to vasculogenesis and re-endothelisation of arteries following intervention for vessel occlusion (Daher, Noel *et al*., 2008). Angiogenesis has been induced through ET binding EDNRB, and inhibited by the EDNRB specific chemical antagonist BQ788 (Salani, Taraboletti *et al*., 2000). Increased migration of ECs *in vitro* was stimulated by ET and completely inhibited with BQ788 (Daher, Noel *et al*., 2008). One hypothesis suggests the role of ET-EDNRB in angiogenesis may be to induce upregulation of MMP-2, necessary for ECM breakdown during vessel growth and migration (Bagnato and Spinella, 2003).

EDNRB has been identified as a modulator of forms of vascular development and remodelling other than arteriogenesis, making EDNRB a possible modulator of arteriogenesis, since many processes, such as breakdown of ECM, are similar in angiogenesis and arteriogenesis. The potential of EDNRB to modulate arteriogenesis has yet to be defined, and is the intent of the results which follow.

5.1.2 Morpholino Antisense Oligonucleotide Knockdown

Morpholino antisense oligonucleotides (MOs) are frequently used to knockdown genes of interest in zebrafish embryos. MOs are short 25 base-pair nucleotides synthesised with a morpholine rather than ribose backbone (Summerton and Weller, 1997). The basic MO structure can be found in figure 1.8. MOs act via steric block to prevent translation of mRNA to peptide at the ribosome, and are complementary to a specific sequence in the mRNA.Splice-site blocking MOs result in modification of pre-mRNA splicing to knockdown a gene's functional sequence (Summerton, 2007). An advantage of splice-site blocking MOs in contrast to start-site blockers, which inhibit translation, is the ability to determine activity through PCR analysis.

However, MO knockdown can suffer from off-target affects instead of, or in addition to, desired specific gene knockdown (Eisen and Smith, 2008). In turn, an observed phenotype may not relate to the gene studied. For instance, it is reported that neural defects observed in 15-20% of MO studies result from activation of p53 and therefore apoptosis (Eisen and Smith, 2008). Eisen and Smith (2008) suggest utilisation of one or more controls to confirm findings are specific: GeneTools standard control MO, specific gene mismatch controls, use of different MOs targeting the same gene, and rescue experimentation.

5.2 Results

Arteriogenesis is dependent, at least in part, on haemodynamic force (Buschmann and Schaper, 1999) with mammalian studies demonstrating the importance of forces such as FSS to development of collateral blood flow following arterial ligation (Eitenmuller, Volger *et al.*, 2006; Pipp, Boehm *et al.*, 2004). In Chapter 4 I demonstrated differential expression of 290 genes with absent haemodynamic force. It is therefore possible that at least some differentially expressed genes modulate arteriogenesis. I began by scrutinising the 290 differentially expressed genes to generate a list of candidates with known functions within vasculature.

5.2.1 Literature Search of Differentially Expressed Genes

To identify potential modulators of arteriogenesis, I scrutinised the 290 differentially expressed genes by performing literature researches utilising the public database www.pubmed.gov. I created a candidate list of genes with known vascular function, genes believed to have greatest possibility of modulating arteriogenesis (figure 5.24 in chapter appendix). *EDNRB* demonstrated significantly decreased expression with absent haemodynamic force. This, combined with their known roles in vascular development and remodelling as summarised above, led me to hypothesise *EDNRB* deficiency may lead to reduced recovery of aortic blood flow following occlusion. The role of each of these genes in arteriogenesis has not been studied, despite demonstrations of their importance in vascular remodelling in mammals (Adams, Wilkinson *et al.*, 1999;

Murakoshi, Miyauchi *et al.*, 2002). These results aim to determine the role these genes may play in modulating arteriogenesis in the models I describe in Chapter 3, utilising morpholino oligonucleotide knockdown. Prior to knockdown, however, I confirmed expression and sequenced these genes in zebrafish embryos.

5.2.2 Expression of EDNRB in Zebrafish Embryos

To confirm expression of *EDNRB* in zebrafish embryos I performed RT-PCR analysis. Total RNA from 36hpf wildtype embryos was reverse transcribed to generate cDNA. This timepoint was utilised since it was the first microarray timepoint. Forward and reverse primer pairs (coloured red in figures 5.1B) designed against Ensembl predicted sequences for *EDNRB* (figure 5.1B) were used to identify expression of the genes by RT-PCR with relevant primer pairs. Expression of *GAPDH* was utilised as positive control. Predicted sequences predict transcripts with the primer pairs of band sizes *EDNRB*: 718bp, and *GAPDH*: 1019bp.

RT-PCR of *EDNRB* demonstrated transcript with band size approximately 800bp, corresponding with the predicted size of 718bp (figure 5.1A). These results thus supported expression of *EDNRB* in zebrafish embryos at 36hpf.

5.2.3 Sequencing Confirms Predicted EDNRB Sequences

Determination of *EDNRB* expression was performed utilising primer pairs designed against the Ensembl automated predicted sequence. It was therefore important to confirm Ensembl automated predicted sequence for *EDNRB*. PCR product from section 5.2.2 was sequenced against the primer pairs at the University's Core Genomics Facility with the aim of visualising possible base-pair alignment alterations. Product was purified to remove excess primer, dNTPs, and non-specific products. Sequence alignment for *EDNRB* (figure 5.2) demonstrated 91% homology between PCR product and predicted sequence. Non-homologous regions are found at either end of the product where primers bind, suggesting true alignment is likely 100% between PCR product and predicted sequence. These results confirm automated predicted sequence of *EDNRB* in zebrafish embryos.

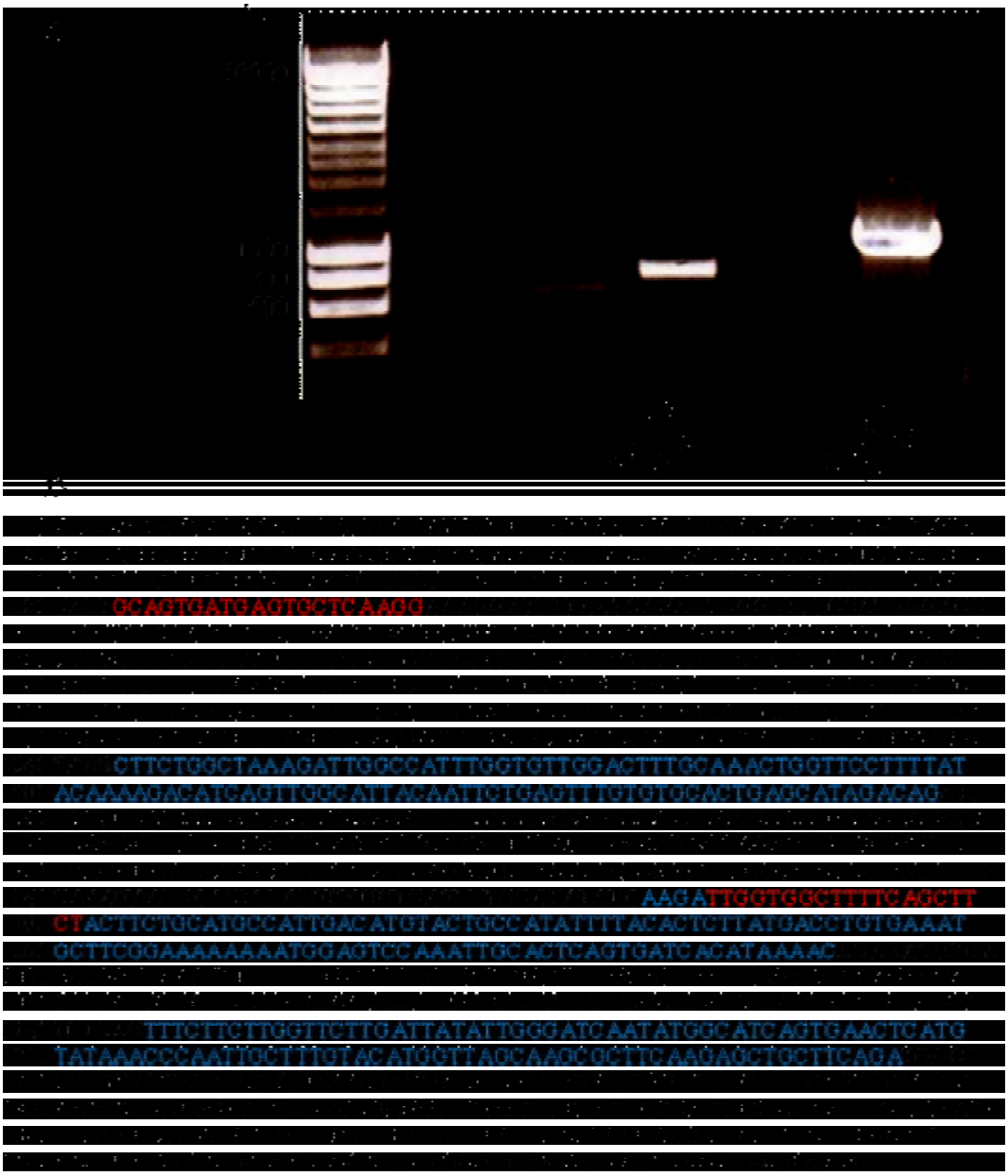

Figure 5.1 Expression of EDNRB in wildtype zebrafish embryos.
PCR analysis with specific primers in A (red base lettering in B) demonstrates expression of *EDNRB* in wildtype embryos. B, Ensembl predicted sequence for *EDNRB*. Black/blue bases indicate alternate exon sequences. Red bases indicate the sequence of primers utilised.

```
Predicted AACCATGCATAGAAAACTATTGCAATAGGTTTATTAATGATTTTGTAATTCTAGCCTACA 60
Sequenced ------------------------------------------------------------

Predicted GACGGGTTGATATCTGTGTTATGCTAAAGAAAACAGTGCTGACTGTTAAATAGTCATGCG 120
Sequenced ------------------------------------------------------------

Predicted TTTCCAAATTATTATGGAAACAAGATGCGTTTTTTGTTTTTTGTTTCTCCTGACTGAACA 180
Sequenced ------------------------------------------------------------

Predicted CATTGCAGTGATGAGTGCTCAAGGAAAGGATTTTAATCAGAGTCGGCTTTCCATGGGACC 240
Sequenced ------------------------------NNNNNNNNNNNNNNGNNTNNNNNGGGNNC 28
                                                    *  *     ***  *

Predicted TTTGTCTCCAACTCAAAAATCTACGATTGTAATAGGAAACCAGATCAACGAGTCCATGCC 300
Sequenced TTTGTCTCCNACTCNAAAATCTACGATTGTAATAGGAAACCNNNTNNACGAGTCCATGCC 88
          ********* **** *************************   *  *************

Predicted TCGGCGACCAAAAGTTTTGCCTCCTATGTGTACAGATCCCACGGAAATCAGGGACACCTT 360
Sequenced TCGGCGACCAAAAGTTTTGCCTCCTATGTGTACAGATCCCACGGAAATCAGGGACACCTT 148
          ************************************************************

Predicted CAAGTATATTAACACCGTGGTTTCATGCCTTGTATTTGTAGTTGGTATAATCGGAAATTC 420
Sequenced CAAGTATATTAACACCGTGGTTTCATGCCTTGTATTTGTAGTTGGTATAATCGGAAATTC 208
          ************************************************************

Predicted CACGCTGCTTAGAATCATTTATAAAAACAAATGCATGCGGAACGGTCCAAATATTCTCAT 480
Sequenced CACGCTGCTTAGAATCATTTATAAAAACAAATGCATGCGGAACGGTCCAAATATTCTCAT 268
          ************************************************************

Predicted TGCAAGTCTGGCGCTTGGGGACCTCTTACACATCATGATAGACATTCCCATCAATGTGTA 540
Sequenced TGCAAGTCTGGCGCTTGGGGACCTCTTACACATCATGATAGACATTCCCATCAATGTGTA 328
          ************************************************************

Predicted TAAGCTTCTGGCTAAAGATTGGCCATTTGGTGTTGGACTTTGCAAACTGGTTCCTTTTAT 600
Sequenced TAAGCTTCTGGCTAAAGATTGGCCATTTGGTGTTGGACTTTGCAAACTGGTTCCTTTTAT 388
          ************************************************************

Predicted ACAAAAGACATCAGTTGGCATTACAATTCTGAGTTTGTGTGCACTGAGCATAGACAGATT 660
Sequenced ACAAAAGACATCAGTTGGCATTACAATTCTGAGTTTGTGTGCACTGAGCATAGACAGATT 448
          ************************************************************

Predicted TCGAGCAGTGTCATCCTGGAACCGCATCAAAGGCATTGGTGTTCCCAAATGGACAGCCAT 720
Sequenced TCGAGCAGTGTCATCCTGGAACCGCATCAAAGGCATTGGTGTTCCCAAATGGACAGCCAT 508
          ************************************************************

Predicted TGAAATCATTCTGATTTGGGTGTTGTCCATTATACTTGCAGTGCCAGAGGCCATTGCCTT 780
Sequenced TGAAATCATTCTGATTTGGGTGTTGTCCATTATACTTGCAGTGCCAGAGGCCATTGCCTT 568
          ************************************************************

Predicted TGACATGATCACAATGGACTACAAAGGAGAGCAGCTCAGGATTTGCCTTCTGCACCCTA- 839
Sequenced TGACATGATCACAATGGACTACAAAGGAGAGCAGCTCANGATTTGCCTTCTGCACCCTAA 628
          ************************************ ********************

Predicted GCAAAGAATCAAGTTTATGCAGGTCAGTTTGCATATATAAAGATTGGTGGCTTTTCAGCT 899
Sequenced GCAAAGAATCAAGTTTATGCAGTTTTATAAG-AAAGCCAAAGATTGNNGNNNNNNNNNNN 687
          ********************** *   *  * * *   ********  *

Predicted TCTACTTCTGCATGCCATTGACATGTACTGCCATATTTTACACTCTTATGACCTGTGAAA 959
Sequenced NNNNN-------------------------------------------------------- 692

Predicted TGCTTCGGAAAAAAAATGGAGTCCAAATTGCACTCAGTGATCACATAAAACAGAGACGTG 1019
Sequenced ------------------------------------------------------------
```

```
Predicted AGGTGGCTAAAACCGTTTTCTGTTTGGTGCTAGTCTTTGCACTGTGCTGGCTTCCACTGC 1079
Sequenced ------------------------------------------------------------

Predicted ATCTTAGTCGTATTCTTCAACGTACAATTTATGATGAAAGGGACCCCAACCGTTGTGAGC 1139
Sequenced ------------------------------------------------------------

Predicted TTCTGAGTTTCTTCTTGGTTCTTGATTATATTGGGATCAATATGGCATCAGTGAACTCAT 1199
Sequenced ------------------------------------------------------------

Predicted GTATAAACCCAATTGCTTTGTACATGGTTAGCAAGCGCTTCAAGAGCTGCTTCAGATCAT 1259
Sequenced ------------------------------------------------------------

Predicted GTCTGTGTTGCTGGTGTCTGCCTCCTGAAATACTAGCCATGGATGACAAACAGTCCTGCA 1319
Sequenced ------------------------------------------------------------

Predicted TAAAGCTGAAGGTAACAGAGCGAGGATCAGCCATAACAGCCATGTCTCCAACAAGTATAC 1379
Sequenced ------------------------------------------------------------

Predicted TTCAAATTAGGCACTGATATGCTTACATGTATCAATGGCCAACAAATTTACTTTAACATT 1439
Sequenced ------------------------------------------------------------

Predicted TAATACTATGCAAATAAAACCATGAACCATAAAATGGTGATATAAAAGGCAAA        1492
Sequence  ------------------------------------------------
```

Figure 5.2 Confirmation of EDNRB ensembl predicted sequence.
The *EDNRB* PCR amplicon underwent sequencing to confirm the Ensembl predicted sequence and demonstrated 91% homology. C = cytosine, G = guanine, T = thymine, A = adenosine, N = not determined, * = sequence match, - = sequence absence. Numbers on right refer to base-pair number of predicted sequence.

To identify regions of homology between *EDNRB* sequences in zebrafish and other model organisms I compared sequence alignments utilising ClustalW (version 2.0.10; www.ebi.ac.uk/Tools/clustalw2/index.html). While the Ensembl predicted sequence were utilised for human, mouse and chick, the zebrafish sequence I determined for the genes were utilised. Regions of homology between species are often functional regions, and thus important to determine.

Alignment of *EDNRB* zebrafish sequence to human, mouse, and chick demonstrated a homology of 61-71% (zebrafish-human 63%, -mouse 61%, -chick 71%). There is significant homology from base-pair 126 onwards between all species aligned (figure 5.3). Human and mouse sequences demonstrate a series of base-pairs prior to the zebrafish sequence (approximately 400 and 140 base-pairs respectively). The regions of sequences demonstrating homology correspond to the majority of exon 1 onward, as can be observed from figure 5.1. A variety of protein domains are therefore possibly homologous between the aligned species, and their roles are described briefly in figure 5.4.

5.2.4 *In situ* Hybridisation Determines EDNRB Expression Pattern

I decided to perform whole-mount *in situ* hybridisation (ISH) to help determine endogenous expression in zebrafish embryos. ISH is commonly utilised to determine gene expression patterns during early development in zebrafish embryos by detecting specific nucleic acid sequences with RNA probes. ISH has a major advantage over antibody immunohistochemistry, since very few antibodies are presently cross-reactive with zebrafish. In addition, reagents and technique have been optimised for zebrafish embryos (Thisse and Thisse, 2008).

ISH was performed at 2 and 4dpf (n=18-24/group) with a probe developed from PCR product as described by Thisse and Thisse (2008). Representative lateral views of *EDNRB* expression pattern can be observed in figure 5.5. At 2dpf (figure 5.5A), a strong line of staining originating at a site above the pericardial sac traverses laterally towards the tail. Its apparent termination is the end of the yolk-sac extension.

```
human ATGAATAAAAGTACTTGTCTGATGGCAGCAGAGACCCCGAGCAAACGGTGGAGGCTACAC 60
mouse ------------------------------------------------------------
chick ------------------------------------------------------------
zfish ------------------------------------------------------------

human TGTCTGGCATTCTCGCAGCGTTTCGTCAGAGCCGGACCCGCCTGCAGCTCAAGGGAGGCG 120
mouse ------------------------------------------------------------
chick ------------------------------------------------------------
zfish ------------------------------------------------------------

human TGCTCCTCTCCCAGAGCAGGCTGGAACCCAGCTGGGTTCCGCCTCCCGGGAAGGTGGTCT 180
mouse ------------------------------------------------------------
chick ------------------------------------------------------------
zfish ------------------------------------------------------------

human CCATTCGTCGCTCTGCATCTGGTTTGTCAGATCCGAGAGGCTCTGAAACTGCGGAGCGGC 240
mouse ------------------------------------------------------------
chick ------------------------------------------------------------
zfish ------------------------------------------------------------

human CACCGGACGCCTTCTGGAGCAGGTAGCAGCATGCAGCCGCCTCCAAGTCTGTGCGGACGC 300
mouse ----------------------------ATGCAATCGCCCGCAAGCCGGTGCGGACGC 30
chick ------------------------------------------------------------
zfish ------------------------------------------------------------

human GCCCTGGTTGCGCTGGTTCTTGCCTGCGGCCTGTCGCGGATCTGGGGAGAGGAGAGAGGC 360
mouse GCCTTGGTGGCGCTGCTGCTGGCCTGTGGCTTCTTGGGGGTATGGGGAGAGAAAAGAGGA 90
chick ------------------------------------------------------------
zfish ------------------------------------------------------------

human TTCCCGCCTGACAGGGCCACTCCG---CTTTTGCAAACCGCAGAGATAATGACGCCACCC 417
mouse TTCCCACCTGCCCAAGCCACGCTGTCACTTCTCGGGACTAAAGAGGTAATGACGCCACCC 150
chick ------------------------------------------------------------
zfish ---------------------------------------------ATGAGTGCTCAAGGA 15

human ACTAAGACCTTATGGCCCAAGGGTTCCAACGCCAGTCTGGCGCGGTCGTTGGCACCTGCG 477
mouse ACTAAGACCTCCTGGACCAGAGGTTCCAACTCCAGTCTGATGCGTTCCTCCGCACCTGCG 210
chick ------------------------------------------------------------
zfish AAGGATTTTAATCAGAGTCGGCTTTCCATGGGACCTTTGTCTCCAACTCAAAAATCTACG 75

human GAGGTGCCTAAAGG---AGACAGGACGGCAGGATCTCCGCCACGCACCATCTCCCCTCCC 534
mouse GAGGTGACCAAAGG---AGGGAGGGGGGCTGGAGTCCCGCCAAGATC---CTTCCCTCCT 264
chick ----------------------------------------------------TCGCTCCCG 9
zfish ATTGTAATAGGAAACCAGATCAACGAGTCCATGCCTCGGCGACCAAAAGTTTTGCCTCCT 135
                                                           *  *  **

human CCGTGCCAAGGACCCATCGAGATCAAGGAGACTTTCAAATACATCAACACGGTTGTGTCC 594
mouse CCGTGCCAACGAAATATTGAGATCAGCAAGACTTTTAAATACATCAACACGATTGTGTCG 324
chick ATGTGCACCGGGCAGACGGAGATCAAGGAGACCTTCAAGTATATCAACACGGTGGTGTCA 69
zfish ATGTGTACAGATCCCACGGAAATCAGGGACACCTTCAAGTATATTAACACCGTGGTTTCA 195
        ***          *  ** ****   * ** ** ** ** ** *****  * ** **

human TGCCTTGTGTTCGTGCTGGGGATCATCGGGAACTCCACACTTCTGAGAATTATCTACAAG 654
mouse TGCCTCGTGTTCGTGCTAGGCATCATCGGGAACTCCACGCTGCTAAGAATCATCTACAAG 384
chick TGCCTGGTGTTCGTCCTGGGCATCATCGGCAACTCCACGCTGTTGCGGATCATCTACAAG 129
zfish TGCCTTGTATTTGTAGTTGGTATAATCGGAAATTCCACGCTGCTTAGAATCATTTATAAA 255
      ***** ** ** **  * ** ** ***** ** ***** **  *  * ** ** ** **

human AACAAGTGCATGCGAAACGGTCCCAATATCTTGATCGCCAGCTTGGCTCTGGGAGACCTG 714
mouse AACAAGTGCATGCGCAATGGTCCCAATATCTTGATCGCCAGTCTGGCTCTGGGAGACCTA 444
chick AACAAGTGCATGAGGAACGGCCCCAACATCCTCATCGCCAGCCTGGCCCTGGGTGACTTG 189
zfish AACAAATGCATGCGGAACGGTCCAAATATTCTCATTGCAAGTCTGGCGCTTGGGGACCTC 315
      ***** ****** * ** ** ** ** **  * ** ** **  **** ** ** *** *
```

```
human CTGCACATCGTCATTGACATCCCTATCAATGTCTACAAGCTGCTGGCAGAGGACTGGCCA 774
mouse CTGCACATCATCATAGACATACCCATTAACACCTACAAGTTGCTCGCAGAGGACTGGCCA 504
chick CTGCACATCATCATCGACATCCCCATCAGCGTCTACAAGCTACTTGCAGAGGACTGGCCC 249
zfish TTACACATCATGATAGACATTCCCATCAATGTGTATAAGCTTCTGGCTAAAGATTGGCCA 375
       * ****** * ** ***** ** ** *     ** *** * ** **  * ** *****

human TTTGGAGCTGAGATGTGTAAGCTGGTGCCTTTCATACAGAAAGCCTCTGTGGGAATCACT 834
mouse TTTGGAGCTGAGATGTGTAAGCTGGTGCCCTTCATACAGAAGGCTTCTGTGGGAATCACA 564
chick TTTGGTGTCGAAATGTGTAAATTAGTGCCCTTCATTCAAAAGGCATCAGTGGGCATCACA 309
zfish TTTGGTGTTGGACTTTGCAAACTGGTTCCTTTTATACAAAAGACATCAGTTGGCATTACA 435
      ***** *  *   * ** **  * ** ** ** ** ** **  * ** ** ** ** **
human GTGCTGAGTCTATGTGCTCTGAGTATTGACAGATATCGAGCTGTTGCTTCTTGGAGTAGA 894
mouse GTGCTGAGTCTTTGTGCTCTAAGTATTGACAGATATCGAGCTGTTGCTTCTTGGAGTCGA 624
chick GTGTTGAGTTTGTGTGCCCTCAGTATAGACAGGTACCGAGCAGTTGCTTCTTGGAGTCGA 369
zfish ATTCTGAGTTTGTGTGCACTGAGCATAGACAGATTTCGAGCAGTGTCATCCTGGAACCGC 495
       *  ***** * ***** ** ** ** ***** *  ***** **  * ** ****   *

human ATTAAAGGAATTGGGGTTCCAAAATGGACAGCAGTAGAAATTGTTTTGATTTGGGTGGTC 954
mouse ATTAAAGGAATTGGGGTTCCAAAATGGACAGCAGTAGAAATTGTTTTAATTTGGGTGGTC 684
chick ATTAAAGGAATTGGAGTGCCAAGGTGGACTGCTGTTGAAATTGTACTCATCTGGGTTATA 429
zfish ATCAAAGGCATTGGTGTTCCCAAATGGACAGCCATTGAAATCATTCTGATTTGGGTGTTG 555
      ** ***** ***** ** ** *  ***** **  * *****  *  * ** *****  *

human TCTGTGGTTCTGGCTGTCCCTGAAGCCATAGGTTTTGATATAATTACGATGGACTACAAA 1014
mouse TCTGTGGTTCTGGCTGTCCCCGAAGCCATAGGTTTTGATATGATTACGTCGGACTACAAA 744
chick TCGGTGGTATTGGCTGTTCCTGAAGCTATTGCATTTGACATGATAACAATGGAGTACAGG 489
zfish TCCATTATACTTGCAGTGCCAGAGGCCATTGCCTTTGACATGATCACAATGGACTACAAA 615
      **  *  *  * ** ** ** ** ** ** *  ***** ** ** **   *** ****

human GGAAGTTATCTGCGAATCTGCTTGCTTCATCCCGTTCAGAAGACAGCTTTCATGCAGTTT 1074
mouse GGAAAGCCCCTAAGGGTCTGCATGCTTAATCCCTTTCAGAAAACAGCCTTCATGCAGTTT 804
chick GGAAAGGATCTCAGAATCTGCCTGCTTCACCCCACACAGAAAACATCCTTTATGATGTTT 549
zfish GGAGAGCAGCTCAGGATTTGCCTTCTGCACCCTA-GCAAAGAATCAAGTTTATGCAGGTC 674
      ***      **  *  * *** * **  * **    ** *  *     ** ***  * *

human TACAAG-ACAGCAAAAGATTGGTGGCTATTCAGTTTCTATTTCTGCTTGCCATTGGCCAT 1133
mouse TACAAG-ACAGCCAAAGATTGGTGGCTGTTCAGTTTCTACTTCTGCTTGCCGCTAGCCAT 863
chick TACAAG-AAAGCTAAAGACTGGTGGCTGTTCAGCTTTTATTTCTGTTTGCCACTGGCTAT 608
zfish AGTTTGCATATATAAAGATTGGTGGCTTTTCAGCTTCTACTTCTGCATGCCATTGACATG 734
           * * *   ***** ******** ***** ** ** *****  ****  *  *

human CACTGCATTTTTTTATACACTAATGACCTGTGAAATGTTGAGAAAGAAAAGTGGCATGCA 1193
mouse CACTGCAGTCTTTTATACCCTGATGACCTGCGAAATGCTCAGGAAGAAGAGCGGTATGCA 923
chick CACAGCACTTTTCTATACTCTCATGACCTGTGAGATGTTACGAAAGAAAAGTGGGATGCA 668
zfish TACTGCCATATTTTACACTCTTATGACCTGTGAAATGCTTCGGAAAAAAAAATGGAGTCCA 794
       ** **  * ** ** ** ** ******** ** *** *  * ** ** *  **  * **

human GATTGCTTTAAATGATCACCTAAAGCAGAGACGGGAAGTGGCCAAAACCGTCTTTTGCCT 1253
mouse GATTGCTTTGAATGATCACTTAAAGCAGAGACGAGAAGTGGCCAAGACAGTCTTCTGCCT 983
chick GATTGCTTTAAATGATCACTTAAAACAGAGACGCGAGGTGGCCAAGACTGTGTTCTGCCT 728
zfish AATTGCACTCAGTGATCACATAAAACAGAGACGTGAGGTGGCTAAAACCGTTTTCTGTTT 854
       *****  * * ******* **** ******** ** ***** ** ** ** ** **  *

human GGTCCTTGTCTTTGCCCTCTGCTGGCTTCCCCTTCACCTCAGCAGGATTCTGAAGCTCAC 1313
mouse GGTCCTCGTGTTTGCTCTCTGTTGGCTTCCCCTTCACCTCAGCCGGATCCTGAAGCTCAC 1043
chick GGTACTTGTTTTTGCCTTGTGTTGGCTTCCACTTCATTTAAGCAGAATATTGAAACTCAC 788
zfish GGTGCTAGTCTTTGCACTGTGCTGGCTTCCACTGCATCTTAGTCGTATTCTTCAACGTAC 914
      *** ** ** *****  * ** ******** ** **  * **  * **  *  * *  **
```

Figure 5.3 EDNRB inter-species homology.

Alignment of *EDNRB* sequences from zebrafish, human, mouse, and chick demonstrates homology between species of between 64 and 70%. Homology is observed for the majority of exons 2-5, suggesting these regions may be functional regions of the gene. Homology over numerous intron:exon boundaries provides a choice for MO splice-site blocker design.

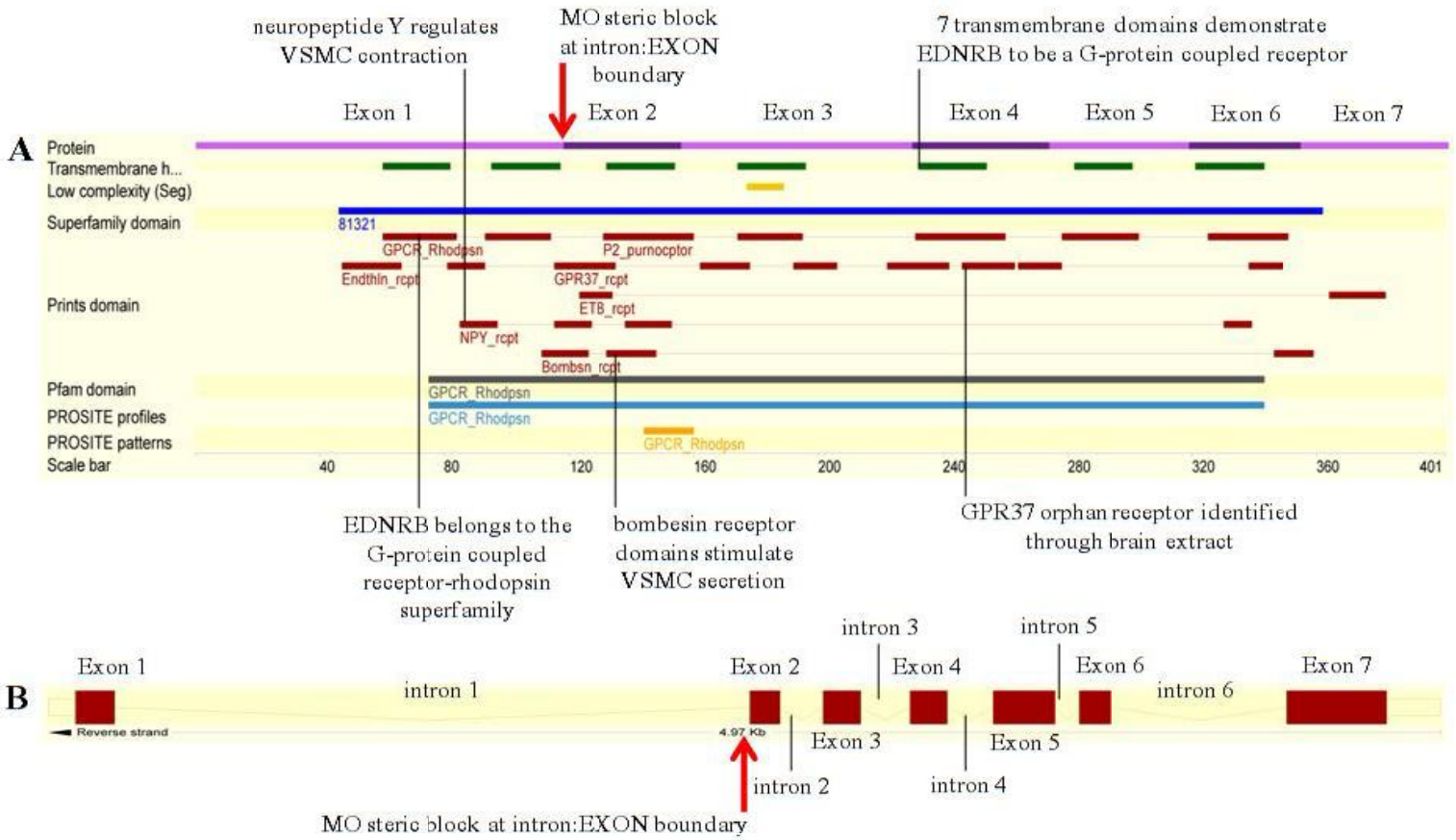

Figure 5.4 EDNRB protein domains.

A demonstrates the different domains within the zebrafish EDNRB protein, with brief descriptions of the roles of the domains. B demonstrates lengths of exons and introns in the EDNRB gene. The location of steric block by the MO utilised (section 5.2.6) is also demonstrated. The scale bar refers to amino acid number. Adapted from information generated by Ensembl version 52 (13/2/09).

This expression pattern concurs with that previously observed (Lister, Cooper *et al.*, 2006) in which the cells are described as presumptive melanocytes (arrow, figure 5.5A). There is also some weak expression immediately dorsal to the line corresponding with the region of SIVs, as well as expression within the brain which corresponds with *EDNRB* as a marker for neural crest cells (Parichy, Ransom *et al.*, 2000).

Despite identical conditions of hybridisation and staining as 2dpf embryos, only weak staining was detectable in 4dpf embryos, suggesting possible decreased *EDNRB* expression from 2 to 4dpf (figure 5.5B). This would concur with my microarray analysis which demonstrated decreased expression in *EDNRB* in control embryos from 48 to 60hpf (log_2 expression at 48hpf: 4.29, 60hpf: 1.36). The strong line of lateral staining observed at 2dpf is no longer observable, presumably a result of completed melanocyte migration or development. Expression in the region of aorta and cardinal vein remains. ET promotes EC proliferation and migration (Cruz, Parnot *et al.*, 2001), components of angiogenesis. Angiogenesis continues to 4dpf in zebrafish embryos (Isogai, Horiguchi *et al.*, 2001), possibly explaining continued levels of *EDNRB* expression in this region. Expression within the head is also still observable at this timepoint.

5.2.5 Determination of Morpholino Concentration for EDNRB Knockdown

Having confirmed expression of *EDNRB* in zebrafish embryos I wished to identify their possible role in modulating arteriogenesis. I chose to perform knockdown experiments, since morpholino antisense oligonucleotides (MOs) are frequently used to knockdown genes of interest in zebrafish embryos. MOs are designed against a gene's sequence, and thus confirmation of base-pair sequence as I performed in section 5.2.3 is important to ensure activity.

A splice-site MO for *EDNRB* (Gene Tools Inc, Oregon, USA) were designed against the confirmed sequence, to perform steric block at regions demonstrating homology when aligned against human, mouse and chick (section 5.2.3). Since multiple exons *EDNRB* demonstrated high levels of homology, the MO were designed to interact with the intron:exon boundary of exon 2.

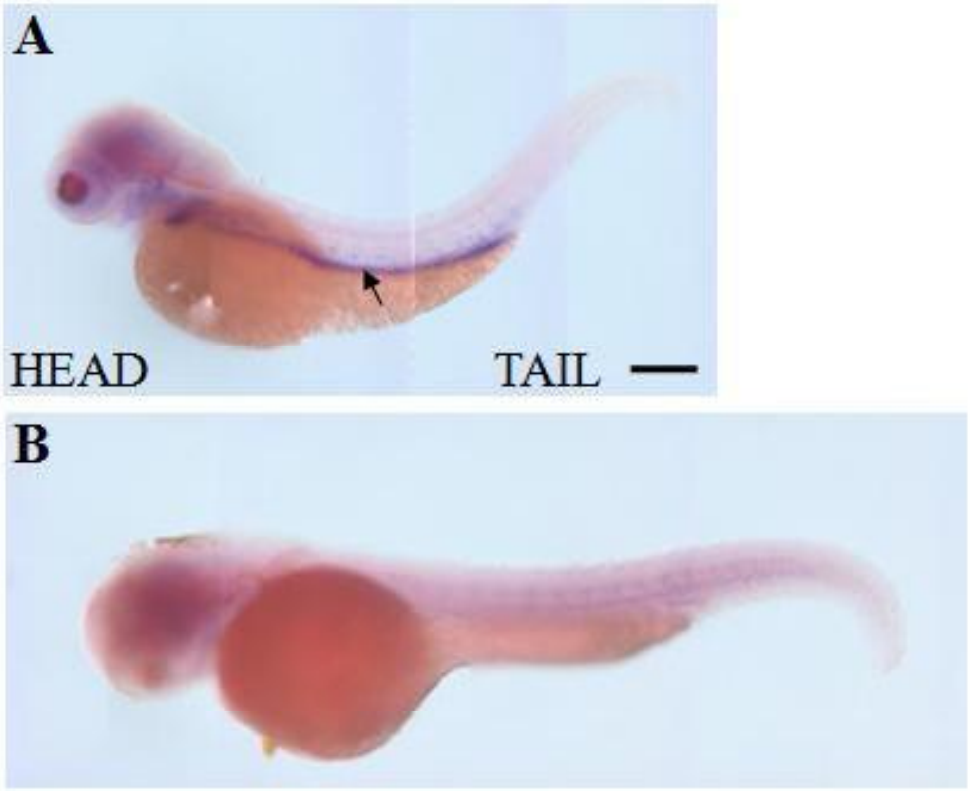

Figure 5.5 *In situ* hybridisation of zebrafish embryos to an EDNRB probe further determines the expression pattern of EDNRB.
48hpf (A) and 96hpf (B) wildtype embryos underwent *in situ* hybridisation to help further determine the expression pattern of *EDNRB* during early development. The results appear to show a fall in expression of *EDNRB* at 96hpf compared to 48hpf. Arrow (A) demarks proposed ventral stripe formed of melanocytes. Each sub-figure comprised of 3-5 images. Scale bar 200μm.

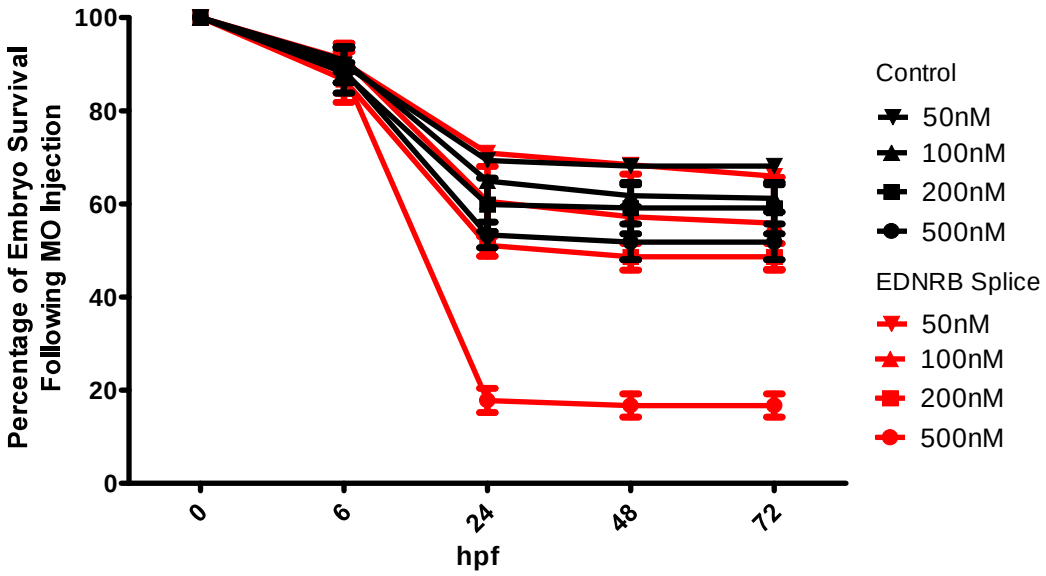

Figure 5.6 Dose-response graph to determine the concentration at which to utilise the EDNRB splice MO.

A concentration of [500nM] *EDNRB* MO led to reduced survival rates for embryos that made utilisation impractical. While a concentration of [50nM] provided the best survival, MO activity was not always detected. A concentration of [100nM] was utilised in further experiments.

To determine the concentration at which the MO should be utilised dose-response experiments were performed to determine embryonic survival over several concentrations (50, 100, 200, 500nM) during the first 3dpf (n=3, total of 120 embryos/group).

Figure 5.6 presents survival rates for embryos injected with *EDNRB* MO in comparison to standard control MO. [50nM] MO demonstrated highest survival rates, however, once more MO activity could not be guaranteed at this concentration. [100nM] and [200nM] shared similar levels of survival (60.5±7.5% and 51.1±2.3% respectively at 24hpf) which corresponded well with survival of embryos injected with control MO (100nM: 65.0±0.9%, 200nM: 59.8±5.7%). [500nM] led to greatly reduced levels of survival compared to embryos injected with the same concentration of control MO, suggesting toxicity. [100nM] *EDNRB* MO was utilised for further experimentation, again to reduce the possibility of non-specific effects caused by toxicity.

5.2.6 EDNRB Morpholinos Knockdown the Gene of Interest

To determine activity of the *EDNRB* MO I performed PCR analysis. Total RNA was extracted from wildtype embryos injected with [100nM] *EDNRB*, or control MO and reverse transcribed generating cDNA. cDNA was then utilised in PCR analysis and gel electrophoresis.

Transcript band shifts were observed with [100nM] *EDNRB* MO at 1 and 5dpf by PCR analysis, demonstrating splice modification by the MO (figure 5.7B) up to 5dpf. No band shifts were observed with cDNA generated from embryos injected with [100nM] control MO. While control bands appear of equal concentration at both 1 and 5dpf at over 200ng, band shifts generated by *EDNRB* splice modification appear reduced at 5dpf (60ng, upper band) compared to 1dpf (100ng, upper band), suggesting a decrease in MO activity from 1-5dpf, as if often observed. It appears MO knockdown induces exon skip, generating transcripts of smaller band sizes. The MO interacts at intron1:exon2 boundary, and may therefore result in 'loss' of several domains including a bombesin receptor domain which can stimulate VSMCs, a neuropeptide Y domain regulating VSMC constriction, or a GPR37 orphan receptor (figure 5.4).

5.2.7 Gross Phenotype of EDNRB Knockdown

In order to determine gross phenotype of *EDNRB* knockdown in zebrafish embryos, I injected wildtype embryos with [100nM] *EDNRB*, or control MO (approximately 40 embryos per group). A further group of 40 sibling embryos were left uninjected with MO. Embryos were then observed under stereomicroscopy at 2 and 5dpf. Wildtype embryos injected with control MO did not demonstrate any altered phenotype compared to uninjected embryos at 2 or 5dpf.

At both timepoints, gross structures including head, trunk, body length, and heart structure appeared comparable under stereomicroscopy. It can thus be deduced that injection of standard control MO does not result in altered physiology of embryos. At 2dpf *EDNRB* knockdown embryos demonstrated previously reported abnormal melanophore pigment cell expression (Lister, Cooper *et al.*, 2006), in addition to severe pericardial oedema and yolk-sac enlargement (figure 5.16). This may result from inhibition of *EDNRB*'s role in renal sodium reabsorption (Bagnall, Kelland *et al.*, 2006) causing fluid imbalances or fluid retention due to hypertension (Murakoshi, Miyauchi *et al.*, 2002). Pericardial oedema continued at 5dpf, leading to a thin, elongated heart but that continued to contract. Yolk-sac enlargement increased from 2-5dpf. Body length is reduced compared to control embryos. In some embryos, slight necrosis to the tail was observed at 5dpf. *EDNRB* phenotype at 5dpf can be seen in figure 5.9 compared to control MO injected siblings. Embryos continued to swim, and react to touch stimuli normally.

5.2.8 Vessel Patterning in EDNRB Knockdown

To determine whether *EDNRB* knockdown resulted in abnormal vascular patterning or development through abnormal vasculogenesis (*de novo* vessel formation through *in situ* differentiation of angioblasts) or angiogenesis (growth and remodelling of primitive vascular networks) I performed confocal microscopy of fli1:eGFP MO injected embryos.

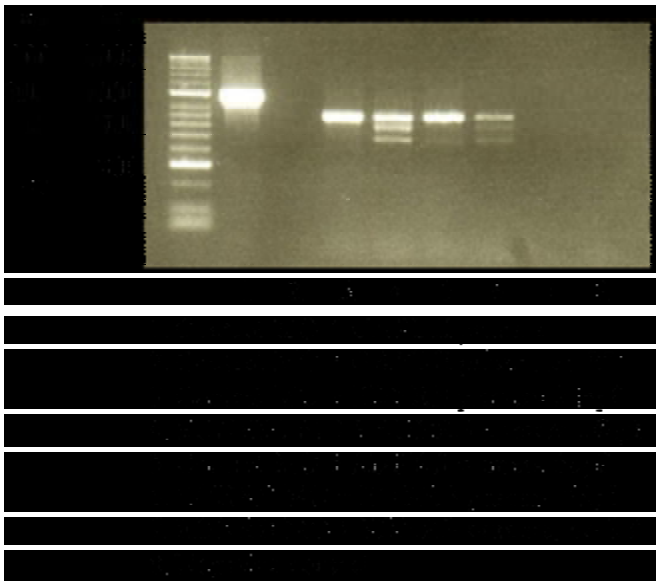

Figure 5.7 Assessing the activity of EDNRB MO by PCR analysis.
PCR analysis was performed on cDNA generated from total RNA extracted at timepoints described in the figure. At 1 and 5dpf splice modification was observed following *EDNRB* splice MO injection leading to observation of multiple bands following EDNRB knockdown. GAPDH expression was utilised as positive control, while no RT lanes were used to demonstrate PCR specificity to the gene of interest.

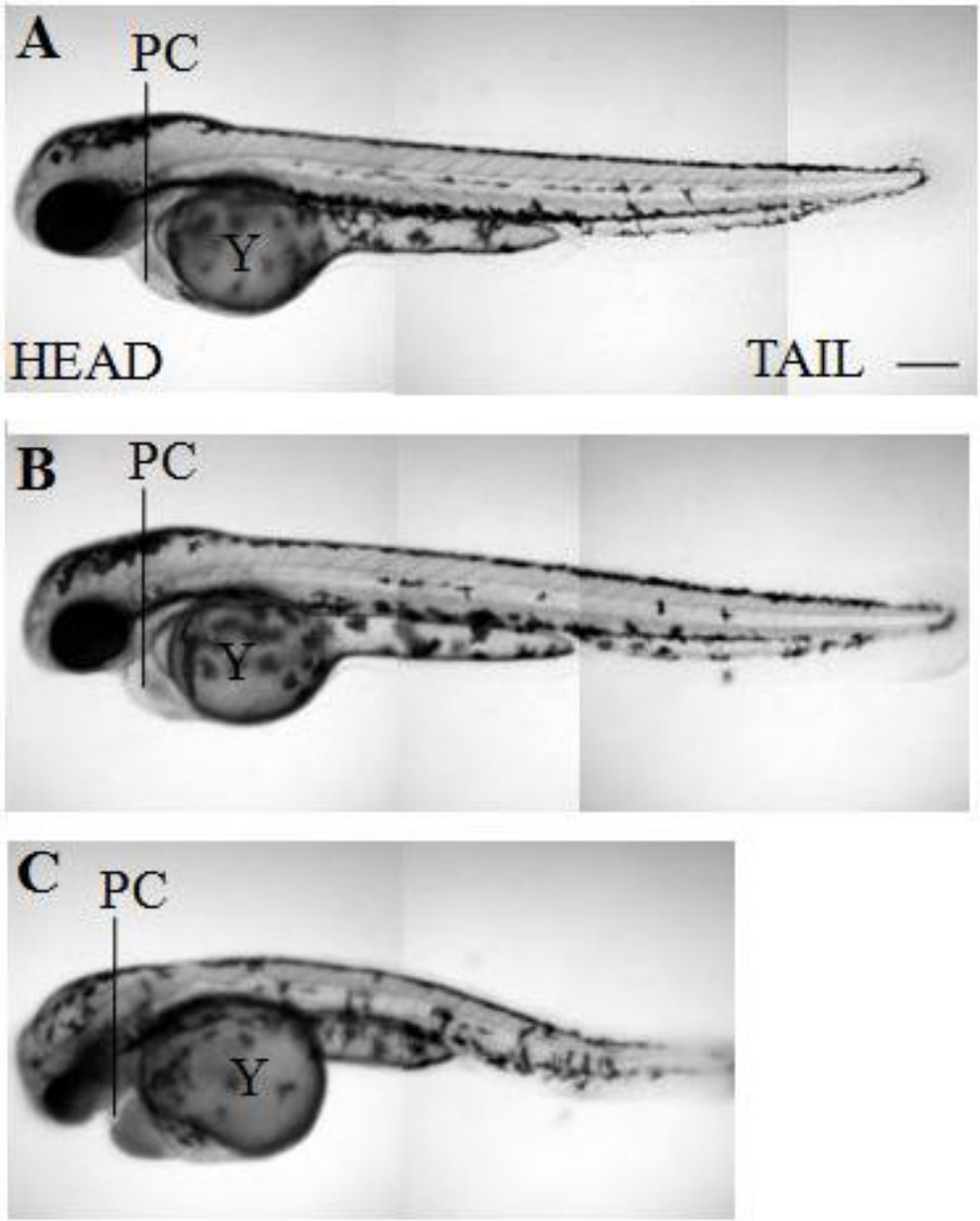

Figure 5.8 Phenotype of EDNRB knockdown in wildtype embryos at 2dpf.
EDNRB knockdown in wildtype embryos at 2dpf (C) resulted in severe pericardial oedema and yolk-sac enlargement on comparison with control MO injected siblings (B) and uninjected siblings (A). Y=yolk-sac, PC=pericardial sac. Representative lateral views complied of 2-3 images. Scale bar 200µm.

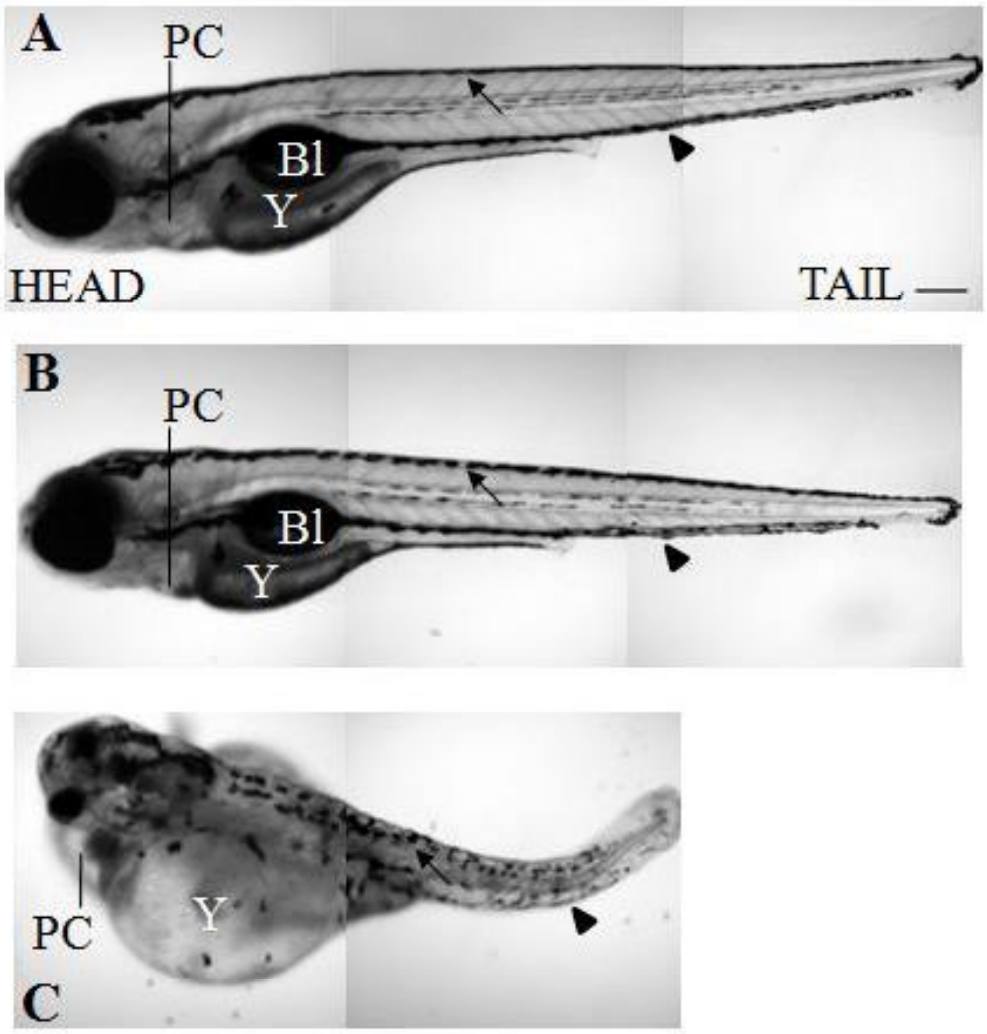

Figure 5.9 Phenotype of EDNRB knockdown in wildtype embryos at 5dpf.
Representative lateral view showing the phenotype observed following *EDNRB* knockdown in wildtype embryos at 5dpf. Pericardial oedema remained in *EDNRB* knockdown wildtype embryos at 5dpf (C). Enlargement of the yolk-sac increases from 2-5dpf. Slight necrosis of the tail was observed in some embryos. In contrast, control MO injected siblings (B) and uninjected siblings (A) looked normal. Arrow denotes site of dorsal stripe, arrowhead site of ventral stripe. Y=yolk-sac, PC=pericardial sac. Each sub-figure compiled from 2-3 images. Scale bar 200μm.

Figure 5.10 EDNRB knockdown does not affect vasculogenesis or angiogenesis.

Representative lateral views at 2dpf of brightfield (A, D, G), fluorescent (B, E, H) and combined (C, F, I) confocal laser-scanning microscopy images of uninjected (A-C), control MO injected (D-F), and *EDNRB* (G-I) knockdown in fli1:eGFP embryos. Vasculogenesis and angiogenesis are observed to have occurred normally in *EDNRB* knockdown embryos, on comparison with control MO injected siblings and uninjected siblings, with no abnormal vessel development or growth. Each sub-figure compiled from 2-3 images. Y=yolk-sac, V=cardinal vein, At=aorta, ISV=intersegmental vessels. Scale bar 200μm throughout.

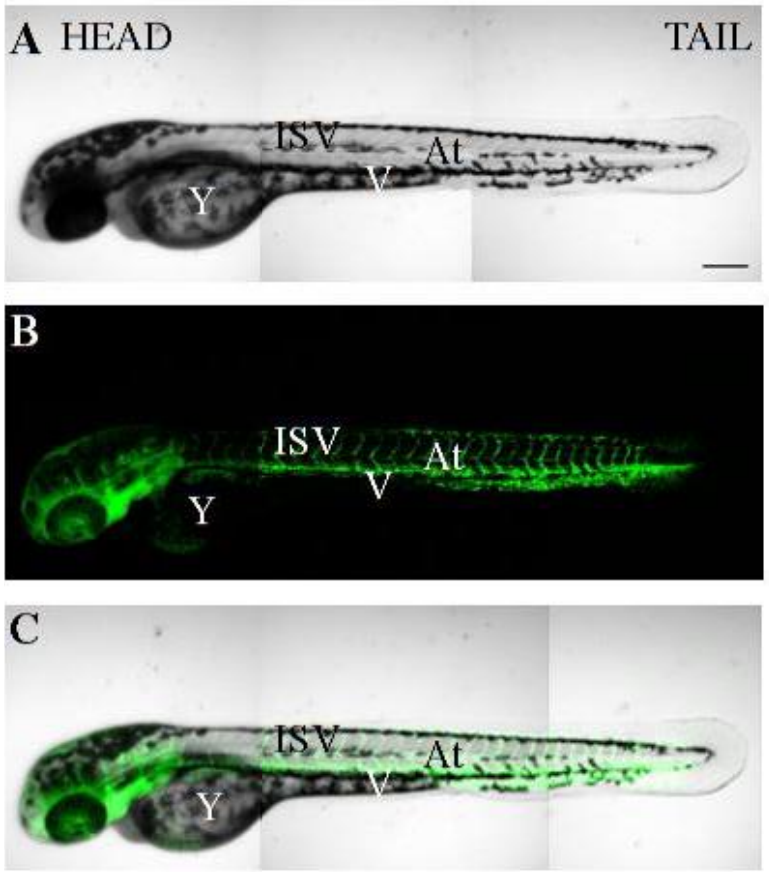

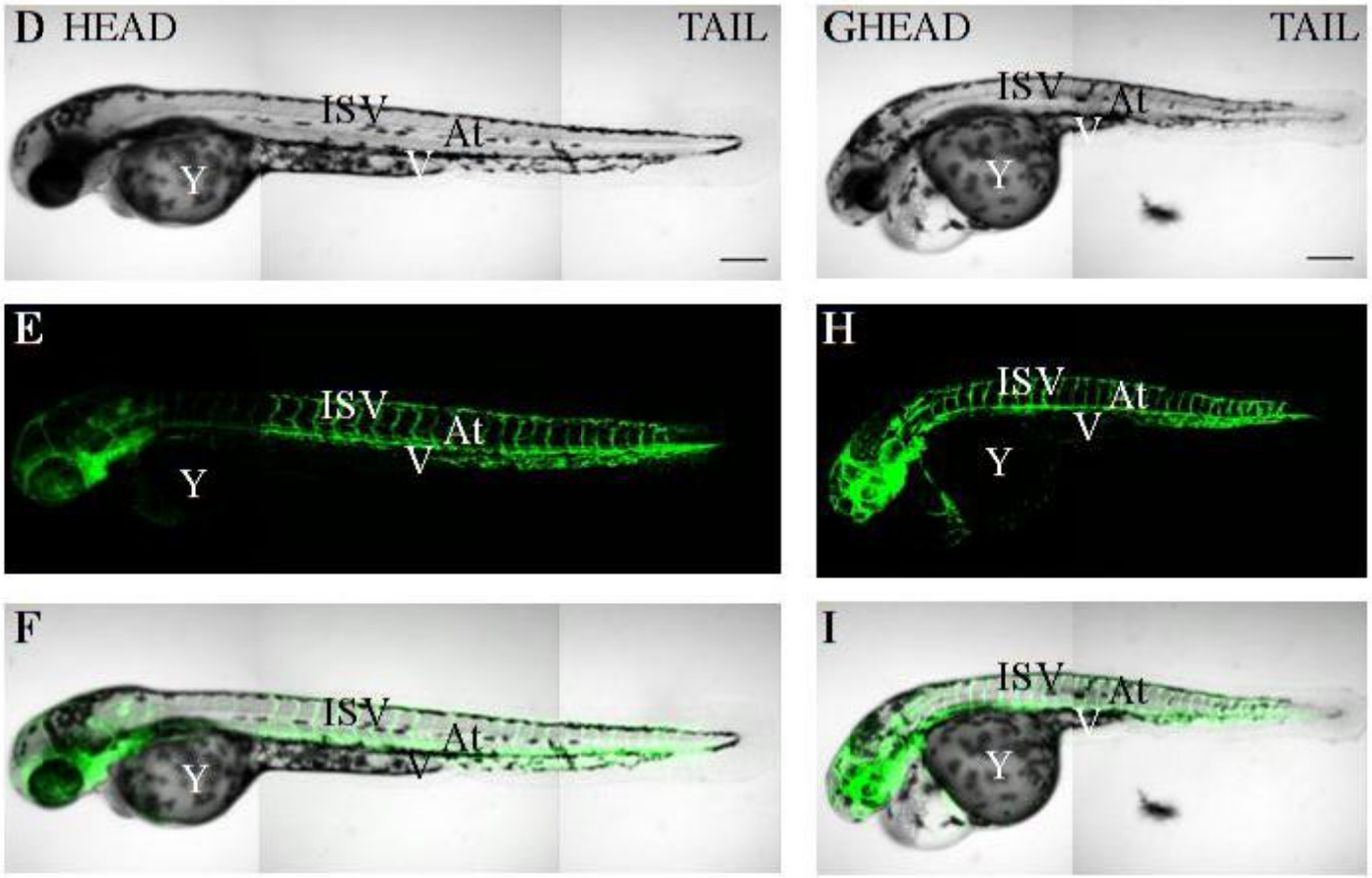
D HEAD
TAIL
ISV
At
V
Y
GHEAD
TAIL
ISV
At
V
Y
E
ISV
At
V
Y
H
ISV
At
V
Y
F
ISV
At
V
Y
I
ISV
At
V
Y

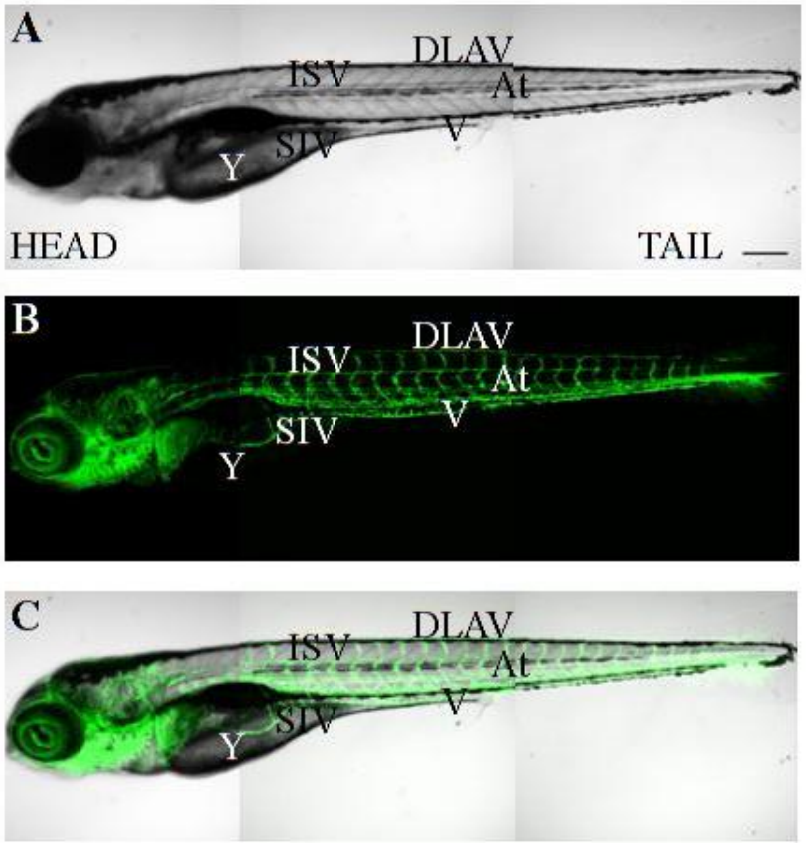

Figure 5.11 The effect of EDNRB knockdown on the vasculature at 5dpf.
Representative lateral views at 5dpf of brightfield (A, D, G), fluorescent (B, E, H) and combined (C, F, I) confocal laser-scanning microscopy images of uninjected (A-C), control MO injected (D-F), and *EDNRB* (G-I) knockdown in fli1:eGFP embryos. At 5dpf, *EDNRB* knockdown embryos demonstrate abnormalities in vessel structure, particularly towards the tail. Each sub-figure compiled from 2-3 images. Y=yolk-sac, V=cardinal vein, At=aorta, ISV=intersegmental vessels, SIV=subintestinal vasculature, DLAV=dorsal longitudinal anastomotic vessels. Scale bar 200μm throughout.

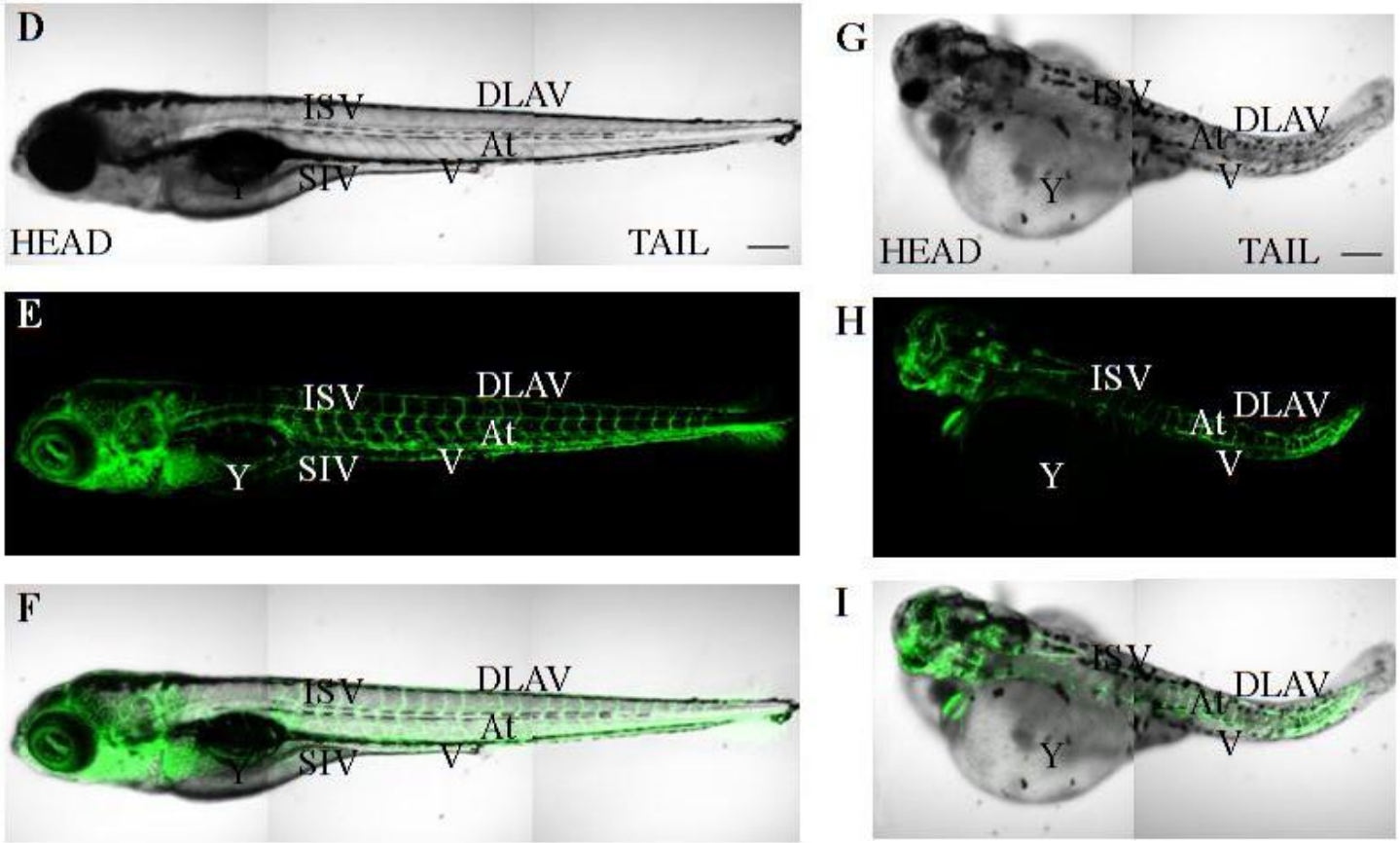
D
ISV
DLAV
At
SIV
V
Y
HEAD
TAIL
G
ISV
DLAV
At
V
Y
HEAD
TAIL
E
ISV
DLAV
At
Y
SIV
V
H
ISV
DLAV
At
Y
V
F
ISV
DLAV
At
Y
SIV
V
I
ISV
DLAV
At
Y
V

Representative embryos were chosen for laser-scanning confocal microscopy at 2 and 5dpf from approximately 40 observed by fluorescent stereomicroscopy. The same embryos were studied at both timepoints.

By 2dpf vasculogenesis, during which aorta and cardinal vein develop, is complete. At 5dpf angiogenesis of ISVs, DLAVs, and SIVs has occurred, with untreated embryos demonstrating a standard vascular pattern (Isogai, Horiguchi *et al.*, 2001). Angiogenesis is responsible for formation of ISVs, DLAVs, and SIVs. 5dpf is also the last timepoint at which recovery of aortic blood flow in *gridlock* embryos was observed (section 5.2.11). Of approximately 40 knockdown embryos per group observed by fluorescent stereomicroscopy at 2dpf, all *EDNRB* knockdown embryos demonstrated normal patterning of aorta and cardinal vein on comparison with wildtype embryos (figure 5.11), suggesting normal vasculogenesis, during which these vessels form (Isogai, Horiguchi *et al.*, 2001).

EDNRB knockdown embryos appear to demonstrate abnormalities in vessel structure, particularly towards the tail. Vessels developed during vasculogenesis that form prior to 2dpf such as dorsal aorta and cardinal vein appear normal, although difficult to observe due to development of severe yolk-sac enlargement. Observation remains obscured at 5dpf. It is particularly difficult to observe aorta and cardinal vein, and determine presence of SIVs due to oedema. While normal patterning and number of ISVs is observed on their formation, and DLAVs develop normally, at 5dpf DLAVs appear abnormal. The vessels demonstrate a more 'looping' phenotype, presumably a response to growth and remodelling necessary as embryos grow. Such a phenotype could be due to loss of EC migratory signals, or inhibited vessel maturation. *EDNRB* has been previously shown to be necessary for correct migration of ECs *in vitro* and *in vivo* (Cruz, Parnot et al., 2001).

5.2.9 Recovery of Aortic Blood Flow with EDNRB Knockdown

Haemodynamic force, including FSS plays a significant role in recovery of aortic blood flow following arterial occlusion (Buschmann and Schaper, 1999). In chapter 4, I demonstrated decreased expression of *EDNRB* in absence of haemodynamic force.

Therefore, it is reasonable to hypothesise *EDNRB* deficiency may lead to reduced recovery of aortic blood flow following occlusion. The role of these genes in arteriogenesis has not been studied, despite demonstrations of their importance in vascular remodelling in mammals (Adams, Wilkinson *et al.*, 1999; Murakoshi, Miyauchi *et al.*, 2002). I therefore wished to determine the potential role of the genes in modulating arteriogenesis.

To do this, I undertook *EDNRB* knockdown in *gridlock* mutant embryos, since the mutants' amenability to high throughput screening suited the experimentation (3 replicates, 30-50 embryos per group per replicate). Recovery of aortic blood flow by 'collateral' vessels in knockdown embryos was determined by binary count of presence or absence of aortic blood flow and compared to embryos injected with standard control MO. *Gridlock* mutants were not affected by MO injection any differently than wildtype embryos, appearing entirely normal, however detailed investigation was not performed and it is possible vessel histology was altered. By 5dpf, *EDNRB* knockdown embryos demonstrate pericardial oedema and severe yolk-sac swelling, as discussed in section 5.2.8. *Gridlock* embryos with *EDNRB* knockdown may therefore demonstrate a phenotype which precludes accurate determination of recovery of blood flow. However, recovery of blood flow was determined to provide preliminary data regarding the role of *EDNRB* in arteriogenesis.

At 2dpf no *EDNRB* knockdown *gridlock* mutant or control MO *gridlock* embryo was found to have aortic blood flow. No significant difference from control MO injecting siblings was observed at 3dpf (control: 26.60±8.95, *EDNRB* knockdown: 13.09±10.16). At 4dpf, a very significant reduction ($P<0.01$) in recovery of aortic blood flow distal to occlusion was observed (control: 63.93±3.41, *EDNRB* knockdown: 27.47±6.61), as demonstrated in figure 5.21. This very significant reduction was maintained at 5dpf (control: 66.73±3.26, *EDNRB* knockdown: 27.50±6.85; power 100%). It seems likely that *EDNRB* controls blood flow, and thus is linked to haemodynamic force, through vasoregulation. Ligand binding of *EDNRB* on VSMCs leads to vasoconstriction, while activation of endothelial *EDNRB* results in NO release inducing vasodilatation (Murakoshi, Miyauchi *et al.*, 2002).

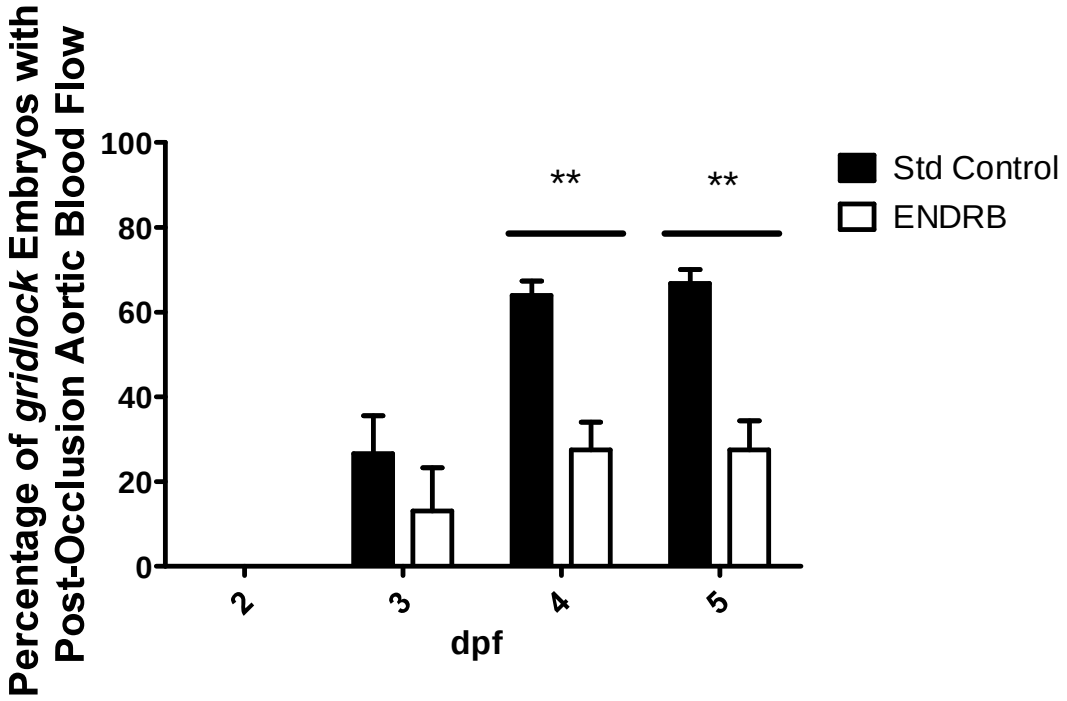

Figure 5.12 The effect of EDNRB knockdown on the acquisition of aortic blood flow distal to the occlusion site in *gridlock* mutant embryos.
EDNRB knockdown *gridlock* mutant embryos do not demonstrate a difference in the acquisition of aortic blood flow distal to the occlusion site compared to control MO injected siblings at 3dpf. At 4dpf, a very significant reduction ($P<0.01$) in the acquisition of aortic blood flow is observed, which was maintained at 5dpf.

Experiments utilising VSMCs in culture have demonstrated a significant upregulation of *EDNRB* mRNA following onset of cyclic stretch, mimicking increases in blood pressure, which were maintained for a further 12h after abolishment of stretch (Cattaruzza, Dimigen *et al.*, 2000). EC-specific inactivation of *EDNRB* leads to increased plasma concentrations of ET and reduced endothelial-dependent vasodilatation (Bagnall, Kelland *et al.*, 2006). Furthermore, *EDNRB* mutant mice suffer significantly reduced levels of vascular remodelling following ligation of the common carotid artery (Murakoshi, Miyauchi *et al.*, 2002). This data therefore concurs with previous data in having found a significant reduction in levels of 'collateral' vessel development with *EDNRB* knockdown/knockout.

5.2.10 Chemical Antagonism of EDNRB does not affect Recovery of Aortic Blood Flow in *gridlock* Mutant Embryos

Since *EDNRB* knockdown in *gridlock* mutant embryos by MO led to significant reductions in the percentage of embryos recovering aortic blood flow, I sought to reproduce the effect by chemical antagonism. Groups of *gridlock* mutant embryos were treated with three concentrations ([0.1], [1], and [5μM]) of the specific EDNRB antagonist BQ788 dissolved in DMSO from 2.5-5dpf. This timepoint was chosen since embryos appear to develop without abnormality to 2dpf (sections 5.2.8 and 5.2.9). BQ788 has not previously been utilised in zebrafish embryos. However BQ788 has been demonstrated to inhibit ET-induced angiogenesis (Salani, Taraboletti *et al.*, 2000) and *in vitro* EC migration (Daher, Noel *et al.*, 2008). A different EDNRB specific antagonist (A-192621) was demonstrated to decrease vascular remodelling following arterial ligation in mice (Murakoshi, Miyauchi *et al.*, 2002).

Gridlock embryos survived BQ788 treatment equally well as wildtype embryos. Survival rates ranged from 86.0±3.1%-100% irrespective of treatment group (n=3, 10-30 embryos per group per replicate), demonstrating good embryonic tolerance. The highest concentration of BQ788 ([5μM]) did not demonstrate a significant difference in heart rate compared to DMSO or untreated control siblings (figure 5.14; $P>0.3$; n=8/group; DMSO control: 156.8±3.76, untreated: 143.3±8.27, BQ788: 145.3±6.63; power 98.95%).

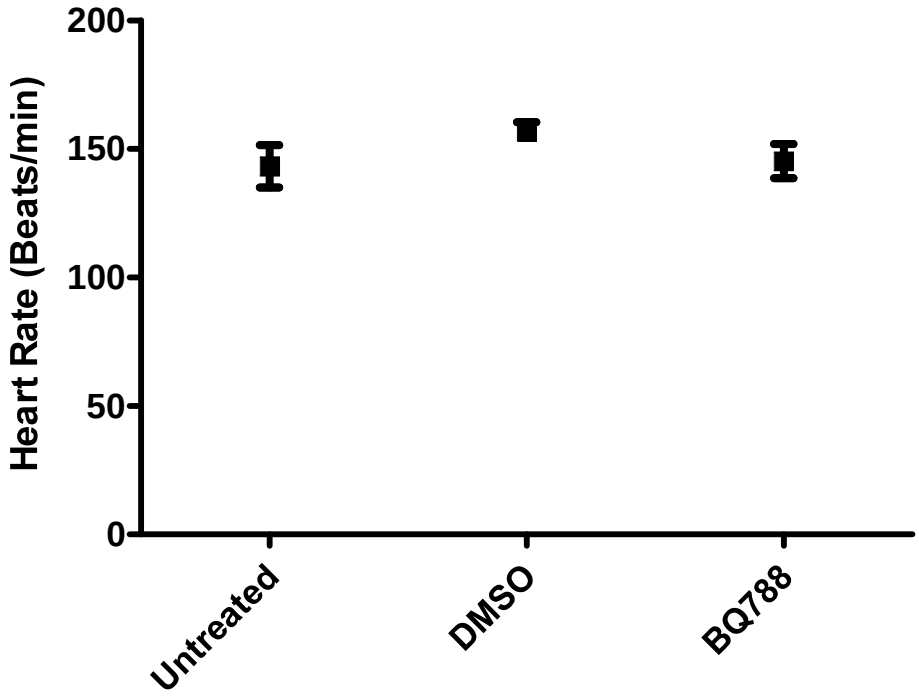

Figure 5.13 The effect of BQ788 on heart rate of *gridlock* mutant embryos at 5dpf.

Incubation from 2.5-5dpf with the EDNRB specific antagonist BQ788 demonstrates no significant difference on heart rates of *gridlock* mutant embryos at 5dpf compared to DMSO or untreated sibling control.

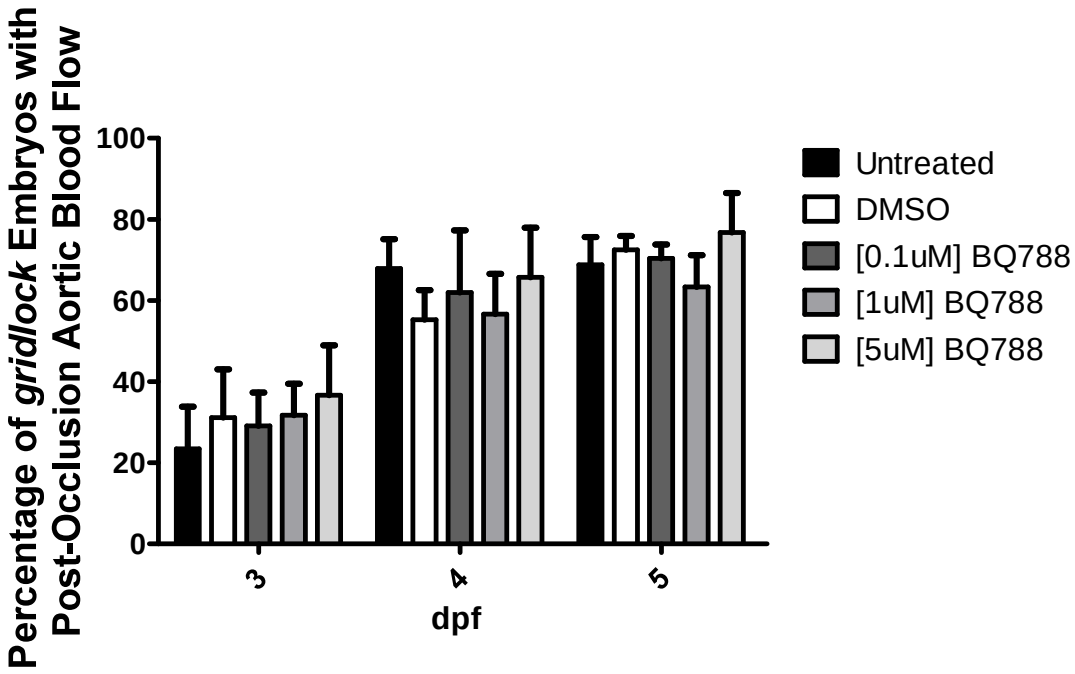

Figure 5.14 The effect of BQ788 on the acquisition of aortic blood flow distal to the occlusion site in *gridlock* mutant embryos.

Incubation from 2.5-5dpf with the EDNRB specific antagonist BQ788 at [0.1], [1], or [5μM] had no significant effect on the acquisition of aortic blood flow distal to the occlusion site in *gridlock* mutant embryos compared to DMSO or untreated sibling control.

This suggests EDNRB deficiency is not altering cardiac contractility. BQ788 has not previously been reported to affect heart rate.

In contrast to the results of *EDNRB* MO knockdown, BQ788 treatment of *gridlock* mutant embryos did not significantly reduce recovery of aortic blood flow (figure 5.23; n=4, 10-20 embryos per group per replicate) at any of the three concentrations. At 2dpf no embryo was observed with aortic blood flow. At 3dpf comparable percentages of embryos recovered aortic blood flow between groups (DMSO: 31.13±11.88%, untreated: 23.43±10.35%, [0.1μM] BQ788: 29.13±8.20%, [1μM] BQ788: 31.75±7.67%, [5μM] BQ788: 36.60±12.68%). Percentages were also comparable between groups at 4dpf (DMSO: 55.25±7.32%, untreated: 67.90±7.29%, [0.1μM] BQ788: 61.93±15.35%, [1μM] BQ788: 56.63±9.97%, [5μM] BQ788: 65.70±12.26%), and 5dpf (DMSO: 72.48±3.41%, untreated: 68.80±6.87%, [0.1μM] BQ788: 70.38±3.45%, [1μM] BQ788: 63.35±7.80%, [5μM] BQ788: 76.80±9.70%; power DMSO v [5 μM] BQ788 90.23%).

BQ788 has not previously been described for utilisation in zebrafish embryos. BQ788 incubation of embryos was performed by immersing embryos in media containing the antagonist. It is therefore possible that BQ788 did not freely diffuse into embryos. Embryos were incubated in BQ788 at 2.5dpf to observe the antagonist's effect after vasculogenesis, and angiogenesis of ISVs, DLAVs, and some SIVs were completed (Isogai, Horiguchi *et al.*, 2001). It is possible that inhibition of EDNRB is required prior to this timepoint in order to cause significant differences in response to arterial occlusion.

5.3 Discussion

Haemodynamic force modulates arteriogenesis (Buschmann and Schaper, 1999). Microarray analysis of zebrafish embryos in presence or absence of physiological haemodynamic force (Chapter 4) demonstrated differential expression of 290 genes between groups. Literature searches identified genes with possible roles in modulation of arteriogenesis through knowledge of other roles within vasculature. For example, although arteriogenesis and angiogenesis are distinct processes, they share mechanistic

traits such as modulation by NO (Yu, deMuinck *et al.*, 2005), and infiltration of monocytes/macrophages (Van Royen, Piek *et al.*, 2001b). *EDNRB* was identified as a possible candidate. Its role in modulating arteriogenesis has not been studied. *EDNRB* modulates blood flow through its involvement in vasoactivity (Murakoshi, Miyauchi *et al.*, 2002), as well as promoting EC proliferation and migration (Cruz, Parnot *et al.*, 2001) a key constituent of angiogenesis. The aim of this chapter was exploitation of zebrafish embryos to determine the role of *EDNRB* in modulating arteriogenesis utilising morpholino oligonucleotide knockdown. Prior to knockdown, I began by confirming expression of *EDNRB* in zebrafish embryos.

5.3.1 Expression of EDNRB in Zebrafish Embryos

In order to confirm expression of *EDNRB* in zebrafish embryos I performed RT-PCR utilising wildtype embryo total RNA extracted at 36hpf and reverse transcribed. RNA extraction was performed at 36hpf since this was the first microarray timepoint. *EDNRB* transcript band size was observed at approximately 800bp (figure 5.1A), corresponding with the predicted band size of 718bp. *GAPDH* control also demonstrated transcript size corresponding with that predicted. Thus, these results confirm expression of *EDNRB* in zebrafish embryos at 36hpf. Transcript band size was determined utilising primer pairs designed against Ensembl predicted sequences. To confirm the sequences PCR product was sequenced at the University's Core Genomics Facility allowing visualisation of potential alterations in base-pair alignment. Product was purified at the facility to remove excess primer, dNTIPs, and non-specific products. Alignment between PCR product and predicted sequence for *EDNRB* demonstrated 91% homology (figure 5.2). Once more, non-homologous regions were identified at either end of the alignment at primer binding locations. This may suggest true alignments are closer to 100% homology. These results confirm the automated predicted sequences for *EDNRB* in zebrafish embryos.

Alignment of *EDNRB* zebrafish sequence to human, mouse, and chick demonstrated a homology of 61-71% with significant homology from base-pair 126 onwards between all aligned species (figure 5.3). The regions of homology correspond to the majority of

exon 1 onward. A variety of protein domains are therefore possibly homologous between the aligned species (discussed in section 5.3.3).

5.3.2 Expression Pattern of EDNRB is Elucidated by ISH

I performed whole-mount *in situ* hybridisation (ISH) to determine expression patterns in zebrafish embryos. ISH is commonly utilised to determine gene expression patterns during early development in zebrafish embryos by detecting specific nucleic acid sequences with RNA probes. It has a major advantage over antibody immunohistochemistry, since few antibodies are cross-reactive with zebrafish. In addition, reagents and technique have been optimised for zebrafish embryos (Thisse and Thisse, 2008). At 2dpf (figure 5.5A), a strong line of staining originating at a site above the pericardial sac traverses laterally towards the tail. It apparently terminates at the end of the yolk-sac extension. This expression pattern concurs with that previously observed (Lister, Cooper *et al.*, 2006) in which the cells are described as presumptive melanocytes (arrow, figure 5.9A). There is weak expression immediately dorsal to the line corresponding with the region of aorta and cardinal vein. This may correspond to vascular cells such as VSMCs expressing *EDNRB* (Cattaruzza, Dimigen *et al.*, 2000), or vascular-associated cells such as macrophages which also express the gene (Miyauchi and Masaki, 1999). Expression within head which corresponds with *EDNRB* expression in neural crest cells (Parichy, Ransom *et al.*, 2000) was also observed. Despite identical conditions of hybridisation at 4dpf, only weak staining was detectable (figure 5.5B). This could suggest decreased expression of *EDNRB* from 2 to 4dpf. As mentioned in the previous section, this would concur with my microarray analysis which demonstrated decreased expression in control embryos from 48 to 60hpf. The strong line of lateral staining is not observable at 4dpf, presumably a result of decreased expression in melanocytes. Expression in the region of aorta and cardinal vein remains. ET promotes EC proliferation and migration (Cruz, Parnot *et al.*, 2001), components of angiogenesis. Angiogenesis continues at 4dpf in zebrafish embryos (Isogai, Horiguchi *et al.*, 2001), perhaps explaining continued levels of *EDNRB* expression in this region. Expression within head is also still observable at this timepoint.

5.3.3 EDNRB Knockdown by Morpholino Injection

Having confirmed expression of *EDNRB* in zebrafish embryos I wished to determine their possible role in modulating arteriogenesis, and did so by performing knockdown with MO. As MOs are designed against a gene's sequence, confirmation of base-pair sequence (section 5.2.3) is important to ensure activity. Splice-site blocking MOs result in modification of pre-mRNA splicing to knockdown a gene's functional sequence (Summerton, 2007). An advantage of splice-site blocking MOs is the ability to determine activity by PCR analysis. To determine the concentration at which MOs should be utilised dose-response experiments were performed to determine embryonic survival over several concentrations during the first 3dpf. MO-induced lethality is most likely during this timepoint since MOs are injected at 1-4 cell stage. Dose-response experiments were performed through alteration of MO concentration, rather than alteration of injected volume, to remove the possibility of non-specific phenotypes resulting from increasing volume.

Survival rates following *EDNRB* knockdown were highest following injection of [50nM] (figure 5.11) however, MO activity was not always detected. [100nM] was utilised in future experiments, since this concentration combined high survival rates with activity. Additionally, [100nM] was the second lowest concentration examined, and is therefore least likely to cause toxicity and non-specific phenotypes. Embryonic survival was the parameter utilised in dose response experimentation. In hindsight, a prudent method may have been a more detailed study of embryos' anatomy and physiology to accurately determine possible alterations.

Transcipt band shifts demonstrated splice modification with injection of *EDNRB* MO at 1 and 5dpf (figure 5.7). The band shifts appeared reduced at 5dpf suggesting decreased MO activity, as is often observed. It appears MO knockdown induces exon skip, generating transcripts of smaller band sizes. The MO interacts at intron1:exon2 boundary, and may therefore result in 'loss' of several domains including a bombesin receptor domain which can stimulate VSMCs, a neuropeptide Y domain regulating VSMC constriction, or a GPR37 orphan receptor (figure 5.4).

5.3.4 Gross Phenotypic Characterisation of EDNRB Knockdown

To determine gross phenotype of *EDNRB* knockdown in zebrafish embryos I injected wildtype embryos with [100nM] *EDNRB*, or control MO. A group of embryos were also left uninjected. Wildtype embryos injected with control MO did not demonstrate altered phenotype on comparison with uninjected embryos at 2 or 5dpf under stereomicroscopy. Gross structures such as head, trunk, heart, and body length are comparable between groups demonstrating injection of MOs does not in itself alter embryonic development.

EDNRB knockdown in wildtype embryos demonstrated abnormal melanocyte pigment cell expression at 2dpf (figure 5.8), as previously described (Lister, Cooper *et al.*, 2006). Embryos also demonstrated severe pericardial oedema and yolk-sac enlargement, which may result from inhibition of EDNRB's role in renal sodium reabsorption (Bagnall, Kelland *et al.*, 2006) causing fluid imbalances or fluid retention due to hypertension (Murakoshi, Miyauchi *et al.*, 2002). By 5dpf (figure 5.9) the pericardial sac of *EDNRB* knockdown embryos had become more oedematous. As a result, the heart became thin and elongated, but continued to contract and pump blood around the vasculature. Body length is reduced compared to control embryos. Some embryos demonstrate slight necrosis of the tail, although embryos continued to swim and react to touch stimuli.

5.3.5 Vessel Patterning in EDNRB Knockdown

To determine the effect of *EDNRB* knockdown on vascular patterning and development through vasculogenesis and angiogenesis, fli1:eGFP transgenic embryos underwent MO injection and observation by fluorescent stereomicroscopy. Representative embryos underwent laser-scanning confocal microscopy at 2 and 5dpf. By 2dpf vasculogenesis, during which aorta and cardinal vein develop, is complete. At 5dpf angiogenic development of ISVs, DLAVs, and SIVs is complete, and wildtype embryos demonstrate a standard reproducible vascular pattern (Isogai, Horiguchi *et al.*, 2001). 5dpf is also the last timepoint at which recovery of aortic blood flow in *gridlock* mutant embryos was determined. At 2dpf, embryos demonstrated normal patterning of aorta and cardinal vein on comparison with control MO embryos (figure 5.10). This suggests normal vasculogenesis in *EDNRB* knockdown embryos. Genetic knockdown of vascular

EDNRB in mice was not reported to result in abnormal vasculogenesis (Murakoshi, Miyauchi *et al.*, 2002).

EDNRB knockdown embryos demonstrated apparent abnormalities in vessel structure, particularly towards the tail, at 5dpf (figure 5.11). Vessels developed prior to 2dpf during vasculogenesis (aorta, cardinal vein) appear normal, although difficult to visualise due to yolk-sac enlargement. It remains difficult to visualise aorta and cardinal vein, and determine presence of SIVs at 5dpf. Normal patterning and number of ISVs is observed on formation. DLAVs also develop normally. However, at 5dpf DLAVs appear abnormal. The vessels demonstrate a 'looping' phenotype, presumably a response to abnormal forms of growth and remodelling that occurs during embryonic growth. Given that vessels remain extant but demonstrate some unusual patterning it may suggest EC migration or vessel maturation is inhibited. *EDNRB* has been shown to be necessary for correct migration of ECs *in vitro* and *in vivo* (Cruz, Parnot et al., 2001). However, the possibility cannot be ruled out that abnormality in patterning, most highly visible at the tail, could also result from the severe phenotypic characteristics of pericardial oedema, yolk-sac enlargement, and slight necrosis to the tail region.

5.3.6 Recovery of Aortic Blood Flow with EDNRB Knockdown

Haemodynamic force including FSS plays a significant role in the recovery of aortic blood flow following arterial occlusion (Buschmann and Schaper, 1999). In chapter 4, I demonstrated decreased expression of *EDNRB* with absent haemodynamic force. Therefore, it is reasonable to hypothesise *EDNRB* deficiency may lead to reduced recovery of aortic blood flow following occlusion. The role of these genes in arteriogenesis has not been studied, despite demonstrations of their importance in vascular remodelling in mammals (Adams, Wilkinson *et al.*, 1999; Murakoshi, Miyauchi *et al.*, 2002). To determine their potential role in modulating arteriogenesis I undertook gene knockdown in *gridlock* embryos, a mutant which undergoes arteriogenesis to recover aortic blood flow (Chapter 3). The high throughput nature of observing recovery of aortic blood flow distal to occlusion in *gridlock* mutants provides a rapid means for determining the effect of potential modulators on arteriogenesis. As discussed in Chapter 1 (section 1.4), observation of arterial blood flow recovery

following occlusion (ligation) in mammals can be limited by disadvantages when compared to zebrafish embryos. These include technical difficulty, prolonged experimental timeframes, and inadequate techniques for identification of collateral vessels of all diameters *in vivo* and serially (Mills, Fischer *et al.*, 2000; Heil, Ziegelhoeffer *et al.*, 2004; Duvall, Robert Taylor *et al.*, 2004). Generation of gene knockdown/knockout mice required would also beget similar disadvantages.

EDNRB knockdown in *gridlock* mutants demonstrated very significant reduction ($P<0.01$) in recovery of aortic blood flow distal to occlusion at both 4 and 5dpf (figure 5.12). While no aortic blood flow was observed at 2dpf, recovery of blood flow in *EDNRB* knockdown *gridlock* embryos was also reduced, though non-significantly, at 3dpf. This suggests *EDNRB* knockdown may have altered *gridlock's* response to aortic occlusion at an early stage prior to first observed recovery of flow at 3dpf. EDNRB is expressed on ECs where endothelin binding induces vasodilatation through release of NO, and also on VSMCs where endothelin binding induces vasoconstriction (Murakoshi, Miyauchi *et al.*, 2002). It has been suggested ET controls vascular tone before development of nervous innervation. For example, NO and ET modulate vascular parameters in *Xenopus laevis* tadpoles prior to onset of autonomic control (Schwerte, Printz *et al.*, 2002). Both FSS and cyclic stretch alter *endothelin* and *EDNRB* expression levels, and ECs are capable of determining alterations in haemodynamic force (Ohura, Yamamoto *et al.*, 2003). Exposure of HUVECs to laminar flow representative of arterial rheology led to significant downregulation of *ET* (McCormick, Eskin *et al.*, 2001), while turbulent flow resulted in upregulation of the endothelin precursor *preproendothelin* (Himburg, Dowd *et al.*, 2007). Significant upregulation of EDNRB mRNA is observed following induction of cyclic stretch to cultured VSMCs (Cattaruzza, Dimigen *et al.*, 2000). Thus, EDNRB expression is not only determined by haemodynamic force acting on vasculature, but can also alter haemodynamic force by its regulation of vasoactivity. This is important to stress, since many genes associated with arteriogenesis are differentially expressed with altered levels of haemodynamic force (Schaper and Ito, 1996). Furthermore, FSS induced by laminar flow is believed responsible for initial dilation of collateral vessels through activation of eNOS (Unthank, Nixon *et al.*, 1996).

EDNRB knockdown may therefore inhibit EDNRB-regulated NO-mediated vasodilatation, preventing recovery of blood flow.

EC-specific inactivation of *EDNRB* in mice reduced endothelial-dependent vasodilatation supporting this hypothesis (Bagnall, Kelland *et al.*, 2006). Inactivation also increased plasma ET concentrations, because clearance by EDNRB was inhibited (Bagnall, Kelland *et al.*, 2006). Plasma ET may have been able to bind VSMC EDNRB and EDNRA both unaffected by EC-specific inactivation, resulting in vasoconstriction, preventing vasodilatation by another means. Although *EDNRB* knockdown by MO in zebrafish embryos was not EC-specific preventing VSMC constriction, EDNRA is unaffected, permitting vasoconstriction on endothelin binding, and thereby inhibiting vasodilatation required for recovery of blood flow.

Evidence demonstrates the importance of monocytes/macrophages to arteriogenesis. Macrophage depletion by *pu.1* knockdown in *gridlock* embryos significantly reduces recovery of blood flow around occlusion (Gray, Packham *et al.*, 2007). MCP-1 is released from shear activated ECs (Van Royen, Piek *et al.*, 2001b), and is the most potent stimulator of monocyte migration (Heilmann, Beyersdorf *et al.*, 2002). MCP-1 promotes monocyte recruitment to collateral vessels following ligation (van Royen, Hoefer *et al.*, 2003). EDNRB is also expressed on monocytes and macrophages (Miyauchi and Masaki, 1999). Therefore *EDNRB* knockdown may result in decreased recruitment or activity of monocytes to remodelling vessels, limiting recovery of aortic blood flow.

5.3.7 Chemical Antagonism of EDNRB does not affect Recovery of Aortic Blood Flow in *gridlock* Mutant Embryos

Since *EDNRB* knockdown in *gridlock* mutant embryos by MO led to significant reductions in percentage of embryos recovering aortic blood flow, I sought to reproduce the effect by chemical antagonism. Groups of *gridlock* mutant embryos were treated with three concentrations of the specific EDNRB antagonist BQ788 from 2.5-5dpf. This timepoint was chosen since embryos appear to develop without abnormality to 2dpf (sections 5.2.7 and 5.2.8). BQ788 has not previously been utilised in zebrafish embryos.

However it has been demonstrated to inhibit ET-induced angiogenesis (Salani, Taraboletti *et al.*, 2000) and *in vitro* EC migration (Daher, Noel *et al.*, 2008). An alternative EDNRB specific antagonist (A-192621) decreased vascular remodelling following arterial ligation in mice (Murakoshi, Miyauchi *et al.*, 2002). Recent research in chick has demonstrated no effect with EDNRB inhibition by BQ788 in physiological development, however alterations in haemodynamic force induced by arterial ligation resulted in significantly reduced 'collateral' vessel development in comparison to control ligated embryos (Ms Emily Hoggar, personal communication). This data provides a further link between EDNRB and altered haemodynamic force.

Gridlock embryos survived BQ788 treatment equally well as untreated control sibling embryos, and demonstrated no alteration in heart rate (figure 5.13). BQ788 treatment of *gridlock* mutant embryos did not significantly reduce recovery of aortic blood flow (figure 5.14) at any of the three concentrations, contrasting with *EDNRB* knockdown. BQ788 has not previously been described for utilisation in zebrafish embryos. Incubation of embryos was performed by immersing embryos in media containing the antagonist. It is therefore possible that BQ788 did not freely diffuse into embryos. Embryos were incubated in BQ788 at 2.5dpf to observe the antagonist's effect after formation of the vessels which remodel during recovery of blood flow in *gridlock* embryos. It is possible inhibition of *EDNRB* is required prior to this timepoint in order to cause significant differences in response to arterial occlusion. The early non-significant reductions in recovery of aortic blood flow observed following *EDNRB* knockdown may support this theory.

5.4 Limitations and Future Work

5.4.1 Effects of EDNRB Knockdown on Recovery of Aortic Blood Flow in *gridlock* Mutant Embryos is not confirmed by Chemical Antagonism

I have demonstrated *EDNRB* knockdown significantly reduces recovery of aortic blood flow distal to occlusion in *gridlock* mutant embryos (figure 5.12). However, these results were not confirmed by chemical antagonism of EDNRB by BQ788 (figure 5.14). The role of EDNRB in modulating arteriogenesis therefore needs confirmation, although

studies in mice (Murakoshi, Miyauchi *et al.*, 2002) and chick (Ms Emily Hoggar, personal communication) suggest a role. Diffusion of BQ788 into embryos should be identified through Western blot and immunoprecipitation, so activity can be confirmed. This would require custom design of antibodies, since no commercially produced antibody against EDNRB is available for use with zebrafish. It would also be beneficial to perform BQ788 treatment of embryos at earlier timepoints, or through different methods of administration. Injection of BQ788 directly into the circulation, in an adaptation of microangiography methodology (Isogai, Horiguchi *et al.*, 2001), may yield differing results. Means are available to determine if BQ788 did freely diffuse into the embryos including mass spectrometry (which would demonstrate the drug's presence, but not its location) and high performance liquid chromatography (HPLC) allowing identification and quantification.

5.4.2 EDNRB Significantly Reduces Recovery of Aortic Blood Flow in *gridlock* Mutant Embryos by an Unknown Mechanism

The mechanism by which EDNRB may modulate arteriogenesis has not been the remit of this work, which was to identify EFNB1 and EDNRB as potential modulators of the process. Work in mice (Murakoshi, Miyauchi *et al.*, 2002) led to the hypothesis that decreased levels of NO may, at least in part, cause the effects seen in zebrafish *gridlock* mutant embryos following *EDNRB* knockdown. It would therefore be of interest to challenge this hypothesis. NO is easily inhibited in the zebrafish embryo with the NOS inhibitor L-NAME, which results in a 97% reduction in levels of nitrite in embryo media (Gray, Packham *et al.*, 2007). NO levels can also be enhanced through use of the NO donor SNP (Pelster, Grillitsch *et al.*, 2005). Utilising these means together with the models of aortic occlusion developed would therefore permit further understanding of the mechanism that associates *EDNRB* with arteriogenesis.

5.5 Conclusion

Utilising a model of zebrafish embryonic arteriogenesis developed in Chapter 3, I have demonstrated a possible role for *EDNRB*, extrapolated from the microarray analysis

discussed in Chapter 4, in modulating arteriogenesis. I have shown expression of *EDNRB* in zebrafish embryos and confirmed predicted sequences, before attempting to demonstrate their localisation within the embryo. While further work is required to confirm my findings, and identify the mechanism by which modulation of arteriogenesis may occur, I have demonstrated significant alteration in arteriogenesis by *EDNRB* knockdown, a gene with significantly decreased expression in absence of blood flow and haemodynamic force when compared to physiological levels. My results thus present microarray analysis of zebrafish embryos as a successful means for determining differential gene expression.

Chapter Six

Modulation of Arteriogenesis by EphrinB1

Chapter 6: Modulation of Arteriogenesis by EphrinB1

Microarray technology (Chapter 4) was utilised to identify a gene set differentially expressed under conditions of absent blood flow, and thereby absent haemodynamic force, compared to controls under physiological levels of blood flow. From 290 genes demonstrating differential expression *EphrinB1* (*EFNB1*) was identified as a candidate for a role in modulating arteriogenesis. *EFNB1* demonstrated significantly decreased expression in the absence of blood flow, leading me to hypothesis *EFNB1* deficiency through knockdown may limit the level of recovery of aortic blood flow observed following occlusion. Despite a demonstration of *EFNB1*'s importance to angiogenesis, its role in arteriogenesis has not been elucidated.

This chapter discusses utilisation of the zebrafish embryo models of arteriogenesis described in Chapter 3 to extrapolate on the microarray analysis obtained in Chapter 4 to determine the role of *EFNB1* in modulating arteriogenesis. The introduction discusses previous research which led me to hypothesise roles for *EFNB1* in modulating arteriogenesis.

6.1 Introduction

6.1.1 Ephrin Signalling Molecules

The ephrin ligand-eph receptor signalling system acts locally since both ligand and receptor tyrosine kinase are bound to a cell's plasma membrane (Pasquale, 2004). Ephrin activity appears dependent upon clustering, and thus membrane association would serve this function (Yancopoulos, Klagsbrun ***et al.***, 1998). While ligand-receptor binding appears promiscuous; ligand and receptor expression is spatially-specific.

EphrinB ligands (B1-B3) and corresponding ephB receptors have roles in vascular development and maintenance, including physiological and pathological angiogenesis (Adams, 2002). Gene expression profiles peak at these times (Frisen, Holmberg ***et al.***,

1999). For example, in human, expression of *ephrinB2* is weaker in homeostatic adult arterial ECs compared to placental arteries or arteries undergoing vascular remodelling (Korff, Braun *et al.*, 2008). It is becoming clear that while ephrinB ligands act in concert, with some potential redundancy, each has a specific function which cannot be entirely compensated for by other members of the family (Adams, Wilkinson *et al.*, 1999). EFNB1 and B2 localise to arterial structures, and ephB3 expressed on some arteries. EFNB1 and ephB3 are again found localised to venous tissue, coexpressed with ephB4 (Adams, Wilkinson *et al.*, 1999; Wang, Chen *et al.*, 1998).

6.1.1.1 EphrinB1

EFNB1 is required during embryonic development. Inactivation in mice resulted in skeletal deformation including polydactyly and cleft palate, as well as perinatal lethality (Compagni, Logan *et al.*, 2003; Davy, Aubin *et al.*, 2004). EFNB1 has been identified as localised to regions of cartilage differentiation (Davy, Aubin *et al.*, 2004), suggesting further roles in embryonic development. EFNB1 has also been implicated in angiogenesis. Angiogenesis has been induced through phosphorylation of tyrosine residues on EFNB1 in ECs *in vitro* (Davy, Aubin *et al.*, 2004; Huynh-Do, Vindis *et al.*, 2002) as well as *in vivo* in mice corneal pocket assay (Kojima, Chang *et al.*, 2007). The role of EFNB1 in angiogenesis, together with roles of other members of the ephrinB family such as ephrinB2 in vessel specification, identify EFNB1 as a potential modulator of other vascular-specific processes such as arteriogenesis.

6.2 Results

Arteriogenesis is dependent, at least in part, on haemodynamic force (Buschmann and Schaper, 1999) with mammalian studies demonstrating the importance of forces such as FSS to development of collateral blood flow following arterial ligation (Eitenmuller, Volger *et al.*, 2006; Pipp, Boehm *et al.*, 2004). In Chapter 4 I demonstrated differential expression of 290 genes with absent haemodynamic force. It is therefore possible that at least some differentially expressed genes modulate arteriogenesis. I began by

scrutinising the 290 differentially expressed genes to generate a list of candidates with known functions within vasculature.

6.2.1 Literature Search of Differentially Expressed Genes

To identify potential modulators of arteriogenesis, I scrutinised the 290 differentially expressed genes by performing literature researches utilising the public database www.pubmed.gov. I created a candidate list of genes with known vascular function, genes believed to have greatest possibility of modulating arteriogenesis. *EFNB1* demonstrated significantly decreased expression with absent haemodynamic force. This, combined with its known roles in vascular development and remodelling, led me to hypothesise *EFNB1* deficiency may lead to reduced recovery of aortic blood flow following occlusion. The role of *EFNB1* in arteriogenesis has not been studied, despite demonstrations of its importance in vascular remodelling in mammals (Adams, Wilkinson *et al.*, 1999; Murakoshi, Miyauchi *et al.*, 2002). These results aim to determine the role *EFNB1* may play in modulating arteriogenesis in the models I describe in Chapter 3, utilising morpholino oligonucleotide knockdown. Prior to knockdown, however, I confirmed expression and sequenced *EFNB1* in zebrafish embryos.

6.2.2 Expression of EFNB1 in Zebrafish Embryos

To confirm expression of *EFNB1* in zebrafish embryos I performed RT-PCR analysis. Total RNA from 36hpf wildtype embryos was reverse transcribed to generate cDNA. This timepoint was utilised since it was the first microarray timepoint. Forward and reverse primer pairs (coloured red in figures 6.1B) designed against Ensembl predicted sequences for *EFNB1* were used to identify expression of the genes by RT-PCR with relevant primer pairs. Expression of *GAPDH* was utilised as positive control. Predicted sequences predict transcripts with the primer pairs of band sizes *EFNB1*: 579bp and *GAPDH*: 1019bp. *EFNB1* demonstrated a transcript with band size of a little under 600bp (figure 6.1A), corresponding well with the predicted transcript band size of 579bp. These results thus supported expression of *EFNB1* in zebrafish embryos at 36hpf.

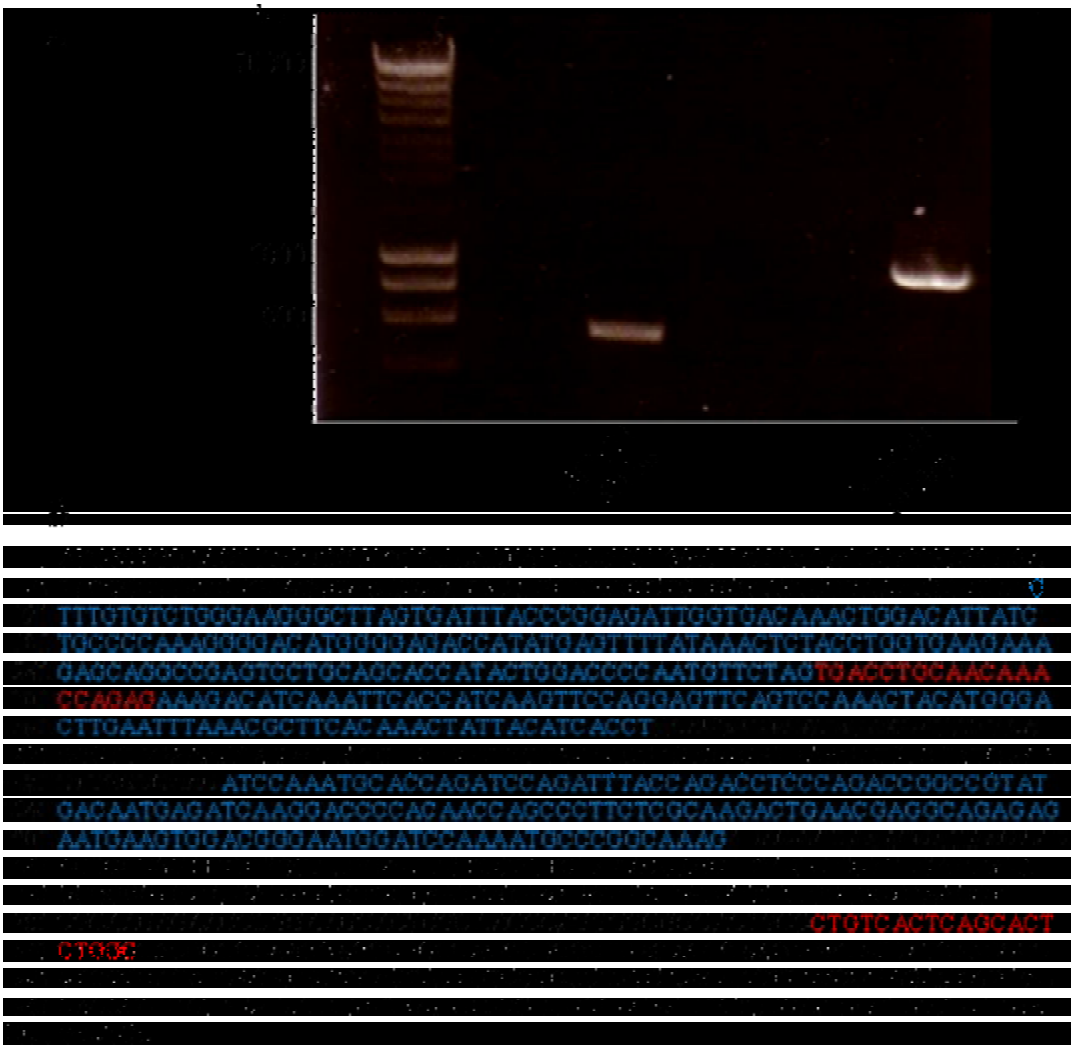

Figure 6.1 Expression of EFNB1 in wildtype zebrafish embryos.
PCR analysis with specific primers in A (red base lettering in B) demonstrates expression of *EFNB1* in wildtype embryos. B, Ensembl predicted sequence for *EFNB1*. Black/blue bases indicate alternate exon sequences. Red bases indicate the sequence of primers utilised to identify expression.

6.2.3 Sequencing Confirms Predicted EFNB1 Sequences

Determination of *EFNB1* expression was performed utilising primer pairs designed against Ensembl automated predicted sequences. It was therefore important to confirm Ensembl automated predicted sequences for *EFNB1*. PCR product from section 6.2.2 was sequenced against the primer pairs at the University's Core Genomics Facility with the aim of visualising possible base-pair alignment alterations. Product was purified to remove excess primer, dNTPs, and non-specific products. Sequence alignment demonstrated a 93% base-pair alignment match between PCR product and predicted sequence for *EFNB1*. Non-homologous regions are found at either end of the product. The *EFNB1* sequence alignment can be observed in figure 6.2. This result confirms the automated predicted sequence for *EFNB1* in zebrafish embryos.

To identify regions of homology between the *EFNB1* sequence in zebrafish and other model organisms I compared sequence alignments utilising ClustalW (version 2.0.10; www.ebi.ac.uk/Tools/clustalw2/index.html). While Ensembl predicted sequences were utilised for human, mouse and chick, the zebrafish sequences I determined for the genes were utilised. Regions of homology between species are often functional regions, and thus important to determine. Zebrafish *EFNB1* demonstrated homology of 64-70% when aligned against human, mouse and chick (figure 6.3; zebrafish-human 66%, -mouse 64%, -chick 70%). Homology between all the species aligned occurred throughout the sequence, with regions of greatest homology occurring from around base-pairs 116-535 and 700-900 (as determined by the zebrafish sequence). These base-pairs correspond to the beginning of exon 2 (figure 6.1) through to the middle of exon 4, and the majority of exon 5. Thus, a variety of protein domains are likely homologous between the species. A brief description of the domains' role is included in figure 6.4.

6.2.4 Determination of Morpholino Concentration for EFNB1 Knockdown

Having confirmed expression of *EFNB1* in zebrafish embryos I wished to identify its possible role in modulating arteriogenesis. A splice-site MO for *EFNB1* (Gene Tools Inc, Oregon, USA) were designed against its confirmed sequence, to perform steric block at regions demonstrating homology when aligned against human, mouse and chick (section 6.2.3).

```
Predicted ATGGCTGGAAGTGACGGCTCGTGGAAATATTACCTCTGGATTCTGACAGCCATGTGCAGA 60
Sequenced ------------------------------------------------------------

Predicted TACGCGTTACCCGCAGCCAAATCACTGGAGTCGGTCGTGTGGAATTCGCAAAATCCCAAG 120
Sequenced ------------------------------------------------------------

Predicted TTTGTGTCTGGGAAGGGCTTAGTGATTTACCCGGAGATTGGTGACAAACTGGACATTATC 180
Sequenced ------------------------------------------------------------

Predicted TGCCCCAAAGGGGACATGGGGAGACCATATGAGTTTTATAAACTCTACCTGGTGAAGAAA 240
Sequenced ------------------------------------------------------------

Predicted GAGCAGGCCGAGTCCTGCAGCACCATACTGGACCCCAATGTTCTAGTGACCTGCAACAAA 300
Sequenced ------------------------------------------------------------

Predicted CCAGAGAAAGACATCAAATTCACCATCAAGTTCCAGGAGTTCAGTCCAAACTACATGGGA 360
Sequenced ----------------ANNNNNNNNNNNNNTTTNNGGNGTTCNGTCNNAACTACATGGGA 44
                         *             **   ** **** ***  ************

Predicted CTTGAATTTAAACGCTTCACAAACTATTACATCACCTCAACGTCTAATGGAACACAGGAA 420
Sequenced CTTGAATTTAAACGCTTCACAAACTATTACATCACCTCAACGTCTAATGGAACACAGGAA 104
          ************************************************************

Predicted GGCTTGGAAAACAGAGAAGGTGGGGTTTGTAGTACGAGATCCATGAAGATCATCATGAAA 480
Sequenced GGCTTGGAAAACAGAGAAGGTGGGGTTTGTAGTACGAGATCCATGAAGATCATCATGAAA 164
          ************************************************************

Predicted GTGGGCCAAGATCCAAATGCACCAGATCCAGATTTACCAGACCTCCCAGACCGGCCGTAT 540
Sequenced GTGGGCCAAGATCCAAATGCACCAGATCCAGATTTACCAGACCTCCCAGACCGGCCGTAT 224
          ************************************************************

Predicted GACAATGAGATCAAGGACCCCACAACCAGCCCTTCTCGCAAGACTGAACGAGGCAGAGAG 600
Sequenced GACAATGAGATCAAGGACCCCACAACCAGCCCTTCTCGCAAGACTGAACGAGGCAGAGAG 284
          ************************************************************

Predicted AATGAAGTGGACGGGAATGGATCCAAAATGCCCGGCAAAGACACAAGAAACCAGAACAAC 660
Sequenced AATGAAGTGGACGGGAATGGATCCAAAATGCCCGGCAAAGACACAAGAAACCAGAACAAC 344
          ************************************************************

Predicted AGTCCCGGTTCTGTGGAAGGAATATTCGGCTCTAAACCAGCTCTCTTCGCTGCCATCGGA 720
Sequenced AGTCCCGGTTCTGTGGAAGGAATATTCGGCTCTAAACCAGCTCTCTTCGCTGCCATCGGA 404
          ************************************************************

Predicted GCGGGCTGTGTGATCTTCCTCCTAATCATAATCATCCTCATCGTCTTGCTCCTCAAGCTT 780
Sequenced GCGGGCTGTGTGATCTTCCTCCTAATCATAATCATCCTCATCGTCTTGCTCCTCAAGCTT 464
          ************************************************************

Predicted CGCAAGAGAACCCGGAAGCACTCGCAACCCAGGGGCGGGACTGCCCTGTCACTCAGCACT 840
Sequenced CGCAAGAGAACCCGGAAGCACTCGCAACCCAGGGGCGGGACTGCCCTGTCACNNNNNNNN 524
          ************************************************

Predicted CTGGCCACGCCCAAAGGAGCCGCCCAGGCCGGCTCAGAGCCAAGTGACATCATCATCCCC 900
Sequenced NNNGGNAAN-------------------------------------------------- 533
             *  *
```

```
Predicted CTGCGGACAACAGAGAATAACTACTGTCCCCACTATGAAAAAGTTAGCGGAGACTATGGA 960
Sequenced ------------------------------------------------------------

Predicted CACCCCGTCTACATAGTGCAGGAAATGCCGCCGCAGAGCCCTGCCAATATCTACTACAAA 1020
Sequenced ------------------------------------------------------------

Predicted GTCTGA                                                      1026
Sequenced ------
```

Figure 6.2 Confirmation of EFNB1 ensembl predicted sequence.
The *EFNB1* PCR amplicon underwent sequencing to confirm the Ensembl predicted sequence. Sequencing demonstrated that the *EFNB1* mastermix shared 93% alignment to the Ensembl predicted sequence. A=adenine, C=cytosine, G=guanine, T=thymine, N=undetermined. *=base-pair alignment, - =absent sequence. Numbers to right denote base sequence number.

```
human ATGGCTCGGCCTGGGCAGCGTTGGCTCGGCAAGTGGCTTGTGGCGATGG-TCGTGTGGGC 59
mouse ATGGCCCGGCCTGGGCAGCGTTGGCTCAGCAAGTGGCTTGTGGCTATGG-TCGTGCTGAC 59
chick ------------------------------------------------------------
zfish ----------ATGGCTGGAAGTGACGGCTCGTGGAAATATTACCTCTGGATTCTGACAGC 50


human GCTGTGCCGGCTCGCCACACCGCTGGCCAAGAACCTGGAGCCCGTATCCTGGAGCTCCCT 119
mouse GCTGTGCCGGCTTGCCACGCCGTTGGCCAAGAACCTGGAGCCCGTGTCCTGGAGCTCTCT 119
chick ------------------------------------------------------TCCTC 5
zfish CATGTGCAGATACGCGTTACCCGCAGCCAAATCACTGGAGTCGGTCGTGTGGAATTCGCA 110
                                                              **


human CAACCCCAAGTTCCTGAGTGGGAAGGGCTTGGTGATCTATCCGAAAATTGGAGACAAGCT 179
mouse TAACCCTAAGTTCCTAAGTGGGAAGGGCTTGGTGATCTACCCGAAGATTGGAGACAAGCT 179
chick TTCTTCCAGATTCATGAGTGGGAAAGGGTTGGTCATCTACCCGGAGATTGGGGACAAACT 65
zfish AAATCCCAAGTTTGTGTCTGGGAAGGGCTTAGTGATTTACCCGGAGATTGGTGACAAACT 170
           * *  **  *   ****** ** ** ** ** ** *** * ***** ***** **


human GGACATCATCTGCCCCCGAGCAGAAGCAGGGCGGCCCTATGAGTACTACAAGCTGTACCT 239
mouse GGACATCATCTGCCCCCGAGCAGAAGCAGGGCGGCCCTACGAGTACTACAAGCTGTACCT 239
chick GGACATTATCTGCCCCAAGGCGGAGCCGTCCAAGCCTTACGAGTACTACAAGCTGTACCT 125
zfish GGACATTATCTGCCCCAAAGGGGACATGGGGAGACCATATGAGTTTTATAAACTCTACCT 230
      ****** *********   *  **          ** ** ****  ** ** ** *****


human GGTGCGGCCTGAGCAGGCAGCTGCCTGTAGCACAGTTCTCGACCCCAACGTGTTGGTCAC 299
mouse GGTGCGGCCAGAGCAGGCGGCTGCTTGCAGCACTGTGCTTGATCCCAATGTACTGGTCAC 299
chick GGTGAAAAAGGACCAGGCAGATGCCTGCAGCACCGTCATGGACCCCAACGTGCTGGTGAC 185
zfish GGTGAAGAAAGAGCAGGCCGAGTCCTGCAGCACCATACTGGACCCCAATGTTCTAGTGAC 290
      ****      ** ***** *   * ** *****  *  * ** ***** **  * ** **


human CTGCAATAGGCCAGAGCAGGAAATACGCTTTACCATCAAGTTCCAGGAGTTCAGCCCCAA 359
mouse TTGCAACAAGCCACACCAGGAAATCCGCTTCACCATCAAGTTCCAAGAGTTCAGCCCCAA 359
chick GTGCAACCGGCCCGAGCAGGAGATCCGCTTCACCATCAAGTTTCAGGAGTTCAGCCCCAA 245
zfish CTGCAACAAACCAGAGAAAGACATCAAATTCACCATCAAGTTCCAGGAGTTCAGTCCAAA 350
      *****    **  *  * ** **    ** *********** ** ******** ** **


human CTACATGGGCCTGGAGTTCAAGAAGCACCATGATTACTACATTACCTCAACATCCAATGG 419
mouse CTACATGGGCCTGGAATTCAAAAAGTACCACGATTACTACATTACATCAACGTCCAATGG 419
chick CTACATGGGCCTGGAGTTCAAGCGGCAGCAGGATTACTTCATCACATCCACCTCTAACGG 305
zfish CTACATGGGACTTGAATTTAAACGCTTCACAAACTATTACATCACCTCAACGTCTAATGG 410
      ********* ** ** ** **           * ** * *** ** ** ** ** ** **


human AAGCCTGGAGGGGCTGGAAAACCGGGAGGGCGGTGTGTGCCGCACACGCACCATGAAGAT 479
mouse GAGCTTGGAGGGACTGGAGAACCGGGAGGGAGGTGTGTGTCGCACCCGCACTATGAAGAT 479
chick GACACTGGATGGCCTGGAGAACCGGGAAGGAGGGGTCTGCCAGACACGCTCCATGAAGAT 365
zfish AACACAGGAAGGCTTGGAAAACAGAGAAGGTGGGGTTTGTAGTACGAGATCCATGAAGAT 470
       *    *** **  **** *** * ** ** ** ** **    **  *  * ********


human CATCATGAAGGTTGGGCAAGATCCCAATGCTGTGACGCCTGAGCAGCTGA--CTACCAG- 536
mouse CGTTATGAAGGTTGGGCAAGATCCAAATGCTGTGACACCCGAGCAGTTGA--CTACCAG- 536
chick CGTCATGAAAGTGGGGCAGGATCCAAACGCGGTGATCCCGGAGCAGCTGA--CGACGAG- 422
zfish CATCATGAAAGTGGGCCAAGATCCAAATGCACCAGATCCAGATTTACCAGACCTCCCAGA 530
      * * ***** ** ** ** ***** ** **       ** **          *  * **


human CAGGCCCAGCAAGGAGGCAGACAACACTGTCAAGATGGCCACACAGGCCCCTGGTAGTCG 596
mouse CCGGCCAAGCAAGGAGTCAGACAACACTGTCAAGACAGCCACACAGGCTCCTGG---TCG 593
chick TCGGCC---CACGCAGCCAGCCAA-------GCGACCGCCCCTCGAGGGCC-------CG 465
zfish CCGGCCGTATGACAATGAGATCAAGGACCCCACAACCAGCCCTTCTCGCAAGACTGAACG 590
       ****        *      ***          *    * *                **
```

```
human GGGCTCCCTGGGTGACTCTGATGGCAAGCATGAGACT--GTGAACCAGGAAGAGAAGAGT 654
mouse GGGATCCCAGGGTGACTCTGACGGCAAGCATGAGACT--GTGAACCAGGAAGAGAAGAGT 651
chick GAGCTGCCGGGGCCA------GGGTCAGCAGGAGGTTCCGTCAACCAGAACGGCCAGGAG 519
zfish AGGCAGAGAGAATGA---AGTGGACGGGAATGGATCCAAAATGCCCGGCAAAGACACAAG 647
        *      *    *       *    * * *           ** * *     *

human GGCCCAGGTGCAAGTGGGGGCAGCAGCGGGGACCCTGATGGCTTCTTCAACTCCAAGGTG 714
mouse GGCCCAGGTGCAGGTGGCGGTGGCAGCGGGGACTCTGACAGCTTCTTCAACTCCAAGGTA 711
chick ACCCAAGGTCC-----------CAGCG---------ATGGGTTCCTGAGCTCCAAAGTC 558
zfish AAACCAGAACAA--------CAGTCCCGGTTCTGTGGAAGGAATATTCGGCTCTAAACCA 699
         * **                 **         *  *  *  *   *** **

human GCATTGTTCGCGGCTGTCGGTGCCGGTTGCGTCATCTTCCTGCTCATCATCATCTTCCTG 774
mouse GCATTGTTCGCAGCCGTCGGCGCCGGCTGTGTCATCTTCCTGCTCATCATCATCTTCTTG 771
chick GCCGTTTTCGCTGCCATCGGCGCGGGCTGCGTCATCTTCATCCTCATCATCATCTTCCTC 618
zfish GCTCTCTTCGCTGCCATCGGAGCGGGCTGTGTGATCTTCCTCCTAATCATAATCATCCTC 759
      **  * ***** **  **** ** ** ** ** ****** * ** ***** *** ** *

human ACGGTCCTACTACTGAAGCTACGCAAGCGGCACCGCAAGCACACACAGC---AGCGGGCG 831
mouse ACAGTCCTACTACTCAAGCTCCGCAAGCGCCATCGCAAGCATACACAGC---AGCGGGCG 828
chick GTCGTCCTCCTGATCAAGATCCGCAAGCGGCACCGGAAGCACACGCAGC---AGCGGGCC 675
zfish ATCGTCTTGCTCCTCAAGCTTCGCAAGAGAACCCGGAAGCACTCGCAACCCAGGGGCGGG 819
         *** * **  * *** * ****** *    ** *****  * ** *    * * *

human GCTGCCCTCTCGCTCAGTACCCTGGCCAGTCCCAAGGGGGGCAGTGGCACAG-CGGGCAC 890
mouse GCTGCCCTCTCGCTCAGTACCCTAGCCAGCCCCAAAGGGGGTAGTGGTACAG-CGGGCAC 887
chick GCAGCCTTGTCCCTCAGCACCTTGGCCAGCCCCAAATG---CAGCGGGAGCG-CCGGCTC 731
zfish ACTGCCCTGTCACTCAGCACTCTGGCCACGCCCAAAGG----AGCCGCCCAGGCCGGCTC 875
       * *** * ** ***** **  * ****  *****  *    **  *    * * *** *

human CGAGCCCAGCGACATCATCATTCCCTTACGGACTACAGAGAACAACTACTGCCCCCACTA 950
mouse CGAGCCCAGCGACATCATCATCCCCTTACGGACTACAGAGAACAACTACTGCCCCCACTA 947
chick AGAGCCCAGCGACATCATCATCCCTTAA------------------------------ 759
zfish AGAGCCAAGTGACATCATCATCCCCCTGCGGACAACAGAGAATAACTACTGTCCCCACTA 935
       ***** ** ********** **

human TGAGAAGGTGAGTGGGGACTACGGGCACCCTGTCTACATCGTCCAAGAGATGCCGCCCCA 1010
mouse TGAGAAGGTGAGTGGGGACTACGGGCATCCTGTCTACATCGTCCAGGAGATGCCCCCTCA 1007
chick ------------------------------------------------------------
zfish TGAAAAAGTTAGCGGAGACTATGGACACCCCGTCTACATAGTGCAGGAAATGCCGCCGCA 995


human GAGCCCGGCGAACATCTACTACAAGGTCTGA 1041
mouse GAGCCCGGCGAACATCTACTACAAGGTTTGA 1038
chick ------------------------------
zfish GAGCCCTGCCAATATCTACTACAAAGTCTGA 1026
```

Figure 6.3 EFNB1 inter-species homology.

Alignment of *EFNB1* sequences from zebrafish, human, mouse, and chick demonstrates homology between species of between 64 and 70%. Homology is observed for the majority of exons 2-5.

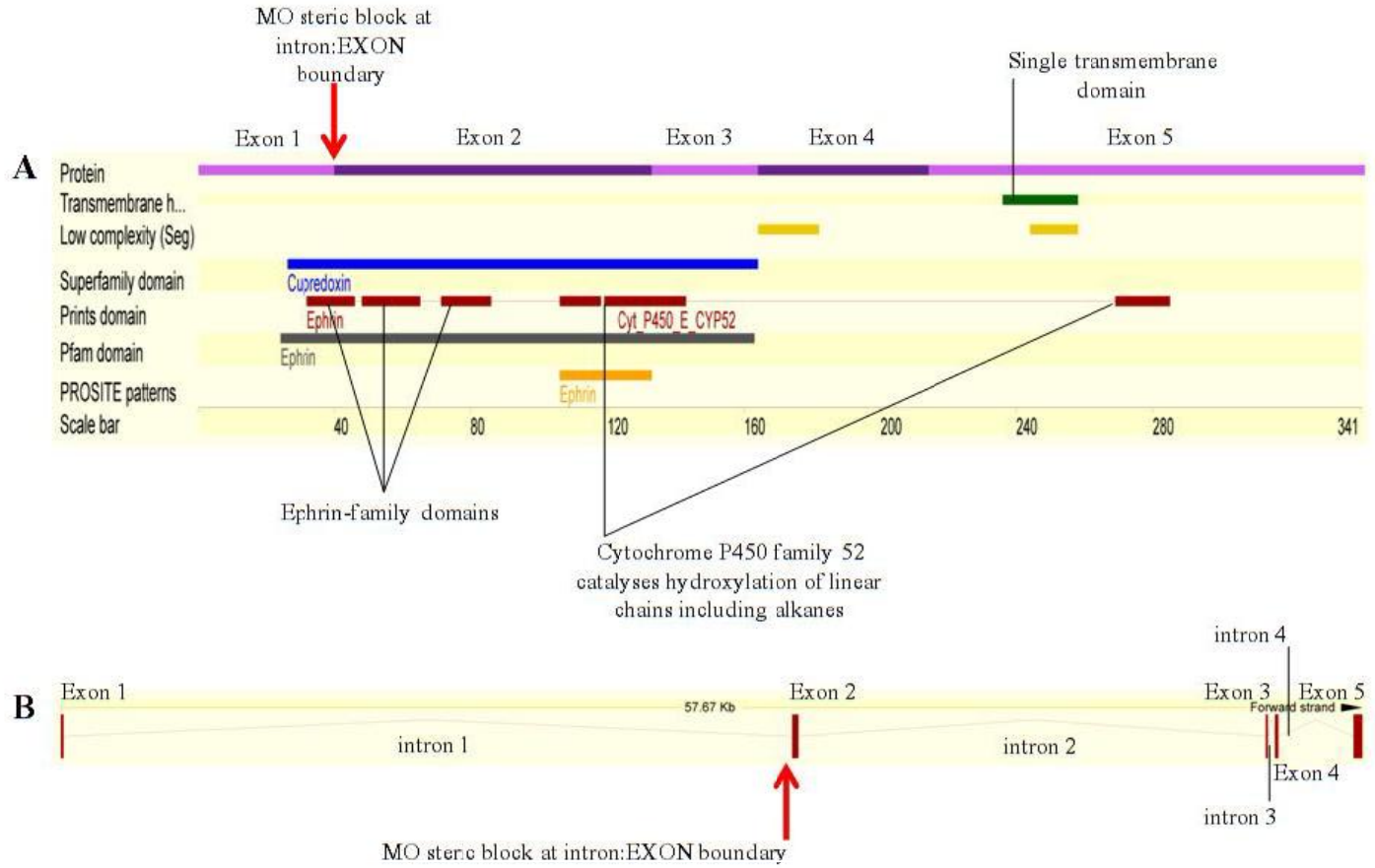

Figure 6.4 EFNB1 protein domains.

A demonstrates the different domains within the zebrafish EFNB1 protein, with brief descriptions of the roles of the domains. B demonstrates the lengths of introns and exons. The location of steric block by the MO utilised (section 5.2.6) is also demonstrated. The scale bar corresponds to amino acid number. Adapted from information generated by Ensembl version 52 (13/2/09).

Since multiple exons demonstrated high levels of homology, MOs were designed to interact with the intron:exon boundary of exon 2. To determine the concentration at which the MOs should be utilised dose-response experiments were performed to determine embryonic survival over several concentrations (50, 100, 200, 500nM) during the first 3dpf (n=3, total of 120 embryos/group).

Highest survival rates for *EFNB1* splice MO injection were recorded injecting a concentration of 50nM (figure 6.5). However, MO activity was not always detected by PCR analysis. Survival rates with [500nM] *EFNB1* MO averaged 21.4±7.4% at 24hpf, making utilisation of the MO at this concentration impractical. Survival rates with [100nM] and [200nM] *EFNB1* MO were similar (100nM: 56.3±16.1%, 200nM: 62.5±22.0%). Therefore, [100nM] was utilised in future experiments, since the lower concentration is least likely to result in non-specific effects caused by toxicity.

6.2.5 EFNB1 Morpholinos Knockdown the Gene of Interest

To determine activity of *EFNB1* MOs I performed PCR analysis. Total RNA was extracted from wildtype embryos injected with [100nM] *EFNB1* or control MO and reverse transcribed generating cDNA. cDNA was then utilised in PCR analysis and gel electrophoresis.

[100nM] *EFNB1* MO resulted in almost complete abolition of normally sized transcript expression at 24hpf (figure 6.6). A highly reduced concentration of cDNA is detected compared to control MO injected embryos whose transcript band was marked by *EFNB1* primers. While more than 200ng DNA is detected in control (lane 3, figure 6.6) by Hyperladder II molecular weight marker, only approximately 50ng cDNA is detected in cDNA generated from *EFNB1* MO injected embryos (lane 4). This suggests a four-fold reduction in *EFNB1* expression with MO. Inducing steric block at the boundary of intron1:exon2, the MO knockdown may result in an early stop to mRNA splicing, since no splice transcripts of different band sizes were observed with RT-PCR (figure 6.6). The beginning of exon2 spans an Ephrin family domain necessary for Ephrin function (figure 6.4). *EFNB1* expression may thus be abolished through an early stop to this domain.

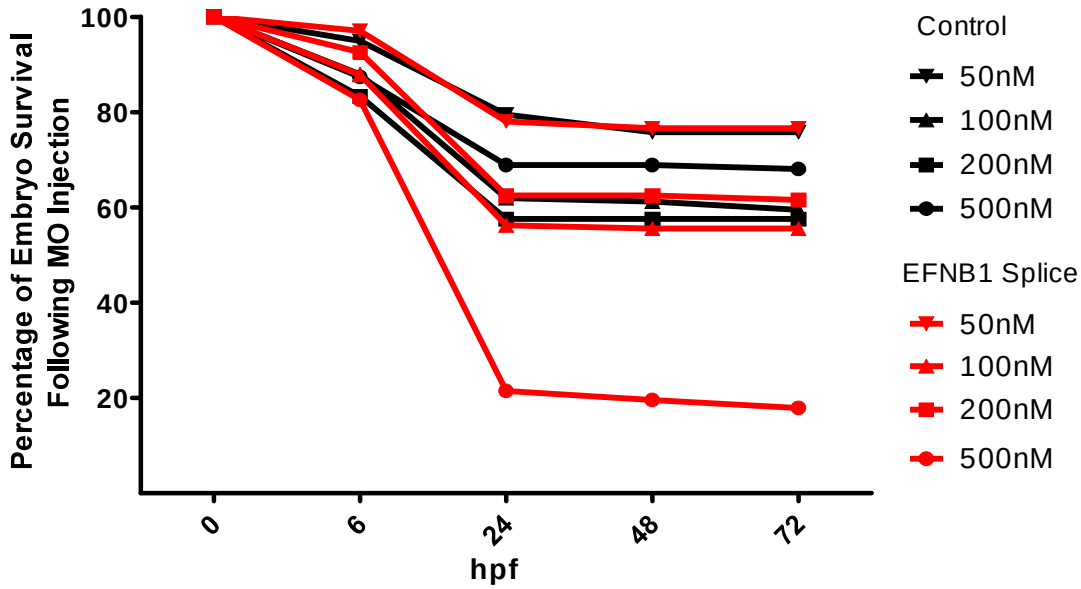

Figure 6.5 Dose-response graph to determine the concentration at which to utilise the EFNB1 splice MO.

A concentration of [500nM] *EFNB1* MO resulted in severely reduced survival rates for embryos. While a concentration of [50nM] provided the best survival, MO activity was not always detected. A concentration of [100nM] was utilised in further experiments.

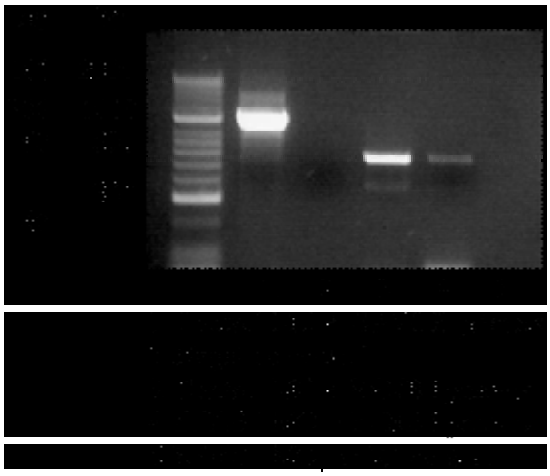

Figure 6.6 Assessing the activity of EFNB1 MO by PCR analysis.
PCR analysis was performed on cDNA generated from total RNA extracted at timepoints described in the figure. A, [100nM] *EFNB1* splice MO led to almost complete abolishment of gene expression at 24hpf.

6.2.6 Gross Phenotype of EFNB1 Knockdown

In order to determine gross phenotype of *EFNB1* knockdown in zebrafish embryos, I injected wildtype embryos with [100nM] *EFNB1* or control MO (approximately 40 embryos per group). A further group of 40 sibling embryos were left uninjected with MO. Embryos were then observed under stereomicroscopy at 2 and 5dpf. Wildtype embryos injected with control MO did not demonstrate any altered phenotype compared to uninjected embryos at 2 or 5dpf.

At both timepoints, gross structures including head, trunk, body length, and heart structure appeared comparable under stereomicroscopy. It can thus be deduced that injection of standard control MO does not result in altered physiology of embryos. At 2dpf, *EFNB1* knockdown embryos did not demonstrate significant gross phenotypic abnormality compared to control injected embryos (figure 6.7), although yolk-sac may be slightly enlarged. At 5dpf, *EFNB1* knockdown embryos presented with slight pericardial oedema and possible deformations of craniofacial ultrastructure observed as a protruding mouth (figure 6.8). *EFNB1* has been identified as localised to regions of cartilage differentiation in mice (Davy, Aubin *et al.*, 2004), and inactivation has resulted in skeletal deformation (Compagni, Logan *et al.*, 2003), which may account for the possible craniofacial deformation. The swim bladder has not inflated, and embryo body length is shorter than control siblings, both characteristics suggestive of delayed development.

6.2.7 Vessel Patterning in EFNB1 Knockdown

To determine whether *EFNB1* knockdown resulted in abnormal vascular patterning or development through abnormal vasculogenesis (*de novo* vessel formation through *in situ* differentiation of angioblasts) or angiogenesis (growth and remodelling of primitive vascular networks) I performed confocal microscopy of fli1:eGFP MO injected embryos. Representative embryos were chosen for laser-scanning confocal microscopy at 2 and 5dpf from approximately 40 observed by fluorescent stereomicroscopy. The same embryos were studied at both timepoints.

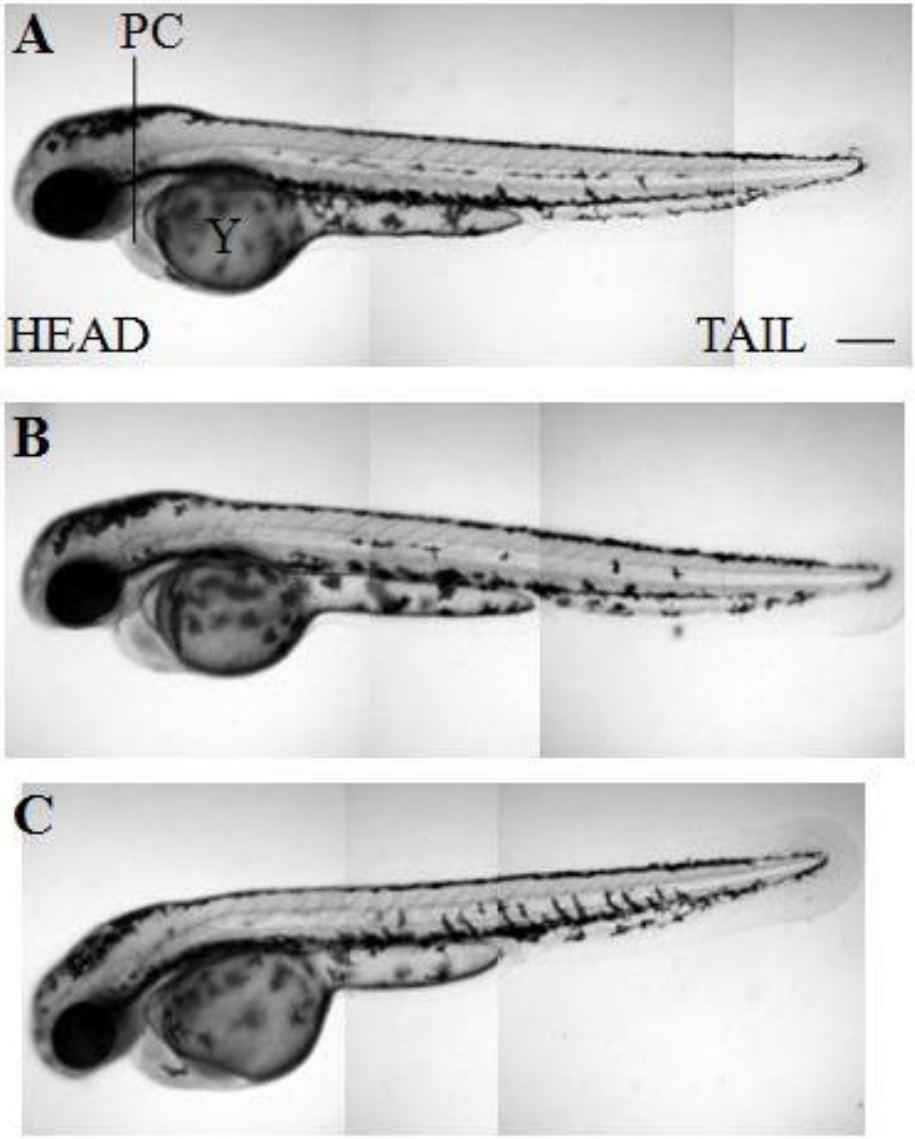

Figure 6.7 Phenotype of EFNB1 knockdown in wildtype embryos at 2dpf.
[100nM] *EFNB1* MO did not result in significant abnormality of wildtype embryos at 2dpf, although the yolk-sac may be slightly enlarged in *EFNB1* knockdown embryos (C) compared to control MO injected siblings (B) or uninjected siblings (A). Representative lateral views compiled from 3 images. Y=yolk-sac, PC=pericardial sac. Scale bar 200μm.

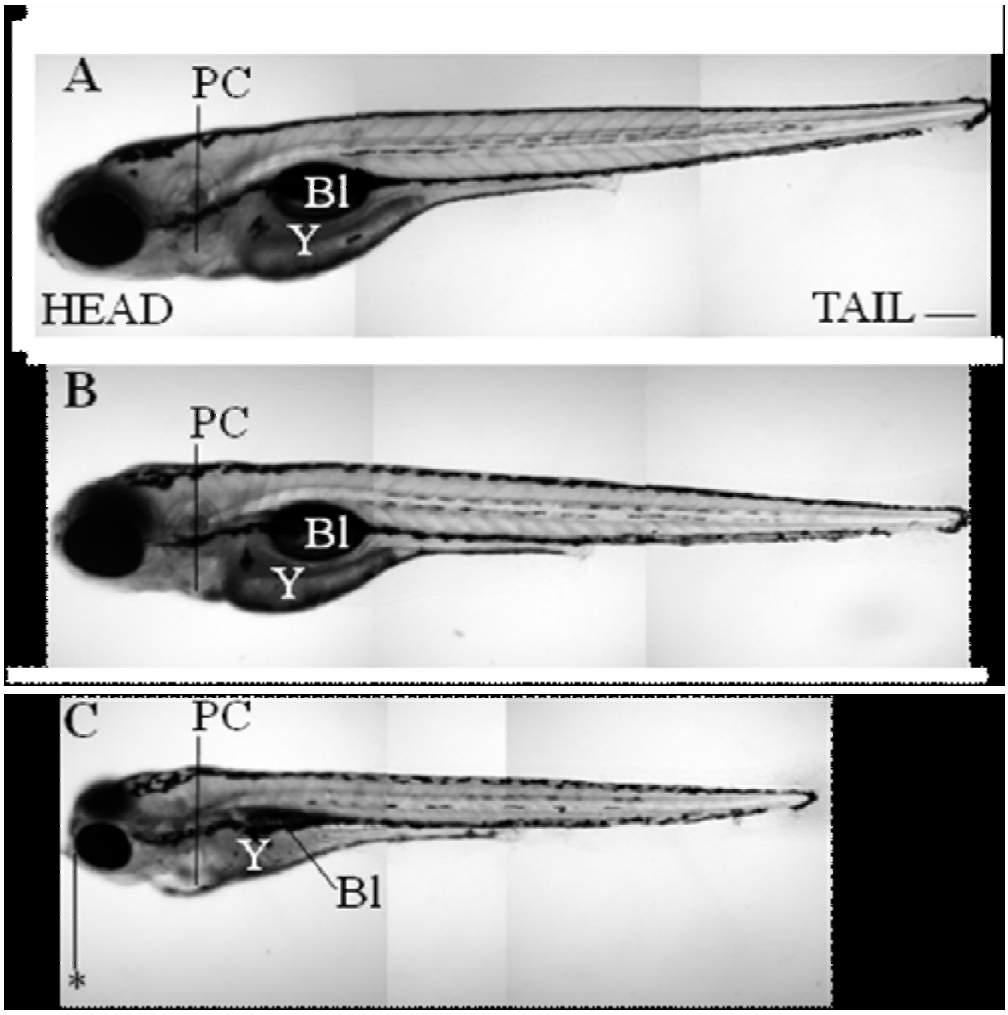

Figure 6.8 Phenotype of EFNB1 knockdown in wildtype embryos at 5dpf.
At 5dpf, *EFNB1* knockdown embryos (C) presented with slight pericardial oedema, and possible deformation of craniofacial structure (*) on comparison with control MO injected siblings (B) or uninjected siblings (A). The swim bladder of *EFNB1* knockdown embryos has not inflated appearing flat in (C), and embryos are shorter than control and uninjected siblings, both characteristics suggestive of delayed development. Y=yolk-sac, Bl=swim bladder, PC=pericardial sac. Representative lateral views compiled of 3 images. Scale bar 200µm.

By 2dpf vasculogenesis, during which aorta and cardinal vein develop, is complete. At 5dpf angiogenesis of ISVs, DLAVs, and SIVs has occurred, with untreated embryos demonstrating a standard vascular pattern (Isogai, Horiguchi *et al.*, 2001). Angiogenesis is responsible for formation of ISVs, DLAVs, and SIVs. 5dpf is also the last timepoint at which recovery of aortic blood flow in *gridlock* embryos was observed. Of approximately 40 knockdown embryos per group observed by fluorescent stereomicroscopy at 2dpf, all *EFNB1* knockdown embryos demonstrated normal patterning of aorta and cardinal vein on comparison with wildtype embryos (figure 6.9), suggesting normal vasculogenesis, during which these vessels form (Isogai, Horiguchi *et al.*, 2001).

All *EFNB1* knockdown embryos demonstrated normal patterning and number of ISVs, and also normal development of DLAVs and communications between aorta, or cardinal vein, and SIVs at 5dpf (figure 6.10). The ISVs, DLAVs and SIVs form later than aorta and cardinal vein, during angiogenesis (Isogai, Horiguchi *et al.*, 2001), which occurs from approximately 30hpf. Their normal patterning in *EFNB1* knockdown embryos suggests angiogenesis is unaffected by *EFNB1* knockdown. Therefore, despite gene knockdown, no vessels failed to form, and no vessel was found to have undergone aberrant angiogenesis by 5dpf.

6.2.8 Recovery of Aortic Blood Flow with EFNB1 Knockdown

In chapter 4, I demonstrated decreased expression of *EFNB1* in absence of haemodynamic force. I thus hypothesise *EFNB1* deficiency may lead to reduced recovery of aortic blood flow following occlusion. The role of these genes in arteriogenesis has not been studied, despite demonstrations of their importance in vascular remodelling in mammals (Adams, Wilkinson *et al.*, 1999; Murakoshi, Miyauchi *et al.*, 2002). I therefore wished to determine the potential role of *EFNB1* in modulating arteriogenesis.

To do this, I undertook *EFNB1* knockdown in *gridlock* mutant embryos, since the mutants' amenability to high throughput screening suited the experimentation (3 replicates, 30-50 embryos per group per replicate).

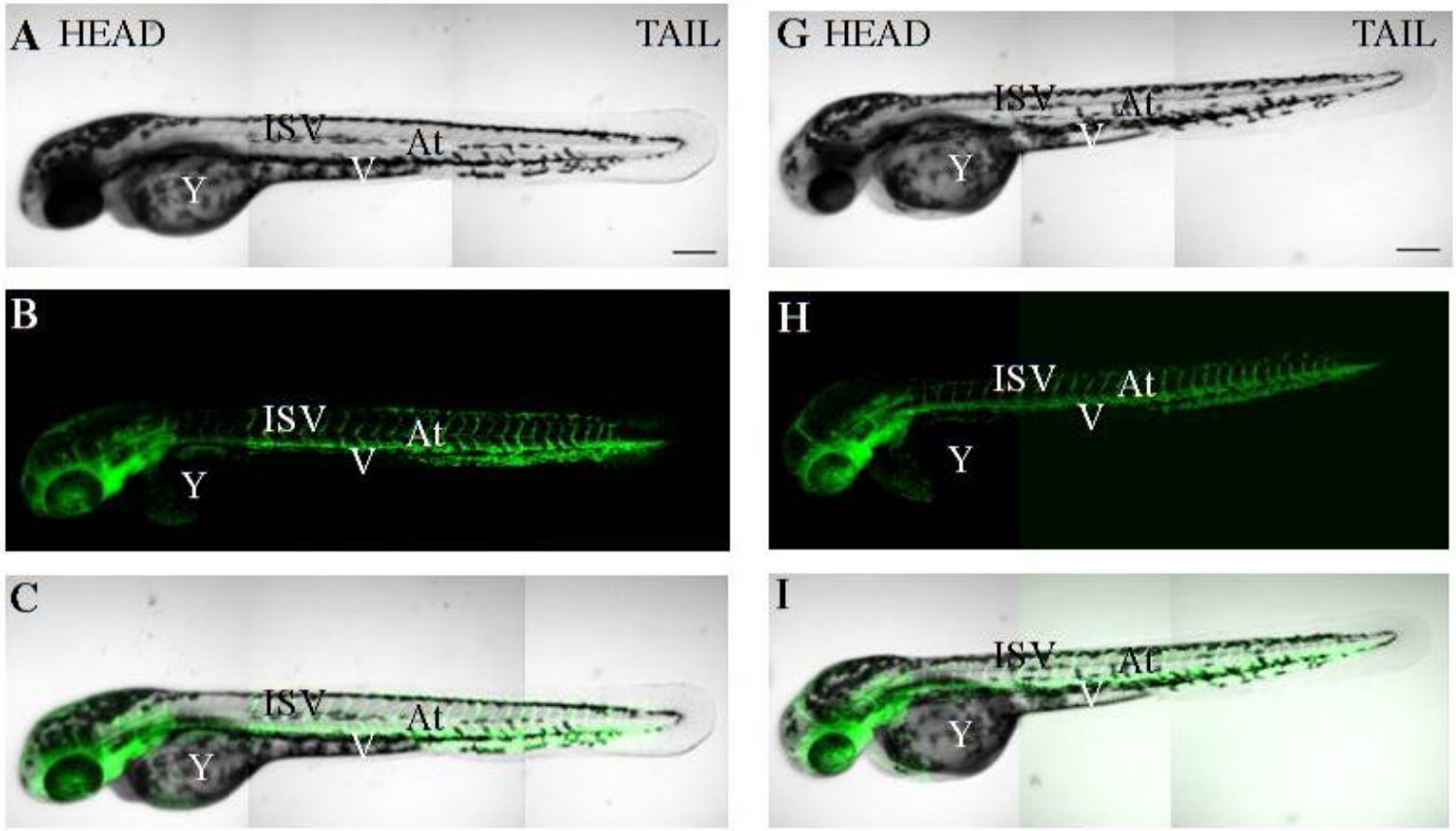
A HEAD
TAIL
ISV
At
V
Y
G HEAD
TAIL
ISV
At
V
Y
B
ISV
At
V
Y
H
ISV
At
V
Y
C
ISV
At
V
Y
I
ISV
At
V
Y

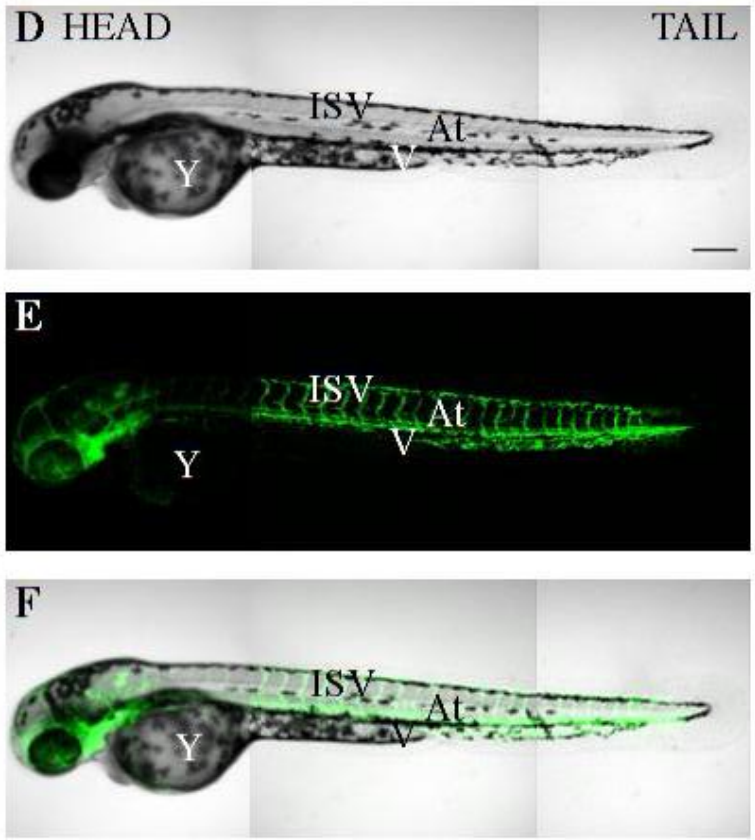

Figure 6.9 EFNB1 knockdown does not affect vasculogenesis or angiogenesis.
Representative lateral views at 2dpf of brightfield (A, D, G) fluorescent (B, E, H) and combined (C, F, I) confocal laser-scanning microscopy images of uninjected (A-C), control MO injected (D-F), and *EFNB1* (G-I) knockdown in fli1:eGFP embryos. Vasculogenesis and angiogenesis are observed to have occurred normally in *EFNB1* knockdown embryos, on comparison with control MO injected siblings and uninjected siblings, with no abnormal vessel development or growth. Each sub-figure compiled from 2-3 images. Y=yolk-sac, V=cardinal vein, At=aorta, ISV=intersegmental vessels. Scale bar 200µm throughout.

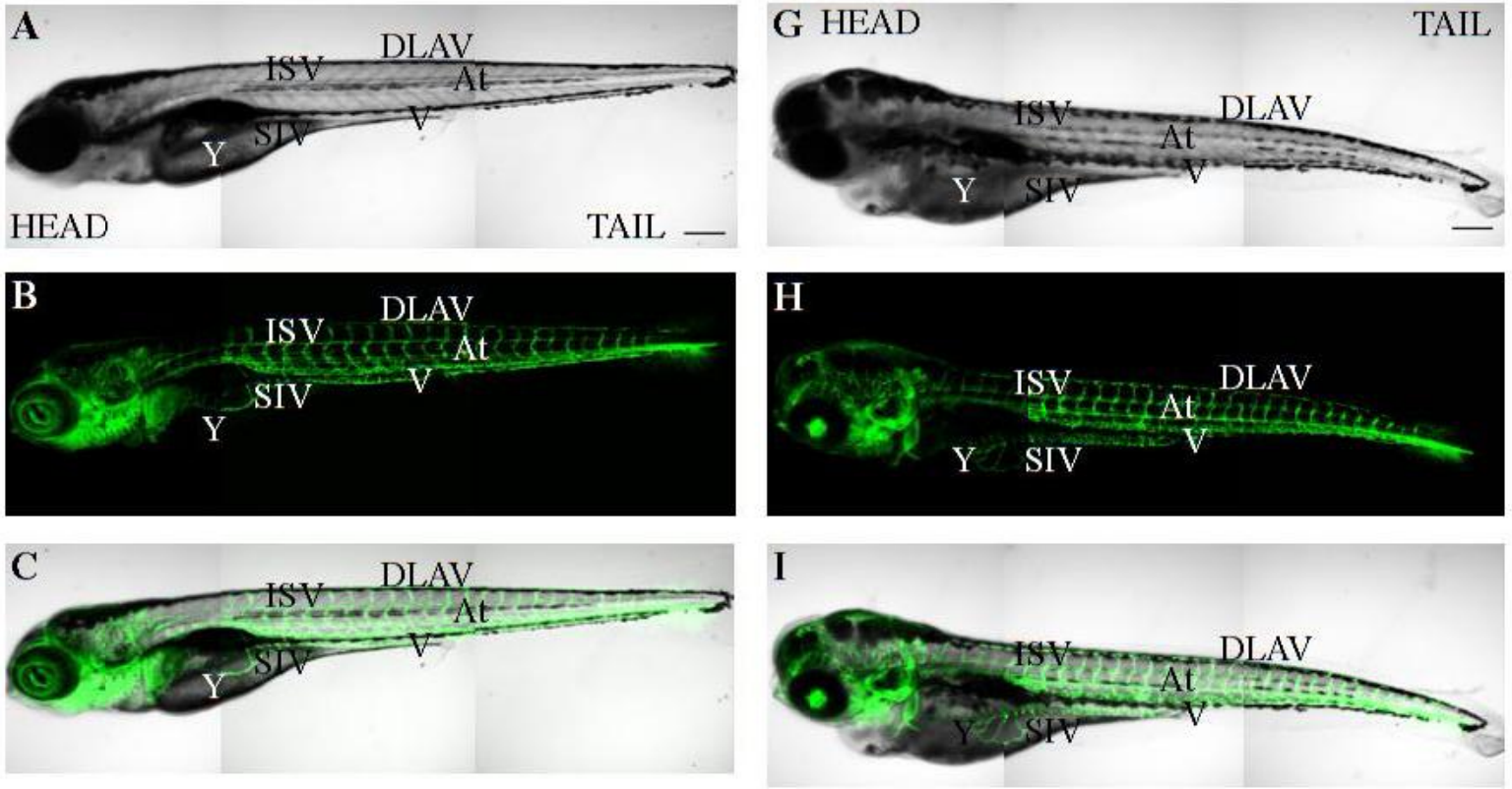
A
ISV
DLAV
At
V
SIV
Y
HEAD
TAIL
G HEAD
TAIL
ISV
DLAV
At
V
Y
SIV
B
ISV
DLAV
At
V
SIV
Y
H
ISV
DLAV
At
V
Y
SIV
C
ISV
DLAV
At
V
SIV
Y
I
ISV
DLAV
At
V
Y
SIV

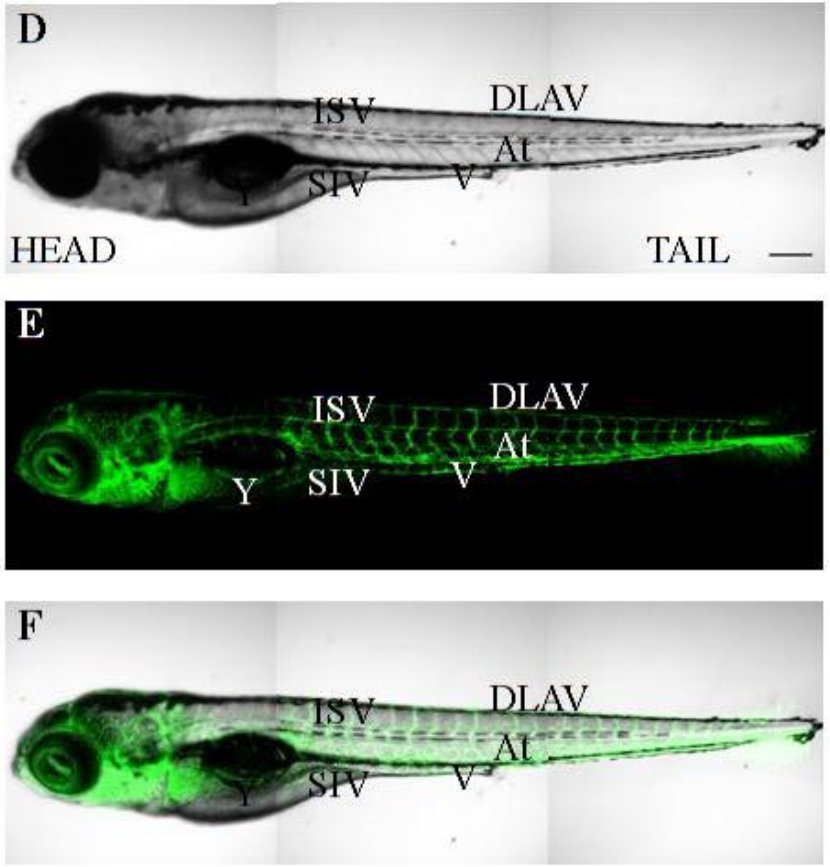

Figure 6.10 The effect of EFNB1 knockdown on the vasculature at 5dpf.
Representative lateral views at 5dpf of brightfield (A, D, G), fluorescent (B, E, H) and combined (C, F, I) confocal laser-scanning microscopy images of uninjected (A-C), control MO injected (D-F), and *EFNB1* (G-I) knockdown in fli1:eGFP embryos. At 5dpf, the vasculature appears normal in *EFNB1* knockdown embryos. Each sub-figure compiled from 2-3 images. Y=yolk-sac, V=cardinal vein, At=aorta, ISV=intersegmental vessels, SIV=subintestinal vasculature, DLAV=dorsal longitudinal anastomotic vessels. Scale bar 200µm throughout.

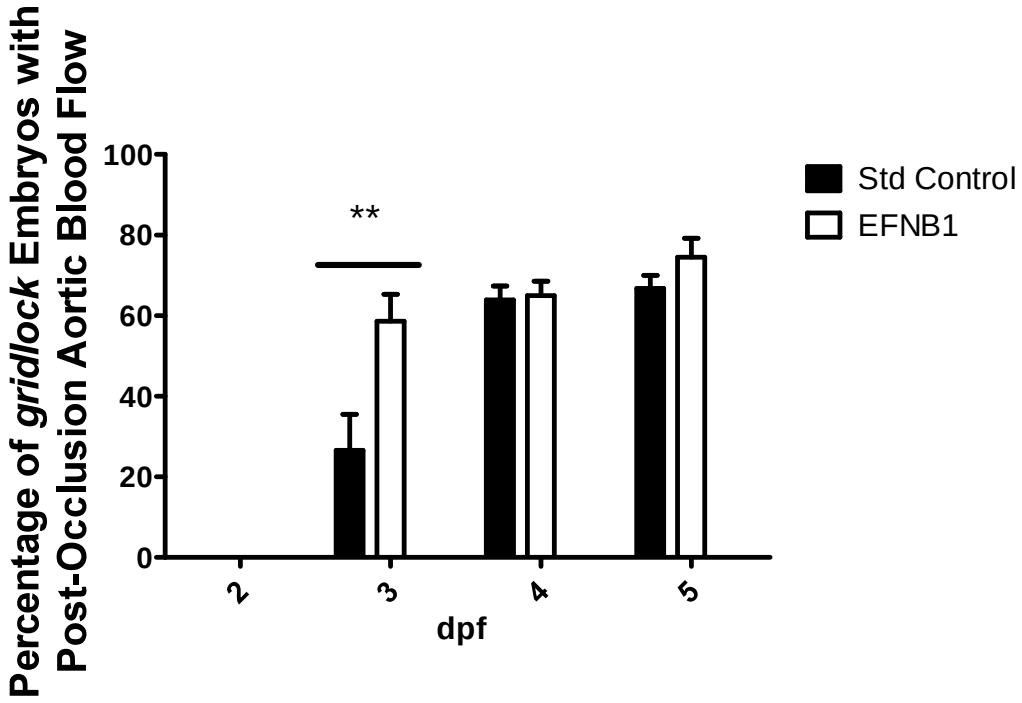

Figure 6.11 The effect of EFNB1 knockdown on the acquisition of aortic blood flow distal to the occlusion site in *gridlock* mutant embryos.
Although a very significant (P<0.01) increase in the acquisition of aortic blood flow distal to the occlusion site is observed in *gridlock* mutant embryos at 3dpf, this significant reduction does not continue to 4 and 5dpf.

Recovery of aortic blood flow by 'collateral' vessels in knockdown embryos was determined by binary count of presence or absence of aortic blood flow and compared to embryos injected with standard control MO.

No *EFNB1* knockdown *gridlock* or control MO *gridlock* embryo was observed with aortic blood flow at 2dpf. At 3dpf, *EFNB1* knockdown in *gridlock* mutant embryos resulted in a very significant ($P<0.01$) increase in recovery of blood flow distal to occlusion compared to control (control: 26.60±8.95%, *EFNB1* knockdown: 58.63±6.68%; power 100%), as seen in figure 6.11. However, by 4dpf this significant increase has been lost (control: 63.93±3.41, *EFNB1* knockdown: 65.03±3.54), and does not recover at 5dpf (control: 66.73±3.26, *EFNB1* knockdown: 74.53±4.71; power 100%) despite similar levels of experimental power. This could result from reductions in MO activity at these later timepoints.

6.3 Discussion

Microarray analysis of zebrafish embryos in presence or absence of physiological haemodynamic force (Chapter 4) demonstrated differential expression of 290 genes between groups. Literature searches identified genes with possible roles in modulation of arteriogenesis through knowledge of other roles within vasculature. For example, although arteriogenesis and angiogenesis are distinct processes, they share mechanistic traits such as modulation by NO (Yu, deMuinck *et al.*, 2005), and infiltration of monocytes/macrophages (Van Royen, Piek *et al.*, 2001b). *EFNB1* was identified as one possible candidate. *EFNB1*'s role in modulating arteriogenesis has not been studied although it has known roles in vascular remodelling including angiogenesis (Adams, 2002). The aim of this chapter was exploitation of zebrafish embryos to determine the role of *EFNB1* in modulating arteriogenesis utilising morpholino oligonucleotide knockdown. Prior to knockdown, I began by confirming expression of *EFNB1* in zebrafish embryos. Since many discussion points refer to the techniques utilised in both this and the previous chapter, reasons justified in Chapter 5 will not be repeated here.

6.3.1 Expression of EFNB1 in Zebrafish Embryos

To confirm expression of *EFNB1* in zebrafish embryos I performed RT-PCR utilising wildtype embryo total RNA extracted at 36hpf and reverse transcribed. RNA extraction was performed at 36hpf since this was the first microarray timepoint. The *EFNB1* transcript demonstrated a band size of just under 600bp (figure 6.1), corresponding well with the predicted band size of 579bp. *GAPDH* control also demonstrated transcript size corresponding with that predicted. Thus, these results confirm expression of *EFNB1* in zebrafish embryos at 36hpf.

Transcript band size was determined utilising primer pairs designed against Ensembl predicted sequences. To confirm the sequences PCR product was sequenced at the University's Core Genomics Facility allowing visualisation of potential alterations in base-pair alignment. Product was purified at the facility to remove excess primer, dNTIPs, and non-specific products. Alignment demonstrated 93% base-pair alignment between PCR product and predicted sequence for *EFNB1* (figure 6.2). Non-homologous regions were found to either end of the alignment at primer binding locations. This result therefore confirms the automated predicted sequences for *EFNB1* in zebrafish embryos.

Alignment of zebrafish *EFNB1* to human, mouse, and chick (figure 6.3) demonstrated homology of 64-70%. Homology occurred throughout the sequence between all the species. Regions of greatest homology corresponded to the beginning of exon 2 (figure 6.1) through to the middle of exon 4, and the majority of exon 5. Thus, a variety of protein domains are likely homologous between the species (figure 6.4).

6.3.2 EFNB1 Knockdown by Morpholino Injection

With confirmed expression of *EFNB1* in zebrafish embryos I wished to determine its possible role in modulating arteriogenesis, and did so by performing knockdown with MO. To determine the concentration at which MOs should be utilised dose-response experiments were performed to determine embryonic survival over several concentrations during the first 3dpf. MO-induced lethality is most likely during this timepoint since MOs are injected at 1-4 cell stage. Dose-response experiments were

performed through alteration of MO concentration, rather than alteration of injected volume, to remove the possibility of non-specific phenotypes resulting from increasing volume.

Survival rates following *EFNB1* knockdown were highest following injection of [50nM] (figure 6.5) however, MO activity was not always detected. [100nM] was utilised in future experiments, since this concentration combined high survival rates with activity. Additionally, [100nM] was the second lowest concentration examined, and is therefore least likely to cause toxicity and non-specific phenotypes.

EFNB1 knockdown resulted in almost complete abolition of gene expression at 24hpf as determined by PCR analysis (figure 6.6). A highly reduced concentration of DNA was detected compared to control MO injected embryos with a possible four-fold reduction in *EFNB1* expression. Inducing steric block at the boundary of intron1:exon2, the MO knockdown may result in an early stop to mRNA splicing, since no splice transcripts of different band sizes were observed with RT-PCR. The beginning of exon2 spans an Ephrin family domain necessary for Ephrin function (figure 6.4). *EFNB1* expression may thus be abolished through an early stop to this domain.

6.3.3 Gross Phenotypic Characterisation of EFNB1 Knockdown

In order to determine gross phenotype of *EFNB1* knockdown in zebrafish embryos I injected wildtype embryos with [100nM] *EFNB1* or control MO. A group of embryos were also left uninjected. Wildtype embryos injected with control MO did not demonstrate altered phenotype on comparison with uninjected embryos at 2 or 5dpf under stereomicroscopy. Gross structures such as head, trunk, heart, and body length are comparable between groups demonstrating injection of MOs does not in itself alter embryonic development. At 2dpf no gross phenotypic abnormality was observed in wildtype embryos injected with *EFNB1* MO, aside from possible slight enlargement of the yolk-sac (figure 6.7). At 5dpf *EFNB1* knockdown embryos demonstrated slight pericardial oedema and possible deformations of craniofacial structures (figure 6.8) which could result from no specific effects of the MO as outlined elsewhere. EFNB1 is localised to regions of cartilage differentiation in mice (Davy, Aubin *et al.*, 2004), and

inactivation results in skeletal deformations (Compagni, Logan *et al.*, 2003), which may account for the observed craniofacial deformation. In addition, the swim bladder appeared uninflated, and embryo body length was reduced compared to control MO injected embryos. Together this may indicate delayed development.

6.3.4 Vessel Patterning in EFNB1 Knockdown

To determine the effect of *EFNB1* knockdown on vascular patterning and development through vasculogenesis and angiogenesis, fli1:eGFP transgenic embryos underwent MO injection and observation by fluorescent stereomicroscopy. Representative embryos underwent laser-scanning confocal microscopy at 2 and 5dpf. At 2dpf, *EFNB1* knockdown embryos demonstrated normal patterning of aorta and cardinal vein on comparison with control MO embryos (figure 6.9). This suggests normal vasculogenesis in knockdown embryos. Although EFNB1 is expressed throughout the vasculature (Adams, Wilkinson *et al.*, 1999), there is no evidence to suggest a role for EFNB1 in vasculogenesis. At 5dpf all *EFNB1* knockdown embryos demonstrated normal patterning of ISVs, DLAVs, and SIVs, and normal number of ISVs compared to control MO injected embryos (figure 6.10). Their normal development suggests angiogenesis is unaffected in *EFNB1* knockdown embryos. Development of communications between aorta, or cardinal vein, and SIVs was also normal. Thus, despite *EFNB1* knockdown, no vessels failed to form, and no vessel was found to have undergone aberrant angiogenesis by 5dpf.

6.3.5 Recovery of Aortic Blood Flow with EFNB1 Knockdown

Since *EFNB1* demonstrated significantly decreased expression in the absence of haemodynamic force I hypothesise *EFNB1* deficiency may lead to reduced recovery of aortic blood flow following occlusion. The role of these genes in arteriogenesis has not been studied, despite demonstrations of their importance in vascular remodelling in mammals (Adams, Wilkinson *et al.*, 1999; Murakoshi, Miyauchi *et al.*, 2002). To determine their potential role in modulating arteriogenesis I undertook gene knockdown in *gridlock* embryos, as described in Chapter 3.

No *EFNB1* knockdown *gridlock* or control MO *gridlock* embryo was observed with aortic blood flow at 2dpf. At 3dpf, *EFNB1* knockdown in *gridlock* mutant embryos resulted in a very significant ($P<0.01$) increase in recovery of blood flow distal to occlusion compared to control (figure 6.11). By 4dpf this significant increase was lost and did not recover at 5dpf. At these timepoints there was no significant difference from control values. These results are possibly due to reductions in MO activity at 4 and 5dpf. Given the short timeframe of increased recovery of aortic blood flow, it is difficult to determine the possible mechanisms involved. Expression in kidney arterioles and glomeruli suggested possible roles in vascular patterning and development (Adams, 2002). Such alterations during development of zebrafish embryos could account for my observation, since vasculature is plastic at this time and undergoes sprouting and regression (Isogai, Lawson *et al.*, 2003). However, I did not determine alterations in vasculature patterning of *EFNB1* knockdown embryos at 2dpf. Utilisation of MOs designed against different regions of *EFNB1*'s sequence may permit validation of this result. Closely related molecules, such as EFNB2, demonstrate an important role in arterial-venous fate decisions at timepoints close to the onset of blood flow (Wang, Chen *et al.*, 1998). It is possible that embryonic expression peaks at this timepoint. If *EFNB1* expression follows a similar pattern lower levels of expression may occur at the later timepoints of 4 and 5dpf, and thus the effect of deficiency may be lessened. This hypothesise could be tested by performed *in situ* hybridisation at all three timepoints.

6.4 Limitations and Future Work

6.4.1 Confirmation of EFNB1 Knockdown

EFNB1 knockdown embryos demonstrated cranio-facial malformations at later timepoints which could result from non specific effects of the *EFNB1* MO. This in turn calls into question the observed effect of *EFNB1* deficiency in the recovery of aortic blood flow in *gridlock* mutants. Although a standard control MO was utilised to limit the risk of observing non specific effects resulting from the injection procedure, it would also be beneficial to compare *EFNB1* knockdown embryos to embryos injected with an *EFNB1* mismatch MO which has no functionality. Together with the experiments

performed, this would allow a determination of the role of specific to non specific effects of MO injection.

6.4.2 EFNB1 Significantly Affects Recovery of Aortic Blood Flow in *gridlock* Mutant Embryos by an Unknown Mechanism

The mechanism by which *EFNB1* knockdown in *gridlock* mutant embryos resulted in significantly increased recovery of aortic blood flow has not been determined. The remit of this work was to identify *EFNB1* as a potential modulator of arteriogenesis. Determination of expression levels at the timepoints at which recovery of aortic flow was observed (i.e. 3-5dpf) by *in situ* hybridisation or Northern blot may indicate one aspect of the mechanism. Lower expression levels at a particular timepoint (for example at 4 and 5dpf) may reduce the 'potential' for *EFNB1* knockdown. Repeating knockdown experimentation with a splice-site MO designed against a different region of the gene may help confirm the results described in this chapter, or provide mechanistic information by affecting the recovery of aortic blood flow in *gridlock* embryos in a different manner. It may also be beneficial to perform similar knockdown experiments utilising a start-site MO inhibiting translation of the entire gene. In this way, the mechanism of action may start to be determined.

6.5 Conclusion

Utilising a model of zebrafish embryonic arteriogenesis developed in Chapter 3, I have demonstrated a possible role for *EFNB1* in modulating arteriogenesis extrapolated from the microarray analysis discussed in Chapter 4. I have demonstrated expression of *EFNB1* in zebrafish embryos and confirmed automated predicted sequences. While further work is required to confirm my findings, and identify the mechanism by which modulation of arteriogenesis may occur, I have shown a significant increase in the recovery of aortic blood flow in *gridlock* mutants in a time specific manner by *EFNB1* knockdown. My results suggest microarray analysis of zebrafish embryos to be a successful means for determining differential gene expression.

Chapter Seven

General Discussion

Chapter 7: General Discussion

In this chapter I bring together the findings from my results chapters (Chapter 3-6) in order to discuss methodology, the position of the research within the field, improvements that may be made to the research, and possible future directions. To do this I begin the chapter with a summary of principle findings.

7. 1 Summary of Principle Findings

The principle novel findings from this work indicate:

- Arteriogenesis in zebrafish embryos is not a phenotypic response to *gridlock* mutation, but a response to vascular occlusion that can occur in wildtype embryos following laser-induced aortic occlusion
- Like mammalian arteriogenesis, recovery of aortic blood flow distal to occlusion site in *gridlock* mutants and wildtype embryos having undergone laser-induced aortic occlusion is modulated by NOS inhibition
- Modulation by NOS inhibition is not a result of modulating vasoactivity or aortic blood velocity, suggesting NO modulation shares a mechanism between zebrafish and mammalian arteriogenesis
- Microarray analysis in the absence of physiological *in vivo* haemodynamic force permits determination of differential gene expression compared to controls providing novel data on genes and gene groups undergoing differential expression
- *EDNRB* and vasoactive genes demonstrated significantly decreased expression in absence of blood flow and haemodynamic force when compared to physiological levels and deficiency significantly suppressed arteriogenesis following knockdown suggesting *EDNRB* modulation of arteriogenesis

- *EFNB1* also demonstrated significantly decreased expression in absence of haemodynamic force. *EFNB1* knockdown resulted in a temporal alteration in recovery of aortic blood flow, demonstrating significantly enhanced flow recovery at 3dpf, but not 4 or 5dpf.

7.2 Methodology

7.2.1 Aortic Occlusion

Utilisation of zebrafish embryos provides an alternative model system for performing cardiovascular research to mammalian models. As an alternative, the methods and protocols utilised demonstrate both positive and negative features.

Utilisation of pre-existing transgenic (fli1:eGFP/gata1:dsRED) and mutant (*gridlock*) embryos provided the opportunity to perform *in vivo* studies of aortic blood flow recovery following both permanent (*gridlock*) and induced aortic occlusion. Thus, *in vivo* confocal microscopy of fli1:eGFP/gata1:dsRED transgenic embryos pre- and post aortic occlusion permitted determination of the existence of vessels capable of remodelling in zebrafish embryos prior to induction of occlusion. The existence of such vessels is a key characteristic of arteriogenesis.

It is unfortunate that induction of aortic occlusion in wildtype embryos was found to be unfeasible at earlier timepoints than 4dpf due to the formation of arterio-venous fistulas in the developing vasculature. In conjunction with Home Office regulation limiting utilisation of zebrafish embryos to 5.2dpf at standard incubation temperatures of 28°C a timepoint at 4dpf limited observation of aortic blood flow recovery to 22 hours. Although this length of time allowed observation of aortic blood flow recovery around the occlusion site in wildtype embryos, it limited observation of vessel maturation and stability that would have occurred over longer timepoints. This in turn limits the data achievable from such studies.

The characterisation of remodelling vessels was also limited by not performing histology. Histology may have determined pre- and post- blood flow recovery vessel

arterio-venous identify through expression of EphrinB2 (arteries) and EphB4 (veins). This would therefore have demonstrated if vessel identity altered following vessel occlusion. Histology for endogenous mediators such as NO, or the enzyme eNOS, pre- and post- blood flow recovery may have demonstrated a difference in expression levels of eNOS in non recruited vessels compared to recruited post- recovery vessels, as has been identified in mammals (Cai, Kocsis *et al.*, 2004a). Thus, performing histological examination of vessels involved in recovery of aortic blood flow may have helped further analyse similarities and differences between mammalian and zebrafish arteriogenesis in vessel identity and expression of endogenous mediators.

7.2.2 Morpholino Knockdown

Morpholino knockdown experiments to determine the role of *EDNRB* (Chapter 5) and *EFNB1* (Chapter 6) in modulation of zebrafish arteriogenesis were performed utilising the generic standard control morpholino generated by GeneTools. The standard control is directed against human β-globin pre-mRNA, a gene not present in zebrafish, and thus acts to control against the process of MO injection (Eisen and Smith, 2008). However, the standard control may not control against specific MO sequences and it may therefore be beneficial to perform additional experiments to MO knockdown utilising specific *EDNRB* or *EFNB1* randomised or nucleotide polymorph MO versions. In contrast, the decision to utilise splice site blocking MOs was advantageous to the research. This type of MO, in comparison to start site blocking MOs, is beneficial in that RNA levels can be determined by PCR and thus deficiency can be determined quickly and simply. It should be noted however that a decreased RNA level does not necessarily equal a decrease in protein.

A further problem with utilisation of MOs is the difficulty in injecting precise, consistent and reproducible volumes, even in performing estimations by injecting volumes into oil measured by graticule. It is therefore possible individual embryos received varying volumes of MO.

7.2.3 Microarray Execution and Validation

Although I believe the microarray comparing gene expression in the presence and absence of haemodynamic force (Chapter 4) was performed well, the extended length of time beyond that originally envisaged required to obtain high quality and high yield RNA necessary for each of the three microarray timepoints prevented validation by real-time PCR. The absence of validation prevents complete confidence in the differential gene expression observed in the absence of haemodynamic force and the subsequent gene knockdown studies performed in Chapters 5 and 6.

It would have been interesting to perform Northern blots of genes of interest to determine changes in RNA levels, and Western blots to observe levels of protein. It would also have been interesting to compare gene expression levels in *tnnt2* with those observed following induced inhibition of cardiac contraction by pharmacological inhibitors such as BDM (2,3-butanedione monoxime). BDM blocks myofibrillar ATPase (Bartman, Walsh *et al.*, 2004), so that at high enough concentrations cardiac contraction is inhibited or reduced to the extent that blood flow is prevented. This experimentation would allow determination of at which point in early development of zebrafish embryos inhibited contraction had the most affect on gene expression.

7.3 Position of the Research within the Field

7.3.1 Utilisation of Zebrafish Embryos in the Study of Arteriogenesis

Arteriogenesis is almost exclusively studied by performing arterial ligation in mammalian models. Ligation induces downstream ischaemia and hypoxia which induces angiogenesis and arteriogenesis, distinct processes from one another (Carmeliet, 2000). Furthermore, arteriogenesis is able to occur in absence of hypoxia (Heil, Eitenmuller *et al.*, 2006; Lee, Stabile *et al.*, 2004). Therefore utilisation of ligation may confuse a study of arteriogenesis. Zebrafish embryos do not suffer hypoxia under standard incubation conditions of 28° Celsius prior to 14 days post fertilisation even in the absence of blood flow (Pelster and Burggren, 1996). I believe this to be an

advantage over mammalian models and permits observation of arteriogenesis independently of angiogenesis.

Despite anatomical differences, early function of the cardiovascular system is similar between zebrafish and mammalian embryos (Schwerte and Fritsche, 2003), making zebrafish embryos a valid model for studying mammalian disease processes such as arteriogenesis. However, differences in gene function thought to have come about during evolution might mean zebrafish may not reflect human disease processes.

Before any determination of genetic modulation I needed to demonstrate that zebrafish embryos underwent arteriogenesis, since the model is novel to the process. The *gridlock* mutant's phenotype is complete and permanent occlusion of the aorta, and recovers aortic blood flow during the first days of development despite maintenance of occlusion. I have demonstrated through laser-induced aortic occlusion of wildtype zebrafish embryos that recovery of aortic blood flow is not a response to *gridlock* mutation, but a response to vascular occlusion that can occur in all embryos. This therefore demonstrates for the first time exploitation of zebrafish embryos is suitable for studying arteriogenesis, and may prove complementary to mammalian models. My utilisation of *gridlock* embryos allowed observation of aortic blood flow recovery without surgery and possible subsequent non-specific cytokine release. *Gridlock* also provided a high-throughput means for determining vessel remodelling. This starting point allowed me to consider endogenous and genetic modulation of arteriogenesis. Determining endogenous modulation and genetic basis of arteriogenesis is important, since arteriogenesis is considered a potential therapeutic target for arterial occlusion resulting from atherosclerosis (Goncalves, Epstein *et al.*, 2001). Present therapies alleviate symptoms but stimulate little or no disease regression (van Royen, Piek *et al.*, 2001a), making further research necessary. Characterisation, by for example gene expression profiling, could provide clinicians with a means of identifying individuals at risk prior to onset of disease, and may allow pharmacogenetic tailoring of treatments to ethnic or gene-specific groups (Weisfeldt and Zieman, 2007), giving a greater likelihood of treatment success.

With the current level of model characterisation zebrafish embryos prove complementary to existing models of arteriogenesis. For instance, the apparent ability of embryos to recovery aortic blood flow following occlusion via remodelling pre-existing vessels suggest arteriogenesis to be an evolutionarily conserved process. Greater model characterisation, including histological determination of possible alterations in collateral vessel gene expression, endogenous molecule expression, and modulation by circulating cells (such as monocytes, currently being performed by Caroline Gray), would permit a greater comparison of aortic blood flow recovery in zebrafish embryos and mammalian models. Observation of embryonic aortic blood flow recovery over longer timepoints into juvenile and adult stages may permit generation of a basic timeplan similar to that possible for mammalian arteriogenesis (figure 1.2). Greater model characterisation and longer observational timepoints may therefore allow determination of similarities and differences between zebrafish and mammalian arteriogenesis, which may in turn allow determination of zebrafish as a complementary or comprehensive stand alone model of arteriogenesis.

7.3.2 Recovery of Aortic Blood Flow Distal to Occlusion Site in Zebrafish Embryos is modulated by NOS inhibition

In order to help unravel the endogenous modulation of arteriogenesis in zebrafish embryos I chose to investigate the role of nitric oxide. eNOS expression has been demonstrated in zebrafish from 3dpf in cardiomyocytes, aorta and cardinal vein (Fritsche, Schwerte *et al.*, 2000). The ease of administering small non-peptide molecules, including L-NAME, via simple diffusion into embryos permitted determination of nitric oxide's role in zebrafish arteriogenesis without the need for gaseous or intravenous drug administration, as is necessary in mammals.

Nitric oxide is well documented to modulate arteriogenesis in mammalian models. Femoral artery ligation of eNOS deficient mice results in decreased collateral blood flow during the first week post ligation, although flow returned to control levels by three weeks post ligation (Mees, Wagner *et al.*, 2007). In corroboration, non-specific inhibition of NOS enzymes by L-NAME administration diminished blood flow in collateral vessels (Yang, Yan *et al.*, 2001). L-NAME has been previously reported to

cause vasoconstriction in zebrafish embryos from 3dpf (Fritsche, Schwerte *et al.*, 2000), demonstrating its activity in zebrafish embryos, as well as the early development of haemodynamic control. Thus, I determined the role of NO in modulation of arteriogenesis in zebrafish embryos by administration of L-NAME to embryo media. I found NOS inhibition led to significant reduction in recovery of aortic blood flow in *gridlock* mutant embryos, suggesting that as in other species and models of vascular occlusion NO modulates 'collateral' vessel formation in zebrafish embryos following aortic occlusion. A significant reduction in aortic blood flow recovery also occurred following NOS inhibition of wildtype embryos having undergone laser-induced aortic occlusion. This data demonstrates that NO modulation is not isolated to modulation of aortic blood flow recovery in *gridlock* mutants and provides further evidence to suggest that like other previously studied species NO modulates 'collateral' vessel development in zebrafish embryos following aortic occlusion.

It has been suggested that observed decreased collateral vessel blood flow with NO inhibition in mammals results from absence of vasodilatation. It was hypothesised that inhibition of vasodilatation stimulated continued remodelling of collateral vessels via sustained elevations in haemodynamic force which would have normalised in control animals through dilatation (Mees, Wagner *et al.*, 2007). However, it has also been hypothesised that the inability of eNOS deficient mice to respond to VEGF is responsible for the observation (Yu, deMuinck *et al.*, 2005), suggesting NO-mediation of VEGF is responsible for decreased collateral blood flow. Although I sort to determine the role of NO in modulation of arteriogenesis, I did not determine the effect of VEGF. I found that NOS inhibition by L-NAME did not significantly reduce aortic blood flow recovery in *gridlock* mutant embryos by modulating either vasoactivity or aortic blood velocity.

NOS inhibition has been shown to cause significant reductions in mammalian heart rate (Jacobi, Sydow *et al.*, 2005), demonstrating modulation of cardiac contractility by NO. It is therefore possible L-NAME decreases percentage recovery of aortic blood flow in zebrafish embryos following occlusion through modulation of cardiac contraction. Decreased heart rate may result in decreased blood flow, intravascular pressure, and

haemodynamic force in remodelling communications resulting in decreased remodelling of those communications. Decreased stroke volume may also result in decreased blood velocity, because blood volume may be decreased. L-NAME treatment of zebrafish embryos resulted in heart rates of 86% of control, thereby concurring with mammalian data which demonstrated heart rate falling by half with L-NAME treatment (Jacobi, Sydow *et al.*, 2005). This may suggest decreased volumes of blood flow caused by falls in heart rate result in decreased percentages of embryos with aortic blood flow recovery.

To determine the effect of decreased heart rate on aortic blood velocity I developed a means of determining velocity by calculating movement of erythrocytes in respect to time. It has previously been difficult to determine haemodynamic parameters in zebrafish embryos due to their small size. During the course of the work, a similar technique was independently published by another group who demonstrated significant reduction of aortic blood velocity in a concentration dependent manner to MS-222 at 2dpf (Malone, Sciaky *et al.*, 2007). This data thus independently demonstrated the technique has the sensitivity necessary in order to measure subtle alterations in haemodynamic parameters in zebrafish embryos. It also demonstrated embryos at the earliest stages of development have the physiological processes necessary for control of haemodynamics. L-NAME treatment did not result in significant alterations in aortic blood velocity suggesting aortic blood velocity is not affected by decreased heart rate. It is possible that inhibition of vasodilatation by L-NAME administration limits the effect of decreased heart rate on aortic blood velocity, maintaining velocity via decreased vessel luminal diameters, and it should be noted that the statistical power of this experiment was found to be 10.3% at the proximal aorta. This fact makes it more difficult to identify changes in velocity, and it is possible increasing the power by studying greater numbers of embryos might identify an effect.

Erythrocyte numbers entering intersegmental vessels of 5 and 6 day post fertilisation zebrafish embryos decrease significantly on L-NAME treatment, as a result of decreased vessel diameter (Fritsche, Schwerte *et al.*, 2000). However, aortic blood velocity was not determined in the study. L-NAME treatment did not affect non-ischaemic (physiologically normal) blood flow in rat muscles (Lloyd, Yang *et al.*, 2001), while it

has significantly reduced limb perfusion in mice (Jacobi, Sydow *et al.*, 2005), perhaps suggesting measurement of different indices accounts for alternative results.

Studying the role of NO mediation in *gridlock* and laser-occluded embryos has therefore enabled me to demonstrate that zebrafish and mammalian arteriogenesis share mechanisms, at least in part, and suggests some level of conservation between arteriogenesis in mammalian and non-mammalian vertebrates.

7.3.3 Microarray Analysis in the Absence of Physiological *in vivo* Haemodynamic Force permits Determination of Differential Gene Expression compared to Controls

Genetic analysis of the effect of haemodynamic force has been performed under varying conditions by many groups; however studies have mostly occurred *in vitro*. Cultured cells generally reside in an environment for a period of days, while ECs can reside in microenvironments in a quiescent state for many months. The significance of this difference is unknown, but might translate to incomplete or deceptive mimicry of *in vivo* conditions (Staton, Lewis *et al.*, 2006). *In vitro* systems are based primarily on single monolayers of cells which contrasts with the *in vivo* environment where cells undergo wide-ranging interactions, including with different cell populations. Furthermore, *in vitro* studies have determined effects of either FSS *or* cyclic stretch to gene expression, while both forces help comprise haemodynamic force *in vivo*.

To my knowledge only one study has performed microarray analysis with the aim of determining gene expression following arterial ligation (Lee, Stabile *et al.*, 2004). Ligation of the femoral artery led to the largest group of differentially expressed genes relating to inflammation despite sham operation of contralateral limbs. I describe the first study to perform microarray analysis in an *in vivo* model which does not induce angiogenesis and arteriogenesis, and is free of hypoxia, as well as surgically-induced gene expression. Exploitation of zebrafish embryos enabled me to identify genes which may modulate arteriogenesis alone. In addition, I performed the microarray utilising total RNA. This method is technically simple, and permits RNA extraction immediately, capturing gene expression as close to conditions of *in vivo* physiology as is possible.

While it enables determination of gene expression for the whole organism, permitting observation of the interaction between physical forces, endogenous modulation and different cell types, it does not enable isolation of vascular-specific gene expression, which is dependent upon further analysis and hypotheses.

Differentially expressed genes included a number previously demonstrated to modulate arteriogenesis in both mammalian models and my models utilising zebrafish embryos. For example, endogenous modulation was represented by differential expression of VEGF. Several studies have demonstrated increased collateral vessel remodelling or increased collateral blood flow following VEGF administration (Kondoh, Koyama *et al.*, 2004; Takeshita, Weir *et al.*, 1996). However, these studies have been performed in models where distinction between ischemic and non-ischemic regions was not made. VEGF upregulation predominantly occurs following binding of hypoxia-inducible factor 1 (HIF-1) to the VEGF promoter (Forsythe, Jiang *et al.*, 1996), suggesting VEGF upregulation occurs under hypoxic conditions. Mammalian studies in which ischemic and non-ischemic regions of muscle were analysed independently found collateral vessel development occurred in regions unaffected by reduced blood flow (Ito, Arras *et al.*, 1997). Other members of Dr. Chico's lab have demonstrated arteriogenesis to occur independently of hypoxia in zebrafish (Gray, Packham *et al.*, 2007). Differential expression of VEGF in the microarray analysis therefore suggests VEGF has a role in modulating alterations in haemodynamic force, and could indeed modulate arteriogenesis. It is possible VEGF modulates arteriogenesis through mediation of NO as has been demonstrated *in vitro* (Hood, Meininger *et al.*, 1998), or conversely through NO-mediation of VEGF (Papapetropoulos, Garcia-Cardena *et al.*, 1997). It is unfortunate that eNOS and iNOS genes, the isoforms of NOS observed and hypothesised to modulate arteriogenesis, were not represented on the GeneChip utilised preventing determination of possible mediation between VEGF and NO.

7.3.4 Differential Expression of Vasoactive Genes in the Absence of Haemodynamic Force

A cluster of vasoactive genes demonstrated significantly decreased gene expression in the absence of haemodynamic force. In order to determine a possible role for these genes in modulating arteriogenesis I performed knockdown experimentation of *EDNRB*. Although a role for EDNRB in angiogenesis and vascular remodelling has been described (Murakoshi, Miyauchi *et al.*, 2002), I am the first to research and find a role for EDNRB in modulation of arteriogenesis. I have demonstrated *EDNRB* knockdown significantly reduces recovery of aortic blood flow distal to occlusion in *gridlock* mutant embryos. While my results were not confirmed by chemical antagonism, studies in mice (Murakoshi, Miyauchi *et al.*, 2002) and chick (Ms Emily Hoggar, personal communication) do suggest a role. The mechanism by which EDNRB may modulate arteriogenesis was not the remit of this work. It is possible that decreased levels of NO may, at least in part, causes the effects seen in zebrafish *gridlock* mutant embryos following *EDNRB* knockdown, and it would be of interest to challenge this hypothesis. NO is easily inhibited in zebrafish embryos with NOS inhibition by L-NAME administration, although L-NAME does not distinguish between NOS isoforms. NO levels can also be enhanced through use of the NO donor SNP (Pelster, Grillitsch *et al.*, 2005). Utilising these means together with the models of aortic occlusion developed would permit further understanding of the mechanism that associates EDNRB with arteriogenesis. Since EDNRB is also expressed in monocytes/macrophages, cells important to collateral vessel remodelling, it would also be of interest to determine the effect of *EDNRB* knockdown on monocyte/macrophage recruitment and activity following arterial occlusion. It is possible that knockdown of *EDNRB* inhibits monocyte/macrophage activity in some way, thereby reducing recovery of aortic blood flow. Given expression of EDNRB in multiple cell-types (ECs, VSMCs, monocytes/macrophages), further research might also lead to isolate which of these cell-types is affected by *EDNRB* reduction. *EDNRB* knockdown in any of these cell-types might reduce recovery of aortic blood flow following occlusion, and it is possible that knockdown in all three contribute to the effect I have observed.

7.3.5 Temporal Alterations in Recovery of Aortic Flow with *EFNB1* Knockdown

EFNB1 knockdown in *gridlock* mutant embryos resulted in a very significant increase in recovery of blood flow distal to occlusion compared to control at 3dpf (figure 6.11) however by 4dpf this significant increase was lost and did not recover at 5dpf. These results are possibly due to reductions in MO activity at 4 and 5dpf. Given the short timeframe of increased recovery of aortic blood flow, it is difficult to determine the possible mechanisms involved. Expression in kidney arterioles and glomeruli suggested possible roles in vascular patterning and development (Adams, 2002). Such alterations during development of zebrafish embryos could account for my observation, since vasculature is plastic at this time and undergoes sprouting and regression (Isogai, Lawson *et al.*, 2003). However, I did not determine alterations in vasculature patterning of *EFNB1* knockdown embryos at 2dpf. Utilisation of MOs designed against different portions of *EFNB1*'s sequence may permit validation of this result. Closely related molecules, such as EFNB2, demonstrate an important role in arterial-venous fate decisions at timepoints close to the onset of blood flow (Wang, Chen *et al.*, 1998). It is possible that embryonic expression peaks at this timepoint. If *EFNB1* expression follows a similar pattern lower levels of expression may occur at the later timepoints of 4 and 5dpf, and thus the effect of deficiency may be lessened. The hypothesis could be tested by performed *in situ* hybridisation at all three timepoints.

7.4 Summary

This work demonstrates that zebrafish embryos are able to undergo a process akin to mammalian arteriogenesis. Though the zebrafish models developed and discussed may prove complementary to existing mammalian models, more work is required to determine the mechanistic and histological similarities and differences that may exist between zebrafish and mammals undergoing vessel remodelling after occlusion. I believe that with this additional data, it may be possible to describe zebrafish embryos as a stand alone comprehensive model for the study of arteriogenesis.

References

ADAMS, R. H. (2002) Vascular patterning by Eph receptor tyrosine kinases and ephrins. *Semin Cell Dev Biol,* 13**,** 55-60.

ADAMS, R. H., WILKINSON, G. A., WEISS, C., DIELLA, F., GALE, N. W., DEUTSCH, U., RISAU, W. & KLEIN, R. (1999) Roles of ephrinB ligands and EphB receptors in cardiovascular development: demarcation of arterial/venous domains, vascular morphogenesis, and sprouting angiogenesis. *Genes Dev,* 13**,** 295-306.

AFFYMETRIX www.affymetrix.com, accessed 16/09/2008.

GeneChip Zebrafish Genome Array Data Sheet.

ADAMS, R. H. (2002) Vascular patterning by Eph receptor tyrosine kinases and ephrins. *Semin Cell Dev Biol,* 13**,** 55-60.

ADAMS, R. H., WILKINSON, G. A., WEISS, C., DIELLA, F., GALE, N. W., DEUTSCH, U., RISAU, W. & KLEIN, R. (1999) Roles of ephrinB ligands and EphB receptors in cardiovascular development: demarcation of arterial/venous domains, vascular morphogenesis, and sprouting angiogenesis. *Genes Dev,* 13**,** 295-306.

AFFYMETRIX www.affymetrix.com, accessed 16/09/2008.

ARMULIK, A., ABRAMSSON, A. & BETSHOLTZ, C. (2005) Endothelial/pericyte interactions. *Circ Res,* 97**,** 512-23.

BABIAK, A., SCHUMM, A. M., WANGLER, C., LOUKAS, M., WU, J., DOMBROWSKI, S., MATUSCHEK, C., KOTZERKE, J., DEHIO, C. & WALTENBERGER, J. (2004) Coordinated activation of VEGFR-1 and VEGFR-2 is a potent arteriogenic stimulus leading to enhancement of regional perfusion. *Cardiovasc Res,* 61**,** 789-95.

BAGATTO, B. & BURGGREN, W. (2006) A Three-Dimensional Functional Assessment of Heart and Vessel Development in the Larva of the Zebrafish (Danio rerio). *Physiol Biochem Zool,* 79**,** 194-201.

BAGNALL, A. J., KELLAND, N. F., GULLIVER-SLOAN, F., DAVENPORT, A. P., GRAY, G. A., YANAGISAWA, M., WEBB, D. J. & KOTELEVTSEV, Y. V. (2006) Deletion of endothelial cell endothelin B receptors does not affect blood pressure or sensitivity to salt. *Hypertension,* 48**,** 286-93.

BAGNATO, A. & SPINELLA, F. (2003) Emerging role of endothelin-1 in tumor angiogenesis. *Trends Endocrinol Metab,* 14**,** 44-50.

BAIK, H. W., KWAK, B. K., SHIM, H. J., KIM, Y. S., LEE, J. B. & KIM, K. S. (2008) A New Ischemic Model Using a Radiofrequency Wire Electrode in a Rabbit Hindlimb. *Cardiovasc Intervent Radiol.*

BAKER, K., WARREN, K. S., YELLEN, G. & FISHMAN, M. C. (1997) Defective "pacemaker" current (Ih) in a zebrafish mutant with a slow heart rate. *Proc Natl Acad Sci U S A,* 94**,** 4554-9.

BARTMAN, T., WALSH, E. C., WEN, K. K., MCKANE, M., REN, J., ALEXANDER, J., RUBENSTEIN, P. A. & STAINIER, D. Y. (2004) Early myocardial function affects endocardial cushion development in zebrafish. *PLoS Biol,* 2**,** E129.

BENJAMIN, L. E., HEMO, I. & KESHET, E. (1998) A plasticity window for blood vessel remodelling is defined by pericyte coverage of the preformed endothelial network and is regulated by PDGF-B and VEGF. *Development,* 125**,** 1591-8.

BERGMANN, C. E., HOEFER, I. E., MEDER, B., ROTH, H., VAN ROYEN, N., BREIT, S. M., JOST, M. M., AHARINEJAD, S., HARTMANN, S. & BUSCHMANN, I. R. (2006) Arteriogenesis depends on circulating monocytes and macrophage accumulation and is severely depressed in op/op mice. *J Leukoc Biol,* 80**,** 59-65.

BERS, D. M. (2002) Cardiac excitation-contraction coupling. *Nature,* 415**,** 198-205.

BERTHIAUME, N., YANAGISAWA, M., LABONTE, J. & D'ORLEANS-JUSTE, P. (2000) Heterozygous knock-Out of ET(B) receptors induces BQ-123-sensitive hypertension in the mouse. *Hypertension,* 36**,** 1002-7.

BLUM, Y., BELTING, H. G., ELLERTSDOTTIR, E., HERWIG, L., LUDERS, F. & AFFOLTER, M. (2008) Complex cell rearrangements during intersegmental vessel sprouting and vessel fusion in the zebrafish embryo. *Dev Biol,* 316**,** 312-22.

BUSCHMANN, I. & SCHAPER, W. (1999) Arteriogenesis Versus Angiogenesis: Two Mechanisms of Vessel Growth. *News Physiol Sci,* 14**,** 121-125.

BUSCHMANN, I. & SCHAPER, W. (2000) The pathophysiology of the collateral circulation (arteriogenesis). *J Pathol,* 190**,** 338-42.

BUSCHMANN, I. R., VOSKUIL, M., VAN ROYEN, N., HOEFER, I. E., SCHEFFLER, K., GRUNDMANN, S., HENNIG, J., SCHAPER, W., BODE, C. & PIEK, J. J. (2003) Invasive and non-invasive evaluation of spontaneous arteriogenesis in a novel porcine model for peripheral arterial obstructive disease. *Atherosclerosis,* 167**,** 33-43.

CAI, W., VOSSCHULTE, R., AFSAH-HEDJRI, A., KOLTAI, S., KOCSIS, E., SCHOLZ, D., KOSTIN, S., SCHAPER, W. & SCHAPER, J. (2000) Altered balance between extracellular proteolysis and antiproteolysis is associated with adaptive coronary arteriogenesis. *J Mol Cell Cardiol,* 32**,** 997-1011.

CAI, W. J., KOCSIS, E., LUO, X., SCHAPER, W. & SCHAPER, J. (2004a) Expression of endothelial nitric oxide synthase in the vascular wall during arteriogenesis. *Mol Cell Biochem,* 264**,** 193-200.

CAI, W. J., KOCSIS, E., WU, X., RODRIGUEZ, M., LUO, X., SCHAPER, W. & SCHAPER, J. (2004b) Remodeling of the vascular tunica media is essential for development of collateral vessels in the canine heart. *Mol Cell Biochem,* 264**,** 201-10.

CARMELIET, P. (2000) Mechanisms of angiogenesis and arteriogenesis. *Nat Med,* 6**,** 389-95.

CARMELIET, P., FERREIRA, V., BREIER, G., POLLEFEYT, S., KIECKENS, L., GERTSENSTEIN, M., FAHRIG, M., VANDENHOECK, A., HARPAL, K., EBERHARDT, C., DECLERCQ, C., PAWLING, J., MOONS, L., COLLEN, D., RISAU, W. & NAGY, A. (1996) Abnormal blood vessel development and lethality in embryos lacking a single VEGF allele. *Nature,* 380**,** 435-9.

CATTARUZZA, M., DIMIGEN, C., EHRENREICH, H. & HECKER, M. (2000) Stretch-induced endothelin B receptor-mediated apoptosis in vascular smooth muscle cells. *FASEB J,* 14**,** 991-8.

CHEN, B. P., LI, Y. S., ZHAO, Y., CHEN, K. D., LI, S., LAO, J., YUAN, S., SHYY, J. Y. & CHIEN, S. (2001) DNA microarray analysis of gene expression in endothelial cells in response to 24-h shear stress. *Physiol Genomics,* 7**,** 55-63.

CHEN, J. N., HAFFTER, P., ODENTHAL, J., VOGELSANG, E., BRAND, M., VAN EEDEN, F. J., FURUTANI-SEIKI, M., GRANATO, M., HAMMERSCHMIDT, M., HEISENBERG, C. P., JIANG, Y. J., KANE, D. A., KELSH, R. N., MULLINS, M. C. & NUSSLEIN-VOLHARD, C.

(1996) Mutations affecting the cardiovascular system and other internal organs in zebrafish. *Development,* 123**,** 293-302.

CHICO, T. J., INGHAM, P. W. & CROSSMAN, D. C. (2008) Modeling cardiovascular disease in the zebrafish. *Trends Cardiovasc Med,* 18**,** 150-5.

CHILDS, S., CHEN, J. N., GARRITY, D. M. & FISHMAN, M. C. (2002) Patterning of angiogenesis in the zebrafish embryo. *Development,* 129**,** 973-82.

CHIU, J. J., CHEN, L. J., CHEN, C. N., LEE, P. L. & LEE, C. I. (2004) A model for studying the effect of shear stress on interactions between vascular endothelial cells and smooth muscle cells. *J Biomech,* 37**,** 531-9.

CLAYTON, J. A., CHALOTHORN, D. & FABER, J. E. (2008) Vascular Endothelial Growth Factor-A Specifies Formation of Native Collaterals and Regulates Collateral Growth in Ischemia. *Circ Res*.

COMPAGNI, A., LOGAN, M., KLEIN, R. & ADAMS, R. H. (2003) Control of skeletal patterning by ephrinB1-EphB interactions. *Dev Cell,* 5**,** 217-30.

COVASSIN, L., AMIGO, J. D., SUZUKI, K., TEPLYUK, V., STRAUBHAAR, J. & LAWSON, N. D. (2006) Global analysis of hematopoietic and vascular endothelial gene expression by tissue specific microarray profiling in zebrafish. *Dev Biol*.

CRUZ, A., PARNOT, C., RIBATTI, D., CORVOL, P. & GASC, J. M. (2001) Endothelin-1, a regulator of angiogenesis in the chick chorioallantoic membrane. *J Vasc Res,* 38**,** 536-45.

CUNNINGHAM, K. S. & GOTLIEB, A. I. (2005) The role of shear stress in the pathogenesis of atherosclerosis. *Lab Invest,* 85**,** 9-23.

DAHER, Z., NOEL, J. & CLAING, A. (2008) Endothelin-1 promotes migration of endothelial cells through the activation of ARF6 and the regulation of FAK activity. *Cell Signal.*

DAVIES, A., BLAKELEY, A. & KIDD, C. (2001) *Human Physiology*, Churchill Livingstone.

DAVY, A., AUBIN, J. & SORIANO, P. (2004) Ephrin-B1 forward and reverse signaling are required during mouse development. *Genes Dev,* 18**,** 572-83.

DE HOON, M., IMOTO, S. & MIYANO, S. (2002) Gene Cluster 3.0. University of Tokyo, Human Genome Centre.

DEAN, A. G., SULLIVAN, K. M. & SOE, M. M. (2008) OpenEpi: Open Source Epidemiologic Statistics for Public Health, Version 2.2.1.

DEINDL, E., BUSCHMANN, I., HOEFER, I. E., PODZUWEIT, T., BOENGLER, K., VOGEL, S., VAN ROYEN, N., FERNANDEZ, B. & SCHAPER, W. (2001) Role of ischemia and of hypoxia-inducible genes in arteriogenesis after femoral artery occlusion in the rabbit. *Circ Res,* 89**,** 779-86.

DEMICHEVA, E., HECKER, M. & KORFF, T. (2008) Stretch-induced activation of the transcription factor activator protein-1 controls monocyte chemoattractant protein-1 expression during arteriogenesis. *Circ Res,* 103**,** 477-84.

DRIEVER, W., SOLNICA-KREZEL, L., SCHIER, A. F., NEUHAUSS, S. C., MALICKI, J., STEMPLE, D. L., STAINIER, D. Y., ZWARTKRUIS, F., ABDELILAH, S., RANGINI, Z., BELAK, J. &

BOGGS, C. (1996) A genetic screen for mutations affecting embryogenesis in zebrafish. *Development,* 123**,** 37-46.

DUVALL, C. L., ROBERT TAYLOR, W., WEISS, D. & GULDBERG, R. E. (2004) Quantitative microcomputed tomography analysis of collateral vessel development after ischemic injury. *Am J Physiol Heart Circ Physiol,* 287**,** H302-10.

EISEN, J. S. & SMITH, J. C. (2008) Controlling morpholino experiments: don't stop making antisense. *Development,* 135**,** 1735-43.

EITENMULLER, I., VOLGER, O., KLUGE, A., TROIDL, K., BARANCIK, M., CAI, W. J., HEIL, M., PIPP, F., FISCHER, S., HORREVOETS, A. J., SCHMITZ-RIXEN, T. & SCHAPER, W. (2006) The Range of Adaptation by Collateral Vessels After Femoral Artery Occlusion. *Circ Res.*

FENG, W., MCCABE, N. P., MAHABELESHWAR, G. H., SOMANATH, P. R., PHILLIPS, D. R. & BYZOVA, T. V. (2008) The angiogenic response is dictated by beta3 integrin on bone marrow-derived cells. *J Cell Biol,* 183**,** 1145-57.

FENG, Y., YANG, J. H., HUANG, H., KENNEDY, S. P., TURI, T. G., THOMPSON, J. F., LIBBY, P. & LEE, R. T. (1999) Transcriptional profile of mechanically induced genes in human vascular smooth muscle cells. *Circ Res,* 85**,** 1118-23.

FISCHER, C., MAZZONE, M., JONCKX, B. & CARMELIET, P. (2008) FLT1 and its ligands VEGFB and PlGF: drug targets for anti-angiogenic therapy? *Nat Rev Cancer,* 8**,** 942-56.

FISHMAN, M. C. & CHIEN, K. R. (1997) Fashioning the vertebrate heart: earliest embryonic decisions. *Development,* 124**,** 2099-117.

FLAMANT, L., TOFFOLI, S., RAES, M. & MICHIELS, C. (2009) Hypoxia regulates inflammatory gene expression in endothelial cells. *Experimental Cell Research,* in press.

FORSYTHE, J. A., JIANG, B. H., IYER, N. V., AGANI, F., LEUNG, S. W., KOOS, R. D. & SEMENZA, G. L. (1996) Activation of vascular endothelial growth factor gene transcription by hypoxia-inducible factor 1. *Mol Cell Biol,* 16**,** 4604-13.

FRISEN, J., HOLMBERG, J. & BARBACID, M. (1999) Ephrins and their Eph receptors: multitalented directors of embryonic development. *EMBO J,* 18**,** 5159-65.

FRITSCHE, R., SCHWERTE, T. & PELSTER, B. (2000) Nitric oxide and vascular reactivity in developing zebrafish, Danio rerio. *Am J Physiol Regul Integr Comp Physiol,* 279**,** R2200-7.

FRYE, S. R., YEE, A., ESKIN, S. G., GUERRA, R., CONG, X. & MCINTIRE, L. V. (2005) cDNA microarray analysis of endothelial cells subjected to cyclic mechanical strain: importance of motion control. *Physiol Genomics,* 21**,** 124-30.

GARCIA-CARDENA, G., COMANDER, J., ANDERSON, K. R., BLACKMAN, B. R. & GIMBRONE, M. A., JR. (2001) Biomechanical activation of vascular endothelium as a determinant of its functional phenotype. *Proc Natl Acad Sci U S A,* 98**,** 4478-85.

GERHOLD, D., RUSHMORE, T. & CASKEY, C. T. (1999) DNA chips: promising toys have become powerful tools. *Trends Biochem Sci,* 24**,** 168-73.

GESSLER, M., KNOBELOCH, K. P., HELISCH, A., AMANN, K., SCHUMACHER, N., ROHDE, E., FISCHER, A. & LEIMEISTER, C. (2002) Mouse gridlock: no aortic coarctation or deficiency, but fatal cardiac defects in Hey2 -/- mice. *Curr Biol,* 12**,** 1601-4.

GONCALVES, L. M., EPSTEIN, S. E. & PIEK, J. J. (2001) Controlling collateral development: the difficult task of mimicking mother nature. *Cardiovasc Res,* 49**,** 495-6.

GRAY, C., PACKHAM, I. M., WURMSER, F., EASTLEY, N. C., HELLEWELL, P. G., INGHAM, P. W., CROSSMAN, D. C. & CHICO, T. J. (2007) Ischemia is not required for arteriogenesis in zebrafish embryos. *Arterioscler Thromb Vasc Biol,* 27**,** 2135-41.

HAFFTER, P., GRANATO, M., BRAND, M., MULLINS, M. C., HAMMERSCHMIDT, M., KANE, D. A., ODENTHAL, J., VAN EEDEN, F. J., JIANG, Y. J., HEISENBERG, C. P., KELSH, R. N., FURUTANI-SEIKI, M., VOGELSANG, E., BEUCHLE, D., SCHACH, U., FABIAN, C. & NUSSLEIN-VOLHARD, C. (1996) The identification of genes with unique and essential functions in the development of the zebrafish, Danio rerio. *Development,* 123**,** 1-36.

HAGA, J. H., LI, Y. S. & CHIEN, S. (2007) Molecular basis of the effects of mechanical stretch on vascular smooth muscle cells. *J Biomech,* 40**,** 947-60.

HALKA, A. T., TURNER, N. J., CARTER, A., GHOSH, J., MURPHY, M. O., KIRTON, J. P., KIELTY, C. M. & WALKER, M. G. (2008) The effects of stretch on vascular smooth muscle cell phenotype in vitro. *Cardiovasc Pathol,* 17**,** 98-102.

HATO, T., TABATA, M. & OIKE, Y. (2008) The role of angiopoietin-like proteins in angiogenesis and metabolism. *Trends Cardiovasc Med,* 18**,** 6-14.

HEIL, M., EITENMULLER, I., SCHMITZ-RIXEN, T. & SCHAPER, W. (2006) Arteriogenesis versus angiogenesis: similarities and differences. *J Cell Mol Med,* 10**,** 45-55.

HEIL, M. & SCHAPER, W. (2004) Influence of mechanical, cellular, and molecular factors on collateral artery growth (arteriogenesis). *Circ Res,* 95**,** 449-58.

HEIL, M., ZIEGELHOEFFER, T., PIPP, F., KOSTIN, S., MARTIN, S., CLAUSS, M. & SCHAPER, W. (2002) Blood monocyte concentration is critical for enhancement of collateral artery growth. *Am J Physiol Heart Circ Physiol,* 283**,** H2411-9.

HEIL, M., ZIEGELHOEFFER, T., WAGNER, S., FERNANDEZ, B., HELISCH, A., MARTIN, S., TRIBULOVA, S., KUZIEL, W. A., BACHMANN, G. & SCHAPER, W. (2004) Collateral artery growth (arteriogenesis) after experimental arterial occlusion is impaired in mice lacking CC-chemokine receptor-2. *Circ Res,* 94**,** 671-7.

HEILMANN, C., BEYERSDORF, F. & LUTTER, G. (2002) Collateral growth: cells arrive at the construction site. *Cardiovasc Surg,* 10**,** 570-8.

HEYDARKHAN-HAGVALL, S., CHIEN, S., NELANDER, S., LI, Y. C., YUAN, S., LAO, J., HAGA, J. H., LIAN, I., NGUYEN, P., RISBERG, B. & LI, Y. S. (2006) DNA microarray study on gene expression profiles in co-cultured endothelial and smooth muscle cells in response to 4- and 24-h shear stress. *Mol Cell Biochem,* 281**,** 1-15.

HIMBURG, H. A., DOWD, S. E. & FRIEDMAN, M. H. (2007) Frequency-dependent response of the vascular endothelium to pulsatile shear stress. *Am J Physiol Heart Circ Physiol,* 293**,** H645-53.

HIRATSUKA, S., MINOWA, O., KUNO, J., NODA, T. & SHIBUYA, M. (1998) Flt-1 lacking the tyrosine kinase domain is sufficient for normal development and angiogenesis in mice. *Proc Natl Acad Sci U S A,* 95**,** 9349-54.

HOEFER, I. E., GRUNDMANN, S., VAN ROYEN, N., VOSKUIL, M., SCHIRMER, S. H., ULUSANS, S., BODE, C., BUSCHMANN, I. R. & PIEK, J. J. (2005) Leukocyte subpopulations and

arteriogenesis: specific role of monocytes, lymphocytes and granulocytes. *Atherosclerosis,* 181**,** 285-93.

HOEFER, I. E., VAN ROYEN, N., BUSCHMANN, I. R., PIEK, J. J. & SCHAPER, W. (2001) Time course of arteriogenesis following femoral artery occlusion in the rabbit. *Cardiovasc Res,* 49**,** 609-17.

HONG, C. C., KUME, T. & PETERSON, R. T. (2008) Role of crosstalk between phosphatidylinositol 3-kinase and extracellular signal-regulated kinase/mitogen-activated protein kinase pathways in artery-vein specification. *Circ Res,* 103**,** 573-9.

HOOD, J. D., MEININGER, C. J., ZICHE, M. & GRANGER, H. J. (1998) VEGF upregulates ecNOS message, protein, and NO production in human endothelial cells. *Am J Physiol,* 274**,** H1054-8.

HOVE, J. R., KOSTER, R. W., FOROUHAR, A. S., ACEVEDO-BOLTON, G., FRASER, S. E. & GHARIB, M. (2003) Intracardiac fluid forces are an essential epigenetic factor for embryonic cardiogenesis. *Nature,* 421**,** 172-7.

HUSS, R., HEIL, M., MOOSMANN, S., ZIEGELHOEFFER, T., SAGEBIEL, S., SELIGER, C., KINSTON, S. & GOTTGENS, B. (2004) Improved arteriogenesis with simultaneous skeletal muscle repair in ischemic tissue by SCL(+) multipotent adult progenitor cell clones from peripheral blood. *J Vasc Res,* 41**,** 422-31.

HUYNH-DO, U., VINDIS, C., LIU, H., CERRETTI, D. P., MCGREW, J. T., ENRIQUEZ, M., CHEN, J. & DANIEL, T. O. (2002) Ephrin-B1 transduces signals to activate integrin-mediated migration, attachment and angiogenesis. *J Cell Sci,* 115**,** 3073-81.

IGNARRO, L. J. (1990) Nitric oxide. A novel signal transduction mechanism for transcellular communication. *Hypertension,* 16**,** 477-83.

ISOGAI, S., HORIGUCHI, M. & WEINSTEIN, B. M. (2001) The vascular anatomy of the developing zebrafish: an atlas of embryonic and early larval development. *Dev Biol,* 230**,** 278-301.

ISOGAI, S., LAWSON, N. D., TORREALDAY, S., HORIGUCHI, M. & WEINSTEIN, B. M. (2003) Angiogenic network formation in the developing vertebrate trunk. *Development,* 130**,** 5281-90.

ITO, W. D., ARRAS, M., SCHOLZ, D., WINKLER, B., HTUN, P. & SCHAPER, W. (1997) Angiogenesis but not collateral growth is associated with ischemia after femoral artery occlusion. *Am J Physiol,* 273**,** H1255-65.

JACOBI, J., SYDOW, K., VON DEGENFELD, G., ZHANG, Y., DAYOUB, H., WANG, B., PATTERSON, A. J., KIMOTO, M., BLAU, H. M. & COOKE, J. P. (2005) Overexpression of dimethylarginine dimethylaminohydrolase reduces tissue asymmetric dimethylarginine levels and enhances angiogenesis. *Circulation,* 111**,** 1431-8.

JACOBI, J., TAM, B. Y., WU, G., HOFFMAN, J., COOKE, J. P. & KUO, C. J. (2004) Adenoviral gene transfer with soluble vascular endothelial growth factor receptors impairs angiogenesis and perfusion in a murine model of hindlimb ischemia. *Circulation,* 110**,** 2424-9.

JAYAPAL, M. & MELENDEZ, A. J. (2006) DNA microarray technology for target identification and validation. *Clin Exp Pharmacol Physiol,* 33**,** 496-503.

JIA, H., KING, I. N., CHOPRA, S. S., WAN, H., NI, T. T., JIANG, C., GUAN, X., WELLS, S., SRIVASTAVA, D. & ZHONG, T. P. (2007) Vertebrate heart growth is regulated by functional antagonism between Gridlock and Gata5. *Proc Natl Acad Sci U S A,* 104**,** 14008-13.

JIN, D. K., SHIDO, K., KOPP, H. G., PETIT, I., SHMELKOV, S. V., YOUNG, L. M., HOOPER, A. T., AMANO, H., AVECILLA, S. T., HEISSIG, B., HATTORI, K., ZHANG, F., HICKLIN, D. J., WU, Y., ZHU, Z., DUNN, A., SALARI, H., WERB, Z., HACKETT, N. R., CRYSTAL, R. G., LYDEN, D. & RAFII, S. (2006) Cytokine-mediated deployment of SDF-1 induces revascularization through recruitment of CXCR4+ hemangiocytes. *Nat Med,* 12**,** 557-67.

JIN, S. W., BEIS, D., MITCHELL, T., CHEN, J. N. & STAINIER, D. Y. (2005) Cellular and molecular analyses of vascular tube and lumen formation in zebrafish. *Development,* 132**,** 5199-209.

JIN, S. W., HERZOG, W., SANTORO, M. M., MITCHELL, T. S., FRANTSVE, J., JUNGBLUT, B., BEIS, D., SCOTT, I. C., D'AMICO, L. A., OBER, E. A., VERKADE, H., FIELD, H. A., CHI, N. C., WEHMAN, A. M., BAIER, H. & STAINIER, D. Y. (2007) A transgene-assisted genetic screen identifies essential regulators of vascular development in vertebrate embryos. *Dev Biol,* 307**,** 29-42.

JONES, E. A., LE NOBLE, F. & EICHMANN, A. (2006) What determines blood vessel structure? Genetic prespecification vs. hemodynamics. *Physiology (Bethesda),* 21**,** 388-95.

KAMEI, M., SAUNDERS, W. B., BAYLESS, K. J., DYE, L., DAVIS, G. E. & WEINSTEIN, B. M. (2006) Endothelial tubes assemble from intracellular vacuoles in vivo. *Nature,* 442**,** 453-6.

KELSH, R. N., HARRIS, M. L., COLANESI, S. & ERICKSON, C. A. (2008) Stripes and belly-spots-A review of pigment cell morphogenesis in vertebrates. *Semin Cell Dev Biol.*

KIBBE, M., BILLIAR, T. & TZENG, E. (1999) Inducible nitric oxide synthase and vascular injury. *Cardiovasc Res,* 43**,** 650-7.

KIM, I., MOON, S. O., KOH, K. N., KIM, H., UHM, C. S., KWAK, H. J., KIM, N. G. & KOH, G. Y. (1999) Molecular cloning, expression, and characterization of angiopoietin-related protein. angiopoietin-related protein induces endothelial cell sprouting. *J Biol Chem,* 274**,** 26523-8.

KIMMEL, C. B., BALLARD, W. W., KIMMEL, S. R., ULLMANN, B. & SCHILLING, T. F. (1995) Stages of embryonic development of the zebrafish. *Dev Dyn,* 203**,** 253-310.

KLABUNDE, R. (2005) *Cardiovascular Physiological Concepts*, Lippincott Williams and Wilkins.

KOJIMA, T., CHANG, J. H. & AZAR, D. T. (2007) Proangiogenic role of ephrinB1/EphB1 in basic fibroblast growth factor-induced corneal angiogenesis. *Am J Pathol,* 170**,** 764-73.

KONDOH, K., KOYAMA, H., MIYATA, T., TAKATO, T., HAMADA, H. & SHIGEMATSU, H. (2004) Conduction performance of collateral vessels induced by vascular endothelial growth factor or basic fibroblast growth factor. *Cardiovasc Res,* 61**,** 132-42.

KORFF, T., BRAUN, J., PFAFF, D., AUGUSTIN, H. G. & HECKER, M. (2008) Role of ephrinB2 expression in endothelial cells during arteriogenesis: impact on smooth muscle cell migration and monocyte recruitment. *Blood,* 112**,** 73-81.

KOWANETZ, M. & FERRARA, N. (2006) Vascular endothelial growth factor signaling pathways: therapeutic perspective. *Clin Cancer Res,* 12**,** 5018-22.

KUBOTA, Y., OIKE, Y., SATOH, S., TABATA, Y., NIIKURA, Y., MORISADA, T., AKAO, M., URANO, T., ITO, Y., MIYAMOTO, T., NAGAI, N., KOH, G. Y., WATANABE, S. & SUDA, T. (2005) Cooperative interaction of Angiopoietin-like proteins 1 and 2 in zebrafish vascular development. *Proc Natl Acad Sci U S A,* 102**,** 13502-7.

KUMAR, D., BRANCH, B. G., PATTILLO, C. B., HOOD, J., THOMA, S., SIMPSON, S., ILLUM, S., ARORA, N., CHIDLOW, J. H., JR., LANGSTON, W., TENG, X., LEFER, D. J., PATEL, R. P. & KEVIL, C. G. (2008) Chronic sodium nitrite therapy augments ischemia-induced angiogenesis and arteriogenesis. *Proc Natl Acad Sci U S A,* 105**,** 7540-5.

LANGHEINRICH, U., VACUN, G. & WAGNER, T. (2003) Zebrafish embryos express an orthologue of HERG and are sensitive toward a range of QT-prolonging drugs inducing severe arrhythmia. *Toxicol Appl Pharmacol,* 193**,** 370-82.

LAWSON, N. D., SCHEER, N., PHAM, V. N., KIM, C. H., CHITNIS, A. B., CAMPOS-ORTEGA, J. A. & WEINSTEIN, B. M. (2001) Notch signaling is required for arterial-venous differentiation during embryonic vascular development. *Development,* 128**,** 3675-83.

LAWSON, N. D. & WEINSTEIN, B. M. (2002) In vivo imaging of embryonic vascular development using transgenic zebrafish. *Dev Biol,* 248**,** 307-18.

LE NOBLE, F., FLEURY, V., PRIES, A., CORVOL, P., EICHMANN, A. & RENEMAN, R. S. (2005) Control of arterial branching morphogenesis in embryogenesis: go with the flow. *Cardiovasc Res,* 65**,** 619-28.

LE NOBLE, F., MOYON, D., PARDANAUD, L., YUAN, L., DJONOV, V., MATTHIJSEN, R., BREANT, C., FLEURY, V. & EICHMANN, A. (2004) Flow regulates arterial-venous differentiation in the chick embryo yolk sac. *Development,* 131**,** 361-75.

LEE, C. W., STABILE, E., KINNAIRD, T., SHOU, M., DEVANEY, J. M., EPSTEIN, S. E. & BURNETT, M. S. (2004) Temporal patterns of gene expression after acute hindlimb ischemia in mice: insights into the genomic program for collateral vessel development. *J Am Coll Cardiol,* 43**,** 474-82.

LEHOUX, S., CASTIER, Y. & TEDGUI, A. (2006) Molecular mechanisms of the vascular responses to haemodynamic forces. *J Intern Med,* 259**,** 381-92.

LEVY, K., AND STANTON (2005) *Berne and Levy Principles of Physiology*, Elvesier Mosby.

LIESCHKE, G. J., OATES, A. C., PAW, B. H., THOMPSON, M. A., HALL, N. E., WARD, A. C., HO, R. K., ZON, L. I. & LAYTON, J. E. (2002) Zebrafish SPI-1 (PU.1) marks a site of myeloid development independent of primitive erythropoiesis: implications for axial patterning. *Dev Biol,* 246**,** 274-95.

LISTER, J. A., COOPER, C., NGUYEN, K., MODRELL, M., GRANT, K. & RAIBLE, D. W. (2006) Zebrafish Foxd3 is required for development of a subset of neural crest derivatives. *Dev Biol,* 290**,** 92-104.

LISTER, J. A., ROBERTSON, C. P., LEPAGE, T., JOHNSON, S. L. & RAIBLE, D. W. (1999) nacre encodes a zebrafish microphthalmia-related protein that regulates neural-crest-derived pigment cell fate. *Development,* 126**,** 3757-67.

LIU, V. W. & HUANG, P. L. (2008) Cardiovascular roles of nitric oxide: a review of insights from nitric oxide synthase gene disrupted mice. *Cardiovasc Res,* 77**,** 19-29.

LIU, X., MILO, M., LAWRENCE, N. D. & RATTRAY, M. (2005) A tractable probabilistic model for Affymetrix probe-level analysis across multiple chips. *Bioinformatics,* 21**,** 3637-44.

LLOYD, P. G., YANG, H. T. & TERJUNG, R. L. (2001) Arteriogenesis and angiogenesis in rat ischemic hindlimb: role of nitric oxide. *Am J Physiol Heart Circ Physiol,* 281**,** H2528-38.

LOCKHART, D. J., DONG, H., BYRNE, M. C., FOLLETTIE, M. T., GALLO, M. V., CHEE, M. S., MITTMANN, M., WANG, C., KOBAYASHI, M., HORTON, H. & BROWN, E. L. (1996) Expression monitoring by hybridization to high-density oligonucleotide arrays. *Nat Biotechnol,* 14**,** 1675-80.

MALEK, A. M., GREENE, A. L. & IZUMO, S. (1993) Regulation of endothelin 1 gene by fluid shear stress is transcriptionally mediated and independent of protein kinase C and cAMP. *Proc Natl Acad Sci U S A,* 90**,** 5999-6003.

MALONE, M. H., SCIAKY, N., STALHEIM, L., HAHN, K. M., LINNEY, E. & JOHNSON, G. L. (2007) Laser-scanning velocimetry: a confocal microscopy method for quantitative measurement of cardiovascular performance in zebrafish embryos and larvae. *BMC Biotechnol,* 7**,** 40.

MAXWELL, M. P., HEARSE, D. J. & YELLON, D. M. (1987) Species variation in the coronary collateral circulation during regional myocardial ischaemia: a critical determinant of the rate of evolution and extent of myocardial infarction. *Cardiovasc Res,* 21**,** 737-46.

MCCORMICK, S. M., ESKIN, S. G., MCINTIRE, L. V., TENG, C. L., LU, C. M., RUSSELL, C. G. & CHITTUR, K. K. (2001) DNA microarray reveals changes in gene expression of shear stressed human umbilical vein endothelial cells. *Proc Natl Acad Sci U S A,* 98**,** 8955-60.

MCGUIGAN, M. R., BRONKS, R., NEWTON, R. U., SHARMAN, M. J., GRAHAM, J. C., CODY, D. V. & KRAEMER, W. J. (2001) Muscle fiber characteristics in patients with peripheral arterial disease. *Med Sci Sports Exerc,* 33**,** 2016-21.

MEES, B., WAGNER, S., NINCI, E., TRIBULOVA, S., MARTIN, S., VAN HAPEREN, R., KOSTIN, S., HEIL, M., DE CROM, R. & SCHAPER, W. (2007) Endothelial nitric oxide synthase activity is essential for vasodilation during blood flow recovery but not for arteriogenesis. *Arterioscler Thromb Vasc Biol,* 27**,** 1926-33.

MILLS, J. D., FISCHER, D. & VILLANUEVA, F. S. (2000) Coronary collateral development during chronic ischemia: serial assessment using harmonic myocardial contrast echocardiography. *J Am Coll Cardiol,* 36**,** 618-24.

MIYAUCHI, T. & MASAKI, T. (1999) Pathophysiology of endothelin in the cardiovascular system. *Annu Rev Physiol,* 61**,** 391-415.

MORIMOTO, H., TAKAHASHI, M., SHIBA, Y., IZAWA, A., ISE, H., HONGO, M., HATAKE, K., MOTOYOSHI, K. & IKEDA, U. (2007) Bone marrow-derived CXCR4+ cells mobilized by macrophage colony-stimulating factor participate in the reduction of infarct area and improvement of cardiac remodeling after myocardial infarction in mice. *Am J Pathol,* 171**,** 755-66.

MOTOIKE, T., LOUGHNA, S., PERENS, E., ROMAN, B. L., LIAO, W., CHAU, T. C., RICHARDSON, C. D., KAWATE, T., KUNO, J., WEINSTEIN, B. M., STAINIER, D. Y. & SATO, T. N. (2000) Universal GFP reporter for the study of vascular development. *Genesis,* 28**,** 75-81.

MURAKOSHI, N., MIYAUCHI, T., KAKINUMA, Y., OHUCHI, T., GOTO, K., YANAGISAWA, M. & YAMAGUCHI, I. (2002) Vascular endothelin-B receptor system in vivo plays a favorable inhibitory role in vascular remodeling after injury revealed by endothelin-B receptor-knockout mice. *Circulation,* 106**,** 1991-8.

NESBITT, W. S., MANGIN, P., SALEM, H. H. & JACKSON, S. P. (2006) The impact of blood rheology on the molecular and cellular events underlying arterial thrombosis. *J Mol Med,* 84**,** 989-95.

OHURA, N., YAMAMOTO, K., ICHIOKA, S., SOKABE, T., NAKATSUKA, H., BABA, A., SHIBATA, M., NAKATSUKA, T., HARII, K., WADA, Y., KOHRO, T., KODAMA, T. & ANDO, J. (2003) Global analysis of shear stress-responsive genes in vascular endothelial cells. *J Atheroscler Thromb,* 10**,** 304-13.

OTROCK, Z. K., MAKAREM, J. A. & SHAMSEDDINE, A. I. (2007) Vascular endothelial growth factor family of ligands and receptors: review. *Blood Cells Mol Dis,* 38**,** 258-68.

PAGANI, M., VATNER, S. F. & BRAUNWALD, E. (1978) Hemodynamic effects of intravenous sodium nitroprusside in the conscious dog. *Circulation,* 57**,** 144-51.

PAPAPETROPOULOS, A., GARCIA-CARDENA, G., MADRI, J. A. & SESSA, W. C. (1997) Nitric oxide production contributes to the angiogenic properties of vascular endothelial growth factor in human endothelial cells. *J Clin Invest,* 100**,** 3131-9.

PARHAM, W. A., BOUHASIN, A., CIARAMITA, J. P., KHOUKAZ, S., HERRMANN, S. C. & KERN, M. J. (2004) Coronary hyperemic dose responses of intracoronary sodium nitroprusside. *Circulation,* 109**,** 1236-43.

PARICHY, D. M., RANSOM, D. G., PAW, B., ZON, L. I. & JOHNSON, S. L. (2000) An orthologue of the kit-related gene fms is required for development of neural crest-derived xanthophores and a subpopulation of adult melanocytes in the zebrafish, Danio rerio. *Development,* 127**,** 3031-44.

PARK, H. J., CHANG, K., PARK, C. S., JANG, S. W., IHM, S. H., KIM, P. J., BAEK, S. H., SEUNG, K. B. & CHOI, K. B. (2008) Coronary collaterals: the role of MCP-1 during the early phase of acute myocardial infarction. *Int J Cardiol,* 130**,** 409-13.

PASQUALE, E. B. (2004) Eph-ephrin promiscuity is now crystal clear. *Nat Neurosci,* 7**,** 417-8.

PELSTER, B. & BURGGREN, W. W. (1996) Disruption of hemoglobin oxygen transport does not impact oxygen-dependent physiological processes in developing embryos of zebra fish (Danio rerio). *Circ Res,* 79**,** 358-62.

PELSTER, B., GRILLITSCH, S. & SCHWERTE, T. (2005) NO as a mediator during the early development of the cardiovascular system in the zebrafish. *Comp Biochem Physiol A Mol Integr Physiol,* 142**,** 215-20.

PETERS, K. G., RAO, P. S., BELL, B. S. & KINDMAN, L. A. (1995) Green fluorescent fusion proteins: powerful tools for monitoring protein expression in live zebrafish embryos. *Dev Biol,* 171**,** 252-7.

PETERSON, R. T., SHAW, S. Y., PETERSON, T. A., MILAN, D. J., ZHONG, T. P., SCHREIBER, S. L., MACRAE, C. A. & FISHMAN, M. C. (2004) Chemical suppression of a genetic mutation in a zebrafish model of aortic coarctation. *Nat Biotechnol,* 22**,** 595-9.

PIPP, F., BOEHM, S., CAI, W. J., ADILI, F., ZIEGLER, B., KARANOVIC, G., RITTER, R., BALZER, J., SCHELER, C., SCHAPER, W. & SCHMITZ-RIXEN, T. (2004) Elevated fluid shear stress enhances postocclusive collateral artery growth and gene expression in the pig hind limb. *Arterioscler Thromb Vasc Biol,* 24**,** 1664-8.

PIPP, F., HEIL, M., ISSBRUCKER, K., ZIEGELHOEFFER, T., MARTIN, S., VAN DEN HEUVEL, J., WEICH, H., FERNANDEZ, B., GOLOMB, G., CARMELIET, P., SCHAPER, W. & CLAUSS, M. (2003) VEGFR-1-selective VEGF homologue PlGF is arteriogenic: evidence for a monocyte-mediated mechanism. *Circ Res,* 92**,** 378-85.

POLLOCK, D. M. & SCHNEIDER, M. P. (2006) Clarifying endothelin type B receptor function. *Hypertension,* 48**,** 211-2.

POSTLETHWAIT, J. H. (2007) The zebrafish genome in context: ohnologs gone missing. *J Exp Zoolog B Mol Dev Evol,* 308**,** 563-77.

RASBAND, W. S. ImageJ 1.34s National Institutes of Health, USA.

RENTROP, K. P., FEIT, F., SHERMAN, W. & THORNTON, J. C. (1989) Serial angiographic assessment of coronary artery obstruction and collateral flow in acute myocardial infarction. Report from the second Mount Sinai-New York University Reperfusion Trial. *Circulation,* 80**,** 1166-75.

REYNOLDS, L. E., WYDER, L., LIVELY, J. C., TAVERNA, D., ROBINSON, S. D., HUANG, X., SHEPPARD, D., HYNES, R. O. & HODIVALA-DILKE, K. M. (2002) Enhanced pathological angiogenesis in mice lacking beta3 integrin or beta3 and beta5 integrins. *Nat Med,* 8**,** 27-34.

RHEE, J. S., BLACK, M., SCHUBERT, U., FISCHER, S., MORGENSTERN, E., HAMMES, H. P. & PREISSNER, K. T. (2004) The functional role of blood platelet components in angiogenesis. *Thromb Haemost,* 92**,** 394-402.

ROMAN, B. L. & WEINSTEIN, B. M. (2000) Building the vertebrate vasculature: research is going swimmingly. *Bioessays,* 22**,** 882-93.

ROSEN, L. S. (2002) Clinical experience with angiogenesis signaling inhibitors: focus on vascular endothelial growth factor (VEGF) blockers. *Cancer Control,* 9**,** 36-44.

SALANI, D., TARABOLETTI, G., ROSANO, L., DI CASTRO, V., BORSOTTI, P., GIAVAZZI, R. & BAGNATO, A. (2000) Endothelin-1 induces an angiogenic phenotype in cultured endothelial cells and stimulates neovascularization in vivo. *Am J Pathol,* 157**,** 1703-11.

SANGUINETTI, G., MILO, M., RATTRAY, M. & LAWRENCE, N. D. (2005) Accounting for probe-level noise in principal component analysis of microarray data. *Bioinformatics,* 21**,** 3748-54.

SCHAPER, W. & BUSCHMANN, I. (1999) Arteriogenesis, the good and bad of it. *Cardiovasc Res,* 43**,** 835-7.

SCHAPER, W. & ITO, W. D. (1996) Molecular mechanisms of coronary collateral vessel growth. *Circ Res,* 79**,** 911-9.

SCHAPER, W. & SCHOLZ, D. (2003) Factors regulating arteriogenesis. *Arterioscler Thromb Vasc Biol,* 23**,** 1143-51.

SCHENA, M., SHALON, D., HELLER, R., CHAI, A., BROWN, P. O. & DAVIS, R. W. (1996) Parallel human genome analysis: microarray-based expression monitoring of 1000 genes. *Proc Natl Acad Sci U S A,* 93**,** 10614-9.

SCHOLZ, D., ITO, W., FLEMING, I., DEINDL, E., SAUER, A., WIESNET, M., BUSSE, R., SCHAPER, J. & SCHAPER, W. (2000) Ultrastructure and molecular histology of rabbit hind-limb collateral artery growth (arteriogenesis). *Virchows Arch,* 436**,** 257-70.

SCHWARZ, E. R., MEVEN, D. A., SULEMANJEE, N. Z., KERSTING, P. H., TUSSING, T., SKOBEL, E. C., HANRATH, P. & URETSKY, B. F. (2004) Monocyte chemoattractant protein 1-induced monocyte infiltration produces angiogenesis but not arteriogenesis in chronically infarcted myocardium. *J Cardiovasc Pharmacol Ther,* 9**,** 279-89.

SCHWERTE, T. & FRITSCHE, R. (2003) Understanding cardiovascular physiology in zebrafish and Xenopus larvae: the use of microtechniques. *Comp Biochem Physiol A Mol Integr Physiol,* 135**,** 131-45.

SCHWERTE, T. & PELSTER, B. (2000) Digital motion analysis as a tool for analysing the shape and performance of the circulatory system in transparent animals. *J Exp Biol,* 203**,** 1659-69.

SCHWERTE, T., PRINTZ, E. & FRITSCHE, R. (2002) Vascular control in larval Xenopus laevis: the role of endothelial-derived factors. *J Exp Biol,* 205**,** 225-32.

SCHWERTE, T., UBERBACHER, D. & PELSTER, B. (2003) Non-invasive imaging of blood cell concentration and blood distribution in zebrafish Danio rerio incubated in hypoxic conditions in vivo. *J Exp Biol,* 206**,** 1299-307.

SEHNERT, A. J., HUQ, A., WEINSTEIN, B. M., WALKER, C., FISHMAN, M. & STAINIER, D. Y. (2002) Cardiac troponin T is essential in sarcomere assembly and cardiac contractility. *Nat Genet,* 31**,** 106-10.

SERLUCA, F. C., DRUMMOND, I. A. & FISHMAN, M. C. (2002) Endothelial signaling in kidney morphogenesis: a role for hemodynamic forces. *Curr Biol,* 12**,** 492-7.

SERLUCA, F. C. & FISHMAN, M. C. (2001) Pre-pattern in the pronephric kidney field of zebrafish. *Development,* 128**,** 2233-41.

SIEKMANN, A. F., COVASSIN, L. & LAWSON, N. D. (2008) Modulation of VEGF signalling output by the Notch pathway. *Bioessays,* 30**,** 303-13.

STATON, C., LEWIS, C. & BICKNELL, R. (Eds.) (2006) *Angiogenesis Assays. A Critical Appraisal of Current Techniques,* John Wiley & Sons, Ltd.

SUMMERTON, J. & WELLER, D. (1997) Morpholino antisense oligomers: design, preparation, and properties. *Antisense Nucleic Acid Drug Dev,* 7**,** 187-95.

SUMMERTON, J. E. (2007) Morpholino, siRNA, and S-DNA compared: impact of structure and mechanism of action on off-target effects and sequence specificity. *Curr Top Med Chem,* 7**,** 651-60.

TAKESHITA, S., WEIR, L., CHEN, D., ZHENG, L. P., RIESSEN, R., BAUTERS, C., SYMES, J. F., FERRARA, N. & ISNER, J. M. (1996) Therapeutic angiogenesis following arterial gene transfer of vascular endothelial growth factor in a rabbit model of hindlimb ischemia. *Biochem Biophys Res Commun,* 227**,** 628-35.

TAKIGAWA, M., SAKURAI, T., KASUYA, Y., ABE, Y., MASAKI, T. & GOTO, K. (1995) Molecular identification of guanine-nucleotide-binding regulatory proteins which couple to endothelin receptors. *Eur J Biochem,* 228**,** 102-8.

TAMMELA, T., ENHOLM, B., ALITALO, K. & PAAVONEN, K. (2005) The biology of vascular endothelial growth factors. *Cardiovasc Res,* 65**,** 550-63.

TANG, G. L., CHANG, D. S., SARKAR, R., WANG, R. & MESSINA, L. M. (2005) The effect of gradual or acute arterial occlusion on skeletal muscle blood flow, arteriogenesis, and inflammation in rat hindlimb ischemia. *J Vasc Surg,* 41**,** 312-20.

TERZI, F., HENRION, D., COLUCCI-GUYON, E., FEDERICI, P., BABINET, C., LEVY, B. I., BRIAND, P. & FRIEDLANDER, G. (1997) Reduction of renal mass is lethal in mice lacking vimentin. Role of endothelin-nitric oxide imbalance. *J Clin Invest,* 100**,** 1520-8.

THATTALIYATH, B., CYKOWSKI, M. & JAGADEESWARAN, P. (2005) Young thrombocytes initiate the formation of arterial thrombi in zebrafish. *Blood,* 106**,** 118-24.

THISSE, C. & THISSE, B. (2008) High-resolution in situ hybridization to whole-mount zebrafish embryos. *Nat Protoc,* 3**,** 59-69.

THOMAS, P. D., CAMPBELL, M. J., KEJARIWAL, A., MI, H., KARLAK, B., DAVERMAN, R., DIEMER, K., MURUGANUJAN, A. & NARECHANIA, A. (2003) PANTHER: a library of protein families and subfamilies indexed by function. *Genome Res,* 13**,** 2129-41.

UNGER, E. F. (2001) Experimental evaluation of coronary collateral development. *Cardiovasc Res,* 49**,** 497-506.

UNTHANK, J. L., NIXON, J. C. & DALSING, M. C. (1996) Inhibition of NO synthase prevents acute collateral artery dilation in the rat hindlimb. *J Surg Res,* 61**,** 463-8.

VAN ROYEN, N., HOEFER, I., BUSCHMANN, I., KOSTIN, S., VOSKUIL, M., BODE, C., SCHAPER, W. & PIEK, J. J. (2003) Effects of local MCP-1 protein therapy on the development of the collateral circulation and atherosclerosis in Watanabe hyperlipidemic rabbits. *Cardiovasc Res,* 57**,** 178-85.

VAN ROYEN, N., PIEK, J. J., BUSCHMANN, I., HOEFER, I., VOSKUIL, M. & SCHAPER, W. (2001a) Stimulation of arteriogenesis; a new concept for the treatment of arterial occlusive disease. *Cardiovasc Res,* 49**,** 543-53.

VAN ROYEN, N., PIEK, J. J., SCHAPER, W., BODE, C. & BUSCHMANN, I. (2001b) Arteriogenesis: mechanisms and modulation of collateral artery development. *J Nucl Cardiol,* 8**,** 687-93.

VAN WEEL, V., TOES, R. E., SEGHERS, L., DECKERS, M. M., DE VRIES, M. R., EILERS, P. H., SIPKENS, J., SCHEPERS, A., EEFTING, D., VAN HINSBERGH, V. W., VAN BOCKEL, J. H. & QUAX, P. H. (2007) Natural killer cells and CD4+ T-cells modulate collateral artery development. *Arterioscler Thromb Vasc Biol,* 27**,** 2310-8.

VILLAR, I. C., FRANCIS, S., WEBB, A., HOBBS, A. J. & AHLUWALIA, A. (2006) Novel aspects of endothelium-dependent regulation of vascular tone. *Kidney Int,* 70**,** 840-53.

WAGNER, S., HELISCH, A., BACHMANN, G. & SCHAPER, W. (2004) Time-of-flight quantitative measurements of blood flow in mouse hindlimbs. *J Magn Reson Imaging,* 19**,** 468-74.

WANG, H. U., CHEN, Z. F. & ANDERSON, D. J. (1998) Molecular distinction and angiogenic interaction between embryonic arteries and veins revealed by ephrin-B2 and its receptor Eph-B4. *Cell,* 93**,** 741-53.

WARREN, K. S. & FISHMAN, M. C. (1998) "Physiological genomics": mutant screens in zebrafish. *Am J Physiol,* 275**,** H1-7.

WEINSTEIN, B. (2002) Vascular cell biology in vivo: a new piscine paradigm? *Trends Cell Biol,* 12**,** 439-45.

WEINSTEIN, B. M., STEMPLE, D. L., DRIEVER, W. & FISHMAN, M. C. (1995) Gridlock, a localized heritable vascular patterning defect in the zebrafish. *Nat Med,* 1**,** 1143-7.

WEISFELDT, M. L. & ZIEMAN, S. J. (2007) Advances in the prevention and treatment of cardiovascular disease. *Health Aff (Millwood),* 26**,** 25-37.

WESTERFIELD, M. (2000) *The Zebrafish Book: A Guide for the Laboratory Use of Zebrafish (Danio rerio). Fourth Edition.*, University of Oregon Press, Eugene.

WINKLER, C., ELMASRI, H., KLAMT, B., VOLFF, J. N. & GESSLER, M. (2003) Characterization of hey bHLH genes in teleost fish. *Dev Genes Evol,* 213**,** 541-53.

YANCOPOULOS, G. D., DAVIS, S., GALE, N. W., RUDGE, J. S., WIEGAND, S. J. & HOLASH, J. (2000) Vascular-specific growth factors and blood vessel formation. *Nature,* 407**,** 242-8.

YANCOPOULOS, G. D., KLAGSBRUN, M. & FOLKMAN, J. (1998) Vasculogenesis, angiogenesis, and growth factors: ephrins enter the fray at the border. *Cell,* 93**,** 661-4.

YANG, H. T., YAN, Z., ABRAHAM, J. A. & TERJUNG, R. L. (2001) VEGF(121)- and bFGF-induced increase in collateral blood flow requires normal nitric oxide production. *Am J Physiol Heart Circ Physiol,* 280**,** H1097-104.

YOSHIZUMI, M., ABE, J., TSUCHIYA, K., BERK, B. C. & TAMAKI, T. (2003) Stress and vascular responses: atheroprotective effect of laminar fluid shear stress in endothelial cells: possible role of mitogen-activated protein kinases. *J Pharmacol Sci,* 91**,** 172-6.

YU, J., DEMUINCK, E. D., ZHUANG, Z., DRINANE, M., KAUSER, K., RUBANYI, G. M., QIAN, H. S., MURATA, T., ESCALANTE, B. & SESSA, W. C. (2005) Endothelial nitric oxide synthase is critical for ischemic remodeling, mural cell recruitment, and blood flow reserve. *Proc Natl Acad Sci U S A,* 102**,** 10999-1004.

ZHONG, T. P., CHILDS, S., LEU, J. P. & FISHMAN, M. C. (2001) Gridlock signalling pathway fashions the first embryonic artery. *Nature,* 414**,** 216-20.

ZHONG, T. P., ROSENBERG, M., MOHIDEEN, M. A., WEINSTEIN, B. & FISHMAN, M. C. (2000) gridlock, an HLH gene required for assembly of the aorta in zebrafish. *Science,* 287**,** 1820-4.